5-1-2015

Modeling Background Radiation using Geochemical Data

Kara Marsac
University of Nevada, Las Vegas, marsac@unlv.nevada.edu

MODELING BACKGROUND RADIATION USING GEOCHEMICAL DATA

By

Kara Marsac

Bachelor of Science in Geology
Eastern Michigan University
2013

A thesis submitted in partial fulfillment of the requirements for the

Master of Science – Geoscience

Department of Geoscience
College of Sciences
The Graduate College

University of Nevada, Las Vegas
May 2015

UNLV | GRADUATE COLLEGE

We recommend the thesis prepared under our supervision by

Kara Marsac

entitled

Modeling Background Radiation Using Geochemical Data

is approved in partial fulfillment of the requirements for the degree of

Master of Science - Geoscience
Department of Geosciences

Pamela Burnley, Ph.D., Committee Chair

Russell Malchow, Ph.D., Committee Member

Elisabeth Hausrath, Ph.D., Committee Member

Ralf Sudowe , Ph.D., Graduate College Representative

Kathryn Hausbeck Korgan, Ph.D., Interim Dean of the Graduate College

May 2015

Abstract

Aerial gamma ray surveys have many applications in geology and science in general, such as locating mining prospects, defining radioactive plumes, and detecting nuclear weapons. Unfortunately there is currently no simple way to separate the natural gamma radiation of soil and rocks from that of contaminants such as radioactive plumes. This project used geochemical data (uranium, potassium and thorium concentrations) collected from national databases, private companies, and the NURE (National Uranium Resource Evaluation) Survey, to create forward models of exposure rates measured by aerial gamma ray surveys. We developed these techniques using an area in north central Arizona known as the Navajo Mines area, chosen for its optimal conditions for aerial gamma ray surveys and readily available survey data. Models based on geochemical analyses from databases were not found to be successful, in part due to lack of data for some units. Models based on NURE data sorted by geologic unit were successful at replicating the aerial gamma ray survey, though units with Uranium mineralization proved difficult. ASTER visualizations were effectively used to create subunits of similar exposure rate within the Chinle Formation which contains multiple lithologies. For alluvial units, models based on drainage basin were attempted with success. With these models we are developing techniques to estimate the natural radiation generated by the rocks and soils of an area, making aerial gamma ray surveys more effective.

Acknowledgements

I'd like to thank Dan Haber for being everything from my field assistant, to my sounding board, to my IT help desk during my 2 years here at UNLV. We continue to make better science together by building off each other's ideas.

I doubt I ever would have been able to finish on time without Jeremiah Smith, who endlessly helped me analyze models. I can't wait to see where you go as a scientist.

Chris Adcock has been invaluable to this project by providing so many remote sensing images and endless guidance.

Racheal Johnsen has been an amazing source of support throughout this experience, and I can't thank her enough for taking so much time to direct me through this process.

Thank you to everyone in the Geoscience Department who made my success at UNLV possible, especially to the office staff, who were always there to answer my endless questions.

I'd like to thank my parents for making all of this possible.

Matt Mullen, I can't thank you enough for being my constant source of support throughout this past year. You've been amazingly kind, and I cannot wait to spend the rest of my life with you.

I'd like to thank my committee:

Libby Hausrath for helping me make the tough decisions about my next step in life and offering great advice. Thank you for being an amazing geochemistry teacher and advisor.

Rusty Malchow for constantly wrestling to get everything stipped on time, for offering an excellent outside perspective on all of my work, and having a constant love of science and endless positive attitude.

Ralf Sudowe for being so patient while teaching a geoscientist health physics, running so many samples for me, and going above and beyond the call of duty.

And finally Pamela Burnley, without you this never would have been possible. I cannot thank you enough for taking a chance on me as a student. My life is infinitely better having had you as an advisor and mentor. Thank you for holding my hand in the beginning and allowing me to grow as an independent scientist. You are the mold that every other advisor should be made with. Thank you for being kind, supportive, and truly creating a family within your office.

Table of Contents

List of Tables

List of Figures

Chapter 1: Introduction

Radiation measurement via aerial gamma ray surveys is important because it can give us insight into the spread of radioactive plumes, the location of nuclear weapons or dirty bombs and where to prospect for important resources (Dickson and Scott, 1997). This radiation can come from natural sources such as soil or bedrock, and from anthropogenic radionuclide contamination including nuclear fallout. Past studies have focused on identifying fallout from nuclear weapons testing (Grasty et al., 1984; Books, 1962), and trying to predict bedrock type from an aerial gamma ray survey (Griscom and Peterson, 1961; Pitkin et al.,1964). Instead, our study attempts to take the measured geochemistry of the bedrock and model the natural background measured in an aerial gamma ray survey. A successful model will allow the natural signal from the bedrock to be subtracted from aerial gamma ray surveys allowing for better detection of valuable ores and hazards.

Airborne gamma-ray spectroscopy measures the gamma radiation emitted at or near the surface of the Earth, from materials such as soil, rock and overburden. When radioactive isotopes decay, alpha, beta, and gamma radiation can be released. Neither alpha nor beta radiation can be used for aerial surveys, because both are released in the form of particles, (an alpha particle is two protons and two neutrons, while a beta particle is only an electron) that interact with nuclei in the rock, soil and air, never making it to detectors (Minty, 1997). Gamma radiation consists of high energy photons and is able to penetrate about 30 cm of rock or soil and a few hundred meters of air. The energy released

during decay is different for each radioactive isotope (Dickson and Scott, 1997).

The decay series of Uranium (U), Potassium (K) and Thorium (Th) are the only

naturally occurring radioactive isotopes that exist in large enough quantities and

decay with high enough energies to be measured during an aerial survey (Minty,

1997); which are typically conducted several hundred feet off the ground. When a

gamma-ray interacts with a scintillation detector, light is released and the

intensity of this light is directly related to the energy of the gamma ray that struck

it (Minty, 1997). Based on the intensity of the light emitted from the scintillation

detector one can figure out which isotope released that gamma ray (Minty, 1997).

K, a common element in rocks and soils, makes up approximately 2% of

the Earth's crust. 0.012% of all K is its radioactive isotope, ^{40}K. When ^{40}K decays

to Argon with a branching ratio of 11%, it releases a gamma ray with a

characteristic energy of 1.46 MeV, making ^{40}K easy to identify in a gamma ray

spectrum. The specific activity of K is low, but it exists in such great quantities

that it can to be detected during aerial surveys (Minty, 1997). K is most abundant

in K-feldspars and micas, making K more prevelant in felsic igneous rocks such

as granite, and less abundant in mafic rocks. When K-rich minerals are

weathered the K may be incorporated in new clay minerals (Dickson and Scott,

1997) that can then be incorporated into soils or sedimentary rocks. Sedimentary

rocks such as arkose, and fine grained sedimentary rocks (shale, mudstone, etc.)

are also rich in K (Ulbrich et al., 2009).

^{232}Th is a radioactive isotope ubiquitous in rocks and soils, with a decay

series that releases a number of gamma rays that can be detected by aerial

gamma ray surveys. ^{232}Th itself does not release any high energy, high intensity

gamma rays when it decays to Radium-228 (Ra). Instead, the subsequent

daughters in its decay series release these gamma rays as they decay to the

final stable daughter isotope, Lead-208 (Pb). The series of discrete gamma rays

released by the daughter isotopes are used to calculate an equivalent Th (eTh)

concentration. Th is much less abundant than K, making up only 12 ppm of the

Earth's crust. Th occurs in significant quantities in minor minerals such as

allanite, monazite, xenotime and zircon (Dickson and Scott, 1997). These

minerals are found mostly in felsic igneous rocks. Zircon and monazite are of

particular importance because they are resistant to weathering and thus remain

in the soil and can accumulate in heavy mineral sands (Ulbrich et al., 2009).

When Th is weathered out of a mineral, it tends to stay in place because of its

low solubility. It can be taken up by clays or iron oxides, and if adsorbed by

colloidal clays, can be transported out of the system. An exception to Th's low

solubility is in acidic environments, and neutral environments in the presence of

organic compounds such as humic acid (Dickson and Scott, 1997).

U is another important contributor to the gamma radiation background that

occurs in many of the same environments, minerals and rocks as Th when in its

reduced state (U^{4+}). The solubility of U is highly affected by the presence of

organic compounds, allowing U to concentrate where organic content is high. In

peat and black shales, U concentrations can reach 10,000 times expected values

(Ulbrich et al., 2009). Unlike Th, U also has an oxidized state (U^{6+}) that is soluble

and therefore mobile. Like Th, ^{238}U does not release high energy, high intensity

3

gamma rays when it decays to ^{234}Th, but the subsequent daughters in its decay series release these gamma rays as they decay to the final stable daughter isotope, ^{206}Pb. The series of discrete gamma rays released by the daughter isotopes are used to calculate an equivalent U (eU) concentration. U occurs in the Earth's crust at a concentration of about 3 ppm, and has two major isotopes: ^{238}U and ^{235}U, with ^{238}U being far more abundant. U occurs in minor quantities in oxides and silicates and along grain boundaries, and in higher concentrations in zircon, monazite and xenotime (Dickson and Scott, 1997).

Disequilibrium can affect the decay series of U and Th, causing eU and eTh to vary from actual U and Th concentrations. U concentration is mainly calculated from the spectra of Bismuth-214, and Th concentration is mainly calculated from the spectra of Thalium-208 (Minty, 1997). In order for this type of measurement to be valid, the isotope and its daughters must be in equilibrium. In a closed system equilibrium occurs after 10 times the length of the half-life of the daughter with the longest half-life has passed if the parent has a significantly longer half-life. Once equilibrium is established, everything in the decay chain will be decaying at such a rate that the number of atoms of each daughter remains constant. Th has very short lived daughters and only requires 40 years to reach equilibrium with its daughters, so Th is rarely found in disequilibrium (Dickson and Scott, 1997). U is much more likely than Th to be in disequilibrium because it takes at least 1.5 million years to reach equilibrium (Dickson and Scott, 1997). Disequilibrium can also occur through the preferential removal of the parent or daughter isotope through weathering. Due to the low mobility of Th and its

daughters in aqueous environments, the Th decay chain is less susceptible to disequilibrium. In contrast, due to the higher solubility of U^{6+} as well as the volatility of its daughter Radon-222 (Rn), a gas that can easily escape both soil and rock, equilibrium in the U decay chain cannot be taken for granted.

Previous studies concerning the relationship between aerial gamma ray surveys and geology have focused on how to discern geologic units from survey results. Aerial gamma surveying of the US began in the 1950s with the ARMS (Aerial Radiological Measurement Survey) aerial gamma ray surveys of areas around nuclear facilities to create a baseline to detect future anomalies (Pitkin et al., 1964). These surveys were not done for the purpose of examining lithology, but the USGS used the data to study the relationship between radiation and geology. Pitkin et al. (1964) summarizes findings in aerial gamma ray surveys and geology comparisons across the US, drawing conclusions such as faults being denoted by higher exposure rates due to leaking radon. Griscom and Peterson (1961) reviewed an aerial gamma ray survey done of the Maryland Piedmont by the USGS itself that found previously unknown mafic intrusions. Moxham (1963) concluded that surface radiation is dominated by contribution from rock, not soil. In the study an equation was also devised to calculate U concentration from net radioactivity. By creating and solving computational models of photon emission, Lovborg and Kirkegaard (1974) and Beck et al. (1972) proposed that exposure rates could be calculated from a linear combination of K, U, and Th concentrations. Grasty et al. (1984) compared the

resulting equations to his own calculated equations and assigned average

constant values seen in Equation 1:

$$D = 1.32\ K + 0.548\ eU + 0.272\ eTh \quad \text{(Equation 1)}$$

Where D is exposure rate in mircoR/hr, K is weight percent K, eU is ppm

U, and eTh is ppm Th. Taking the ARMS program further, from 1973 to 1980, an

aerial gamma ray survey known as the NURE (National Uranium Resource

Evaluation) survey was done by the Atomic Energy Commission for the purpose

of evaluating U resources in the US. Most of the continental US was flown with

10 km line spacing. The data are reported as K, U and Th concentrations, and

exposure rate may be calculated using Equation 1. More recent research using

aerial gamma ray surveys and geology has focused primarily on exploration for

U, Th, and precious metals (Mernagh and Miezitis, 2008; Dickson and Scott,

1997; Dickson, 1995). Dickson and Scott (1997) discuss using K, U and Th ratios

in aerial gamma ray surveys to find metal ore deposits. Dickson (1995) studied

equilibrium across Australia, and found that aerial gamma ray survey

interpretation would not be affected by disequilibrium. Mernagh and Mietzitis

(2008) provide an overview of Th resources in Australia, including an aerial

gamma ray survey of the majority of Australia and table of average U, K, Th

concentrations for basic rock types.

While averages of radioactive isotope content in each rock type have been

published (Mernagh and Miezitis, 2008; Dickson and Scott, 1997), rocks are

highly variable. The ranges of concentration of radioactive isotopes are too wide

and overlapping to be able to take these concentrations from an aerial gamma ray survey and predict what rock type is on the ground (Dickson and Scott, 1997). However, aerial gamma ray surveys can be used to see boundaries between adjacent geologic units (Griscom and Peterson, 1961; Pitkin et al., 1964; Moxham, 1963), and trends can be seen in radioelement content and rock type.

The purpose of this study is to create a way to model background radiation emanating from surficial rocks and soils using geochemical data and geologic maps. This would allow for simple identification of anomalies in the survey, assisting in ore location and national security. Comparing a radiation model created from geochemical data and an aerial gamma ray survey can become difficult as a real world survey has additional components such as ubiquitous background radiation from other sources adding to the total radiation, and vegetation attenuating gamma rays. According to Minty (1997) background radiation from the equipment itself, cosmic radiation, and radon in the atmosphere are also measured during aerial gamma ray surveys; these signals are measured and subtracted out of the spectrum to correctly interpret the concentrations of U, K and Th which are being modeled with geochemical data. The radiation measured during an aerial gamma ray survey can possibly be obscured by the presence of vegetation, and there is currently no way to adjust the spectra for this minor effect. Vegetation absorbs radiation that would be read by an aerial survey, thus making it appear as if the concentration of radioactive isotopes is less than it actually is (Minty, 1997), thus an arid environment with

little vegetation should be an optimal candidate for modeling an aerial gamma ray survey. Another complication with aerial gamma ray surveys is due to aeolian addition. In temperate climates, soil is typically formed from the weathering of the bedrock it sits on, which is why the concentration of radioactive isotopes in soil is usually correlated to the concentration of radioactive isotopes in the bedrock. In aeolian addition, an important process in the formation of arid desert soils, dust is transported into the area that has no relation to the bedrock it is deposited on. Books (1962) examined an aerial gamma ray survey of the Los Angeles area, and concluded only generalizations can be made between geology and radiation in the area, because alluvium does not generally overlie parent rock.

Chapter 2: Methods

In this research we focused on modelling background radiation from an area in north central Arizona, near Cameron, AZ (Figure 1). Located in and around the Navajo Nation, this area was mined for U from the 1940s through the 1960s (Hendricks, 2001). The study area was chosen because a high resolution aerial gamma ray survey was performed by personnel of the Remote Sensing Laboratory located in Las Vegas, Nevada, (a facility of the U.S. Department of Energy, National Nuclear Security Administration Nevada Operations Office),from 1994-1999 to assess the risk associated with exposure to radiation in this area. This area has optimal conditions for aerial gamma ray surveys: sparse vegetation and an arid environment.

In order to predict exposure rates, geolocated geochemical data containing U, K, Th concentrations were obtained from national databases (USGS, IEDA, and GeoRoc) and DIR Exploration, a private U mining company (Table 1). The USGS data was accessed through the IEDA database, providing over 350 data points, mostly of volcanic rocks. These analyses vary in whether or not they include U, K and Th. GeoRoc yielded 10 additional data points all of which were basalt analyses and included only K data. We also obtained geolocated data from a private uranium mining company, DIR Exploration, who provided over 170 U concentrations for rocks of unspecified type in our mapping area. These data were then sorted and culled for internal consistency. The geochemical data was synthesized into a single data set and sorted with ArcMap by geologic unit based on its reported location and the 2007 USGS map

(Billingsley et al., 2007) (Figure 2). Geochemical data occurring outside the

modeling area was included in the dataset, if it was from a bedrock unit that also

occurred in the modeling area. No alluvial unit data was brought into the dataset

from outside the modeling area. The meta data associated with each of the

analyses provided by these databases varied greatly based on what the

contributor chose to include, in many cases the rock type of the sample was not

reported; geologic units were rarely reported.

Data points were examined, and discarded or moved to an appropriate

unit based on whether or not the description was consistent with the geologic unit

assigned by location. If the author of the geochemical analysis stated that the

sample was from a unit other than the one that occurred at its geolocation, it was

moved to the author's specified unit. If the rock type of the data point was not

consistent with the description of the geologic map unit (Billingsley et al., 2007), it

was discarded. Most chemical analyses do not include a full set of U, K, and Th

concentrations, the majority only contain K concentrations. For samples that had

multiple analyses using different methods, the geochemical data were combined

by choosing the most accurate method of analysis for each U, K, and Th

concentration. This left us with 552 geochemical data points out of over 1000

original data points for 31 geologic units. For the 2 bedrock units that did not

have a full suite of associated U, K, and Th concentrations, average

concentrations from an Australian geochemical survey (Dickson and Scott, 1997;

Bruce Dickson, personal communication) and data from Mernagh and Miezitis

(2008), were used to fill in these missing concentrations, as the arid climate

mimics that of the southwestern United States. An average was taken of the concentration of each U, K and Th for all major rock types present in the unit based on the USGS description (Billingsley et al., 2007). TRmhm (Holbrook and Moqui Members of the Moenkopi Fm) was created entirely from the data from the Australian survey. The second unit was a small volcanic unit, Qbt, that contained only K concentration. Ten alluvial units (which cover about 10% of the modeling area) had no associated geochemical data points. The majority of the data is associated with 2 geologic units: Pkh with 184 data points and Qa2 with 227. Table 1 gives the number of data points per unit.

Mean, median, and standard deviation were calculated for K, U and Th concentrations for each unit (Table 1). Mean values can be skewed by large outliers, especially with regards to U, since this area hosts ore grade U concentrations, in some cases up to 17,000 ppm U. Thus median concentrations were used and converted into exposure rate, a measure of radiation, using Equation 1. This allowed us to compare the geochemical model (GM) to aerial gamma ray exposure rate data.

The National Security Technologies, LLC (NSTec), Aerial Measuring System (AMS) section provided us with a digital data set for the exposure rate map published in Hendricks (2001). This survey data, consisting only of exposure rate values, was also sorted by geologic unit using ArcMap. The mean, median, and standard deviations of exposure rate were calculated for each unit (Table 2).

NURE aerial survey data was obtained from the USGS database. In the study area there are 8 East/West NURE flight lines through the area and 1

North/South flightline (Figure 3). This survey reports eU, K and eTh concentrations, thus Equation 1 was used to calculate total exposure rate. ArcMap was used to sort this data by the geologic unit to create a NURE model (NM) for direct comparison to the other data sets. All data sets (including the geologic map) were reprojected to the global coordinate system WGS 1984 used by the NURE dataset for accurate comparison.

Alluvial units were modelled in 2 ways: by geologic unit and by drainage basin. Drainage basins for the Little Colorado River and its tributaries were manually drawn in ArcMap based on DEMs (Digital Elevation Models) (Figure 4). Nineteen basins were identified, each representing a separate main tributary and all the streams in its headwater. Geologic units identified as alluvium within each drainage basin were joined into single alluvial units, resulting in 19 alluvial units (Figure 5). AMS exposure rate data occurring within alluvial units was sorted into these 19 alluvial units to create a new standard AMSDB, (AMS Drainage Basin) to compare with NURE models created in the same way. Geochemical data had to be resampled from databases as some basins extended almost 50 km outside of the modeling area. NURE data was resampled for the entirety of the drainage basins and used to create three separate models. The first model includes all NURE data present in drainage basins (AN); the second model is all NURE data present in the drainage basins excluding points located over rock units within the study area (ANNR); and the last model is NURE data only within the study area, excluding points located over rock units (SAONR).

To minimize the possible effect of geolocation uncertainties, data points within 50 meters of a geologic unit boundary were eliminated from NURE and AMS data sets, creating "buffer" models (NBM and AMSB respectively). The footprint of an aerial gamma ray survey point is approximately 91 meters, thus data points within 50 meters of a geologic boundary may have a significant contribution from more than one unit, the buffer mitigates this possible source of uncertainty. The 50 m buffer was also applied to the 19 drainage basin alluvial units for the AMS data (AMSBB) and the NURE data through the SAONR model (SAONRB).

Remote sensing models were created for the TRcs and TRcp members of the Chinle Formation, both sedimentary units that showed large standard deviations in the AMS data. Each of these members consists of many different lithologies, including sandstone, limestone, conglomerate and shale. These rock types all have potentially different average K, U, Th content, making it difficult to assign single K, U, and Th concentrations to these very widespread units. Satellites, such as the Terra satellite, collect data over a wide range of the electromagnetic spectra, including UV and infrared. Data from ASTER (Advanced Spaceborne Thermal Emission and Reflection Radiometer), an instrument aboard Terra, were used to separate geologic units into mineralogically similar subunits. Each of the 14 bands gives different information about the same area, highlighting lithological differences, emphasizing different minerals (van der Meer et al., 2012) or vegetation. Combination images or 'visualizations' were created by combining three bands from the ASTER science

package on the Terra satellite in ENVI. A 7-3-1 band combination image, which discriminates lithology, and a 2-6-10 band combination image, which highlights alteration, were used for the study area. Ratio images were created by making a ratio of the intensities of the 2 ASTER bands. A 2/1 ratio image, which highlights ferric iron on the surface, and a 4/5 ratio image, which highlights the clay mineral laterite, were used for the study area. Both types of images highlight differences in lithology and were classed into 5 classes of differing lithology. They were then polygonised in ArcMap and unioned with the Chinle Fm geologic map to create 5 subunits for each of the Chinle's 2 main members, creating up to 10 subunits in total. NURE data occurring in the Chinle Fm was sorted into these subunits to create a new model for the Chinle Fm, which was compared to AMS survey data sorted into the same subunits. Geochemical data was not considered for this type of modeling, as there were only 11 geochemical analyses for TRcp and 6 for TRcs, not enough data points to create a significant model.

To determine if there were systematic differences in AMS and NURE survey exposure rates, a point to point comparison was made, where the AMS data point closest to each NURE data point was selected and the exposure rates were compared. A histogram of the differences between the exposure rates of each pair points is shown in Figure 6. The histogram was fitted with a gaussian distribution, yielding an average difference in exposure rate of 0.972 microR/hr with a standard deviation of 1.91. This average difference was added to NURE based models to account for the systematic offset between the two aerial gamma ray surveys.

Chapter 3: Results

The AMS measured exposure rate over the study area is shown in Figure 7. The mean and median AMS exposure rate calculated for each geologic unit is given in Table 2. The average standard deviation of AMS data separated into geologic units is 1.44. When the 50 m buffer was applied, one geologic unit, a small isolated dune unit, Qbd, lost all AMS data. However this unit also lacked geochemical data as well as NURE data. Almost 50% of the AMS data was eliminated by adding this buffer. This lowered the standard deviation of exposure rate grouped by geologic unit, the average standard deviations dropped from 1.44 to 1.24

The average difference between the exposure rate predicted by the geochemical model (GM) and the AMS measured exposure rate ranged from 5.81 microR/hr to -235.94 microR/hr. The average absolute difference is 19.60 microR/hr. Values for the GM are reported in Table 3. Only 2 units used data from the Australia geochemical survey. The first of these units was a sedimentary rock unit, TRmhm, that was created entirely from the data from the Australian survey. The second was a small volcanic unit, Qbt, that contained only K concentration; Australian survey was used to estimate and fill the gaps for U and Th.

The NM (NURE model) had an average absolute difference in exposure rate from the AMS data of 0.62 microR/hr. The average standard deviation of the NM is 1.26. Values for NM are reported in Table 4.

The addition of the 50 m buffer to both data sets lowered the average absolute difference between the AMS and NURE exposure rates (AMSB and

15

NBM) to 0.51 microR/hr. The average standard deviation of the NURE data is 1.25. Values for AMSB and NBM are reported in Table 5.

For drainage basins three NURE models were tested: AN, ANNR, and SAONR. For AN the average of the absolute value of exposure rate difference is 0.97 microR/hr. Values for AN are reported in Table 6. For the ANNR model the average absolute difference in exposure rate is 1.06 microR/hr. Values for ANNR are reported in Table 7. For SAONR the average of the absolute value of exposure rate difference is 0.65 microR/hr. This model lacked data for one basin. Values for SAONR are reported in Table 8.

The average of the absolute differences in exposure rate between SAONRB and the AMSBB is 0.65 microR/hr. Values for SAONRB are reported in Table 9.

The average of the absolute differences in exposure rate between NURE and AMS data for the 2-6-10 image of the Chinle Fm is 0.92 microR/hr for TRcp and 0.86 microR/hr for TRcs. The average standard deviation of the AMS data sorted into the Chinle subunits created by the 2-6-10 visualization is 1.70 for both TRcp and TRcs. The average of the standard deviations of the NURE model are 1.22 for TRcp and 1.16 for TRcs. Values for the 2-6-10 image are reported in Table 10 and 11. Figure 8 displays the 2-6-10 image and classes. Figure 9 is a large scale comparison of a satellite image of the geology overlain by the classes created from the 2-6-10 image for a small area within the Chinle. The average of the absolute differences in exposure rate between NURE and AMS data for the 2/1 image is 0.77 microR/hr for TRcp and 0.75 microR/hr for TRcs. The average

standard deviations of the NURE model are 1.4 for TRcp and TRcs. Values for

the 2/1 image are reported in Table 10 and 11. The average of the absolute

differences in exposure rate between NURE and AMS data for the 7-3-1 image

was 1.18 microR/hr for TRcp and 0.69 microR/hr for TRcs. The average standard

deviations of the AMS data sorted into the 7-3-1 subunits is 2.43 for TRcp and

2.31 for TRcs. The average standard deviations of the NURE model are 1.53 for

TRcp and 1.62 for TRcs. Values for the 7-3-1 image are reported in Tables 10

and 11. The 4/5 image has an average of the absolute differences in exposure

rate between NURE and AMS data of 1.1 microR/hr.

Chapter 4: Discussion

The goal of this study is to use preexisting geochemical data and geologic maps to predict exposure rate measured in aerial gamma ray surveys. Such a predictive modeling capability would allow for better evaluation of anomalies in surveys, and thus location of both hazards and possible mineral resources. In order for a background model to be useful it needs to predict the probability of obtaining a given exposure rate at any particular location. With these predictions a small standard deviation is necessary to illustrate accuracy in the method from area to area. This would indicate that there is geochemical significance to how we are modeling exposure rate. A standard deviation of exposure rate smaller than the standard deviation of the whole data set indicates a background radiation unit is more homogenous, and thus significant. A successful model is defined by how well the model matches the AMS data for the defined background radiation unit. A model with an average exposure rate difference of less than ±1 microR/hr with the AMS data is defined as successful because the uncertainty of aerial gamma ray survey measurements is approximately 10%, and an average background radiation from the surface of the Earth is approximately 10 microR/hr.

Models created with sets of NURE data had the lowest standard deviations, and thus the highest unit homogeneity. For NURE data the lowest standard deviation is 1.25, occurring when data was sorted by drainage basin and by geologic unit with a 50 meter buffer. The NURE data set as a whole has a standard deviation of 1.77, so the model creates a noticeable decrease.

18

For AMS data, the lowest standard deviation is 1.19, present when data was sorted by geologic unit and a 50 meter buffer was applied. The AMS data set as a whole has a standard deviation of 2.41, so the sorting and culling of data creates a significant improvement of the standard deviation. AMS data was also sorted by the 2-6-10 visualization for the entire study area, resulting in an average standard deviation of 1.88. This justifies sorting AMS data into geologic units, as it creates units of more uniform exposure rate than the whole data set, and the AMS data set sorted into remote sensing units.

Models based on geochemistry were not found to be successful in this area. This could be due to a number of factors, but most likely related to outliers, preferred sampling, and lack of data. While median concentrations were used to mitigate outliers, for units with less than 5 data points, outliers had a large effect. For example, TRmw had three geochemical data points, but only 2 of the samples had U concentrations, and one of 840 ppm, over 2 orders of magnitude higher than the crustal average of 3 ppm. This outlier U concentration lead to an exposure rate of 243 microR/hr, much higher than the average of the AMS data at 8.26 microR/hr. Another hypothesis as to why the geochemical model did not work for this particular area is the large volume of U mining that occurred in this area, many of these samples could be related to prospecting. A possible issue that could explain units with much higher exposure rates than the AMS data (TRmw and TRmss) is a sampling bias. This could have occurred where samples collected in this area were focused mostly on U prospecting, and thus samples of high U concentration are more likely to be in the databases. It would be valuable

to further explore using geochemistry to model aerial gamma ray surveys in an area lacking significant radioelement mineralization. Another problem with this model is possible geolocation issues. Qa2 has 225 samples that were recorded to have been collected in the exact same location. The USGS data is self-reporting and thus does not contain a minimum number of recorded decimals in latitude and longitude, leading to uncertainty in where a sample was actually collected. The database also has no way of connecting data collected with possible published work, making it impossible to perform checks on data with published maps or contact authors. These data points were of similar rock type that could have occurred in Qa2, and thus were not culled. Overall, our geochemical model tended to under predict exposure rate, and it is unclear why this occurred.

Alluvial units are difficult to model based on geochemical sample data because of the heterogeneous nature of alluvial units. A sample that is collected and analyzed for U, K, and Th is not going to represent the variation occurring within the unit. Alluvial units are also categorized by age and how they were formed, so many times a single alluvial unit occurs in many points within the study area, possibly with vastly different parent rocks.

More success was had with modeling bedrock units based on geochemical data. For example, Pkh, a limestone and sandstone unit, had an average difference of 0.93 microR/hr. This is most likely due to the fact that there were 184 data points within this unit, so the variation within the unit would be represented.

The most successful models were based on the NURE aerial gamma ray survey data set sorted into geological units. These models are probably more successful because aerial gamma ray survey data is being compared to aerial gamma ray survey data, so factors such as vegetation, soil moisture and radon in the soil are included in both datasets. These factors would present additional considerations moving forward with modeling gamma radiation with geochemistry, as they would have to be factored into Equation 1. NM and the AMS data sorted into geologic units had low standard deviations, and thus more homogenous units. The difference between NM and the AMS data had an average of 0.62 microR/hr, a successful model. The addition of a 50 meter buffer improved the homogeneity of the AMS data set and the overall difference between the model and the AMS data set (Figure 10). The overall average difference between the model and the AMS data was 0.51 microR/hr, while the average difference of the medians was 0.46 microR/hr. The overall improvement of results with the buffer indicates that the buffer is removing data points that are being contributed to by more than one geologic unit.

Drainage basin models were not as successful as models based on geologic units, but could be a viable option in other study areas. The best basin model was the SAONR model, which included the least amount of data. The average difference between the SAONR model and the AMS model is 0.65 microR/hr. The average standard deviation of AMS data was 1.5, and the average standard deviation of the SAONR model is 1.25. This is most likely the best basin model because AMS and NURE data are being compared for the

same areas, whereas the ANNR model and the AN model take data from outside the study area, where there is no AMS data. The addition of the 50 m buffer to the SAONR model made little difference to the overall results. The average difference between the model and the AMS data was 0.65microR/hr. The average standard deviation of the AMS data was 1.41 and the average standard deviation of the SAONR model with buffer was 1.33. With the addition of this buffer only 30% of the data was lost.

Using remote sensing to model the TRcp and TRcs members of the Chinle Fm was successful in that the average difference between the models and the AMS data decreased, and the standard deviations of each data set for these units was lowered. The model with the most homogenous units was based on the 2-6-10 visualization, providing lower standard deviations than the NURE buffer model. The success of this image, which emphasizes alteration, over other images points to a possible relationship between alteration and exposure rate.

Of interest is also the trend observed in all of the models (excluding AN), of the average difference in exposure rate between the median AMS and median NURE data being significantly lower than the difference between the mean AMS and mean NURE data. For example, for the 2/1 model the difference is approximately a 40% change. This could indicate that the median is minimizing the skew of the dataset.

The correction constant of 0.972 microR/hr that was added to NURE data to account for the systematic offset between the NURE and AMS aerial surveys

was remarkably successful. The average between the two data sets was significantly improved for all of our models involving NURE data by adding this simple constant. Studies of other areas will need to be done to see if the amount of correction needed varies from location to location.

A concern to be addressed is the applicability of this method to the rest of the United States, where optimal conditions for aerial gamma ray surveys are not present. As NURE data is available for a majority of the continental US, and a comparison between aerial gamma ray surveys is being made, factors such as increased vegetation and soil moisture should not affect the success of this model (Moxham, 1963; Griscom & Peterson, 1961). However, if NURE data were at its lowest density (one line every 10 km), there could be a problem of lack of data in other areas. Whether this kind of modeling is replicable in countries other than the US depends on the public availability of pre-existing aerial gamma ray survey data for the area in question.

Chapter 5: Conclusion

This study has explored a number of methods for creating homogenous background radiation units to successfully model background gamma radiation in the environment. The use of NURE data and geologic maps has proved to create the most successful models, with the addition of a 50 meter buffer generating further successful models. It is possible the success of these models is due to the fact that they are comparing two aerial gamma ray surveys, so the same screening and environmental factors affect each one.

Geochemical data did not produce successful models, possibly due to lack of data or sampling bias. Further work on the relationship between radiation measurements and geochemical analysis could assist in improving these models.

The 2-6-10 ASTER visualization highlighting alteration successfully improved models of the TRcs and TRcp members of the Chinle Fm.

It is important to remember that our definition of success was provided to us by AMS. While some of these techniques may not fit within their narrow range of success, in the event of a nuclear disaster these techniques could still prove useful.

The further research and use of these techniques to model background radiation will allow for easier recognition of anomalies on aerial gamma ray surveys, and thus location of valuable resources and hazards.

Chapter 6: Tables

Table 1: Geochemical Data

Geo Unit	Number of Data Points	Mean U (ppm)	Median U (ppm)	Standard Deviation U	Mean Th (ppm)	Median Th (ppm)	Standard Deviation Th	Mean K (wt%)	Median K (wt%)	Standard Deviation K
Pkh	184	185.26	1.45	1670.25	6.54	6.52	5.23	0.65	0.37	0.95
Qa1	18	37.02	1.80	88.12	11.90	11.90	1.27	0.93	0.88	0.51
Qa2	228	1.63	0.98	1.51	9.78	3.65	11.35	1.48	1.17	0.98
Qae	4	1.37	1.50	0.32				0.96		
Qbt	2							1.58		0.48
Qd	1							0.70		
Qes	1	1.50								
Qf	1	1.10								
Qg1	2	1.90						1.09		
Qg3	1	13.40			6.79			0.02		
Ql	7	4.64	6.38	3.19	24.43	32.20	18.51	1.62	0.91	1.38
Qs	8	1.71	1.60	0.59	1.40	1.40	1.84	0.26	0.10	0.37
Qv	63	1.62	1.40	0.95	4.78	4.78	4.21	0.56	0.31	0.49
Tbpb	4	0.78			2.74			0.91	0.91	0.02
TRcp	11	16.67	4.80	33.45	14.90	13.70	5.32	1.21	1.20	0.50
TRcs	6	14.95	5.14	21.76	17.53	15.70	7.92	1.59	1.30	1.27
TRmss	4	1088.52	40.90	2121.25	8.11		2.15	2.05	2.30	0.96
TRmw	3	421.57		591.76	33.95		25.67	2.11	2.30	0.45
TRco	1	2.94			4.90			1.60		
Total	**552**									

Table 1: Displays only collected geochemical data, units with values filled in from Dickson and Scott (1997) survey in Table 3.

Table 2: AMS Data

Geo Unit	Avg AMS Aerial Survey Exposure Rate (µR/hr)	Median AMS Exp Rate (µR/hr)	AMS Std Dev
Pkh	3.99	3.87	0.83
Qa1	8.36	7.95	1.99
Qa2	8.15	7.82	1.97
Qae	8.25	7.89	2.18
Qbt	6.39	6.54	0.91
Qd	7.00	6.64	1.10
Qes	7.50	7.23	1.62
Qf	7.06	7.03	1.30
Qg1	7.65	7.47	1.40
Qg3	7.64	7.19	1.80
Ql	4.61	4.55	0.82
Qs	7.12	6.80	1.73
Qv	8.29	8.30	1.50
Tbpb	5.72	5.83	0.61
TRcp	9.64	9.29	2.45
TRcs	9.44	9.35	2.09
TRmss	6.47	6.18	0.93
TRmw	7.35	7.39	1.51
Ts	5.81	5.82	0.17
QTg4	6.90	6.48	1.81
QTg5	7.63	7.67	1.17
Qg2	7.86	7.16	3.00
Qa3	8.11	8.35	1.35
Qdb	6.81	7.42	0.48
Qdl	7.72	7.50	1.25
Qdp	7.71	7.50	1.22
Qtr	4.65	4.17	1.20
TRco	6.40	6.35	1.02
TRmhm	8.08	7.83	1.58
Qps	7.21	6.40	2.22

Average: **1.44**

Table 3: Geochemical Model Results

Geo Unit	Avg AMS Aerial Survey Exposure Rate (µR/hr)	Geochemistry Calculated Exposure Rate (µR/hr)	Difference (µR/hr)
Pkh	3.99	3.06	0.93
Qa1	8.36	5.28	3.09
Qa2	8.15	3.07	5.07
Qae	8.25		
Qbt	6.39	3.44*	2.95
Qd	7.00		
Qes	7.50		
Qf	7.06		
Qg1	7.65		
Qg3	7.64	9.22	-1.58
Ql	4.61	13.46	-8.85
Qs	7.12	1.77	5.35
Qv	8.29	2.48	5.81
Tbpb	5.72	2.37	3.34
TRcp	9.64	7.94	1.70
TRcs	9.44	8.80	0.63
TRmss	6.47	27.66	-21.18
TRmw	7.35	243.29	-235.94
Ts	5.81		
QTg4	6.90		
QTg5	7.63		
Qg2	7.86		
Qa3	8.11		
Qdb	6.81		
Qdl	7.72		
Qdp	7.71		
Qtr	4.65		
TRco	6.40	5.06	1.34
TRmhm	8.08	5.98*	2.10
Qps	7.21		
		Average:	**19.60**

Table 3: To get a calculated exposure rate units had to have K, U and Th data.

*These values were calculated using Dickson and Scott (1997, whole survey provided by Bruce Dickson) and Mernagh and Miezitis (2008)

Table 4: NURE Model Results

Geo Unit	Avg AMS Exp Rate (μR/hr)	Avg NURE Exp Rate (μR/hr)	Difference (μR/hr)	Median AMS Exp Rate (μR/hr)	Median NURE Exp Rate (μR/hr)	Difference (μR/hr)	AMS Std Dev	NURE Std Dev
Pkh	3.99			3.87			0.83	
Qa1	8.36	8.48	-0.11	7.95	7.96	0.00	1.99	2.34
Qa2	8.15	7.55	0.60	7.82	7.45	0.37	1.97	1.20
Qae	8.25	7.69	0.55	7.89	7.82	0.07	2.18	1.30
Qbt	6.39	7.53	-1.15	6.54	7.67	-1.13	0.91	0.82
Qd	7.00	7.41	-0.42	6.64	7.16	-0.52	1.10	1.34
Qes	7.50	7.58	-0.09	7.23	7.34	-0.11	1.62	1.76
Qf	7.06	6.95	0.10	7.03	6.86	0.17	1.30	1.28
Qg1	7.65	7.96	-0.31	7.47	7.82	-0.35	1.40	1.59
Qg3	7.64	7.52	0.12	7.19	6.62	0.57	1.80	2.39
Ql	4.61	5.51	-0.91	4.55	5.48	-0.93	0.82	0.79
Qs	7.12	7.52	-0.40	6.80	7.41	-0.61	1.73	1.57
Qv	8.29	7.65	0.64	8.30	7.60	0.70	1.50	1.37
Tbpb	5.72	6.05	-0.34	5.83	6.37	-0.55	0.61	0.89
TRcp	9.64	8.53	1.12	9.29	8.75	0.54	2.45	1.49
TRcs	9.44	8.77	0.67	9.35	8.67	0.69	2.09	1.60
TRmss	6.47			6.18			0.93	
TRmw	7.35	8.12	-0.77	7.39	7.84	-0.45	1.51	0.72
Ts	5.81			5.82			0.17	
QTg4	6.90	6.84	0.06	6.48	7.05	-0.57	1.81	1.54
QTg5	7.63	6.83	0.80	7.67	6.83	0.84	1.17	0.23
Qg2	7.86	8.38	-0.52	7.16	8.70	-1.54	3.00	2.39
Qa3	8.11	9.48	-1.37	8.35	9.48	-1.13	1.35	
Qdb	6.81			7.42			0.48	
Qdl	7.72	6.88	0.84	7.50	6.88	0.61	1.25	0.63
Qdp	7.71	8.06	-0.35	7.50	8.16	-0.66	1.22	0.77
Qtr	4.65			4.17			1.20	
TRco	6.40	7.36	-0.96	6.35	7.54	-1.18	1.02	0.89
TRmhm	8.08	6.52	1.56	7.83	6.81	1.02	1.58	1.28
Qps	7.21	6.41	0.79	6.40	6.41	-0.02	2.22	0.18
Average:			**0.62**			**0.61**	**1.44**	**1.26**

Table 5: NURE Buffer Model Results

Geo Unit	Average AMS Buffer Exp Rate (µR/hr)	Average NURE Buffer Exp Rate (µR/hr)	Difference (µR/hr)	Median AMS Buffer Exp Rate (µR/hr)	Median NURE Buffer Exp Rate (µR/hr)	Difference (µR/hr)	AMS Buffer Std Dev	NURE Buffer Std Dev
Pkh	3.75			3.81			0.54	
Qa1	8.20	8.43	-0.22	7.85	7.90	-0.05	1.81	2.32
Qa2	8.13	7.59	0.54	7.70	7.51	0.19	2.04	1.18
Qae	8.33	7.68	0.66	7.97	7.82	0.15	1.94	1.29
Qbt	6.86	7.28	-0.42	6.71	7.04	-0.34	0.76	0.81
Qd	6.86	7.30	-0.44	6.59	6.97	-0.39	0.95	1.35
Qes	7.43	7.81	-0.38	7.08	7.62	-0.54	1.56	1.71
Qf	7.04	6.86	0.18	7.01	6.81	0.20	0.98	1.05
Qg1	7.38	7.77	-0.39	7.35	7.51	-0.16	1.05	1.65
Qg3	7.50	6.82	0.68	6.98	6.35	0.64	1.71	1.65
Ql	4.49	5.48	-0.99	4.47	5.31	-0.84	0.48	0.86
Qs	6.29	7.25	-0.96	6.01	7.13	-1.11	1.03	1.49
Qv	8.21	8.84	-0.62	8.34	8.06	0.28	1.42	1.16
Tbpb	5.83	6.15	-0.32	5.93	6.37	-0.44	0.55	0.86
TRcp	10.01	8.87	1.14	9.65	8.98	0.67	2.43	1.13
TRcs	9.47	8.51	0.96	9.43	8.49	0.94	1.98	1.32
TRmss	6.18			6.10			0.51	
TRmw	7.98	8.24	-0.26	8.13	8.21	-0.08	0.94	0.76
Ts	5.80			5.82			0.11	
QTg4	6.64	6.81	-0.17	6.17	7.10	-0.93	1.59	1.34
QTg5	7.61			7.47			0.98	
Qg2	7.12	6.94	0.18	6.53	6.83	-0.30	1.91	0.99
Qa3	7.81			8.01			1.36	
Qdb								
Qdl	7.31			7.49			0.45	
Qdp	7.76	8.08	-0.32	7.78	8.08	-0.30	1.59	
Qtr	4.20			4.12			0.27	
TRco	6.39	7.20	-0.81	6.31	7.32	-1.01	0.72	0.85
TRmhm	8.26	8.13	0.13	8.11	8.13	-0.02	1.22	
Qps	6.78			6.16			1.50	
		Average:	**0.51**			**0.46**	**1.19**	**1.25**

Table 6: Basin AN Model Results

Basin	Avg AMS Exp Rate (µR/hr)	Avg AN Exp Rate (µR/hr)	Difference (µR/hr)	Median AMS Exp Rate (µR/hr)	Median AN Exp Rate (µR/hr)	Difference (µR/hr)	AMS Std Dev	AN Std Dev
A	7.41	7.33	0.08	7.24	7.25	-0.01	1.27	1.62
B	7.00	7.20	-0.20	6.82	7.16	-0.35	0.91	1.57
C	9.26	8.48	0.78	8.85	8.39	0.46	2.52	1.17
D	8.98	6.06	2.92	8.80	5.68	3.12	1.79	1.73
E	9.35	10.51	-1.16	9.30	10.71	-1.42	0.82	1.80
F	7.75	6.28	1.47	7.75	5.52	2.23	1.23	2.28
G	7.57	5.48	2.09	7.62	5.31	2.31	0.93	1.44
H	7.77	7.73	0.05	7.61	7.46	0.15	1.54	1.65
I	8.66	6.06	2.60	8.33	5.63	2.71	2.01	1.76
J	9.34	8.27	1.07	9.06	8.79	0.26	2.71	2.87
K	6.22	7.33	-1.11	5.54	6.86	-1.32	2.18	2.27
L	6.99	4.88	2.11	7.26	4.87	2.39	1.20	0.77
M	6.61	7.06	-0.45	6.65	6.84	-0.19	0.70	1.36
N	6.70	5.62	1.08	6.53	5.40	1.13	0.74	1.50
O	7.14	7.04	0.09	6.73	6.74	-0.01	1.82	1.82
P	6.93	6.97	-0.05	6.94	6.90	0.04	0.97	1.39
Q	6.94	6.72	0.21	6.80	6.50	0.30	1.67	1.26
R	7.26	6.91	0.35	7.31	7.01	0.31	0.19	1.09
S	7.67	7.15	0.52	7.28	7.23	0.05	3.27	1.05
		Average:	**0.97**			**0.99**	**1.50**	**1.60**

Table 7: Basin ANNR Model Results

Basin	Avg AMS Exp Rate (µR/hr)	Avg ANNR Exp Rate (µR/hr)	Difference (µR/hr)	Median AMS Exp Rate (µR/hr)	Median ANNR Exp Rate (µR/hr)	Difference (µR/hr)	AMS Std Dev	ANNR Std Dev
A	7.41	6.98	0.43	7.24	6.69	0.54	1.27	1.53
B	7.00	6.95	0.05	6.82	6.87	-0.06	0.91	1.57
C	9.26	8.39	0.87	8.85	8.34	0.52	2.52	1.24
D	8.98	5.94	3.04	8.80	5.60	3.20	1.79	1.63
E	9.35	10.58	-1.24	9.30	10.74	-1.44	0.82	1.79
F	7.75	5.84	1.92	7.75	4.95	2.80	1.23	2.18
G	7.57	5.48	2.10	7.62	5.30	2.31	0.93	1.43
H	7.77	7.98	-0.20	7.61	7.64	-0.03	1.54	1.75
I	8.66	5.77	2.89	8.33	5.45	2.89	2.01	1.53
J	9.34	7.67	1.67	9.06	8.09	0.96	2.71	3.54
K	6.22	6.90	-0.68	5.54	6.22	-0.68	2.18	2.25
L	6.99	4.88	2.11	7.26	4.87	2.39	1.20	0.77
M	6.61	7.08	-0.48	6.65	6.84	-0.19	0.70	1.38
N	6.70	5.62	1.08	6.53	5.40	1.13	0.74	1.50
O	7.14	7.00	0.14	6.73	6.78	-0.05	1.82	1.70
P	6.93	6.98	-0.05	6.94	6.91	0.03	0.97	1.39
Q	6.94	6.70	0.24	6.80	6.50	0.30	1.67	1.21
R	7.26	6.91	0.35	7.31	7.01	0.31	0.19	1.09
S	7.67	7.09	0.58	7.28	7.19	0.09	3.27	1.07
		Average:	**1.06**			**1.05**	**1.50**	**1.61**

Table 8: Basin SAONR Model Results

Basin	Avg AMS Exp Rate (µR/hr)	Avg SAONR Exp Rate (µR/hr)	Difference (µR/hr)	Median AMS Exp Rate (µR/hr)	Median SAONR Exp Rate (µR/hr)	Difference (µR/hr)	AMS Std Dev	SAONR Std Dev
A	7.41	8.62	-1.21	7.24	8.76	-1.52	1.27	1.07
B	7.00	7.82	-0.82	6.82	7.75	-0.93	0.91	1.17
C	9.26	8.36	0.89	8.85	8.34	0.52	2.52	1.37
D	8.98	7.99	0.99	8.80	7.93	0.87	1.79	0.97
E	9.35	8.43	0.92	9.30	8.33	0.97	0.82	0.24
F	7.75	7.25	0.50	7.75	7.29	0.46	1.23	1.36
G	7.57	7.92	-0.35	7.62	7.92	-0.30	0.93	0.65
H	7.77	8.03	-0.26	7.61	7.70	-0.09	1.54	1.79
I	8.66	8.13	0.53	8.33	7.97	0.36	2.01	1.29
J	9.34	10.19	-0.85	9.06	9.33	-0.27	2.71	2.78
K	6.22	8.02	-1.80	5.54	7.68	-2.14	2.18	2.27
L	6.99			7.26			1.20	
M	6.61	6.93	-0.33	6.65	6.67	-0.01	0.70	1.32
N	6.70	6.20	0.50	6.53	6.21	0.32	0.74	0.60
O	7.14	7.13	0.01	6.73	6.88	-0.15	1.82	1.75
P	6.93	6.14	0.78	6.94	5.74	1.20	0.97	1.20
Q	6.94	6.70	0.24	6.80	6.50	0.30	1.67	1.21
R	7.26	7.06	0.20	7.31	7.21	0.11	0.19	0.49
S	7.67	7.22	0.46	7.28	7.39	-0.11	3.27	0.97
	Average:		0.65			0.59	1.50	1.25

Table 9: Basin SAONR Buffer Model Results

Basin	Avg AMS Buffer Exp Rate (µR/hr)	Avg SAONR Buffer Exp Rate (µR/hr)	Difference (µR/hr)	Median AMS Buffer Exp Rate (µR/hr)	Median SAONR Buffer Exp Rate (µR/hr)	Difference (µR/hr)	AMS Buffer Std Dev	SAONR Buffer Std Dev
A	7.22	8.54	-1.31	6.87	8.68	-1.80	1.20	1.10
B	6.95	7.73	-0.77	6.76	7.75	-0.99	0.87	1.15
C	9.23	8.39	0.84	8.86	8.34	0.52	2.37	1.25
D	8.74	8.05	0.70	8.47	8.01	0.46	1.86	1.02
E	9.14			9.04			0.61	
F	7.64	8.29	-0.65	7.67	8.29	-0.62	0.88	
G	7.46			7.50			0.76	
H	7.50	7.90	-0.40	7.33	7.60	-0.27	1.39	1.80
I	8.49	8.00	0.49	8.10	7.58	0.52	1.95	1.35
J	9.09	10.60	-1.50	8.82	9.29	-0.48	2.39	3.38
K	5.62	6.76	-1.14	5.19	6.59	-1.39	1.58	1.25
L	6.94			7.28			1.04	
M	6.62	6.88	-0.26	6.68	6.60	0.07	0.68	1.30
N	6.66	6.23	0.43	6.51	6.22	0.29	0.68	0.59
O	7.05	6.84	0.21	6.70	6.88	-0.18	1.62	0.81
P	6.84	6.25	0.59	6.92	5.69	1.22	0.84	1.34
Q	6.69	6.71	-0.02	6.64	6.58	0.06	1.39	1.21
R								
S	7.57	7.16	0.41	7.27	7.39	-0.12	3.23	1.03
	Average:		**0.65**			**0.60**	**1.41**	**1.33**

Table 10: TRcp Remote Sensing Models

Unit	Avg AMS Exp Rate (µR/hr)	Avg NURE Exp Rate (µR/hr)	Difference (µR/hr)	Median AMS Exp Rate (µR/hr)	Median NURE Exp Rate (µR/hr)	Difference (µR/hr)	AMS Std Dev	NURE Std Dev
TRcp	9.64	8.53	1.12	9.29	8.75	0.54	2.45	1.49
2-6-10								
TRcp2A	10.26	8.73	1.53	9.84	8.73	1.11	2.46	0.83
TRcp3A	9.28						0.19	
TRcp4A	9.91	8.74	1.18	9.52	8.97	0.55	2.43	1.47
TRcp5A	7.82	7.78	0.04	7.46	7.86	-0.40	1.72	1.35
2/1		Average:	**0.92**			**0.52**	**1.70**	**1.22**
TRcp1B	10.00	8.76	1.23	9.76	8.97	0.79	1.75	1.32
TRcp2B	9.95	8.76	1.18	9.31	8.97	0.34	2.71	1.20
TRcp3B	9.45	8.66	0.79	9.05	8.92	0.13	2.63	1.54
TRcp4B	8.57	7.95	0.62	8.31	7.89	0.42	2.22	1.44
TRcp5B	7.87	7.83	0.04	7.31	7.94	-0.63	1.55	1.52
7-3-1		Average:	**0.77**			**0.46**	**2.17**	**1.40**
TRcp1C	10.41			9.74			2.67	
TRcp2C	10.32	8.53	1.78	9.98	8.66	1.32	2.26	1.63
TRcp3C	10	8.65	1.36	9.72	8.83	0.89	2.49	1.51
TRcp4C	9.83	8.58	1.25	9.39	8.92	0.47	2.48	1.62
TRcp5C	8.8	8.47	0.33	8.58	8.67	-0.09	2.23	1.35
4/5		Average:	**1.18**			**0.69**	**2.43**	**1.53**
TRcp1D	9.55	8.67	0.89	9.21	8.94	0.26	2.42	1.44
TRcp2D	9.36	8.36	1.00	9.04	8.55	0.49	2.32	1.40
TRcp3D	9.64	8.55	1.09	9.27	8.93	0.34	2.41	1.47
TRcp4D	9.50	8.23	1.27	9.21	8.43	0.78	2.29	1.35
TRcp5D	10.15	8.84	1.31	9.92	9.07	0.85	2.74	1.45
		Average:	**1.11**			**0.55**	**2.44**	**1.42**

Table 11: TRcs Remote Sensing Models

Unit	Avg AMS Exp Rate (µR/hr)	Avg NURE Exp Rate (µR/hr)	Difference (µR/hr)	Median AMS Exp Rate (µR/hr)	Median NURE Exp Rate (µR/hr)	Difference (µR/hr)	AMS Std Dev	NURE Std Dev
TRcs	9.44	8.77	0.67	9.35	8.67	0.54	2.09	1.6
2-6-10								
TRcs2A	9.54	8.73	0.83	9.55	8.46	1.09	2.46	0.83
TRcs3A	9.16		0.96	8.89	8.20	0.69	0.19	
TRcs4A	9.39	8.74	0.58	9.33	8.78	0.55	2.43	1.47
TRcs5A	8.40	7.78	1.08	8.37	7.45	0.92	1.72	1.35
2/1		**Average:**	**0.86**			**0.81**	**1.70**	**1.22**
TRcs1B	9.57	8.88	0.69	9.36	8.65	0.71	2.22	0.99
TRcs2B	10.05	8.94	1.10	9.70	8.84	0.86	2.88	1.46
TRcs3B	9.67	9.39	0.29	9.56	9.30	0.26	2.02	1.51
TRcs4B	9.19	8.56	0.64	9.24	8.44	0.80	1.73	1.53
TRcs5B	8.81	7.79	1.02	8.90	8.00	0.90	1.70	1.49
7-3-1		**Average:**	**0.75**			**0.71**	**2.11**	**1.40**
TRcs1C	9.4	8.46	0.93	9.43	8.35	1.08	1.44	1.35
TRcs2C	9.33	8.84	0.48	9.38	8.83	0.55	1.63	1.47
TRcs3C	9.22	8.57	0.65	9.24	8.58	0.66	1.88	1.42
TRcs4C	9.88	9.1	0.79	9.52	8.88	0.64	2.93	2.01
TRcs5C	9.6	9.01	0.59	9.12	8.49	0.63	3.68	1.85
4/5		**Average:**	**0.69**			**0.69**	**2.31**	**1.62**
TRcs1D	9.39	8.91	0.48	9.34	9.03	0.31	2.26	1.26
TRcs2D	9.09	8.21	0.88	9.06	8.17	0.90	1.91	1.26
TRcs3D	9.42	8.66	0.76	9.36	8.57	0.80	2.03	1.42
TRcs4D	9.17	8.25	0.92	9.14	8.08	1.06	2.33	1.92
TRcs5D	9.72	9.18	0.54	9.59	9.06	0.53	1.90	1.68
		Average:	**0.71**			**0.72**	**2.09**	**1.51**

Chapter 7: Figures

Figure 1: Relationship Between Geology and Radiation
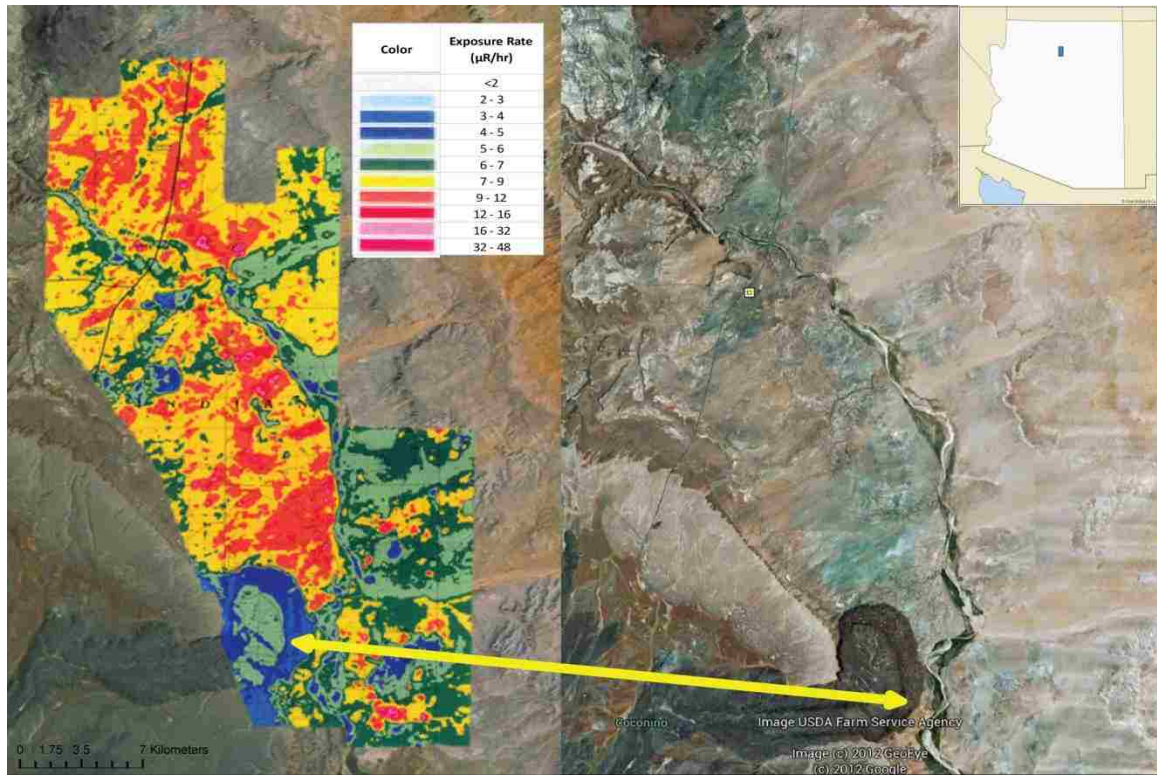
Figure 1: Aerial gamma ray survey of the study area done by AMS (left), satellite image (right, from USDA Farm Service). The yellow arrow points to an oval blue ring on the aerial gamma ray survey, that corresponds to a basalt flow on the satellite image.

Figure 2: Geochemical Data
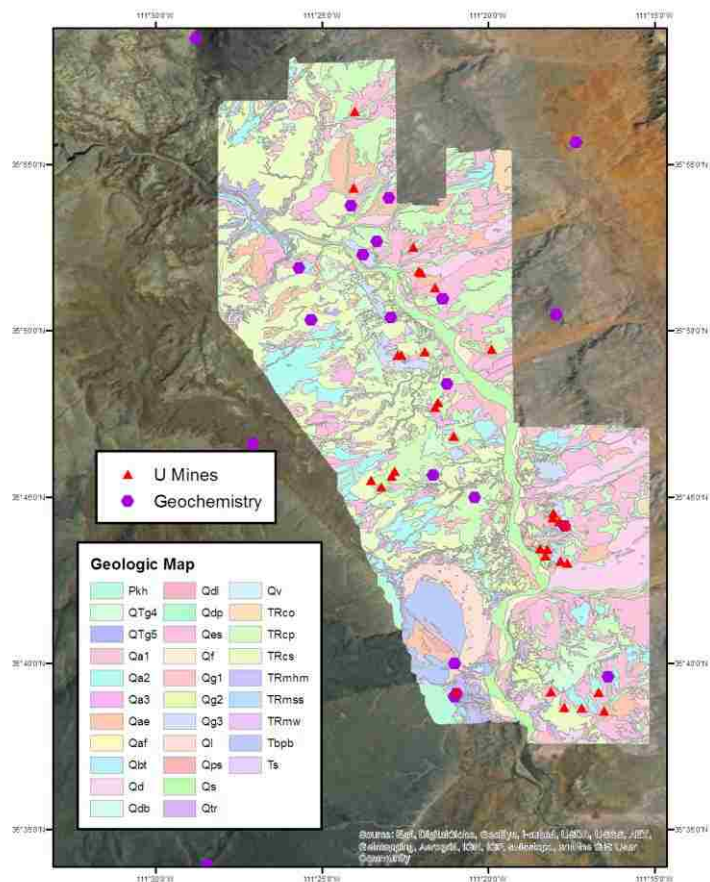
Figure 2: Distribution of geochemical data points and location of uranium mines is indicated with symbols. Geologic reference map of the study area.

Figure 3: NURE Data Distribution
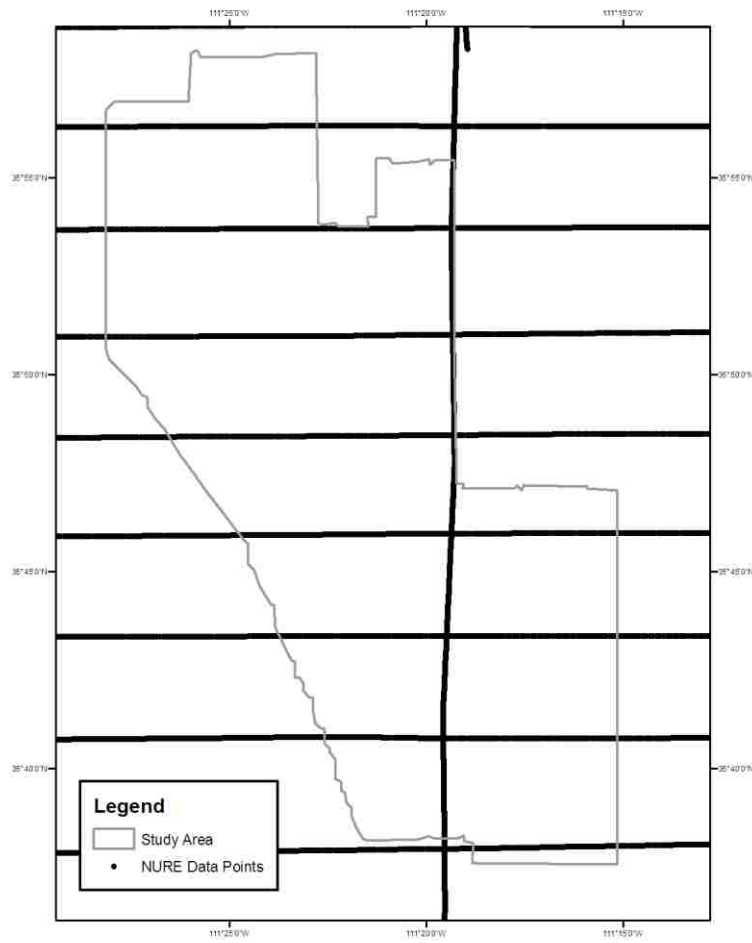
Figure 3: Grey outline indicates modeling area. NURE aerial survey data points occur every 100 to 200 ft along the line, so individual data points are not visible.

Figure 4: Drainage Basins
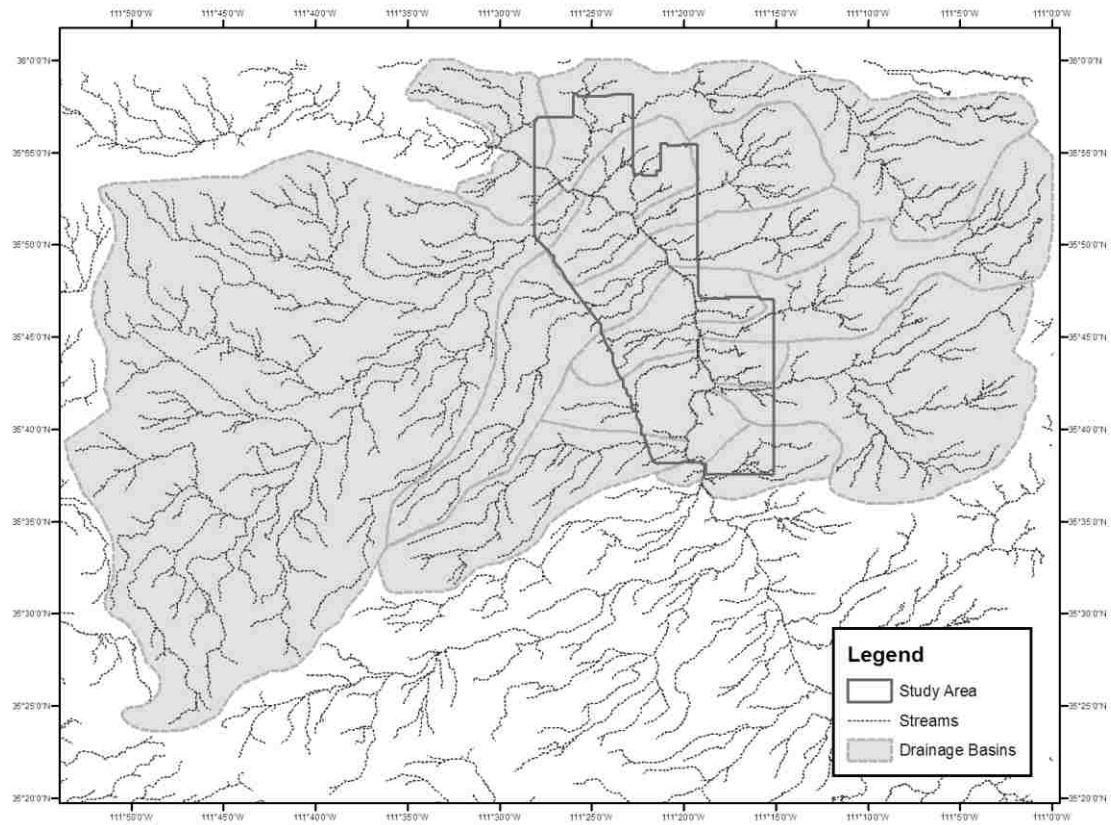
Figure 4: Map of the Little Colorado River and its tributaries. Drainage basins that overlap the study area are shown in grey.

Figure 5: Alluvial Units Sorted by Drainage Basin
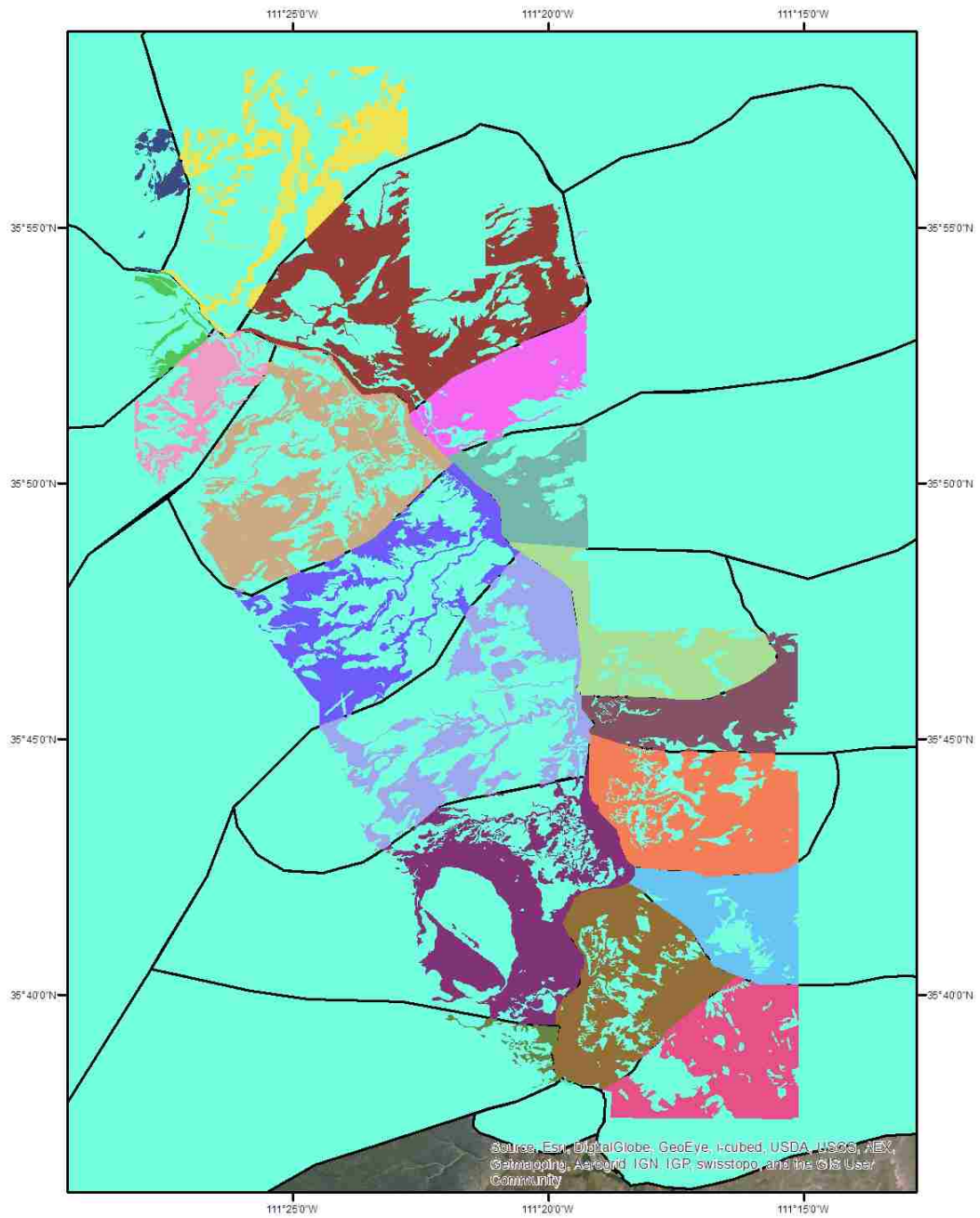
Figure 5: Map of the 19 alluvial units created by joining the alluvial units in each basin.

Figure 6: NURE Correction Constant
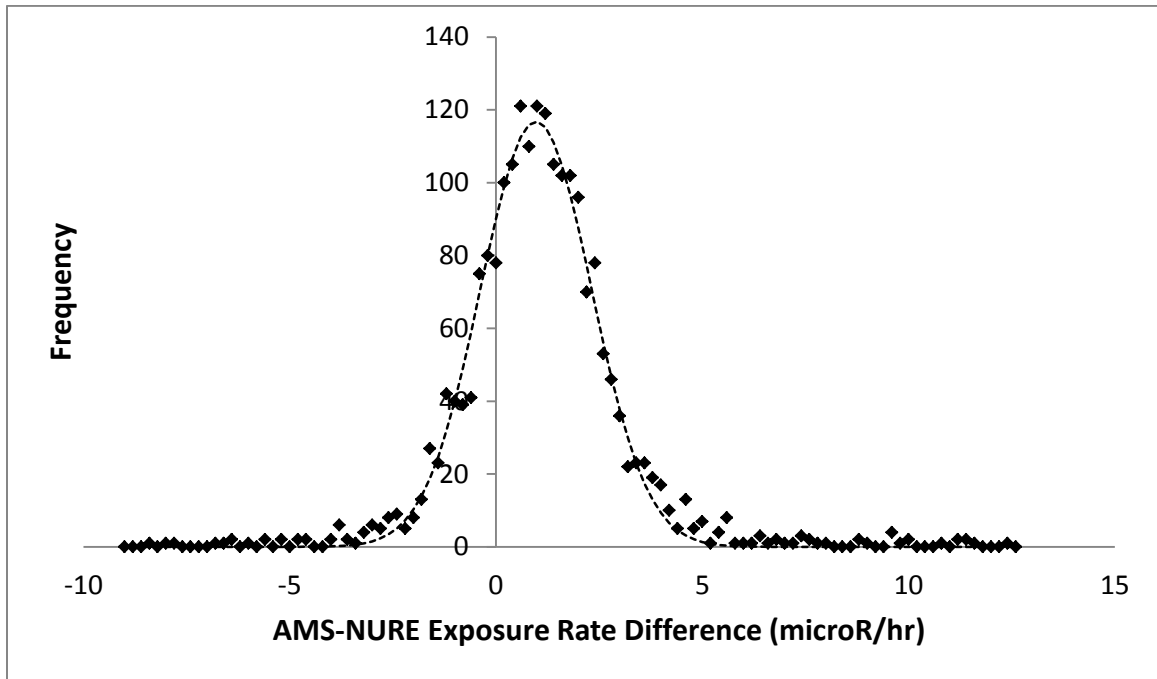
Figure 6: Histogram displaying point to point comparison of AMS and NURE data.

Figure 7: AMS Exposure Rate Distribution
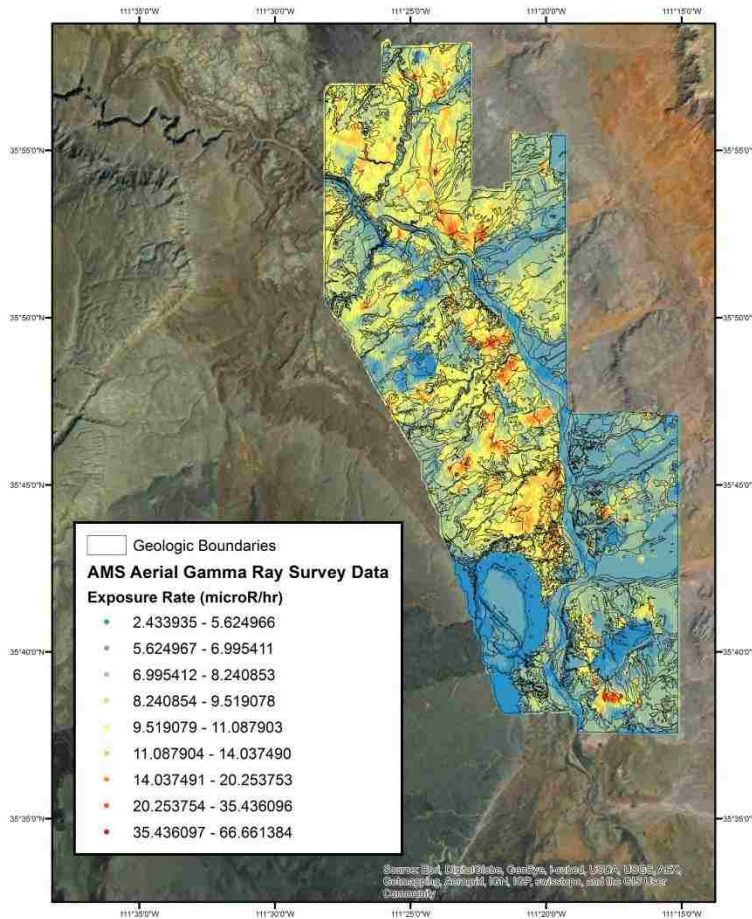
Figure 7: The distribution of exposure rate over the study area. Geologic boundaries are displayed for context.

Figure 8: 2-6-10 Visualization
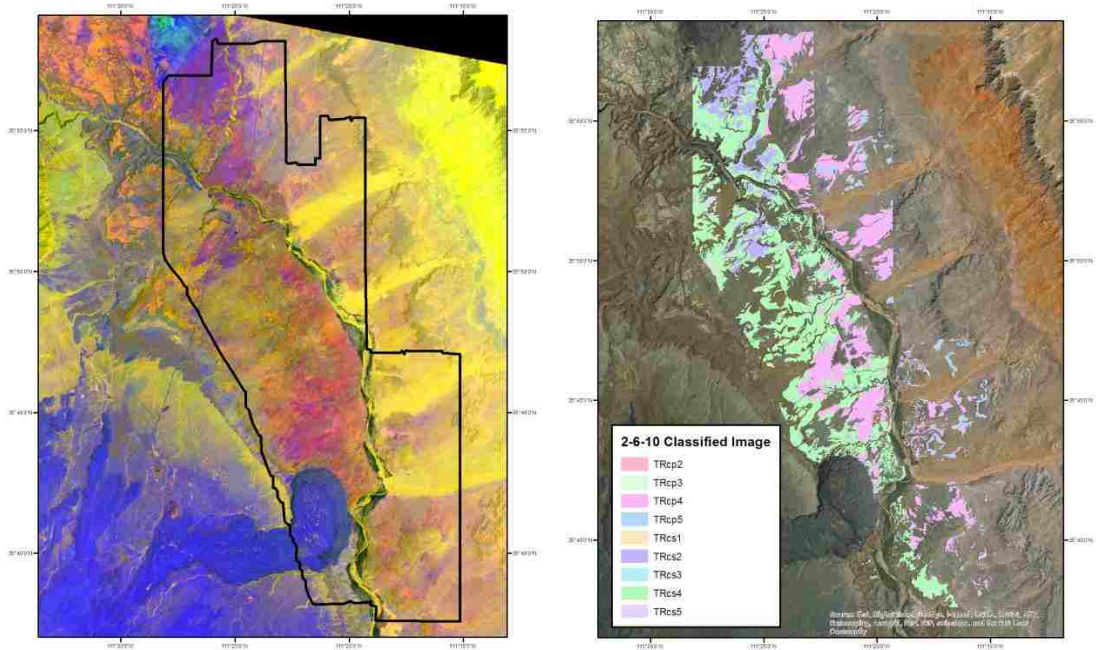
Figure 8: 2-6-10 ASTER visualization (left), classification of TRcs and TRcp based on 2-6-10 (right).

Figure 9: 2-6-10 Visualization Geology Comparison
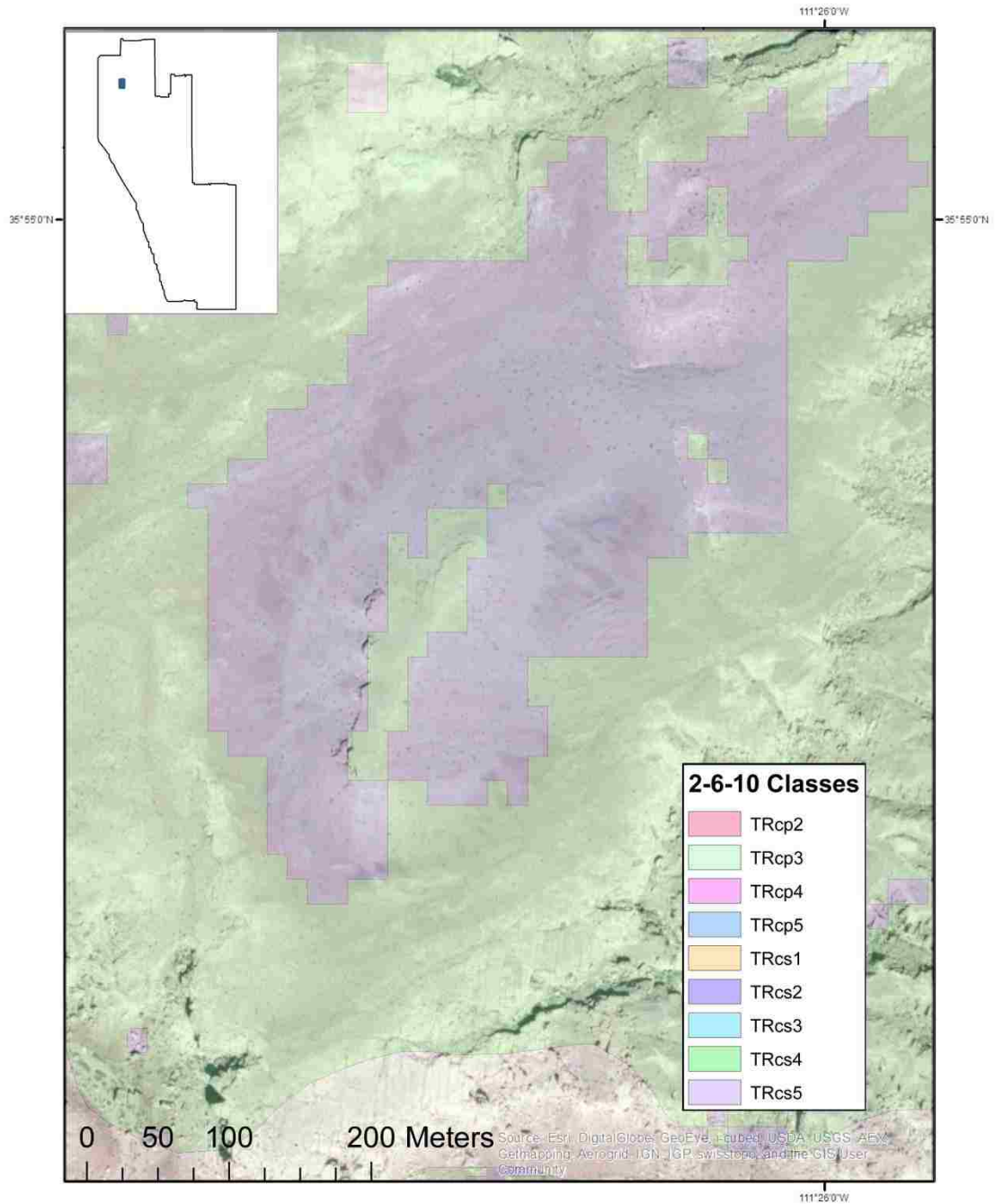
Figure 9: Close up of 2-6-10 classes in relationship to geologic formations on satellite image.

Figure 10: NURE Buffer Model Results
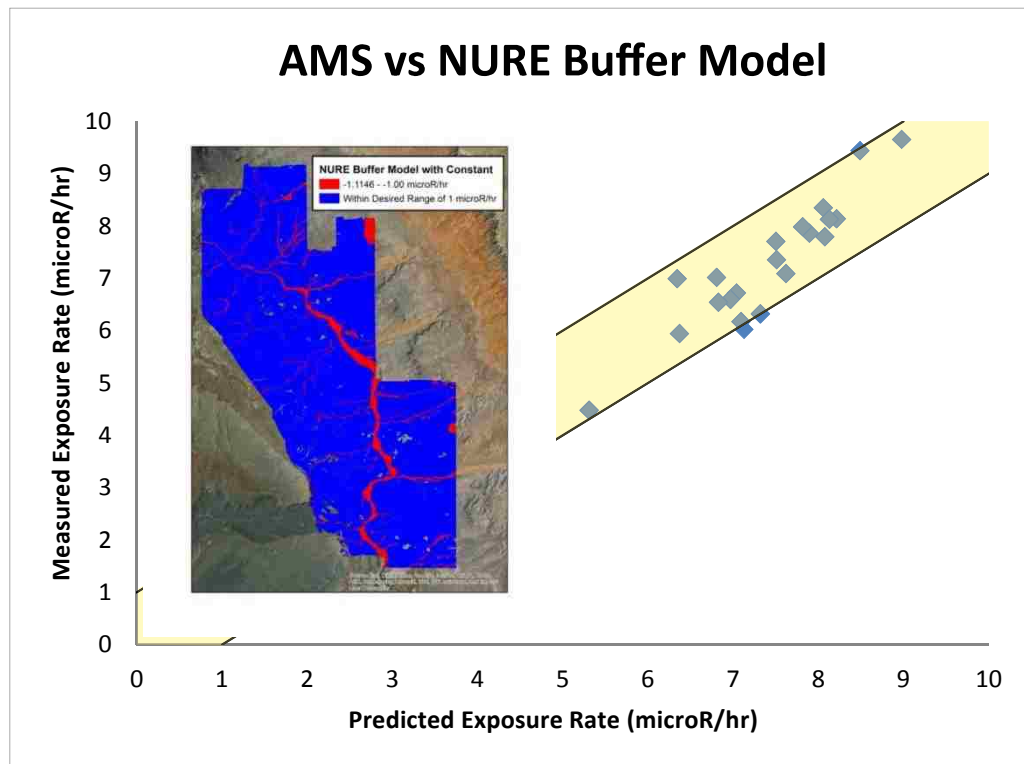
Figure 10: Predicted exposure rate by the NURE Buffer model, versus the measured AMS exposure rate for each unit. The shaded yellow area is our desired range of exposure rates. The inset maps shows the geologic units within this desired range in blue, and those outside the range in red.

Appendix: Unit Reports

Parent Units

Qbt: Brunhes (Pleistocene) age basalt flow, USGS classifies as clinopyroxene-olivine and alkali-olivine basalt with a groundmass rich in glassy plagioclase (Billingsley et al., 2007). We have 2 data points in this unit from the USGS and NAVDAT, both only list Potassium weight percent. NAVDAT reports rock type as basalt which is consistent with the unit, so no data points will be eliminated.

Qbt Field Notes: We were not able to reach this small unit as it was fenced in.

	K (wt %)	U (ppm)	Th (ppm)
mean	1.5814	N/A	N/A
Standard deviation	0.4755	N/A	N/A
range	0.6724	N/A	N/A
median	1.5814	N/A	N/A
mode	N/A	N/A	N/A

Qbt NURE Histogram:

Qbt AMS Histogram:

Qbt AMS Data

Frequency (y-axis: 0, 5, 10, 15, 20, 25, 30, 35, 40, 45, 50)

Exposure Rate (microR/hr) (x-axis: 0, 0.6, 1.2, 1.8, 2.4, 3, 3.6, 4.2, 4.8, 5.4, 6, 6.6, 7.2, 7.8, 8.4, 9, 9.6, 10.2)
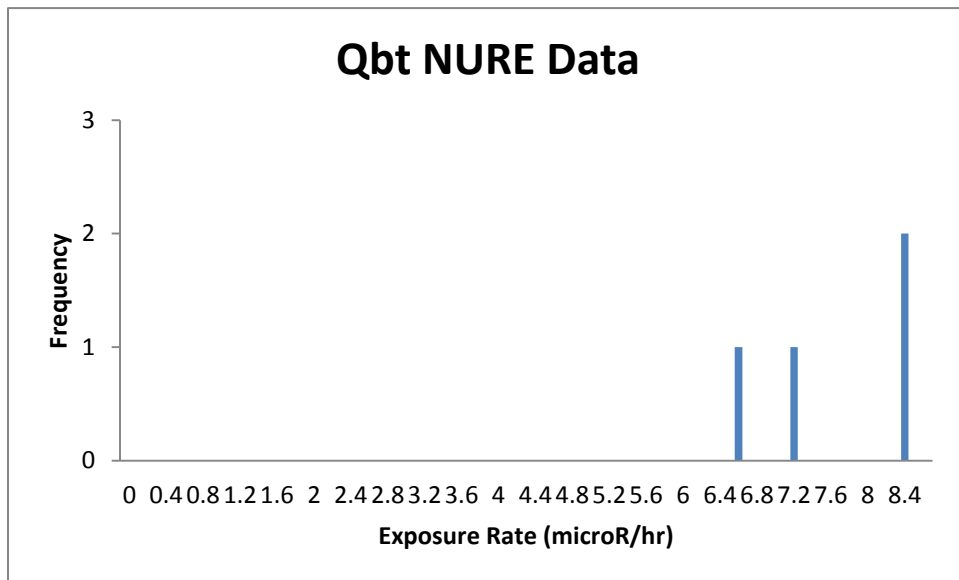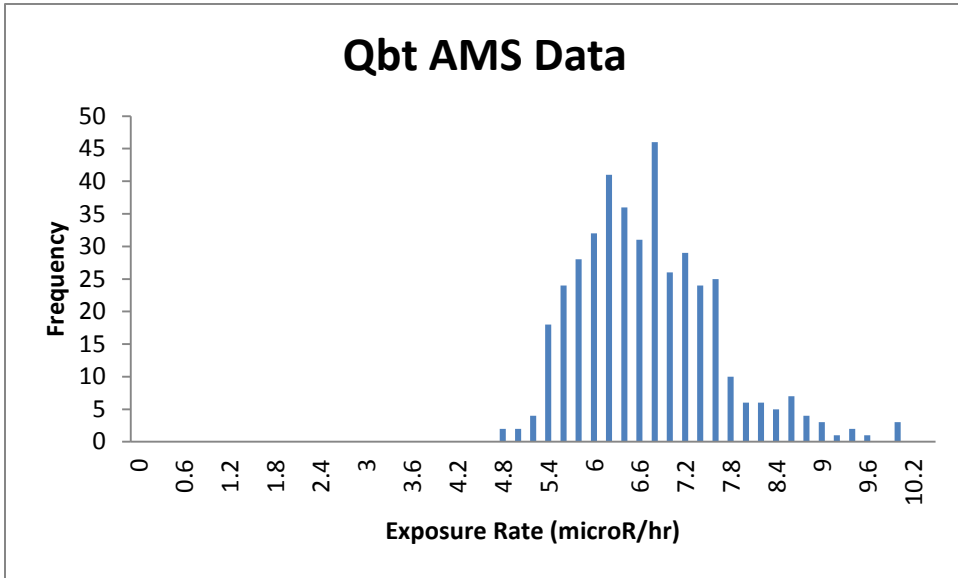
There are only 4 NURE Qbt survey points, so a full comparison cannot be made, but both occur over the same range of values and have means within error. The AMS data is right skewed.

Qbt 50 m Buffer NURE Histogram:

Qbt NURE Buffer Data

Frequency (y-axis: 0, 1)

Exposure Rate (microR/hr) (x-axis: 0, 0.4, 0.8, 1.2, 1.6, 2, 2.4, 2.8, 3.2, 3.6, 4, 4.4, 4.8, 5.2, 5.6, 6, 6.4, 6.8, 7.2, 7.6, 8, 8.4)
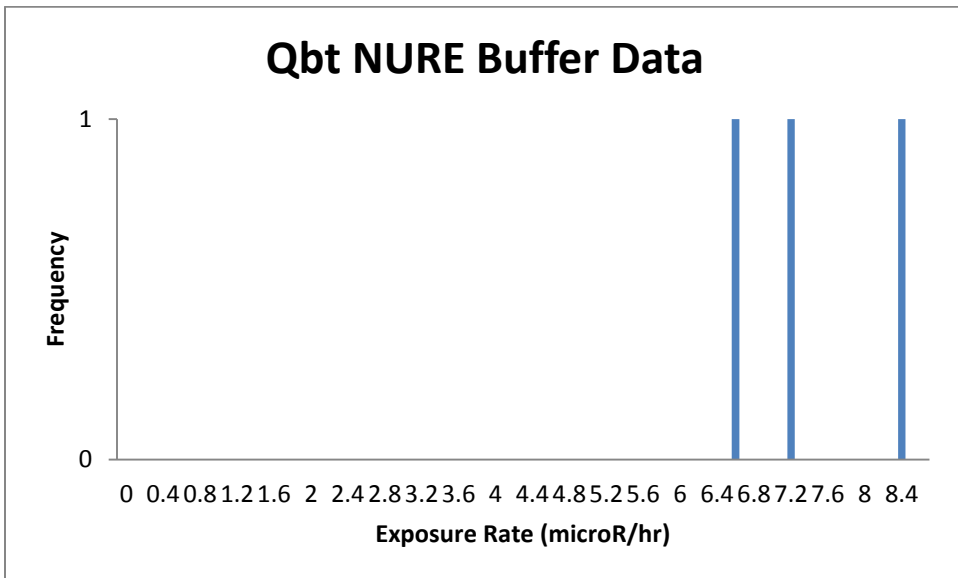
Qbt 50 m Buffer AMS Histogram:

Qbt AMS Buffer Data
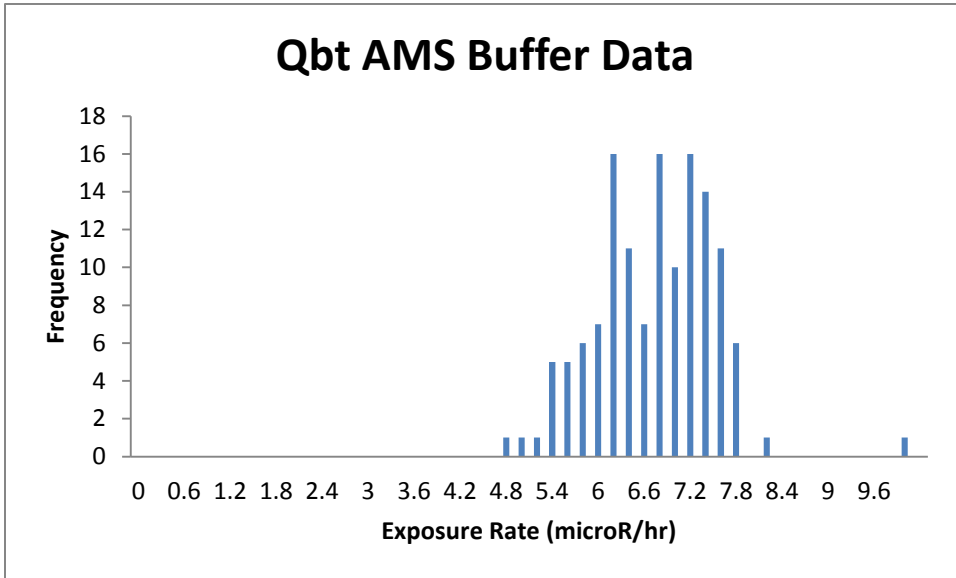
Qbt AMS Distribution: This unit occurs in the northern part of the area, and has a no apparent overall trends, and the exposure rate ranges from 4.625 to 9.811 microR/hr. The unit does not appear like a basalt flow from the aerial imagery.

Qbt AMS Exposure Rate Data
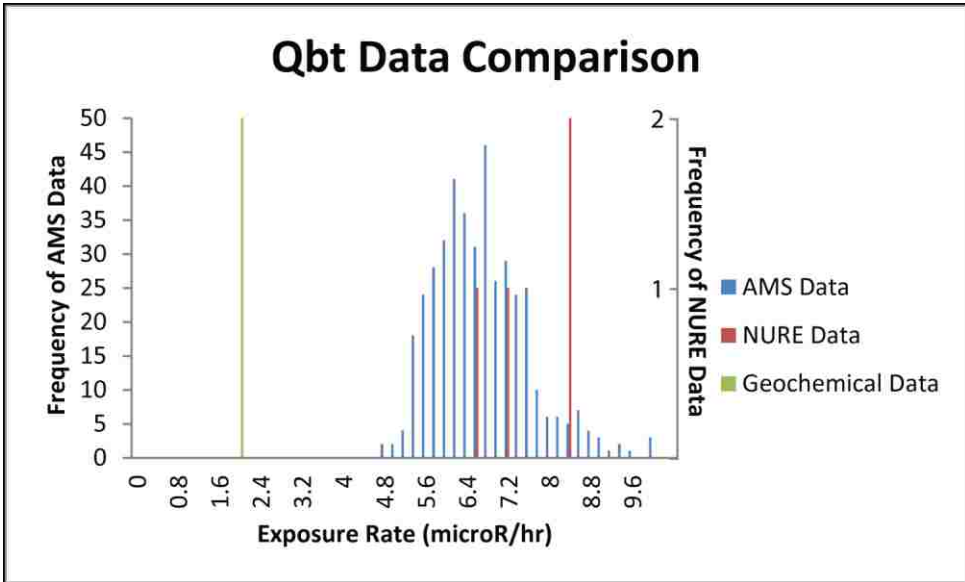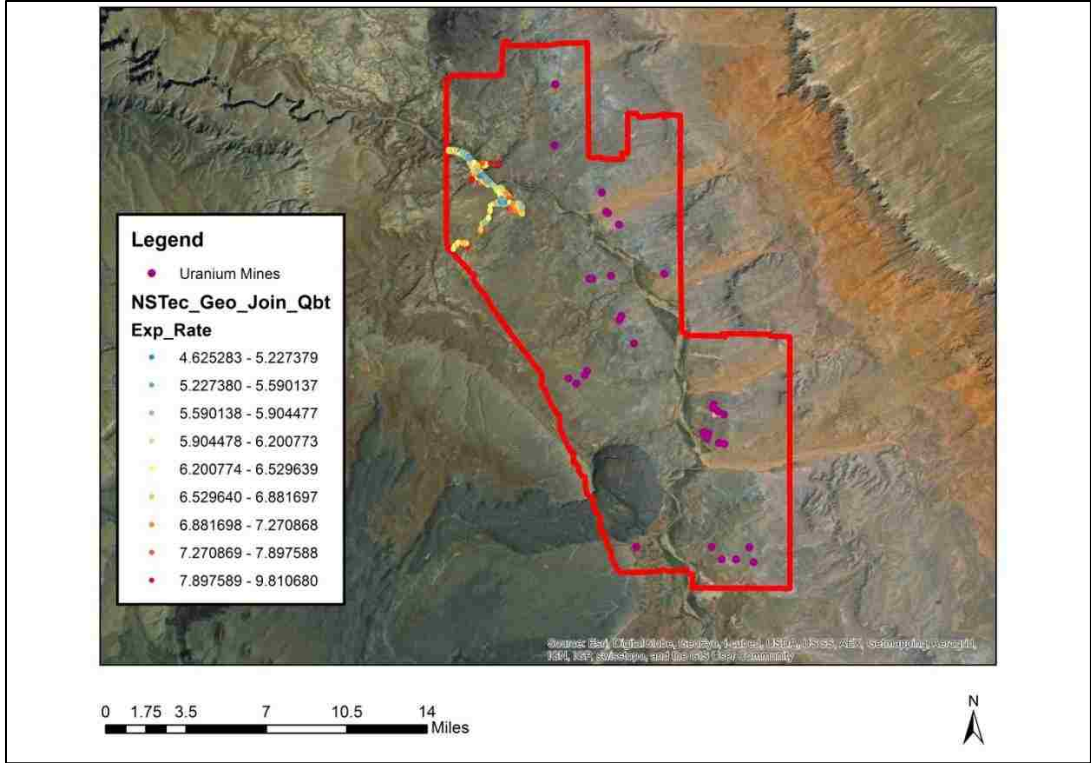
Tbpb: This unit is identified by the USGS as a Pleistocene (K-Ar age: 2.43±0.32Ma) basalt flow know as Black Point. It is a plagioclase-aphyric basalt with large amounts of plagioclase and olivine phenocrysts in a feldspathic groundmass (Billingsley et al., 2007). There are 4 data points in this unit from NAVDAT and the USGS, all are identified as basalt, consistent with Tbpb, so no data points will be removed. Only one data point provides U and Th concentration: 0.78 ppm U and 2.74 ppm Th. George Ulrich is identified as working on this basalt flow and also dating the flow, he worked extensively in this area and wrote several field guides. This leads me to think there may be many more data points on this basalt flow that are not currently known to us. I have been unsuccessful in contacting him, as he has been retired for some time.

Tbpb Field Notes: Basalt clasts are overall smaller, dominated by medium to coarse sand, and 2 mm+ clasts, largest is fist sized. Less aeolian material here. Unclear why this is categorized as the basalt flow itself, no bedrock present as far as we can tell over the whole basalt flow.
Similar to Qes cool but some additional eolian material.

This is not consistent with the USGS description which states the basalt flow 'weathers smooth'. The basalt flow was so covered in alluvium we never actually saw its surface. We were confused as to why this unit was called Tbpb instead of another alluvium unit. Soil was developed with moderate vegetation, not consistent with the reported smooth basalt flow.

	K (wt %)	U (ppm)	Th (ppm)
mean	0.91	N/A	N/A
Standard deviation	0.0249	N/A	N/A
range	0.0498	N/A	N/A
median	0.91	N/A	N/A
mode	N/A	N/A	N/A
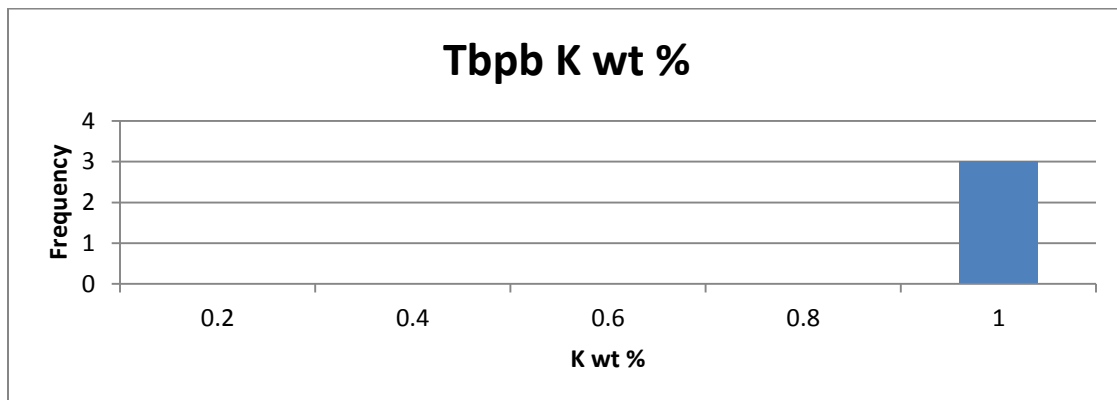
Tbpb NURE Histogram:
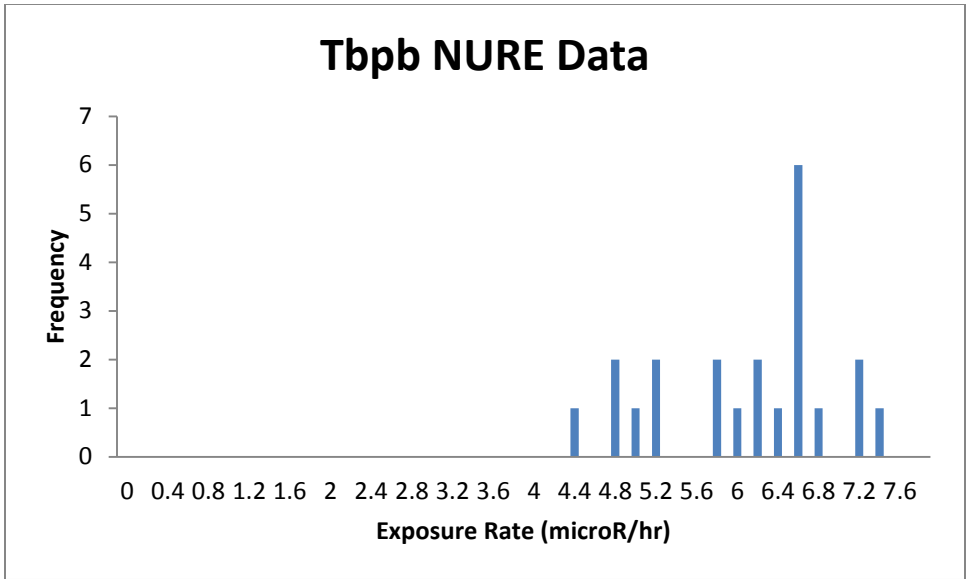
Tbpb AMS Histogram:
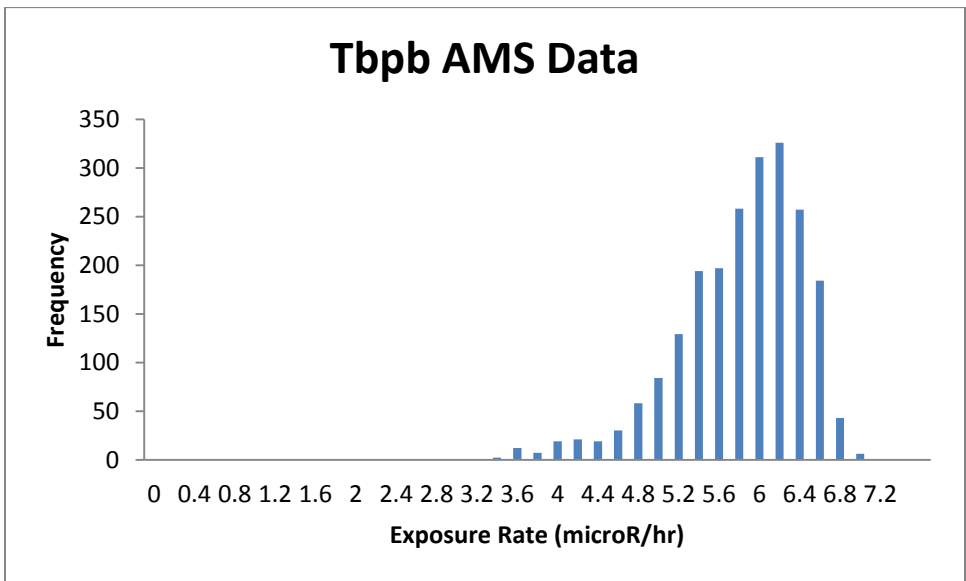
This unit lacks enough NURE data to make a full curve, and the difference between AMS and NURE data is over error, with AMS being higher. The AMS data is also left skewed, which would only go towards helping the means be closer together.

Tbpb 50 m buffer NURE Distribution:

Tbpb NURE Buffer Data
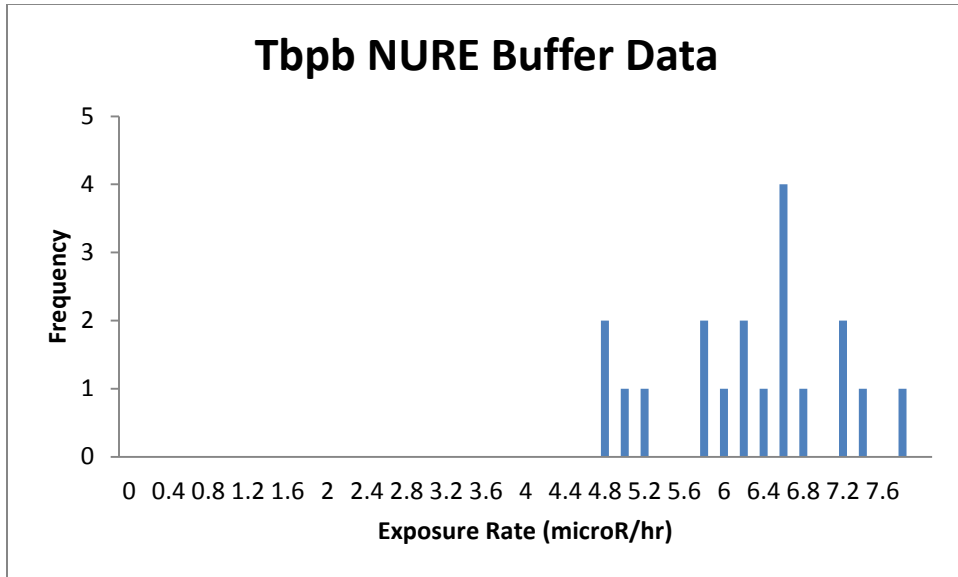
Tbpb 50 m buffer AMS Distribution:

Tbpb AMS Buffer Data
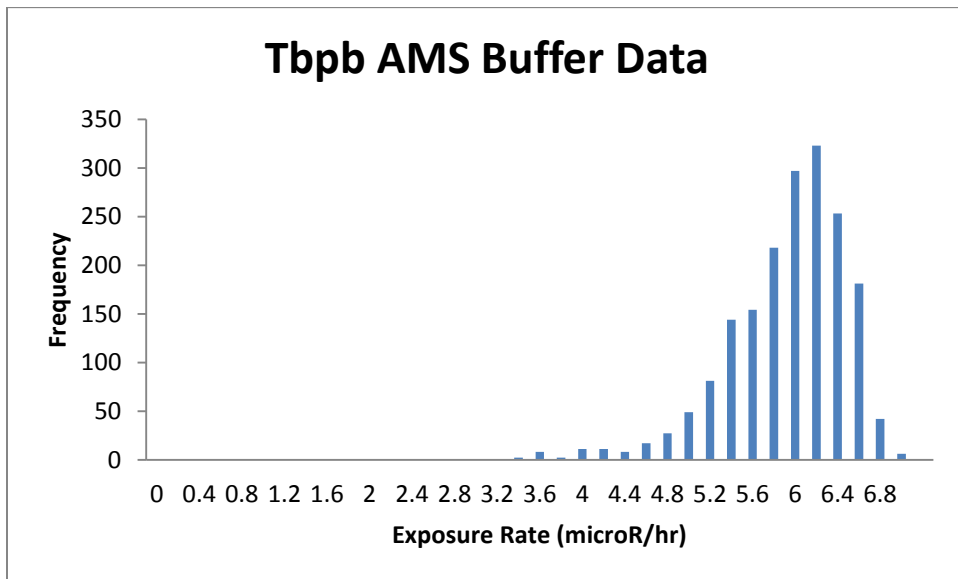
Tbpb AMS Distribution: This unit is the black point basalt flow. It tends to be cool on the rim and hot on the inside, but the range of exposure rates is small, from 3.476 to 6.885 microR/hr.

Tbpb AMS Exposure Rate Data
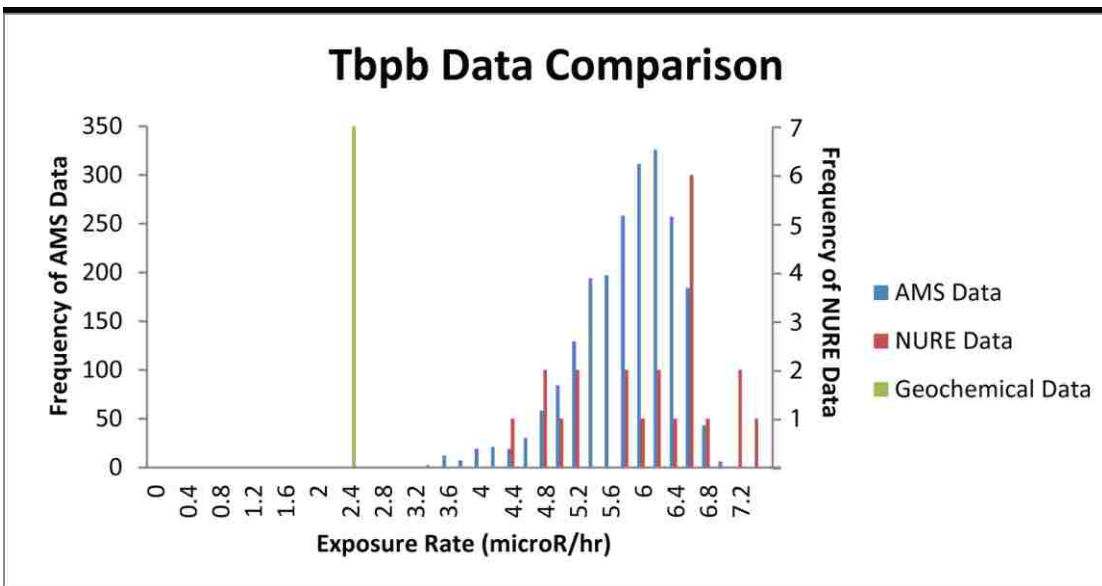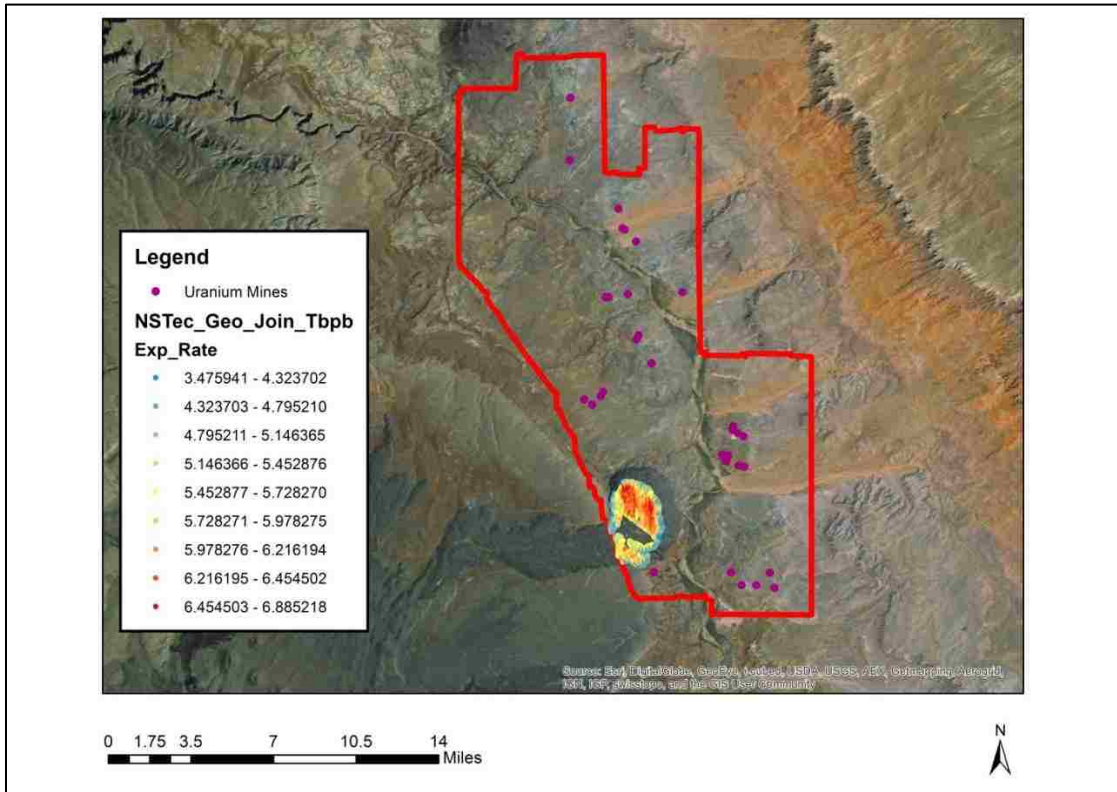
TRco: Owl Rock Member of the Chinle Formation, contains cherty limestone, siltstone and sandstone (Billingsley et al., 2007). There was a single point added to this unit because of a collector's classification. It was identified as a limestone, with 1.6 wt % K, 2.94 ppm U, and 4.9 ppm Th.

TRco Field Notes: Red limestone with grey alteration spots. Some are more green than grey in alteration. Little bit of chert, not much, more in very thin layers than in nodules. Grey sometimes looks like separate beds. Limestone is blueish in places.
Reddish limestone with blue/grey alteration. Not much chert. Bedrock is massive

It's important to note that we observed this unit north of the field area where it was accessible, but still within the quad the USGS described. Field description of a cherty limestone is consistent with USGS description. However, the USGS lists the color as white to purple, while we noticed some green and blue staining, the limestone was in majority red.

TRco NURE Histogram:
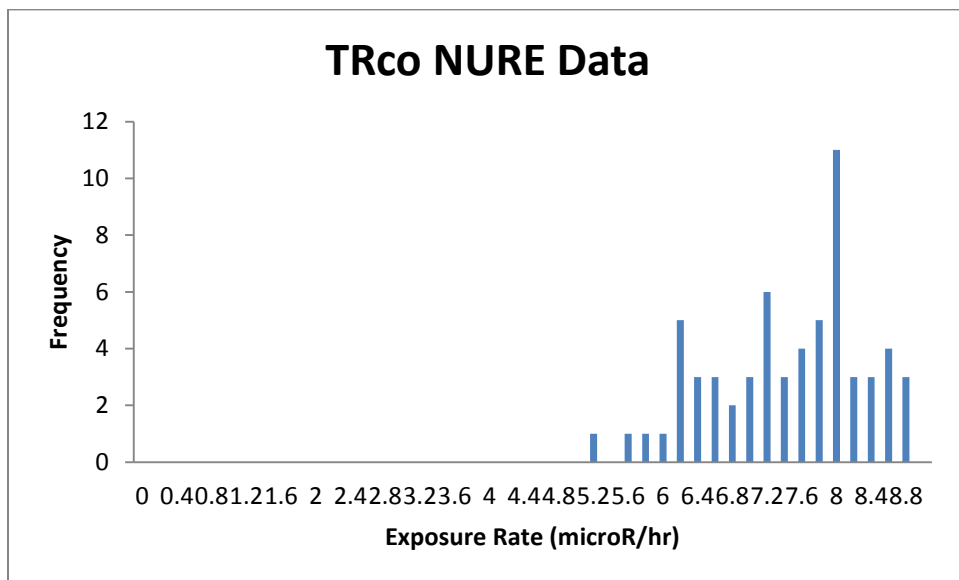
TRco AMS Histogram:
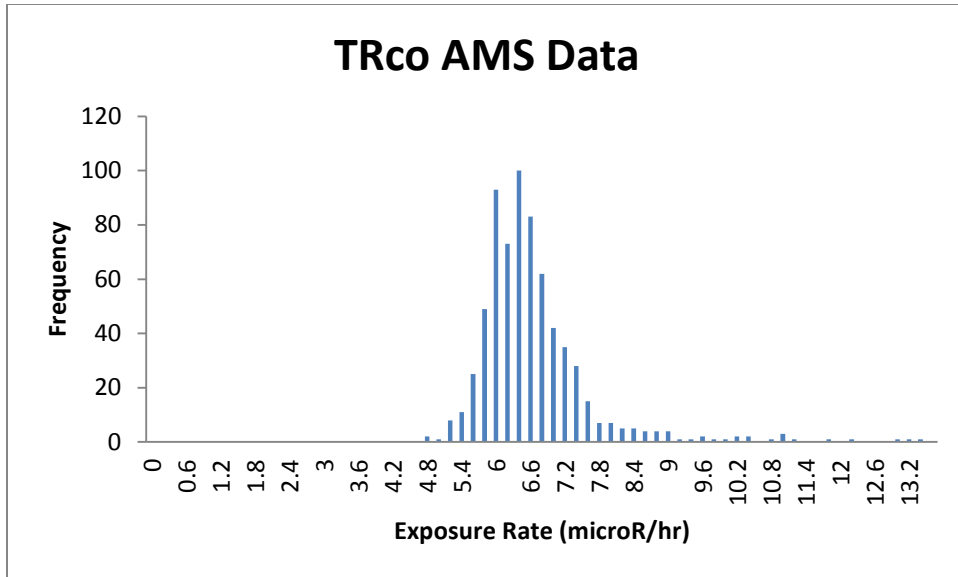
TRco 50 m buffer NURE Histogram:
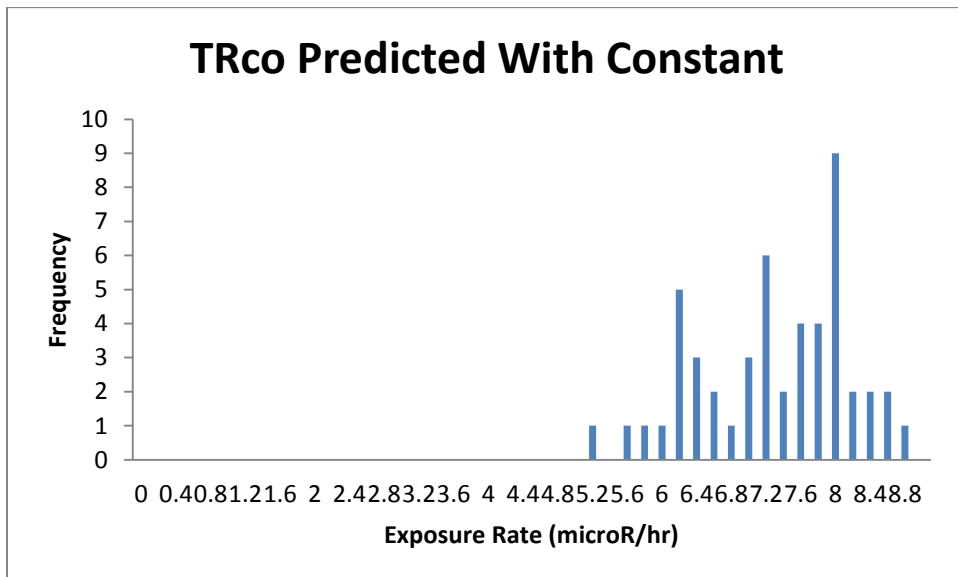
TRco 50 m buffer AMS Histogram:
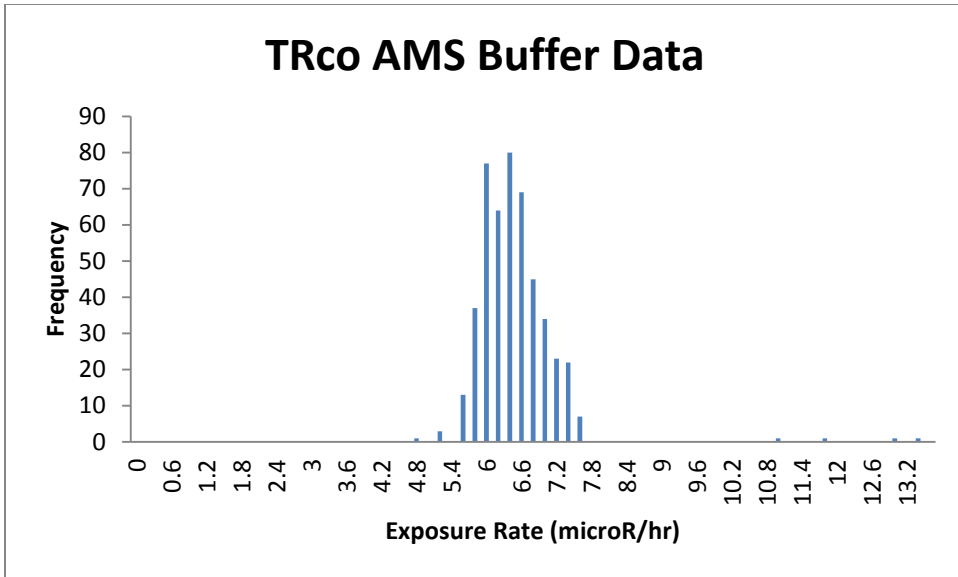
TRco AMS Distribution: We can see very little of this unit as a whole so we do not get any sense of overall trends we may see in this unit. The exposure rate range of this unit is from 4.677 to 13.241.

TRco AMS Exposure Rate Data

TRco Data Comparison
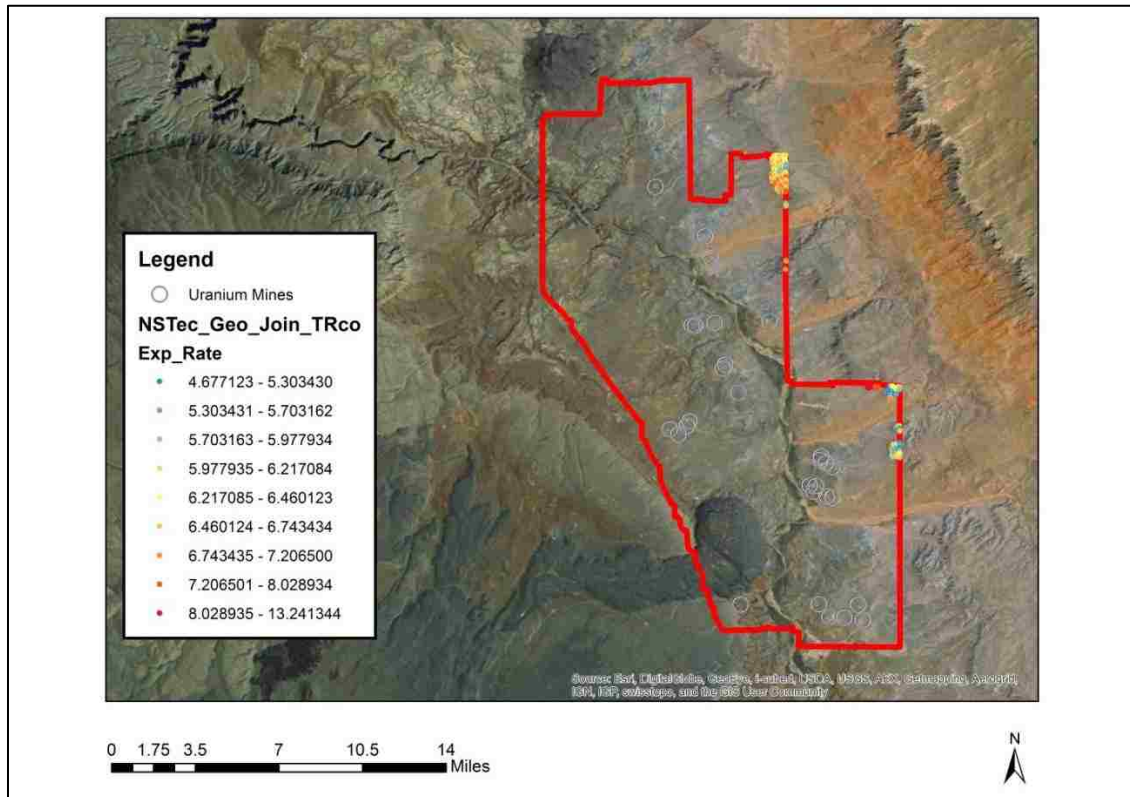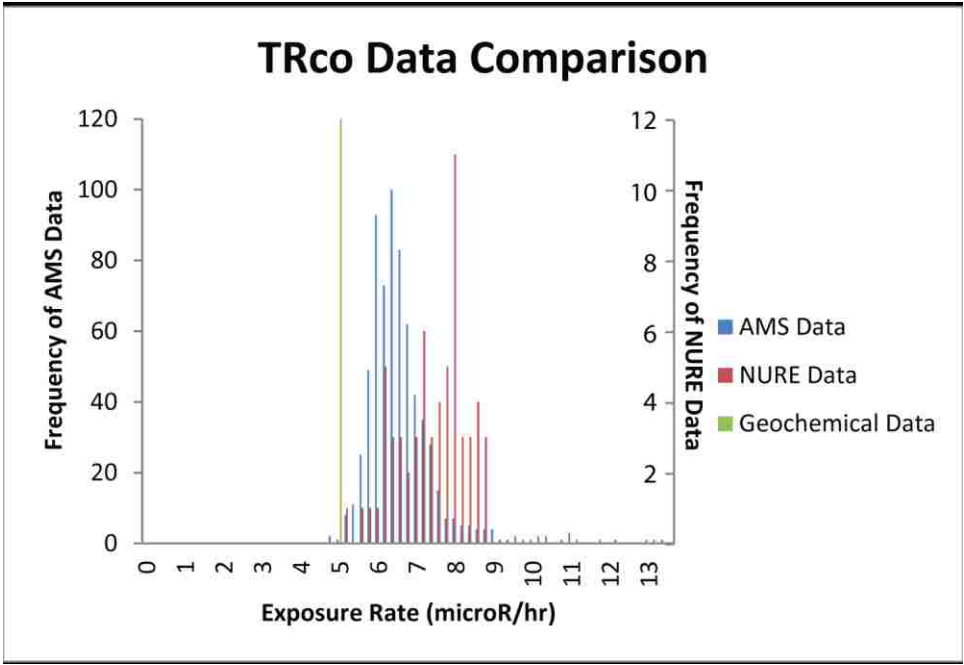
TRcp: The USGS identifies this unit as the Petrified Forest Member of the Chinle Formation, consisting of mudstone, siltstone, and sandstone (Billingsley et al., 2007). One of the rock samples was identified by the collector as being part of the Owl Rock Member of the Chinle Formation, TRco. This sample was also limestone, which is not consistent with TRcp. This point was moved to TRco. There are 11 data points in this unit. Identified rock types are shale, mudstone and conglomerate.

TRcp average Field Notes: This area is more grey than blue, though some areas have blue staining, though more areas have a reddish/purple staining. Surface is broken up mudcracks of grey clay, partially cemented, homogenous. Float is large, mostly fist sized, rounded to subangular, chert and basalt. Blue grey mud cracks. Fine grey dust. Some about 5 cm clasts, mostly chert. Some grey sandstone outcrops. Massive no beds. Fine grained. No vegetation.

TRcp hot Field Notes: Lots of exposed bedrock in this area, could explain why this area is hotter. Grey mud cracked soil with chert and basalt on top. Grey is red stained in areas, no blue. Not laterally continuous, small exposed area, ground is very hard, no exposed bedrock. Sparse vegetation. Grey mudcracked surface partially covered by gravels less than 2 cm. Gravel mostly cherts, some outcrops at grey sandstone. But not much. Sparse to moderate grasses, some shrubs.

TRcp average Field Notes: The road was washed out and we were unable to reach TRcp average.

These field observations are consistent with the USGS description as a greyish blue mudstone or siltstone with significant amounts of clays. This is also the unit where we observed petrified logs in the southwest of the field area, this makes sense as it is the Petrified Forest Member and presence of these fossils is noted in the USGS description. Based on the threatening signage present and the local gift shop, we think most of the petrified wood has been pillaged from this unit.

	K (wt %)	U (ppm)	Th (ppm)
mean	1.2112	16.6714	14.9043
Standard deviation	0.4980	33.4485	5.3215
range	2.1170	89.63	13.69
median	1.2	4.8	13.7
mode	1.2	N/A	N/A

TRcp K wt %

TRcp U ppm
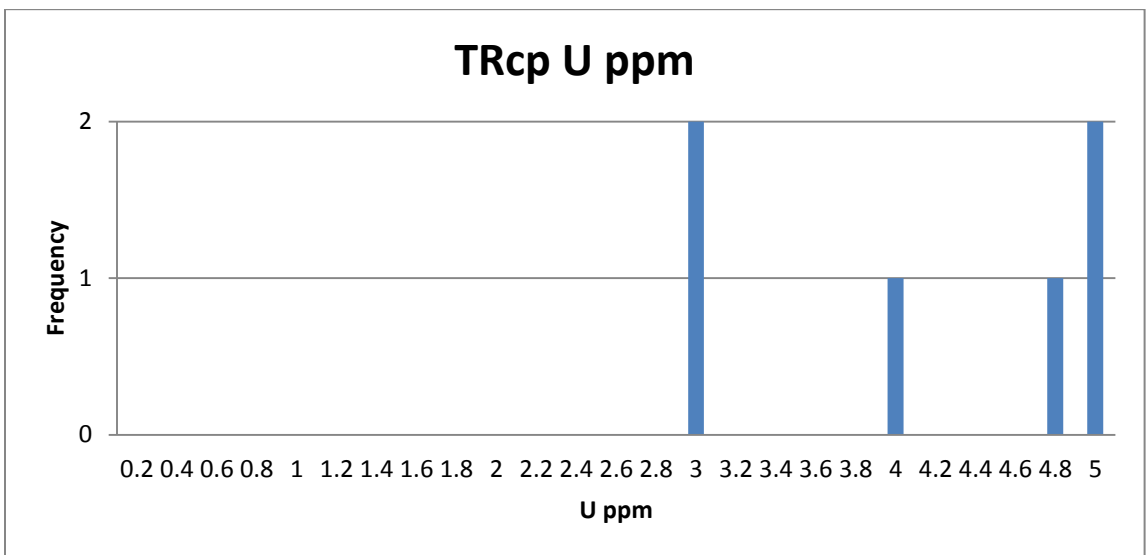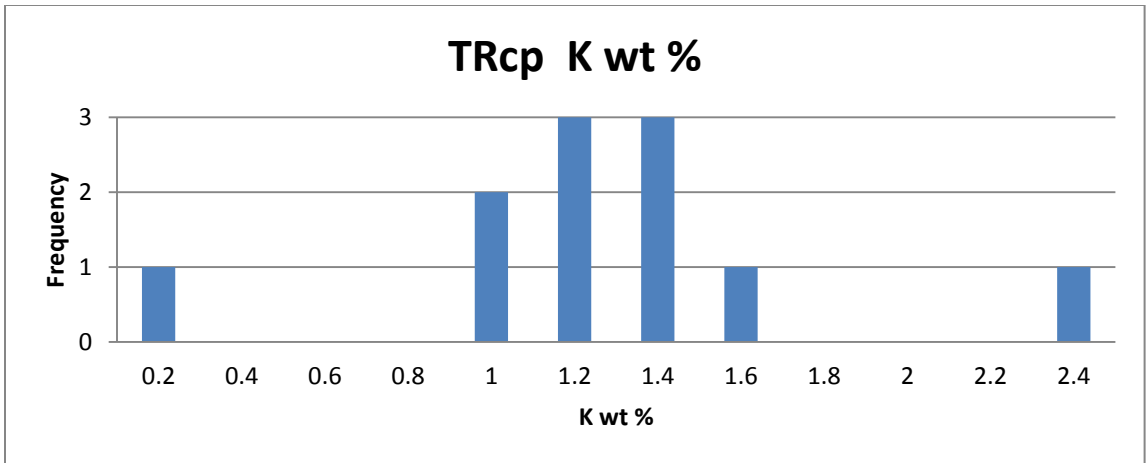
In the conglomerate there is an outlier U value of 92.5 ppm not shown on the histogram.

TRcp Th ppm
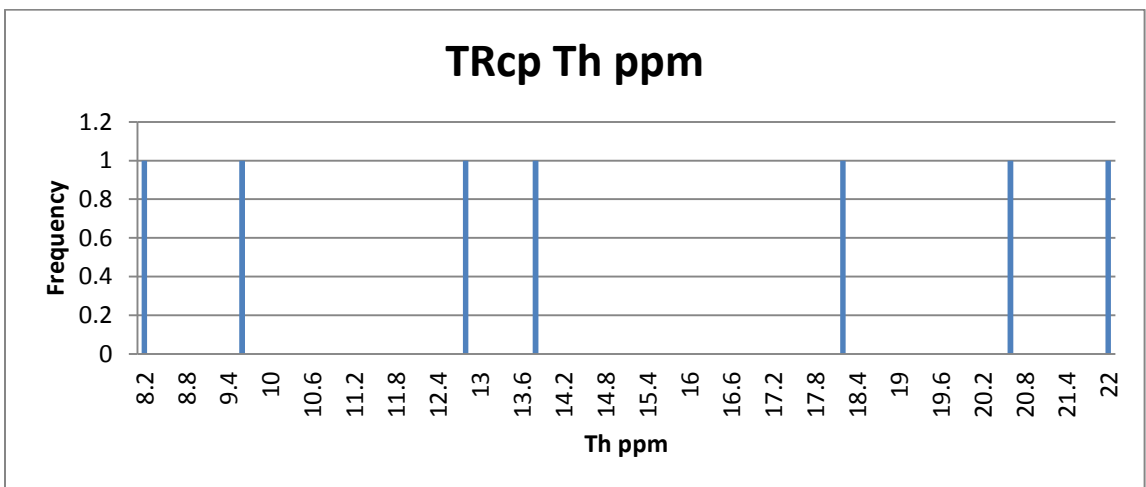
TRcp Soil: The soil on TRcp is described as low relief desert scrub on top of shale (USGS, 2004), this is consistent with the TRcp rock unit description. There is only one soil chemistry data point with 18 ppm Th and 4 ppm U. This is consistent with the rock unit median values of 13.7 ppm Th and 4.8 ppm U.

TRcp NURE Histogram:
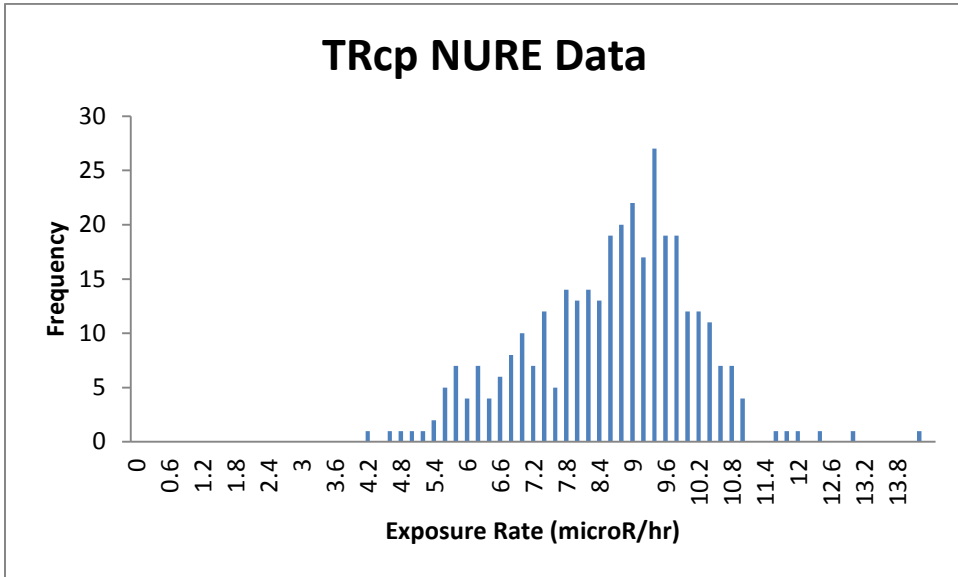
TRcp AMS Histogram:
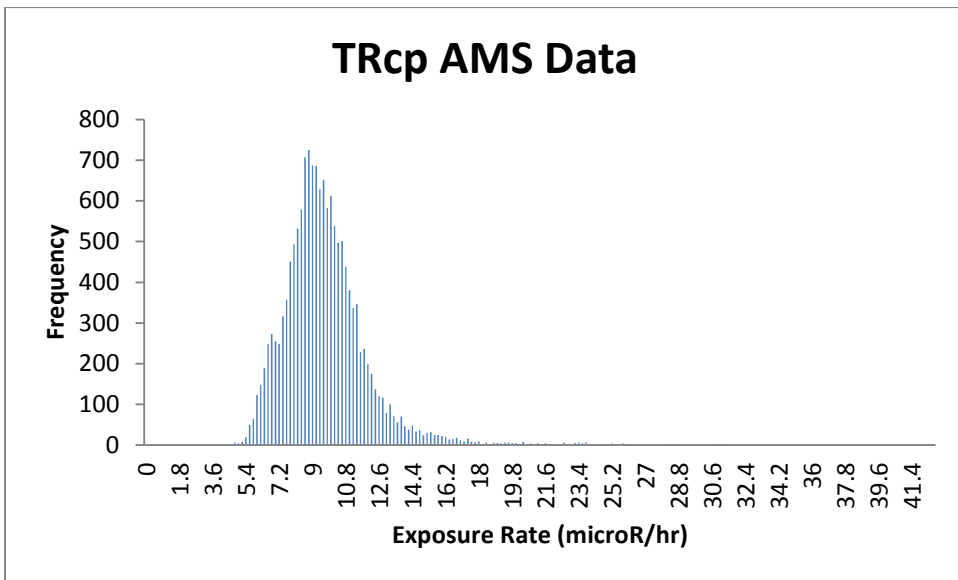
The AMS and NURE average values are significantly far apart, this could be due to the extremely large skew on the AMS data, going to over 40 microR/hr.

TRcp with 50m NURE buffer histogram:
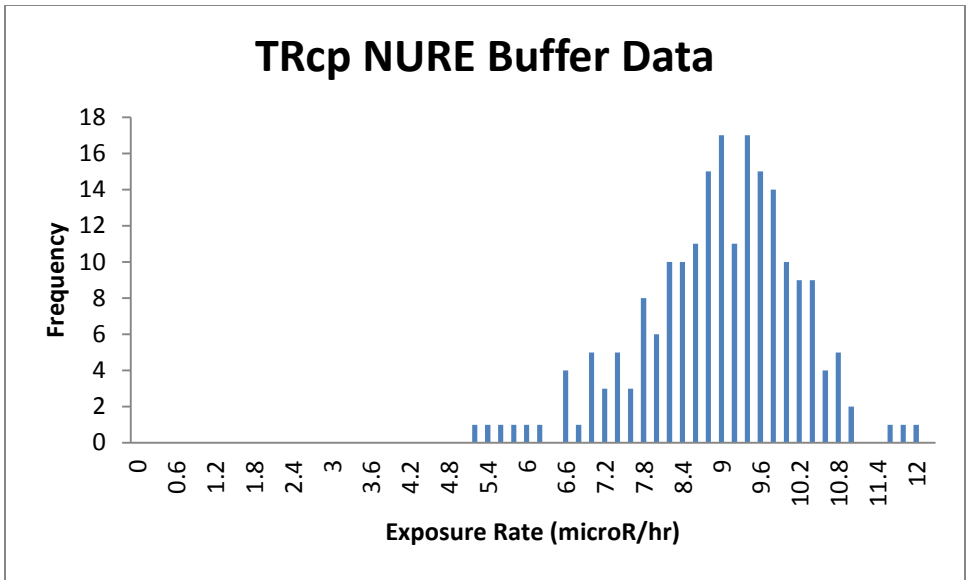
TRcp with 50m AMS buffer histogram:
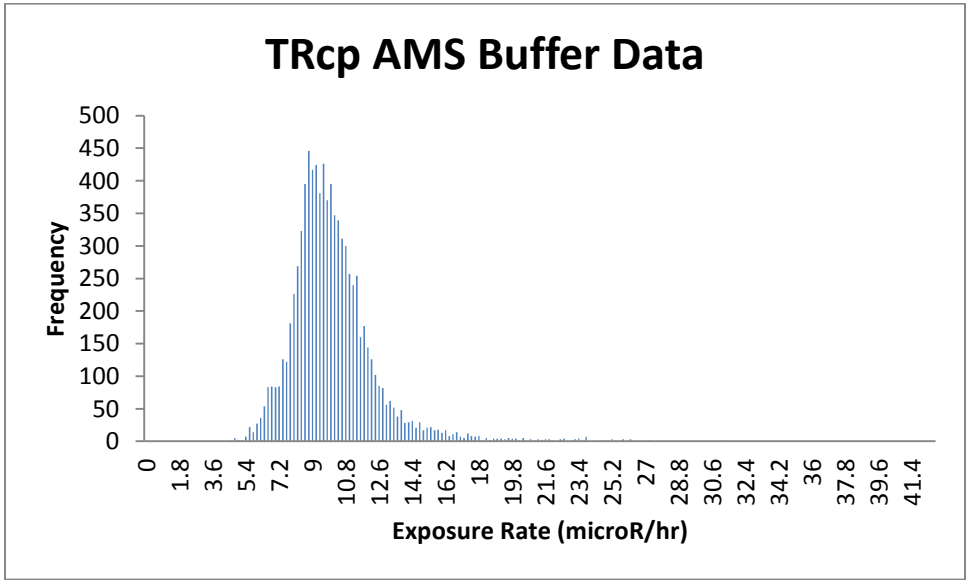
TRcp AMS Distribution: This unit is widely distributed throughout the area, and tends to be cooler in the east than the west. This unit has a large range of exposure rates, from 4.583 to 43.515.

TRcp AMS Exposure Rate Data
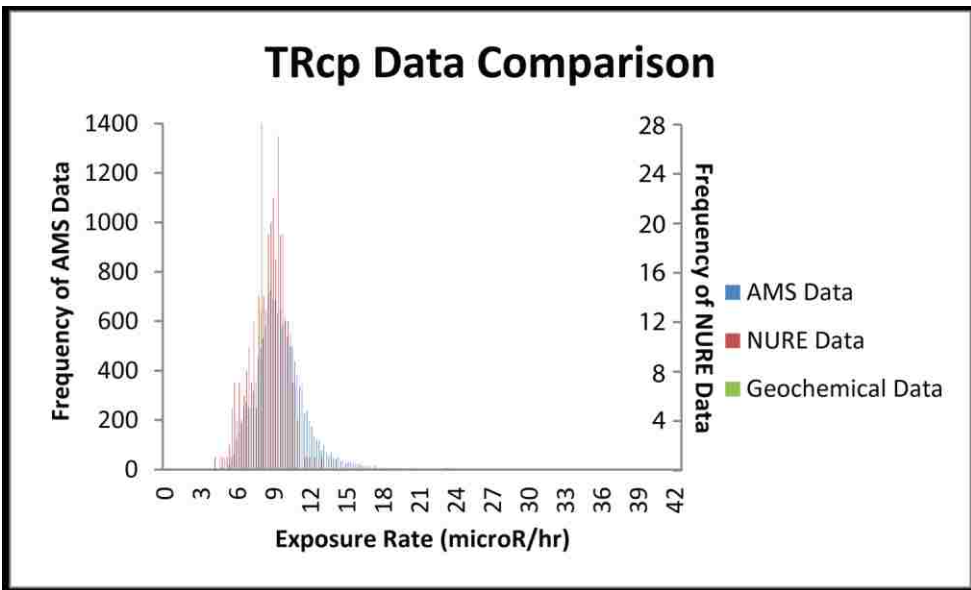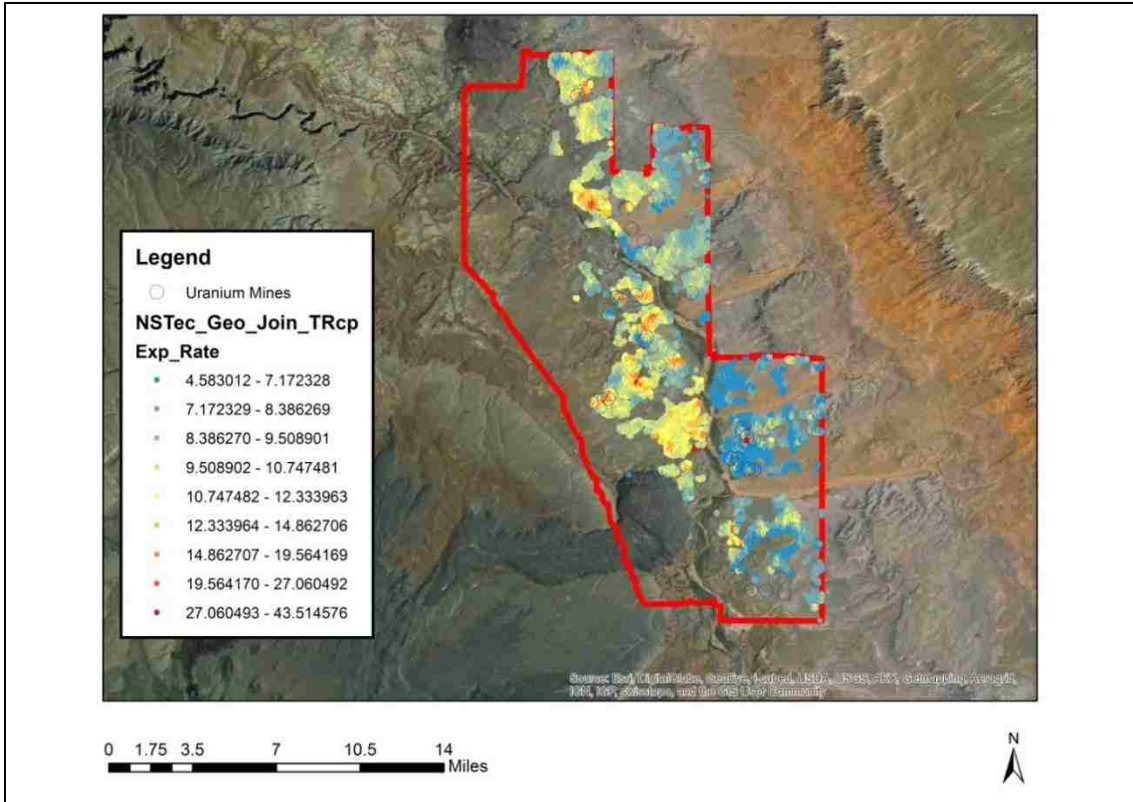
TRcs: The USGS identifies this unit as the Shinarump Member of the Chinle Formation, consisting of sandstone, siltstone, mudstone and conglomerate. They estimate a breakdown of this member to be 75% sandstone, 20% conglomerate, and 5% mudstone/siltstone. Conglomerate contains pebbles of quartzite and a black siliceous material. This unit was mined for Uranium in the Little Colorado River valley starting about 60 years ago, with uranium occurring in the sandstone and petrified wood material (Billingsley et al., 2007). One sample was identified by the collector as coming from the Moenkopi Formation. Based on this sample's description as a red sandstone it most likely belongs to TRmw, the only member of the Moenkopi Formation identified by the USGS to have red sandstone. This sample was moved to TRmw. After eliminating sample repeats, there are 6 data points from the USGS in this rock unit. Identified rock types include sandstone and conglomerate, consistent with TRcs.

TRcs average Field Notes: Huge variation, covered with alluvium and every few feet another rock type dominates the alluvium. We found what we believe to be exposed bedrock and put the detector on the bedrock. Alluvium clasts are large and angular. Many egg size or larger. Chert, sandstone and basalt dominate. Bedrock exposed is highly weathered, varies from grey to white to red sandstone. Sandstone is coarse and poorly sorted, subangular grains, not evolved. Consists mostly of quartz (dominate) then rock fragments and feldspar.

White to red medium grained sandstone mostly covered by 5 cm chert clasts and eolian sand. Sparse vegetation. Basaltic sand in parts.

TRcs hot Field Notes: Lots of exposed bedrock in this area, could explain why this area is hotter. Fine sand, no clasts, homogenous, medium vegetation. Large exposures of outcrop in this area are red and white sandstone. Cause of high radiation is probably this sandstone: poorly sorted, very coarse sandstone, mostly quartz, with feldspar and rock fragments, grains sub angular. Cross bedding present.
Red and white sandstone. Fine eolian sand of same character. Moderate shrubs and grasses. Few clasts aside from weathered in place sandstone.

TRcs cool Field Notes: The road was washed out and we were not able to reach this location.

These field observations are consistent with the USGS description of a brown to white conglomeritic sandstone with cross beds present. However, no siltstone, mudstone, or conglomerate were observed.

	K (wt %)	U (ppm)	Th (ppm)
mean	1.5868	14.96	17.525
Standard deviation	1.2670	21.7592	7.9185
range	3.1759	45.24	17.9
median	1.2985	5.14	15.7
mode	N/A	N/A	N/A
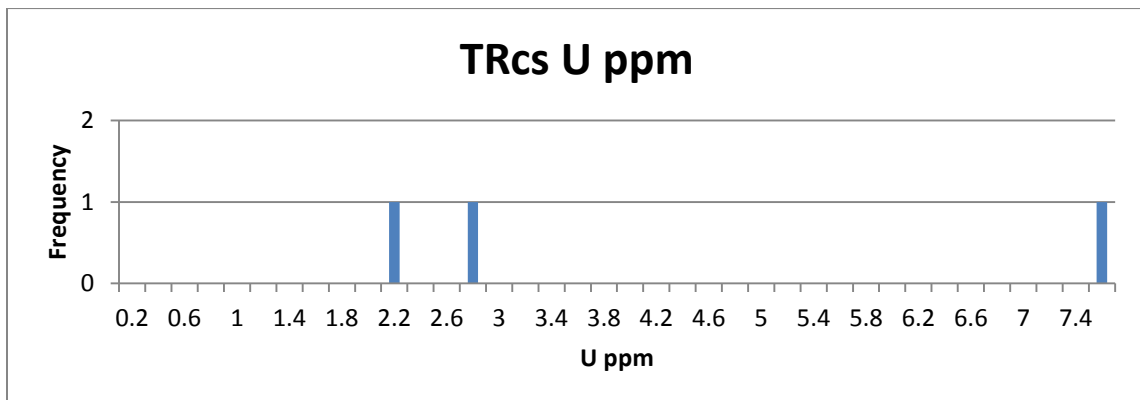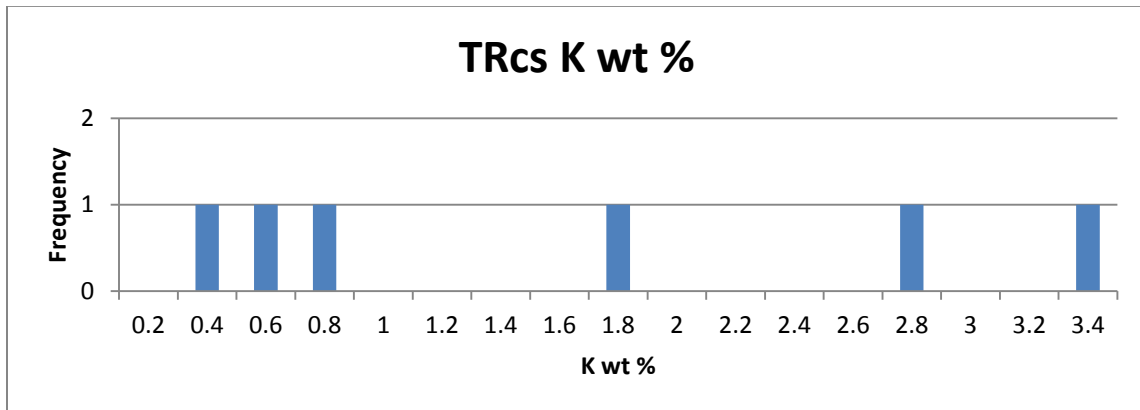
There is one outlier U concentration of 47.4 ppm in the conglomerate not displayed on the histogram.
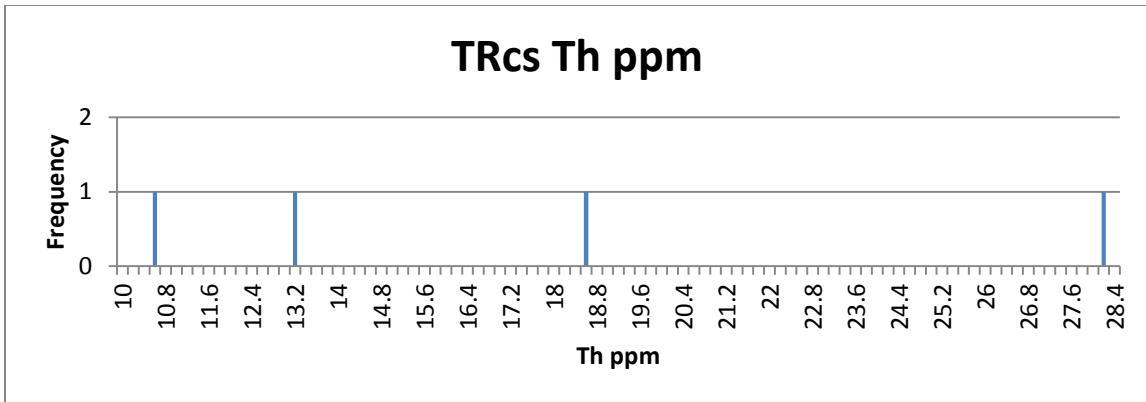
TRcs NURE Histogram:
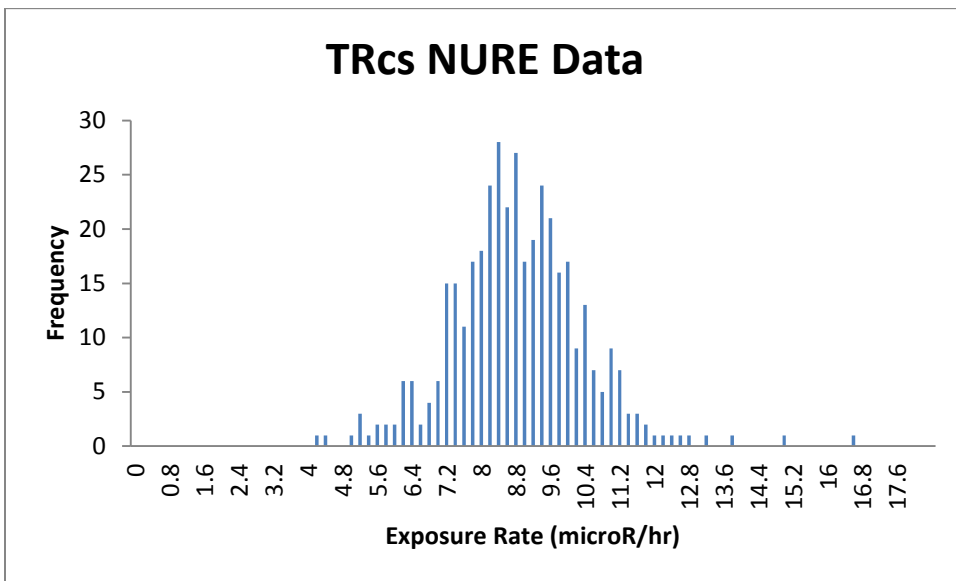
TRcs AMS Histogram:
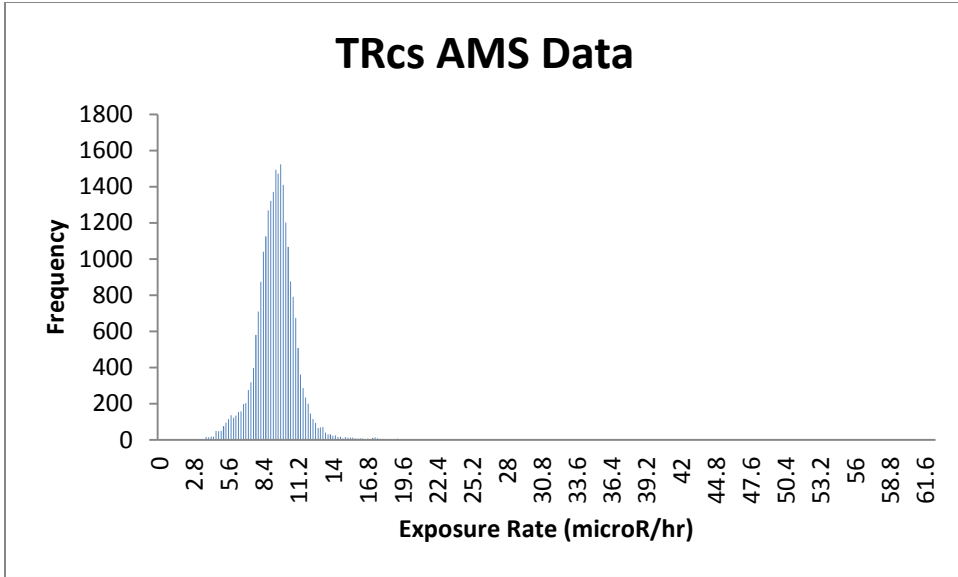
TRcs AMS Data

While the averages are very different, they have about the same central peak coming in at around 8. The AMS data is right skewed, going as high as 62.9, which is probably what's causing the discrepancy between means.

TRcs with 50 m NURE buffer histogram:

TRcs NURE Buffer Data
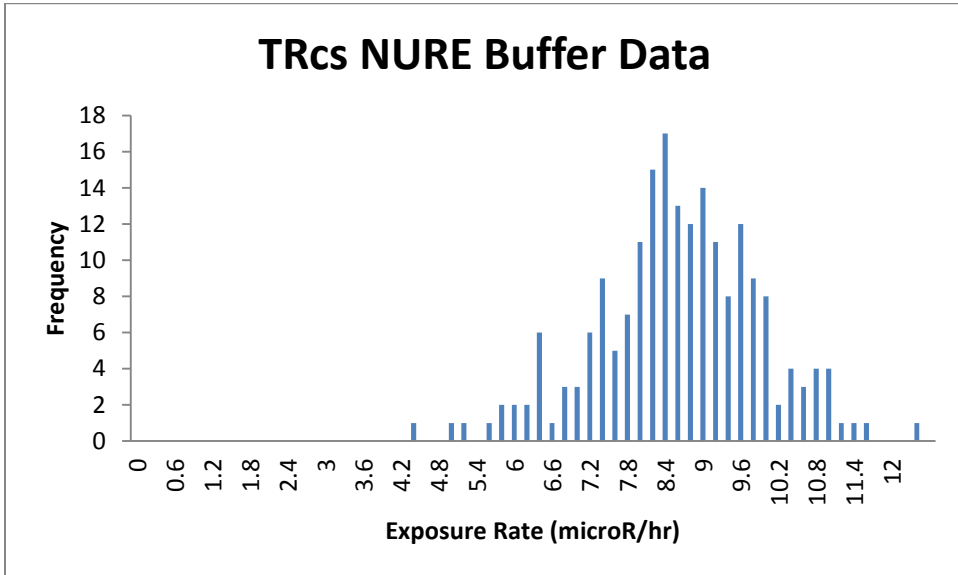
TRcs with 50m AMS buffer histogram:

TRcs AMS Buffer Data
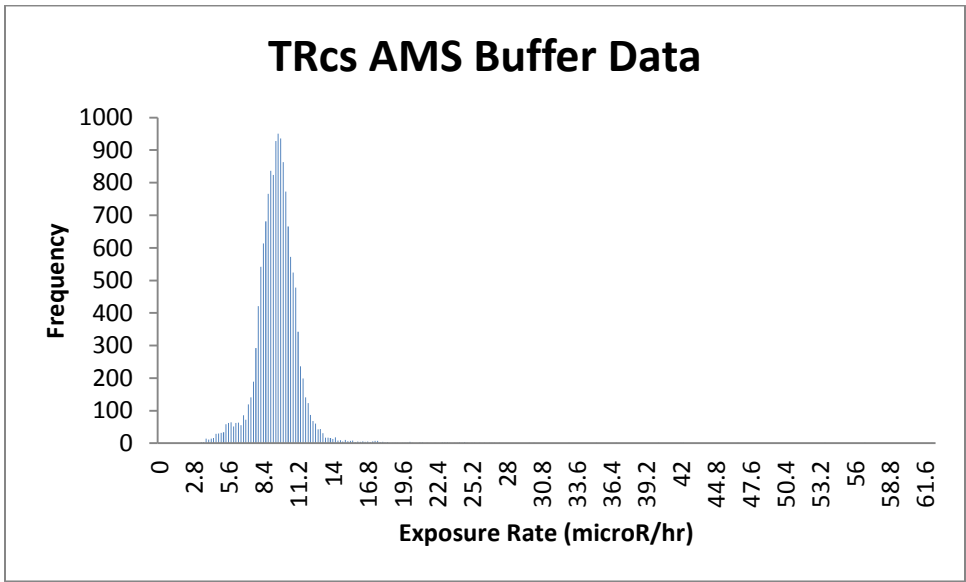
TRcs AMS Distribution: This unit occurs widely throughout the area, with no general trends, but many localized hot spots. This unit has one of the largest ranges of exposure rates, from 3.202 to 65.749

TRcs AMS Exposure Rate Data

TRcs Data Comparison
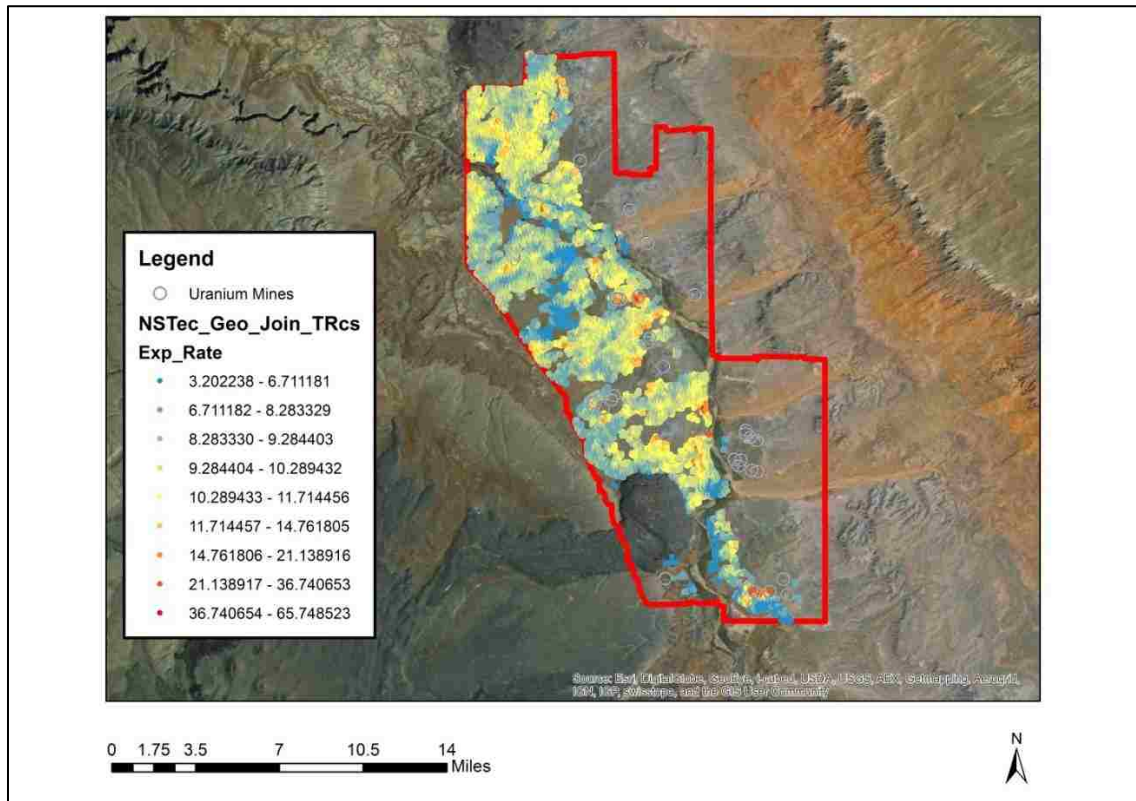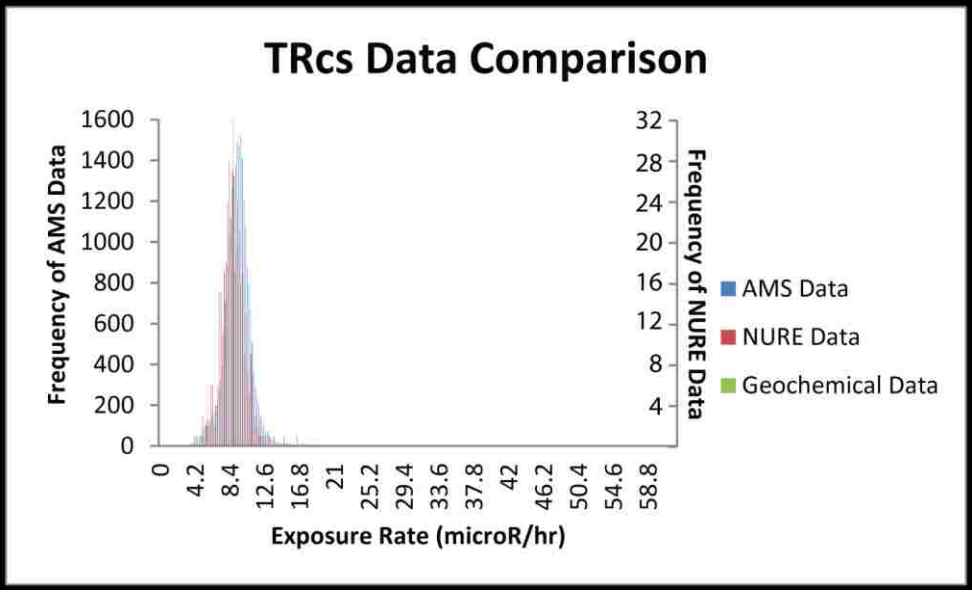
TRmss: The USGS identifies this unit as the Shnabkaib Member of the Moenkopi Formation, consisting of early Triassic sandstone and calcareous siltstone (Billingsley et al., 2007). There are 3 data points in this unit from the USGS, and a drill core that was originally reported as Pkh. There are 2 reported Th concentrations of 9.63 and 6.59 ppm. There are 4 reported U concentrations of 2.27, 6.6, 75.2 and 4270 ppm. It should be noted that the sample containing 4270 ppm U was taken from the Riverview Mine.

TRmss Field notes: Thinly bedded, fine-grained, sandstone. Fissile. Contains ripple marks. Fissile. Contains marks that look like vugs, pitting? This unit appears continuous with no variation. Sandstone appears highly evolved, mainly composed of quartz. Layer of broken rock present on surface, beneath that fines (clay). Thin bedded sandstone. Fine grained medium red. Ripple marks medium. Vegetation mostly dry grasses.

Field description of fine grained sandstone is consistent with USGS description, however the USGS lists the color as light brown, and it was definitely red in the field.

	K (wt %)	U (ppm)	Th (ppm)
mean	2.05	1088.5175	8.11
Standard deviation	0.9574	2121.2514	2.1496
range	2	4267.73	3.04
median	2.3	40.9	8.11
mode	N/A	N/A	N/A
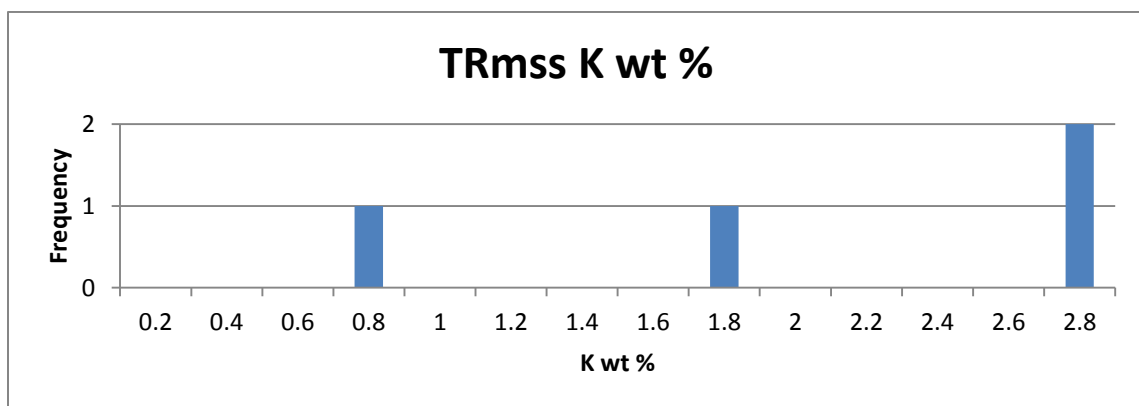
TRmss AMS Histogram:
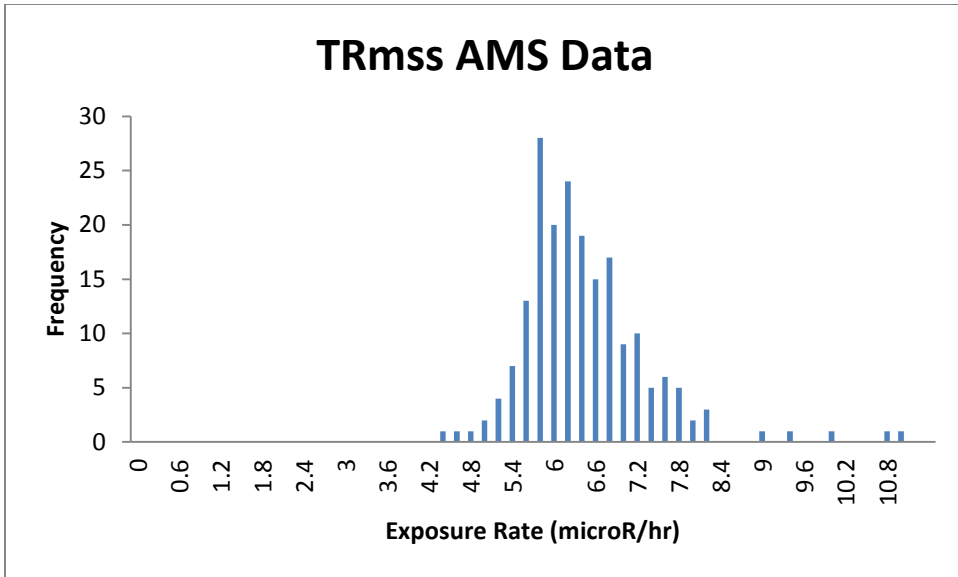
TRmss 50 m buffer AMS Histogram:
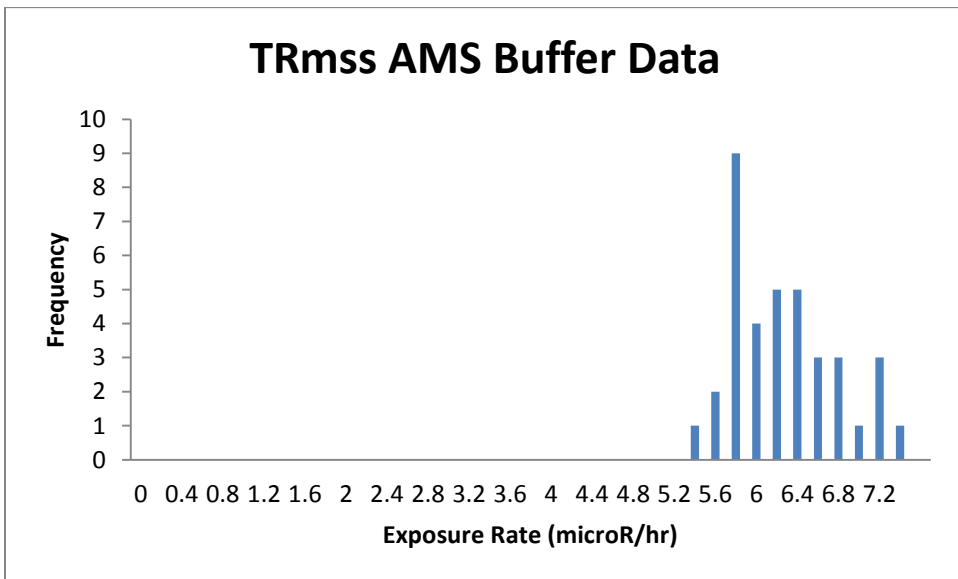
TRmss AMS Distribution: This unit is part of the hogback, and seems to have a no pattern in variation. The exposure rate varies from 5.056 to 11.616.

TRmss AMS Exposure Rate Data

Legend

○ Uranium Mines

NSTec_Geo_Join_TRmss

Exp_Rate

- 5.056144 - 5.514959
- 5.514960 - 5.822745
- 5.822746 - 6.152597
- 6.152598 - 6.474616
- 6.474617 - 6.809365
- 6.809366 - 7.114880
- 7.114881 - 7.890693
- 7.890694 - 9.209180
- 9.209181 - 11.615553

0   1.75 3.5   7   10.5   14
Miles

N
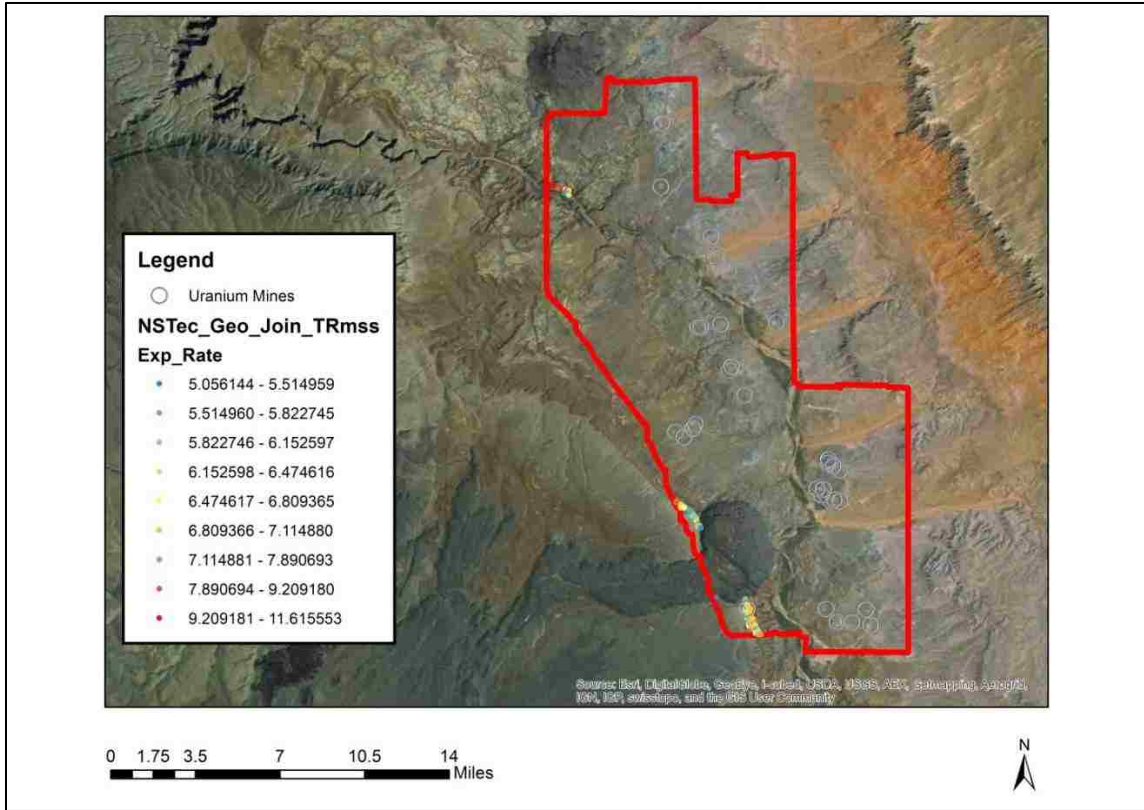
TRmw: The USGS identifies this unit as the Wupatki Member of the Moenkopi Formation, consisting of early Triassic sandstone, siltstone and mudstone (Billingsley et al., 2007). One sample was eliminated because the reported rock type of basalt wasn't consistent with TRmw. A data point originally from TRcs was added due to the collector's notes that it was from TRmw. There are 3 data points total in this unit from USGS. The reported rock type is conglomerate. There are 2 reported Th concentrations of 52.1 and 15.8 ppm in the conglomerate. There are 2 reported U concentrations of 3.13 and 840 ppm in the conglomerate. There seems to be a trend across the units that conglomerates have very high concentrations of U.

TRmw Field Notes: No basalt float. Very Fine grained sandstone. No variation throughout unit. Excellent ripple marks. Sample taken home. Red in color, some layers grey.
Dark red sandstone, some asymmtrical ripple marks. Fine grained. Sparse flowery vegetation.

No conglomerate was observed in the field area, inconsistent with the rock types reported by the USGS database. Red, fine grained sandstone observed in the field is consistent with the USGS unit description. No mudstone was observed.

	K (wt %)	U (ppm)	Th (ppm)
mean	2.1141	421.565	33.95
Standard deviation	0.4487	591.7565	25.6680
range	0.8378	836.87	36.3
median	2.3	421.565	33.95
mode	N/A	N/A	N/A

TRmw NURE Histogram:

TRmw NURE Data

Frequency / Exposure Rate (microR/hr)

TRmw AMS Histogram:

TRmw AMS Data

Frequency / Exposure Rate (microR/hr)
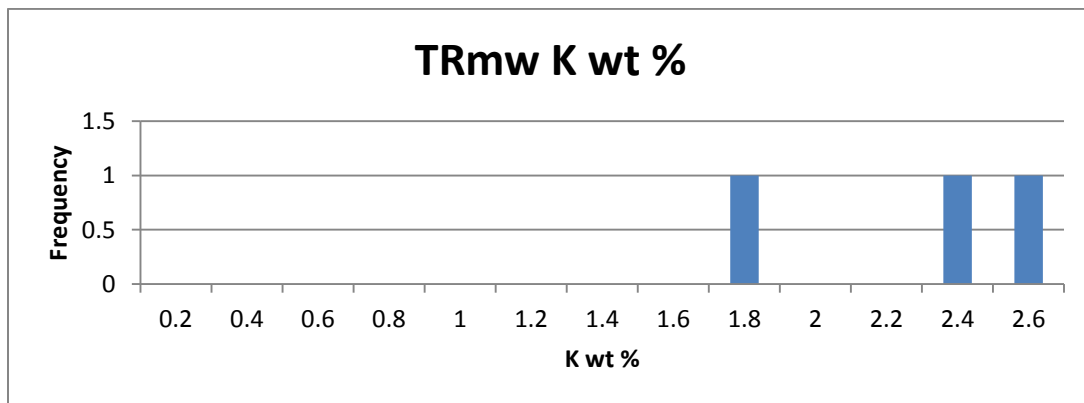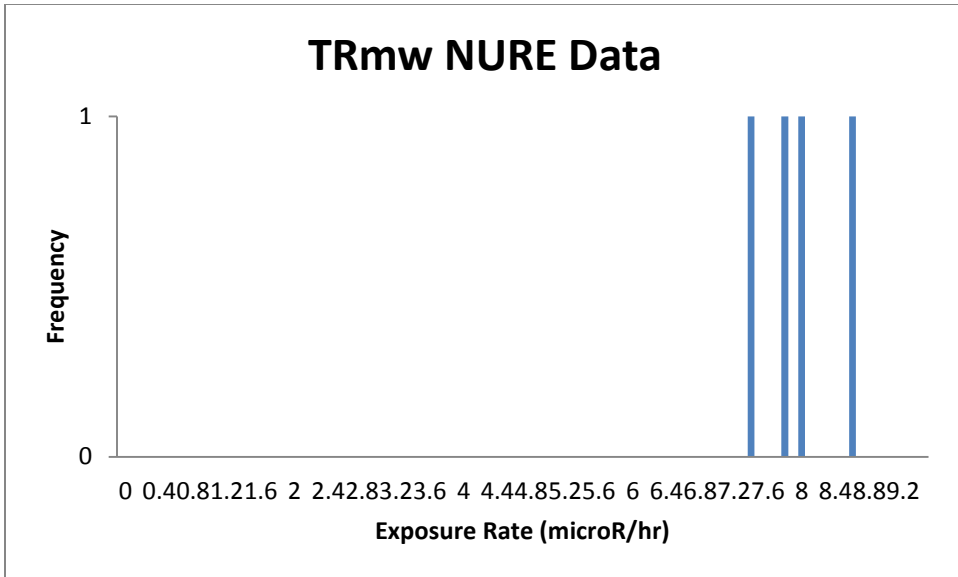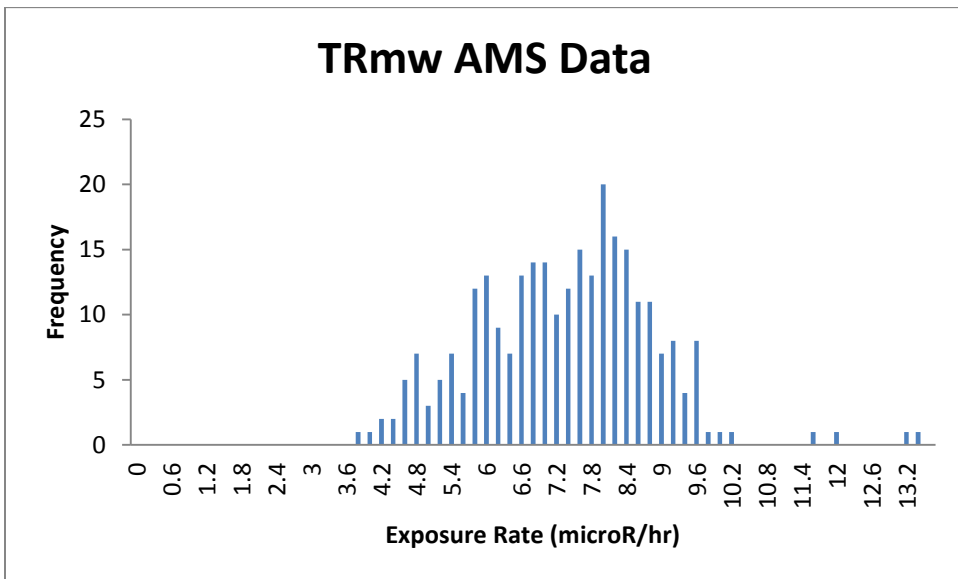
These means are significantly different, and neither histograms is skewed, this difference is probably due to the fact that the NURE data only has 10 data points.

TRmw 50 m buffer NURE Histogram:

TRmw NURE Buffer Data
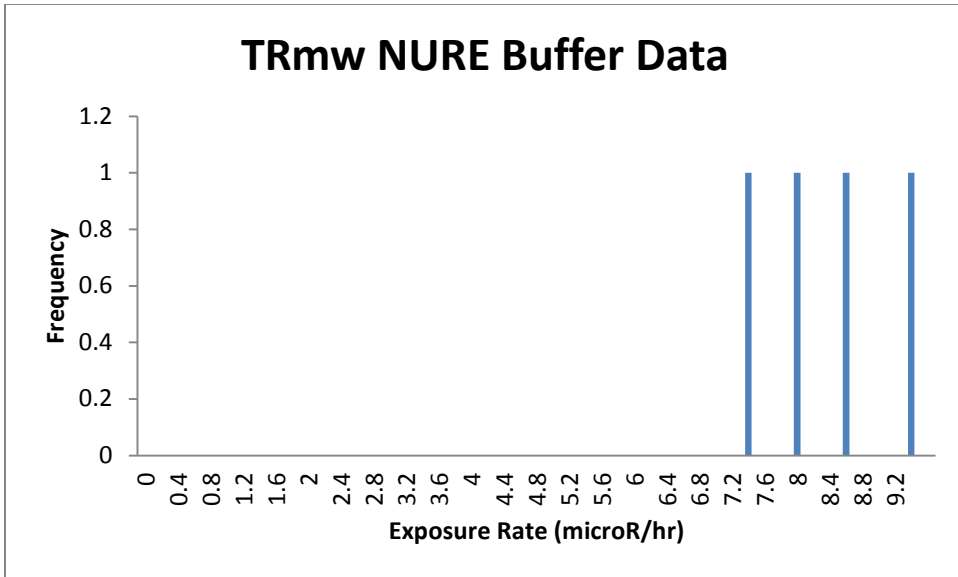
TRmw 50 m buffer AMS Histogram:

TRmw AMS Buffer Data
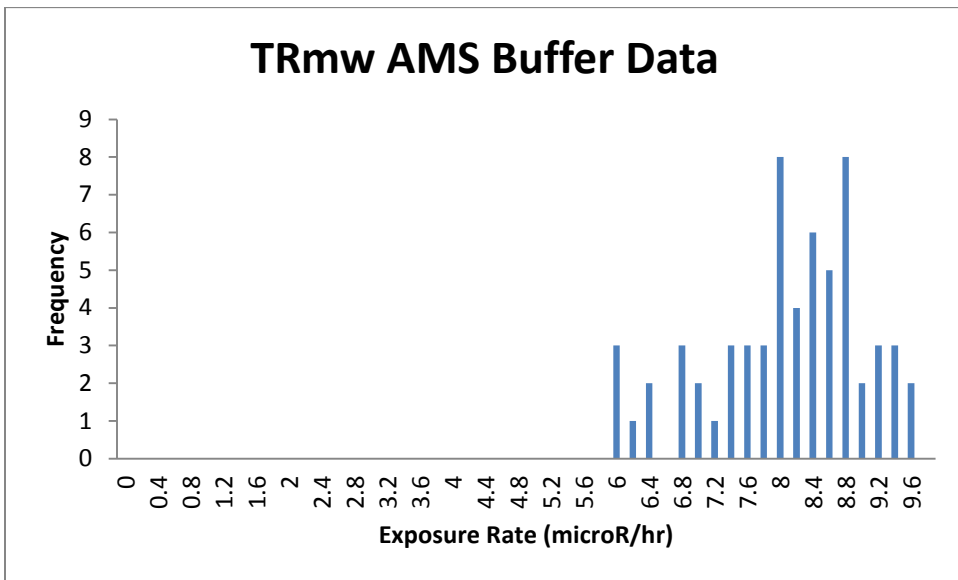
TRmw AMS Distribution: This unit follows the general trend of the other units, with cooler values in the south and hotter values in the north. What's interesting is in the north there are cool and hot points bordering each other.

TRmw AMS Exposure Rate Data
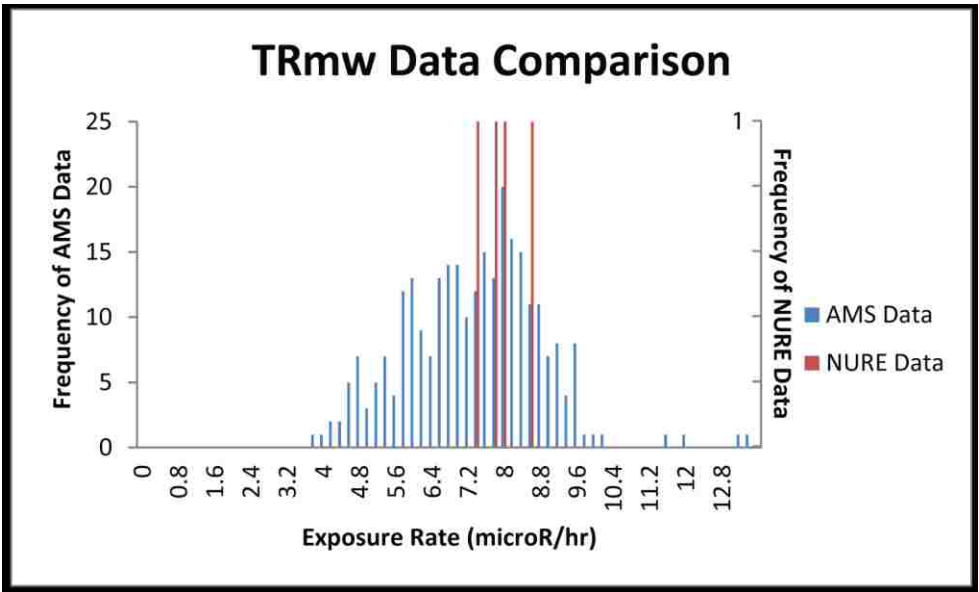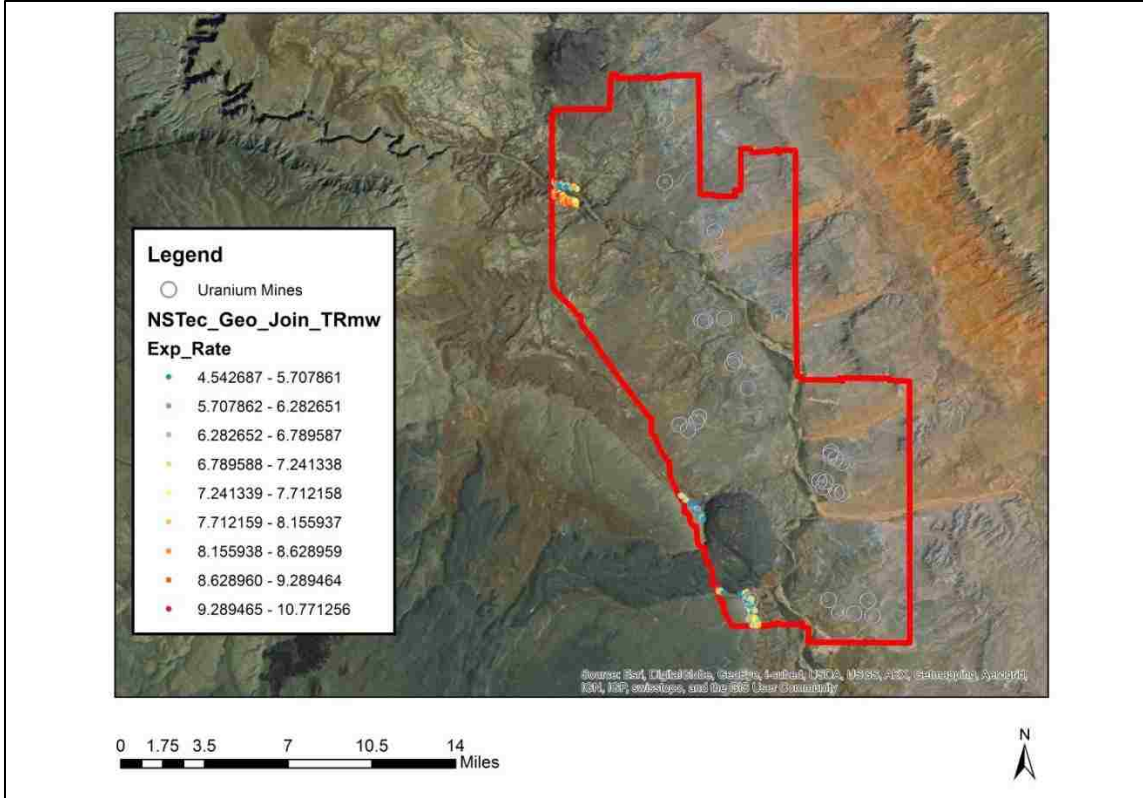
Pkh: Harrisburg Member of the Kaibab Formation, early Permian in age. Contains gypsum, siltstone, sandstone and limestone (some with chert) (Billingsley et al., 2007). We originally had 244 data points within this unit, from the DIR, USGS, and NAVDAT. Rock types that were identified in the data include basalt, limestone, sandstone, dolomite, conglomerate, and one point each andesite and rhyolite. DIR did not record rock type but reported they focused largely on sandstone. This unit has one third of our data, but occupies under 10% of the mapping area. One of these data points is labeled as being from the Moenkopi Formation, and is a drill core. Data points labelled as basalt, andesite or rhyolite were removed from Pkh, and the points labeled Moenkopi Formation were moved to TRmss. While these points were not specified to be TRmss, the listed rock type of calcareous very fine grained sandstone is consistent with the listed rock types in TRmss. Also each rock sample was limited to one data point. This left us with 184 Pkh data points, though only 7 have Th concentrations as K and Th concentrations were removed for all DIR data points.

Pkh Field Notes: Fine grained, well sorted, sandstone bedrock exposed, weathering is in a limestone style, must be a limey sandstone. In the float there is chert and conglomerate. Chert is bright orange only. Medium vegetation cover. Mostly limey sandstone occuring as float. Some bedrock. Some vegetation cover. Occasional basaltic boulders, chert and pendent formation in the limey sandstone.

This description is overall consistent with the USGS description, which mentions part of Pkh contains chert. Conglomerate was present as float, and Dan recorded that there was one piece of basalt float, which could explain the USGS reported rock types.

	K (wt %)	U (ppm)	Th (ppm)
mean	0.6525	185.26	6.5386
Standard deviation	0.9459	1670.2507	5.2315
range	4.1938	16599.7	13.1
median	0.37	1.45	6.52
mode	0.04	1.9	N/A

Mean values tend to be skewed by outliers, especially in the case of Uranium because of this area's richness in Uranium, so median values are more representative of the data points. Because of the wealth of data points for this area we are confident about our representative values for radioelement concentration.

Pkh U ppm
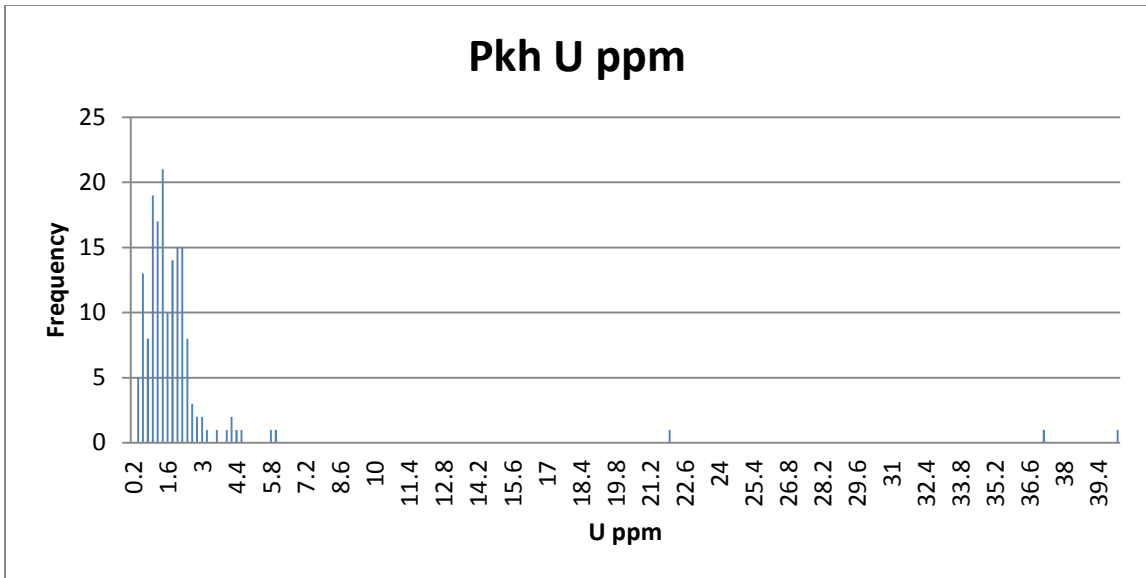
There are 2 outliers not displayed on the graph collected by the USGS in the same location (35.65, -111.35) from siltstone and conglomerate of 16600 and 13800 ppm Uranium. A flaw of some of the data collected from IEDA, originally recorded by the USGS, is that there will be in excess of ten data points recorded at the same location, with multiple different rock types listed. To me this is suspect because the coordinates are only taken out to the second decimal places, which is not up to industry standard (4 decimal places).

Pkh K wt %

Pkh Th ppm
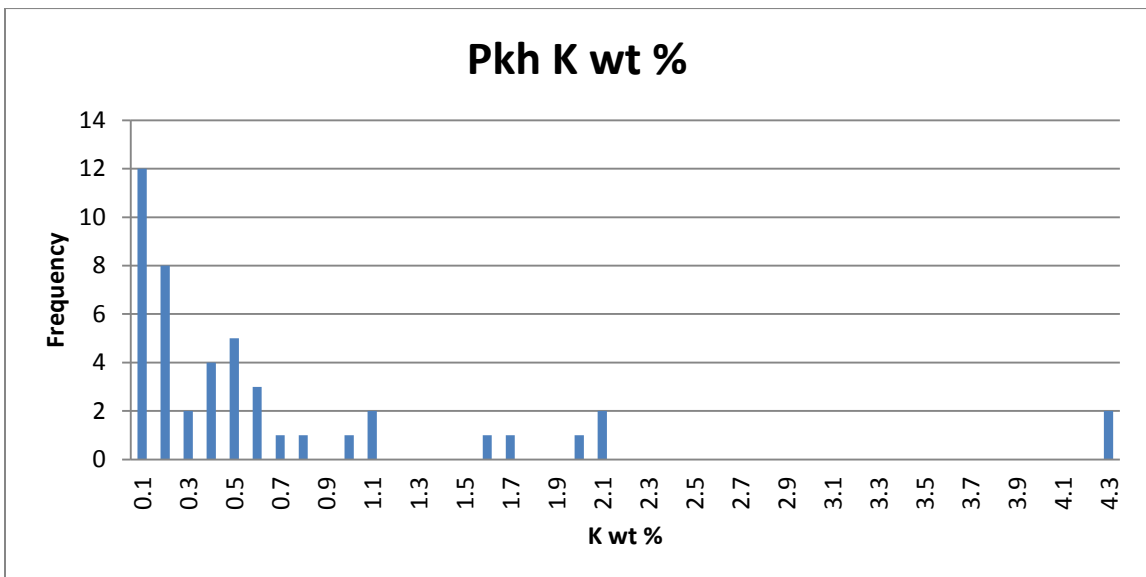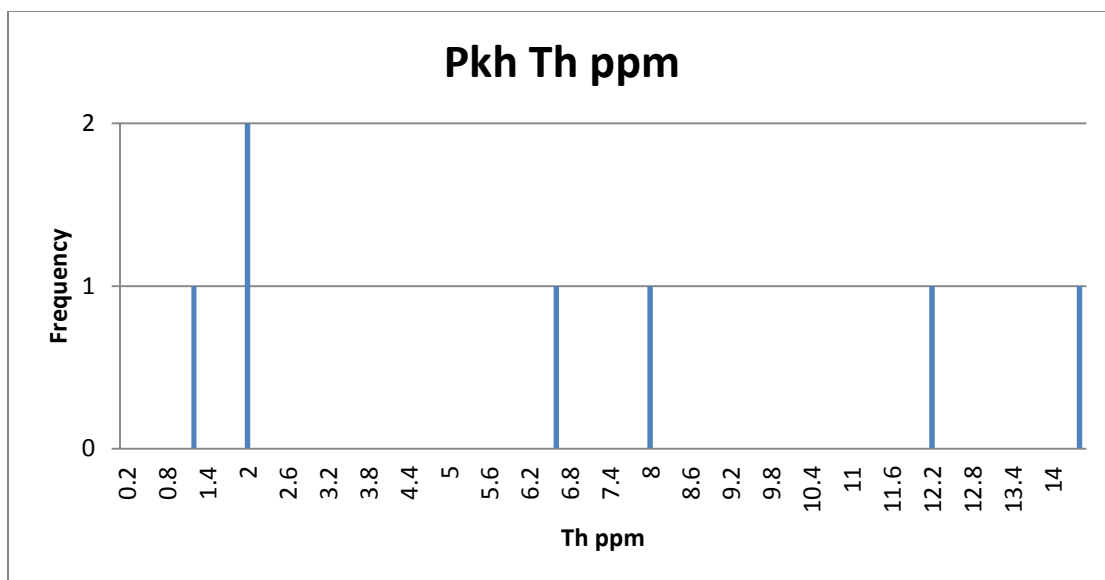
Pkh soil: is defined as tan, fine to coarse grained sand, with moderate to sparse vegetation (USGS, 2004). Points have been recorded to overlay unconsolidated valley fill and volcanic rock, inconsistent with Pkh. There are 4 points total, only one of which has a Th concentration, reported as 7.56 ppm.

	K (wt %)	U (ppm)	Th (ppm)
mean	1.8225	2.14	7.56
Standard deviation	0.1776	0.0490	N/A
range	0.4	0.1	N/A
median	1.815	2.13	7.56
mode	N/A	2.1	N/A

Comparing the soil mean values to the rock median values, the soil has higher values of K, U, and Th. Though it should be taken into account that there is only one Th measurement, which could be skewing the results, as there were rock samples with Th measurements over 7.56 ppm. There are also few U and K measurements, so the difference could simply be a lack of data. Overall, the soil averages exist in the ranges of the rock data which is a positive outcome.

Pkh Soil K wt %

Pkh Soil U ppm

Pkh AMS Histogram:

Pkh AMS Data

A histogram titled "Pkh AMS Data" with Frequency (0 to 200) on the y-axis and Exposure Rate (microR/hr) on the x-axis ranging from 0 to 9.6. The distribution peaks around 4 with a frequency near 185, with a long right tail.
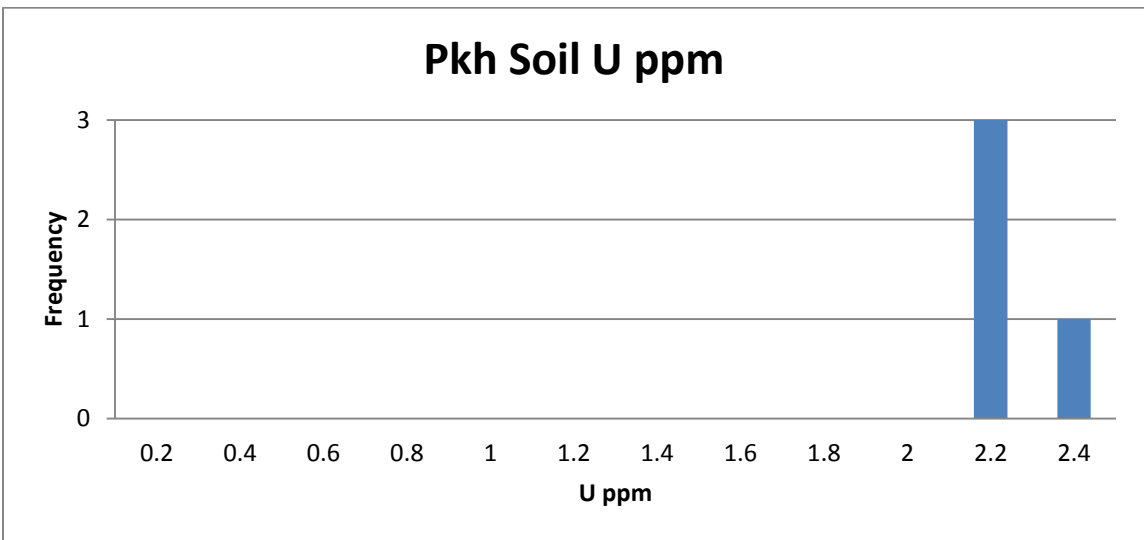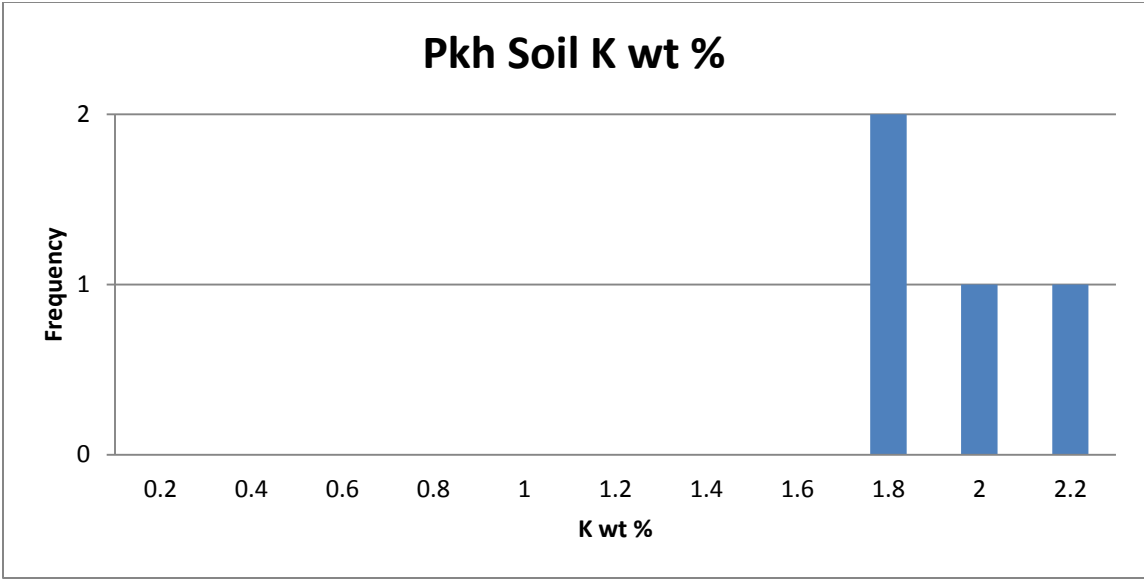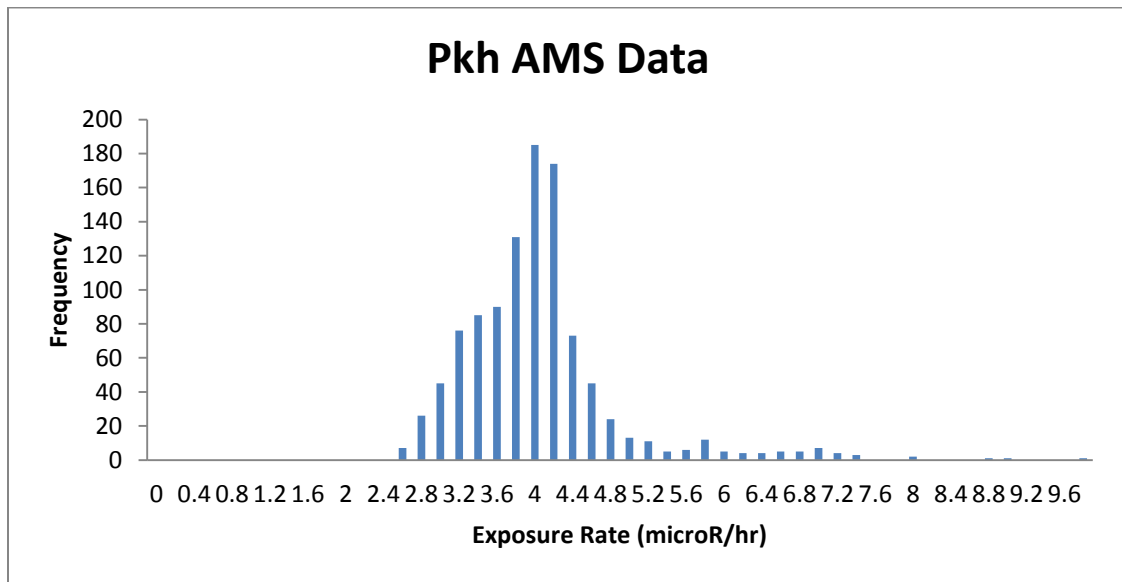
There are only 8 NURE points that occurred within Pkh, so a curve is not formed.

Pkh with 50m AMS buffer histogram:

Pkh AMS Buffer Data

A histogram titled "Pkh AMS Buffer Data" with Frequency (0 to 180) on the y-axis and Exposure Rate (microR/hr) on the x-axis ranging from 0 to 7.2. The distribution peaks around 4 with a frequency near 160, with a right tail.
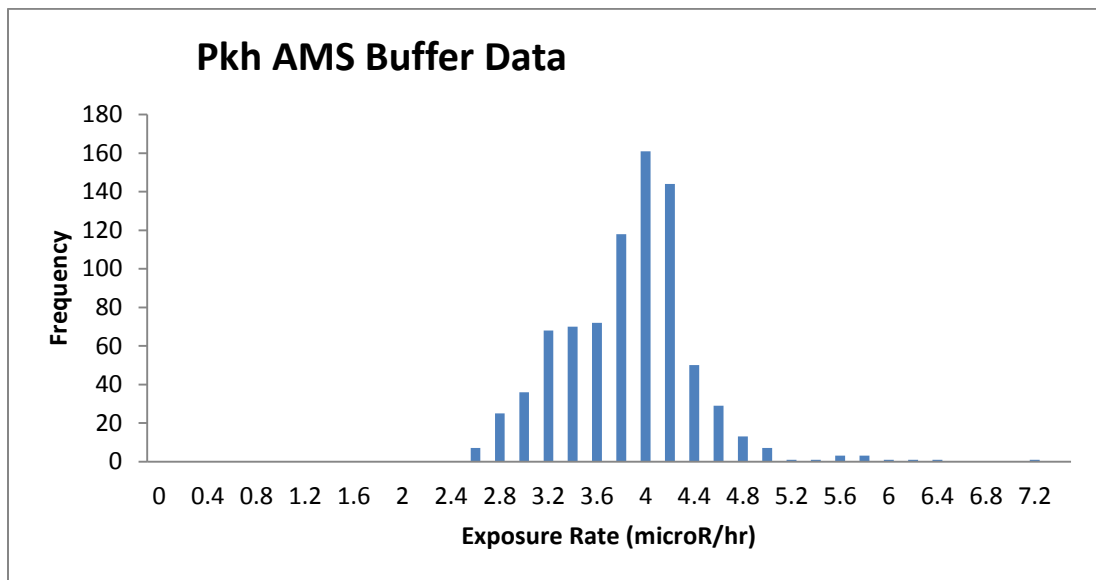
Pkh AMS Distribution: Pkh occurs in two main areas, on the western edge of Black Point, and north there is an exposure at the river. By Black Point there is a clear trend in the AMS exposure rate data with lower exposure rates towards the west and higher in the east, and there is a corresponding Uranium mine bordering the 'hot' east portion. All of the data points in the north have relatively high exposure rates. In this unit exposure rates vary from 2.434 to 9.665. This

unit only occurs in the southwest portion of the map and thus does not display the overall trends seen in other units in the area.

Pkh AMS Exposure Rate Data
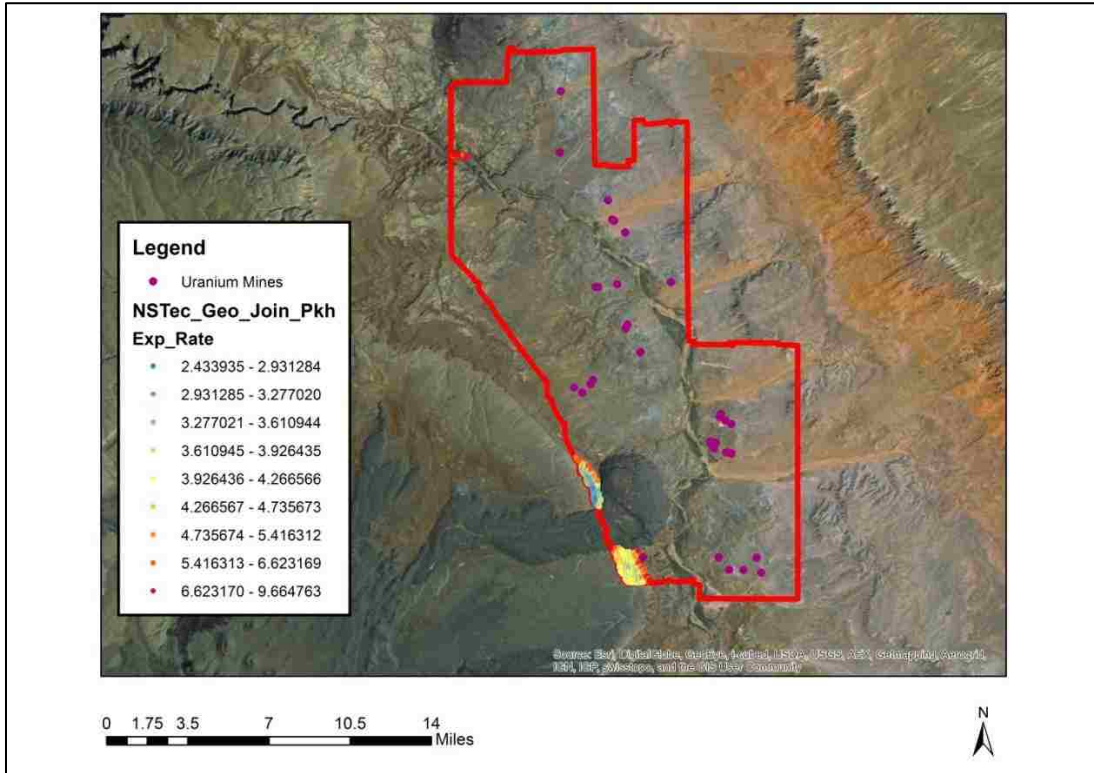
Daughter Units

Qaf: This is a manmade unit, consisting of Holocene sediment and unidentified bedrock that was excavated during construction. Importantly it contains talus from Uranium mining activity (Billingsley et al., 2007). We have 3 data points for this unit from the USGS after eliminating duplicates from the same rock sample. This unit could contain any rock types based on the fact it is a manmade formation, no data points will be eliminated. One sample was identified as latite, while the rest were unidentified. The latite sample is also the only one that reported Th and U concentrations. The Thorium and Uranium values for this unit are quite high, which could be related to the uranium mining talus the USGS states is present in this unit.

Qaf Field Notes: As this is a manmade unit it was not visited during field work.

	K (wt %)	U (ppm)	Th (ppm)
mean	2.2559	9.45	49.9
Standard deviation	0.7603	N/A	N/A
range	1.3220	0	0
median	2.6897	9.45	49.9
mode	N/A	N/A	N/A
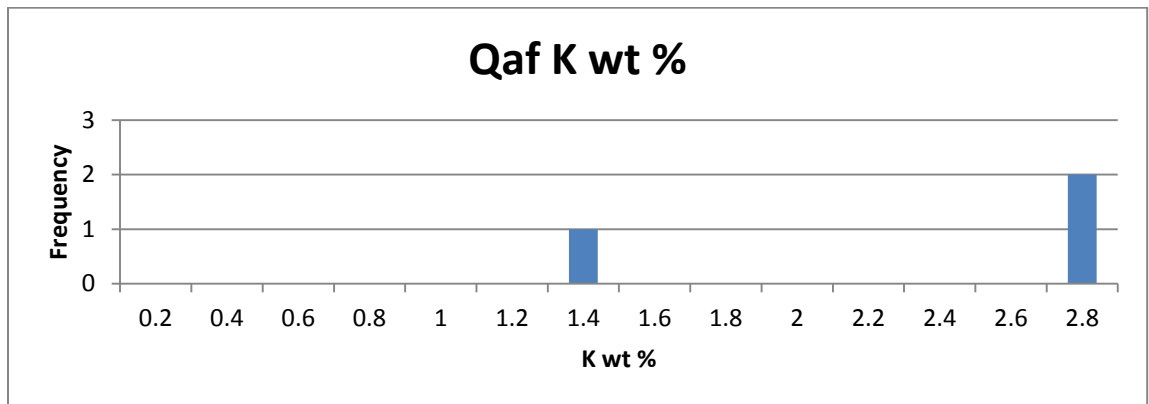
The latite sample has a Thorium measurement of 49.9 ppm and a Uranium measurement of 9.45 ppm.

Qaf Soil: There is one soil sample for Qaf, it is described as a coarse, tan, sand with moderate vegetation occurring on unconsolidated valley fill (USGS, 2004). Valley fill is consistent with Qaf, as Qaf is a talus and Holocene sediment unit. It has a K wt % of 1.7% and a U concentration of 2.2 ppm. The K and U are lower than that of the rock unit, but this could be largely due to the small amount of points for both the rock and soil.

Qaf NURE Histogram:

Qaf NURE Data

Frequency

Exposure Rate (microR/hr)

Qaf AMS Histogram:

Qaf AMS Data

Frequency

Exposure Rate (microR/hr)
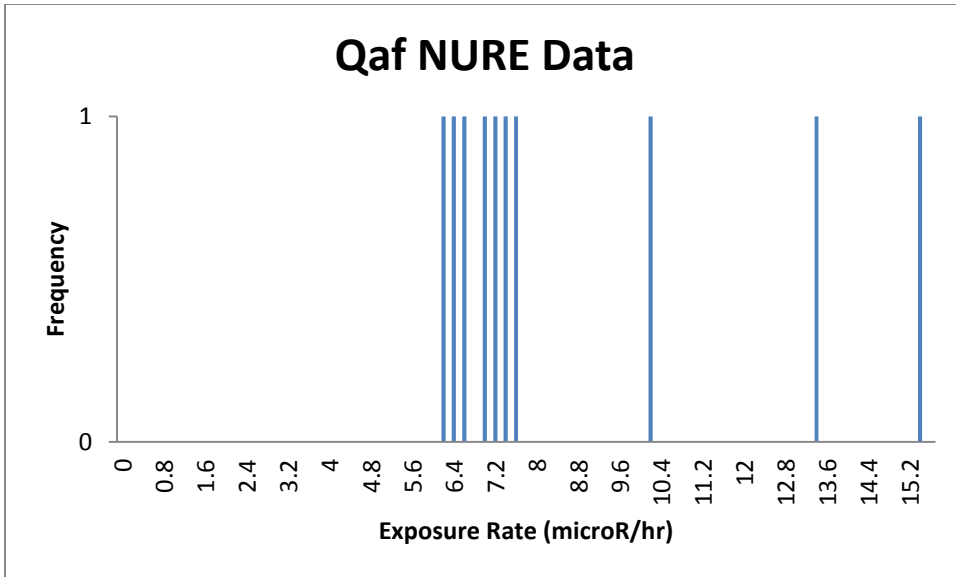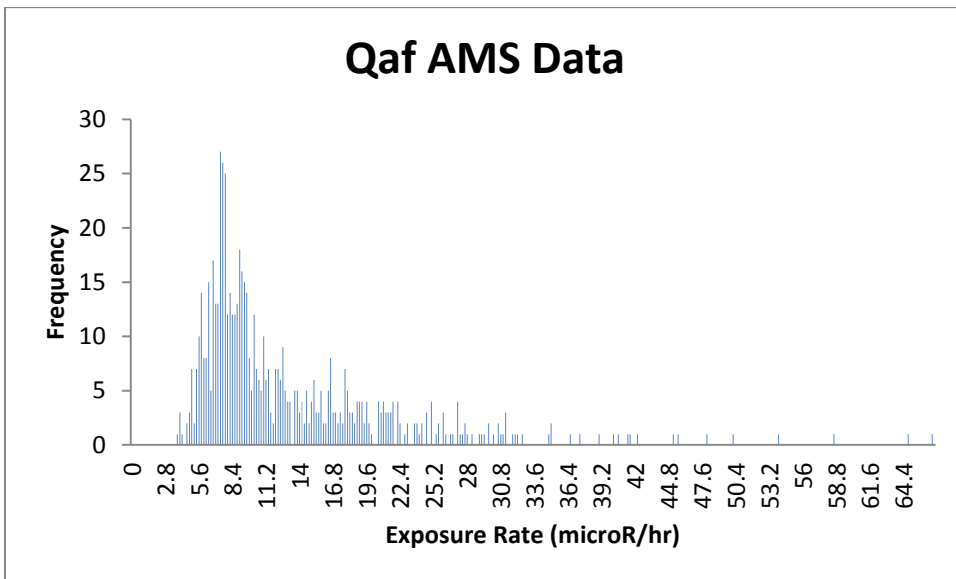
The AMS mean is almost twice that of the NURE data, this is probably due to the fact that there are only 7 NURE survey data points and the AMS data is highly right skewed.

Qaf 50 m buffer NURE Histogram:
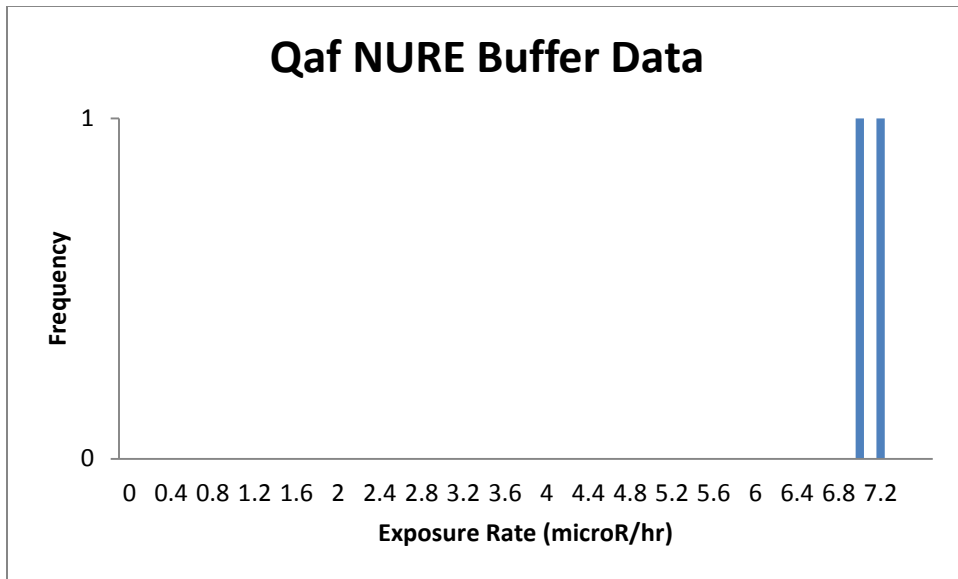
Qaf 50 m buffer AMS Histogram:
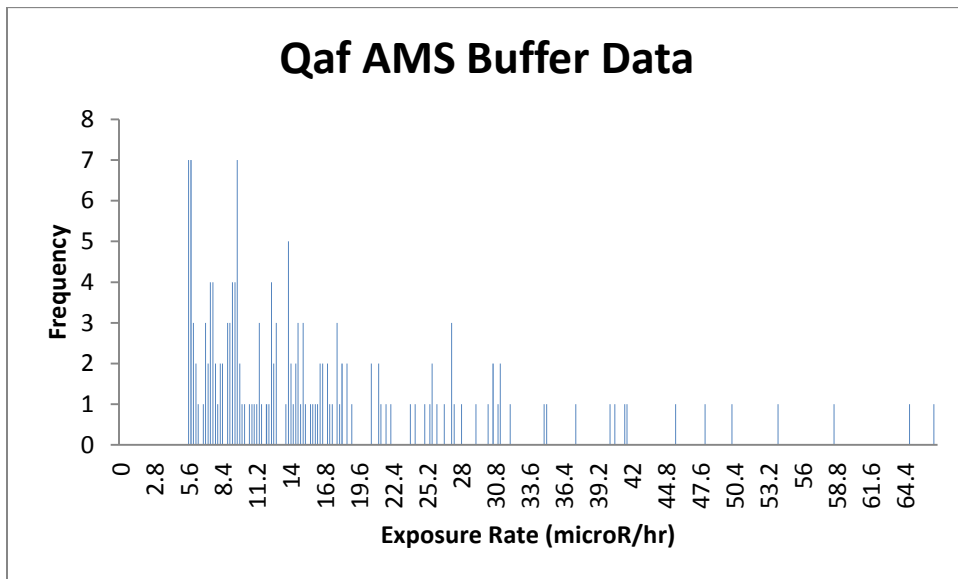
Qaf AMS Distribution: This unit is widely distributed but occurs in small quantities. This makes sense as it is a manmade construction unit, which is obvious by its high concentration in the uranium mine areas. This unit has a very wide range in exposure rate, from 3.88 to 66.661, most likely due to the presence of uranium talus, and the fact that this unit is not defined by a common geology.

Qaf AMS Exposure Rate Data
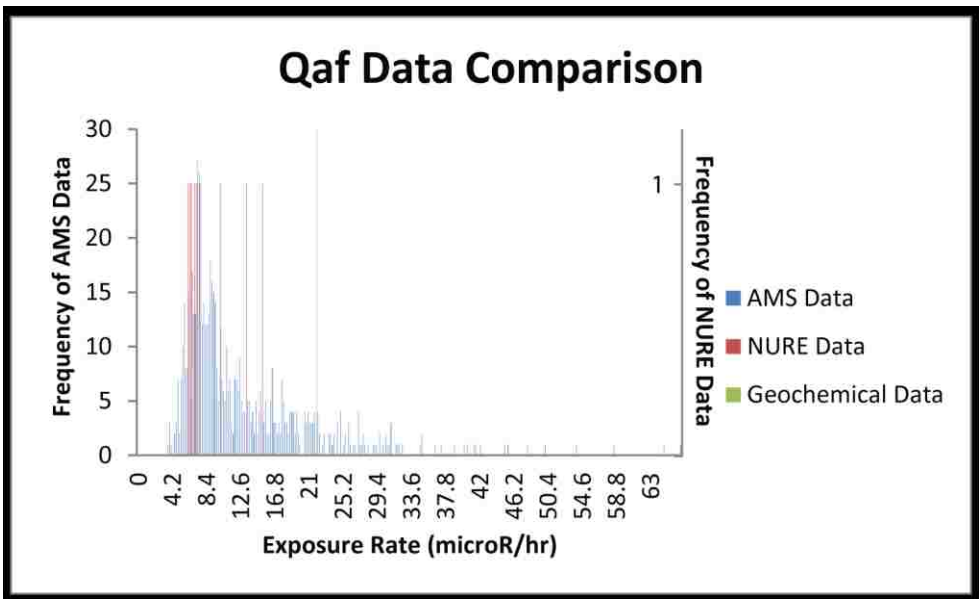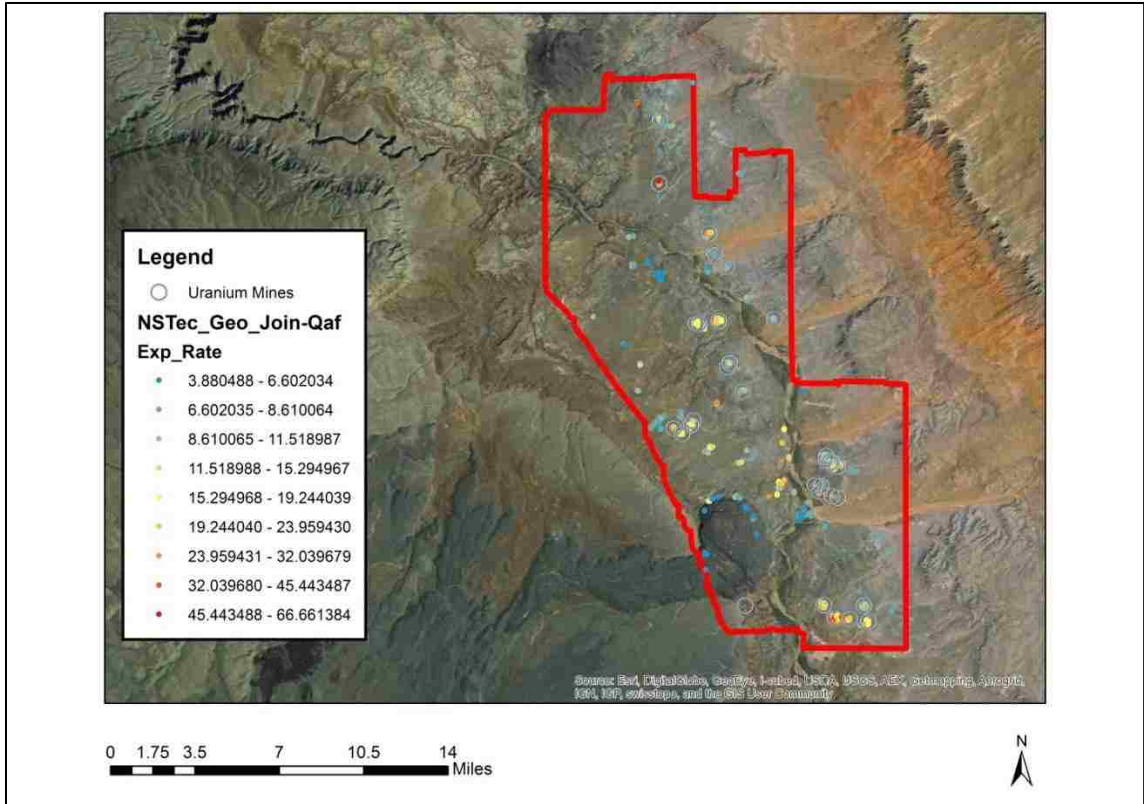
Qs: The USGS classifies this unit as poorly sorted, Holocene age, stream channel deposits, ranging in grain size from silt to gravel (Billingsley et al., 2007). No comment is made on composition, so it is difficult to compare accuracy to the reported rock types of limestone and basalt, as a part of stream sediments will be coming from outside the mapping area. All data points will remain in Qs, as a stream channel deposit it could easily contain all listed rock types. There are 8 data points in this unit from the USGS and DIR. Thorium concentration is not well represented, as only 1 data point has Th ppm.

Qs Field Notes: No data could be collected from this unit, one point was off a cliff and the other was down a road that washed out.

	K (wt %)	U (ppm)	Th (ppm)
mean	0.3	1.7065	2.7
Standard deviation	0.3867	0.5913	N/A
range	1.05	2.018	N/A
median	0.12	1.6	2.7
mode	N/A	1.6	N/A
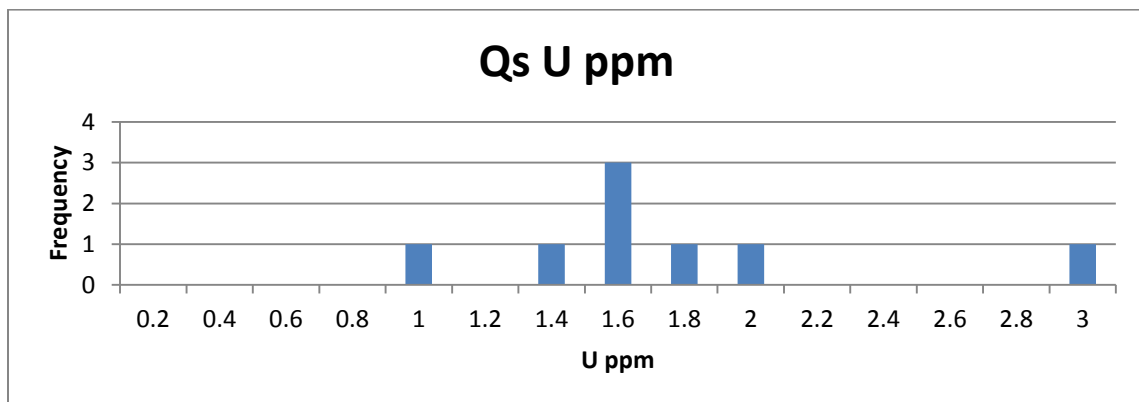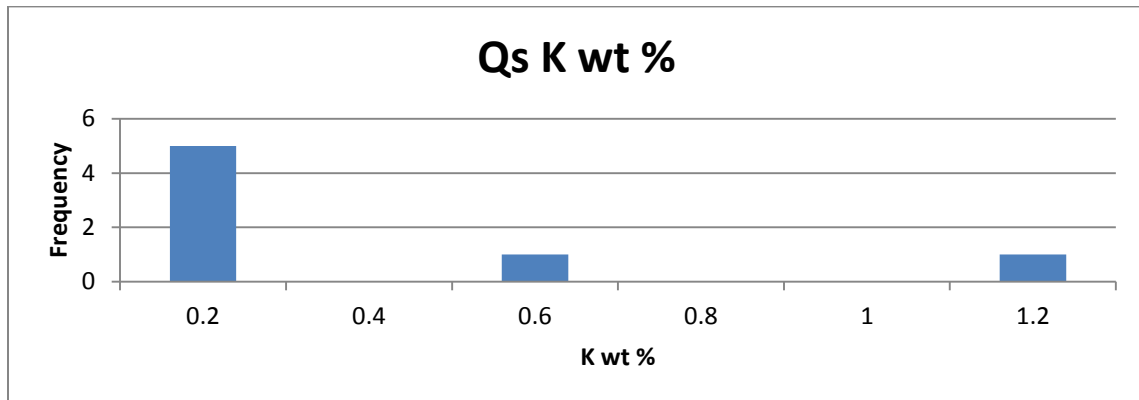
There is only one listed Th concentration of 2.7 ppm.

Qs Soil: This soil is described as occurring on volcanic rock of low relief and sparse vegetation (USGS, 2004). This could be consistent with Qs, as it is a stream channel deposit and could easily contain volcanic rock which frequently occurs in the mapping area. There are 2 data points within this soil.

	K (wt %)	U (ppm)	Th (ppm)
mean	1.6495	3.12	10.38
Standard deviation	0.4943	0.5515	0.8768
range	0.699	0.78	1.24
median	1.6495	3.12	10.38
mode	N/A	N/A	N/A

The soil has higher concentrations of U, K and Th. The soil unit has a mean K concentration of over ten times that of the median concentration of the rock unit, a mean U concentration about twice that of the median concentration of the rock unit, and a mean Th of almost 4 times that of the rock median.

Qs NURE Histogram:
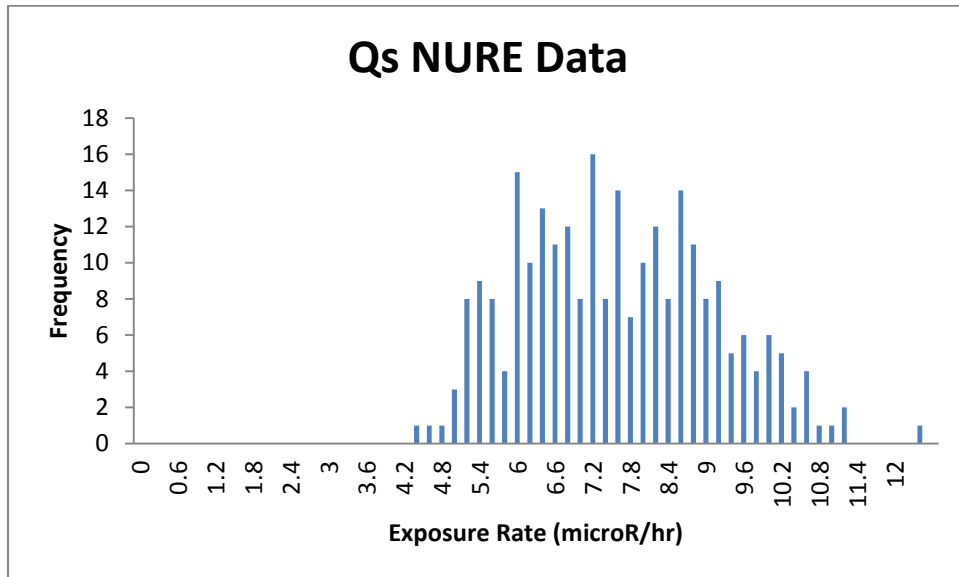
Qs AMS Histogram:
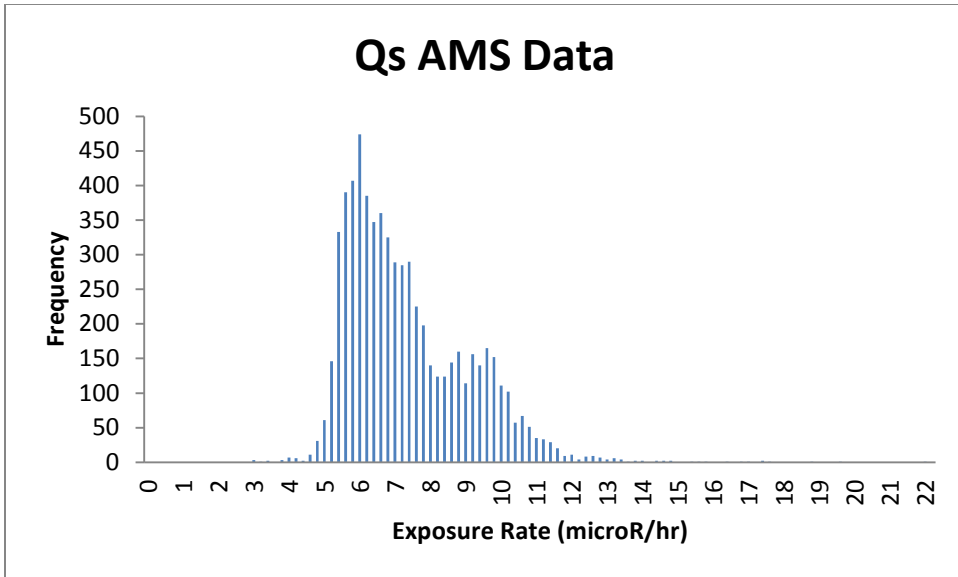
These histograms are almost within error. They both are right skewed, but the AMS histogram is significantly more so, which is probably causing the difference that is above error.

Qs 50 m buffer NURE Histogram:
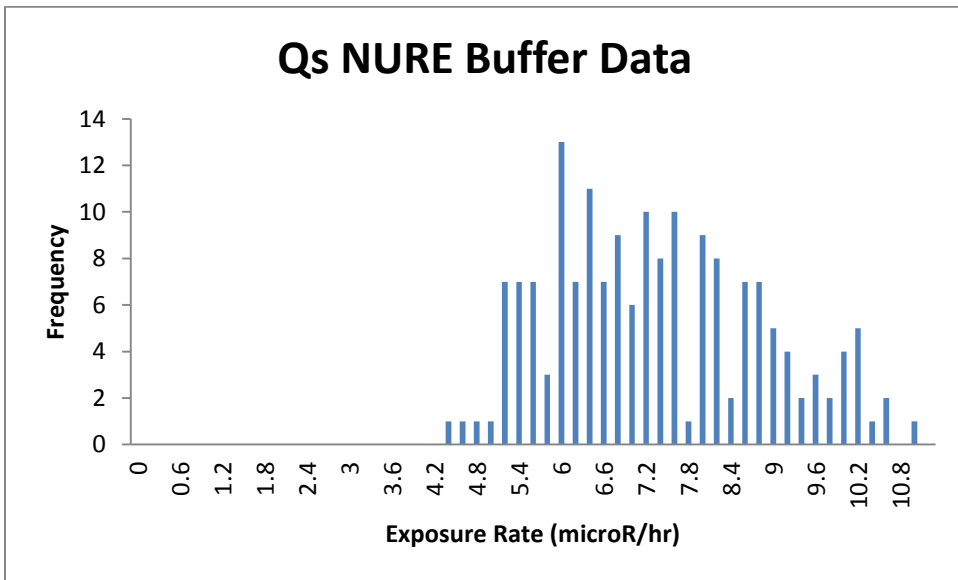
Qs 50 m buffer AMS Histogram:

Qs AMS Buffer Data
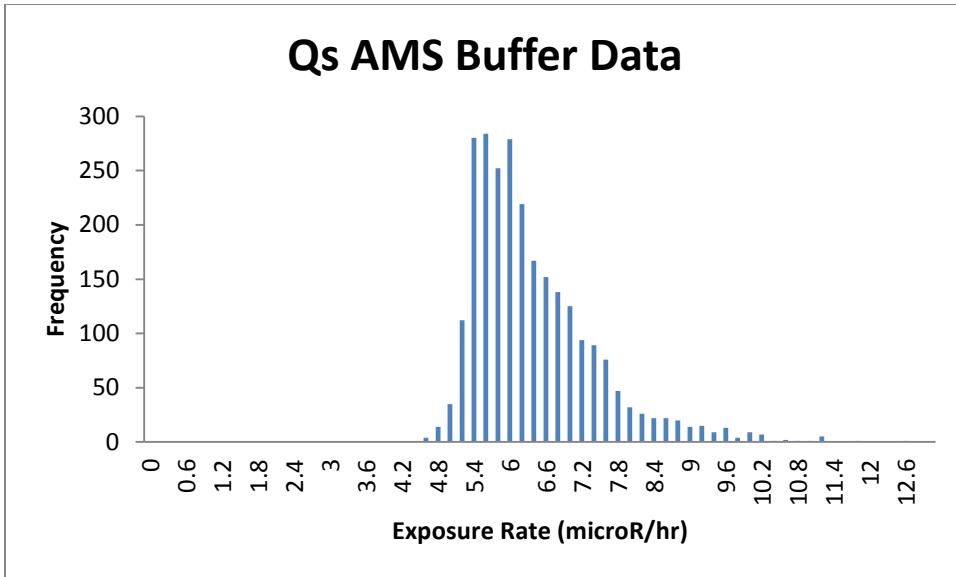
Qs AMS Distribution: This widespread alluvial unit shows clear trends. It is cooler in the southeast and gets warmer as one moves to the northwest, and overall is cooler in the Little Colorado River than it is in the tributaries. There is a stark contrast in the south between east and west of the river. There are also localized hot spots throughout this unit, some corresponding to uranium mines. The exposure rate range of this unit is from 3.634 to 16.368.

Qs AMS Exposure Rate Data
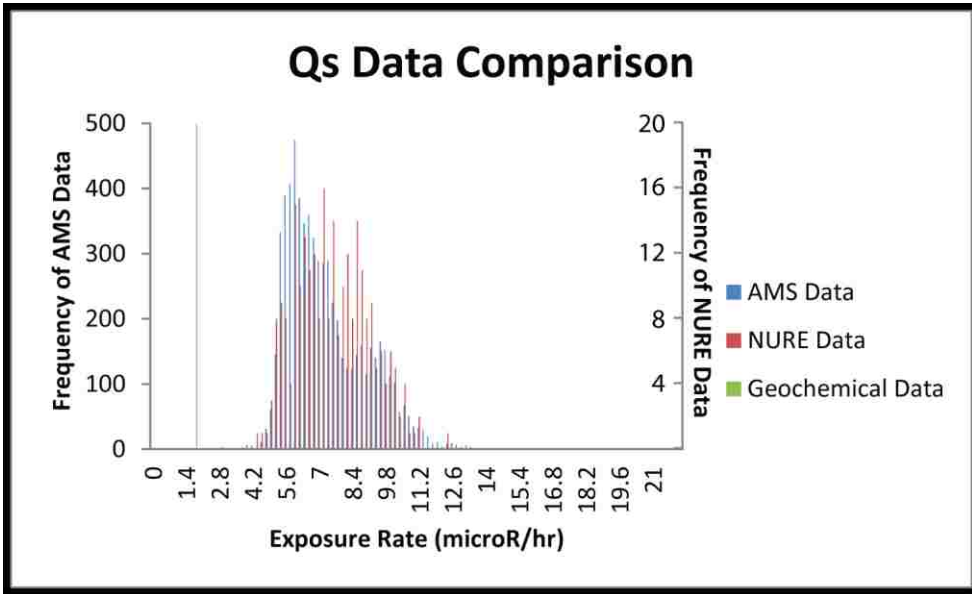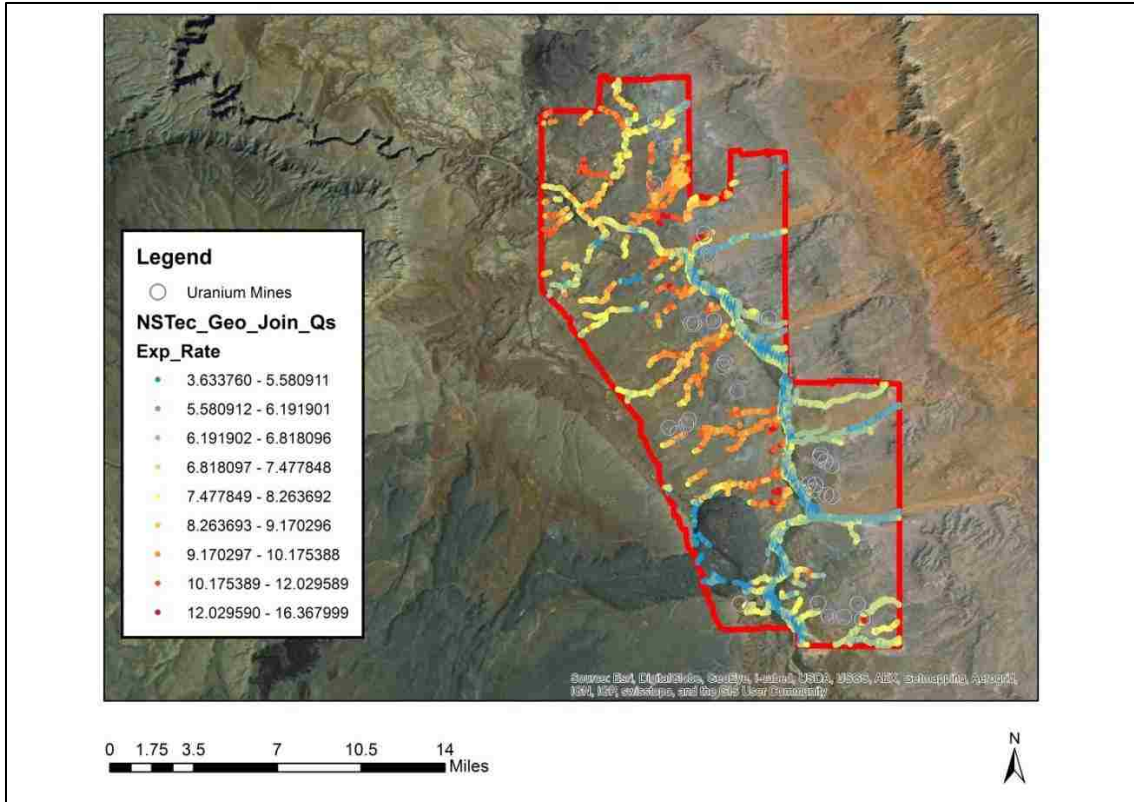
Qf: The USGS classifies this unit as Holocene flood-plain deposits of clay to sand size with little clay, it is partially cemented by gypsum and calcite (Billingsley et al., 2007). One point has a reported rock type of basalt, which is not consistent with Qf, so this point was eliminated. Thus there is only one data point for this unit from DIR. It is of an unidentified rock type and contains 1.1 ppm Uranium.

Qf Field Notes: Silty/clay dirt with no cement. Clasts of limestone, sandstone and chert. Not an even distribution in size, location or type of clasts. Medium to sparse vegetation. Some small aeolian dune build up in vegetation. No basalt. Exposed slightly mud cracked red brown soil. Few clasts of limestone and chert. Moderate shrubs.

　　　No basalt was seen in this area, consistent with eliminating the point labelled basalt. This unit was inconsistent with the USGS description as some clasts were present and we observed it to be mostly clay, the opposite of what is listed by the USGS. We also did not find it to be partially cemented as listed in the USGS description.

Qf NURE Histogram:
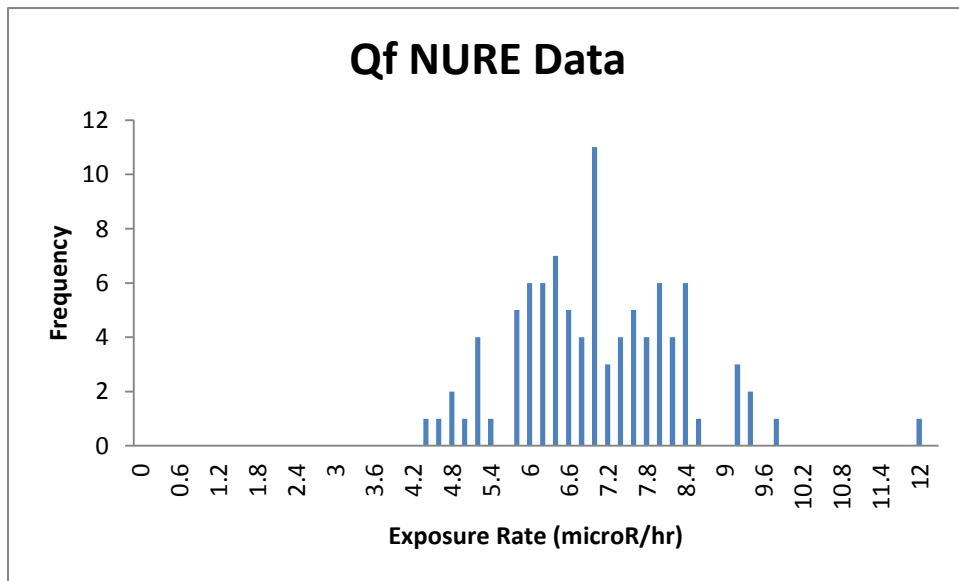
Qf AMS Histogram:
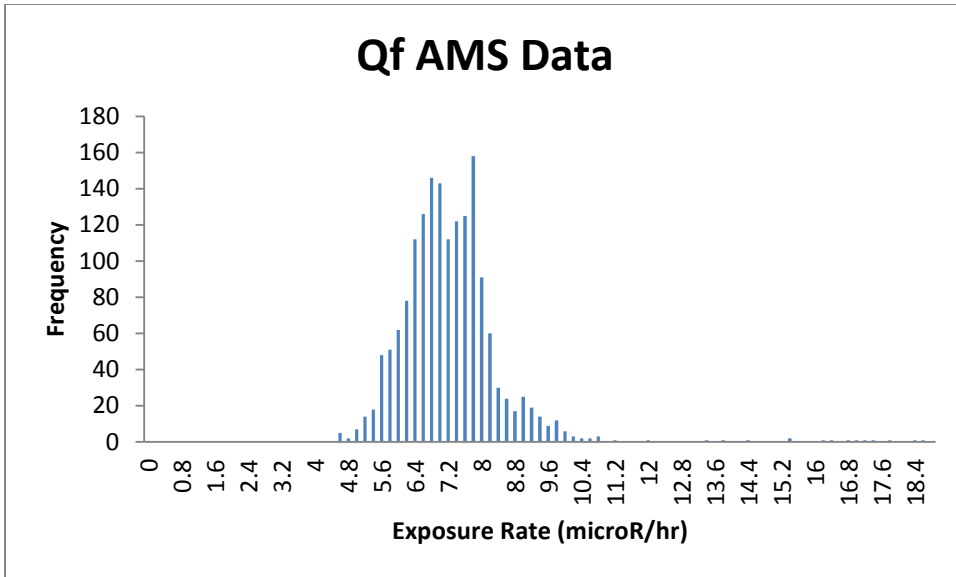
Qf AMS Data

The differences in means is probably due to the right-skewedness of the AMS data, however the medians do not appear to be within error either.

Qf 50 m buffer NURE Histogram:

Qf NURE Buffer Data
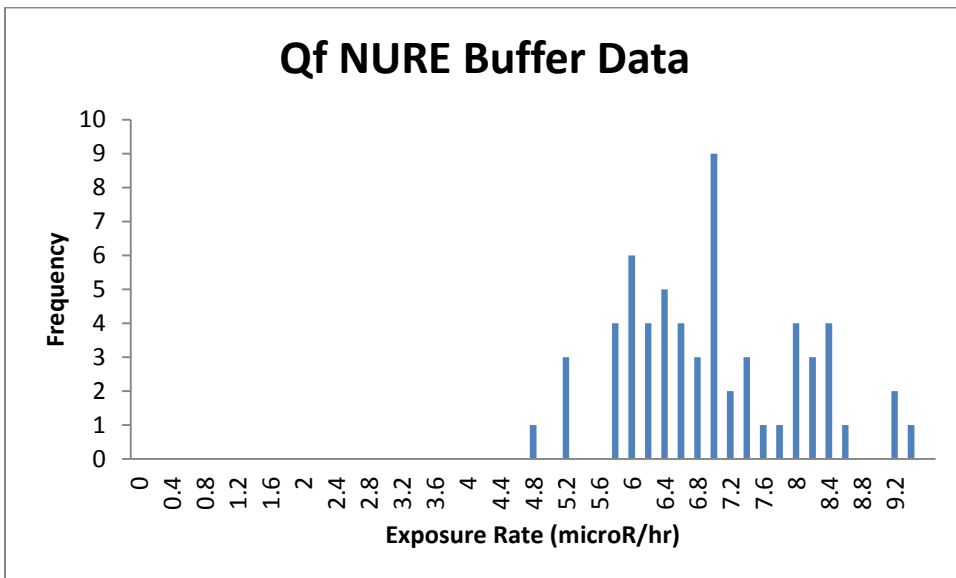
Qf 50 m buffer AMS Histogram:
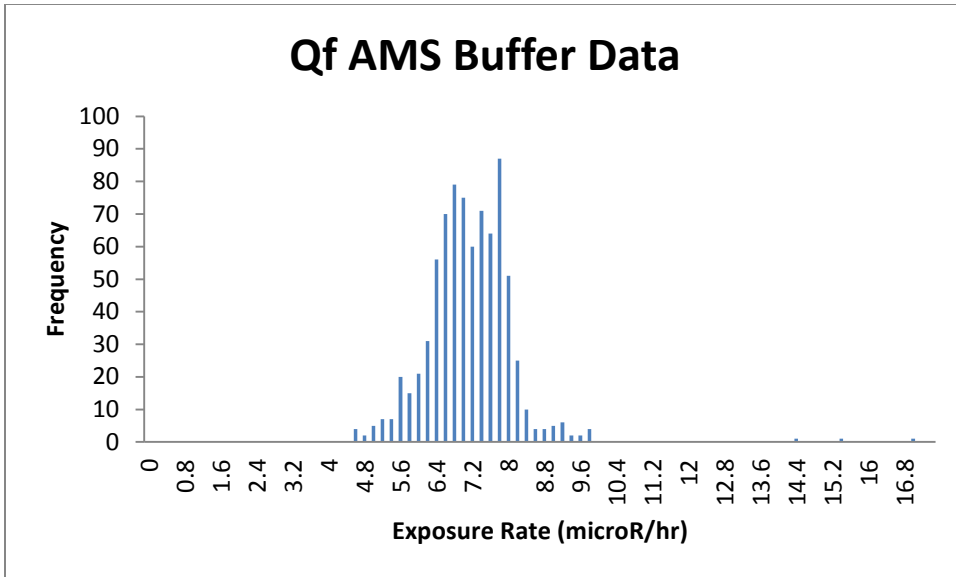
Qf AMS Distribution: This unit occurs mainly in the river bed, and the exposure rates do not display any overall trend. The range is from 4.477 to 18.43.

Qf AMS Exposure Rate Data

Qf Data Comparison
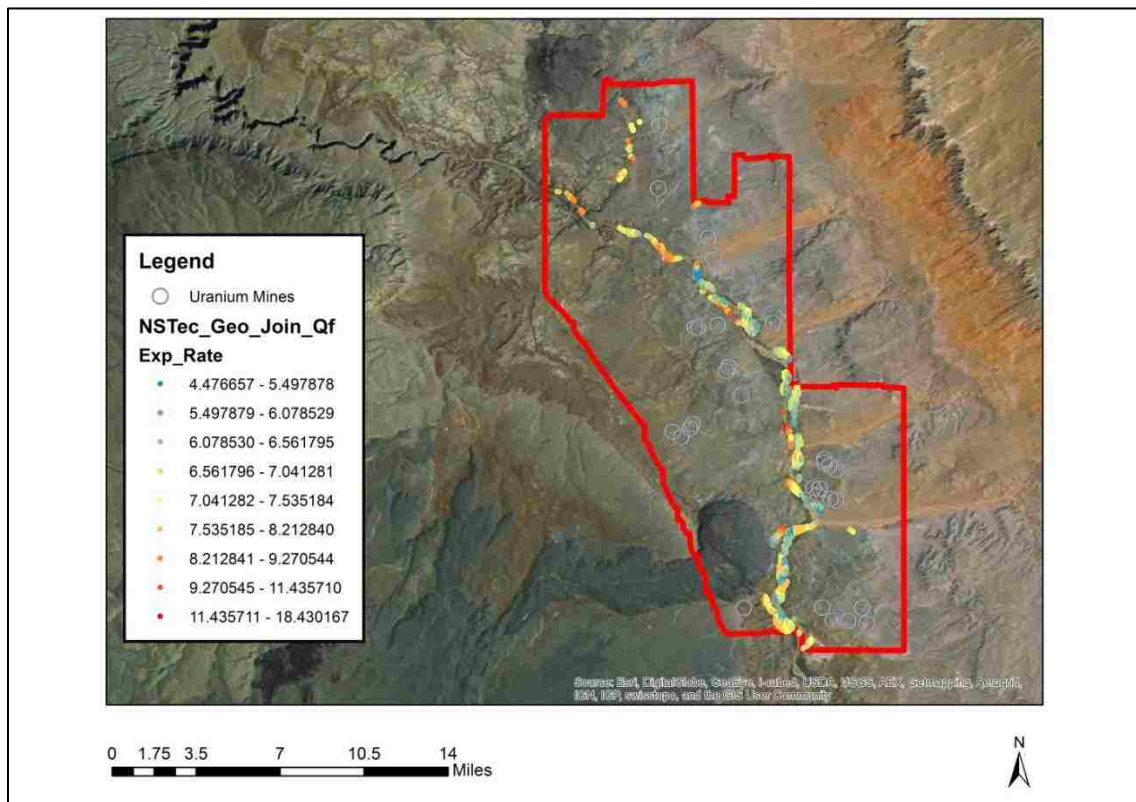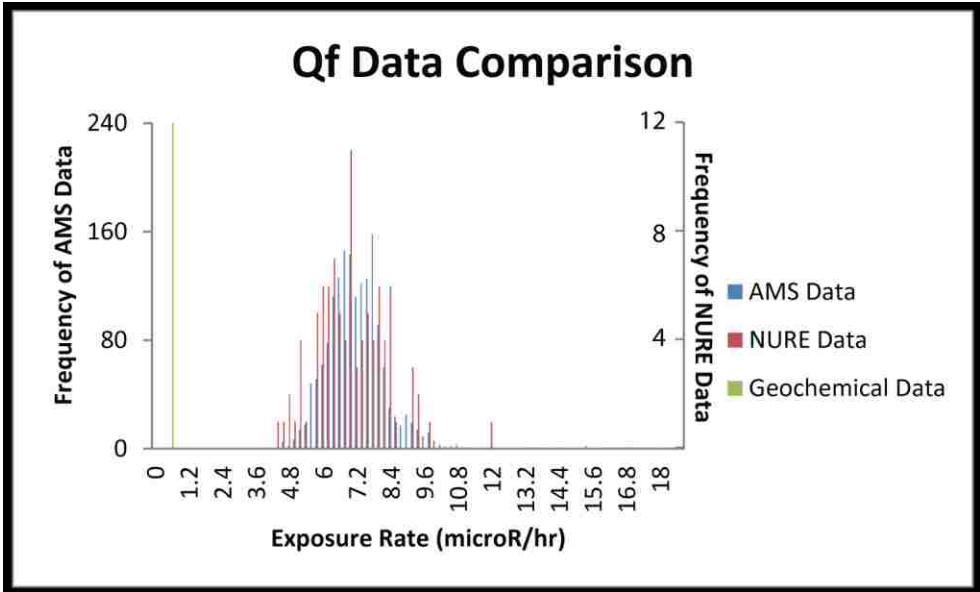
Qd: USGS classifies as Holocene age dune sand and sand sheets. Sand ranges from fine to coarse grained, and consists of quartz and chert from Pkh (Billingsley et al., 2007). We only have one data point for this unit from the USGS, it is listed as a glassy basaltic ash from the Lou-Lan interdune. This is consistent with Qd as a dune sand unit. The USGS only reported Potassium weight percent, and it is listed as 0.6973%. However, the composition of this data point is not consistent with a mainly quartz sand unit and thus may not be representative of Qd.

Qd Field Notes: Dune sands, very homogenous, asymmetrical ripples. Moderately vegetated. Sand is very fine, made up mostly of quartz (85%) and rock fragments (15%), grains are subrounded. No variation in unit. Eolian sand deposits. Dunes. Moderate to dense shrubs. Fine sand, light brown in color, no clasts.

These field observations are consistent with the USGS description of Qd as mostly quartz sand with some rock fragments. No ash was seen in the field as reported by the USGS rock database. This is the only data point for Qd, and should be removed, thus we will have no data for Qd.

Qd NURE Histogram:

Qd AMS Histogram:

Qd AMS Data

Frequency vs **Exposure Rate (microR/hr)**
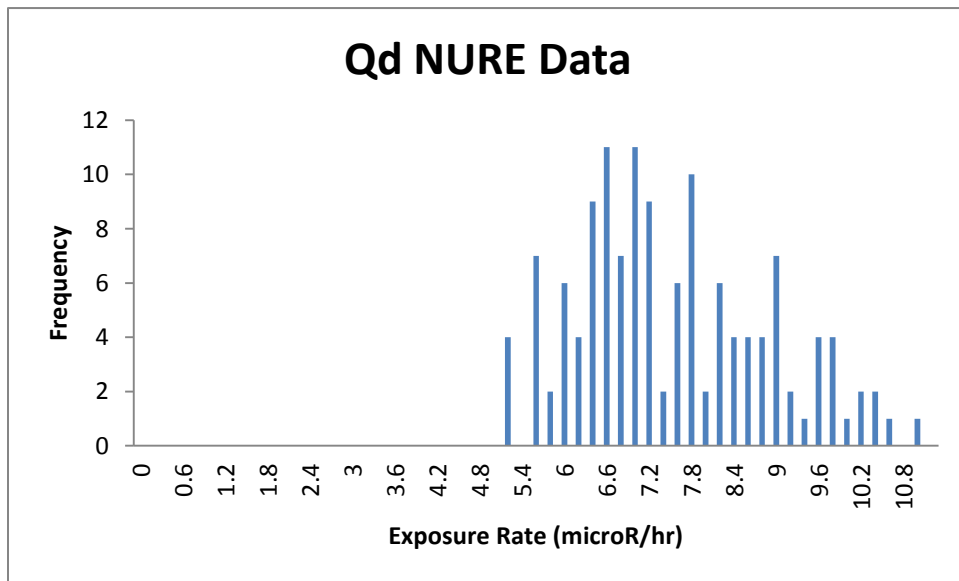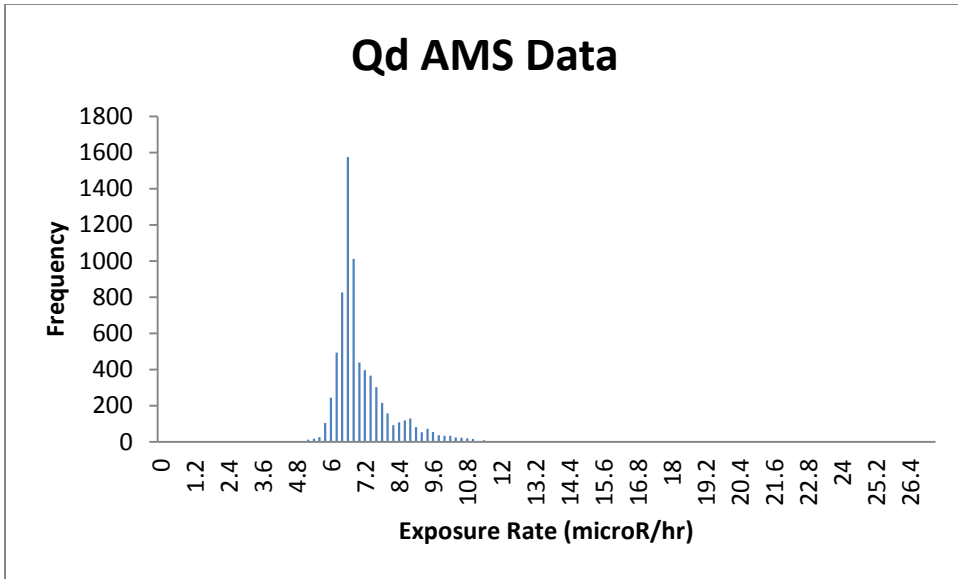
These histograms are pretty far off, neither the measured means of the observed means are close to one another. The mean difference can be explained by the AMS data being right skewed, but the observed median difference cannot.

Qd 50 m buffer NURE Histogram:

Qd NURE Buffer Data

Frequency vs **Exposure Rate (microR/hr)**
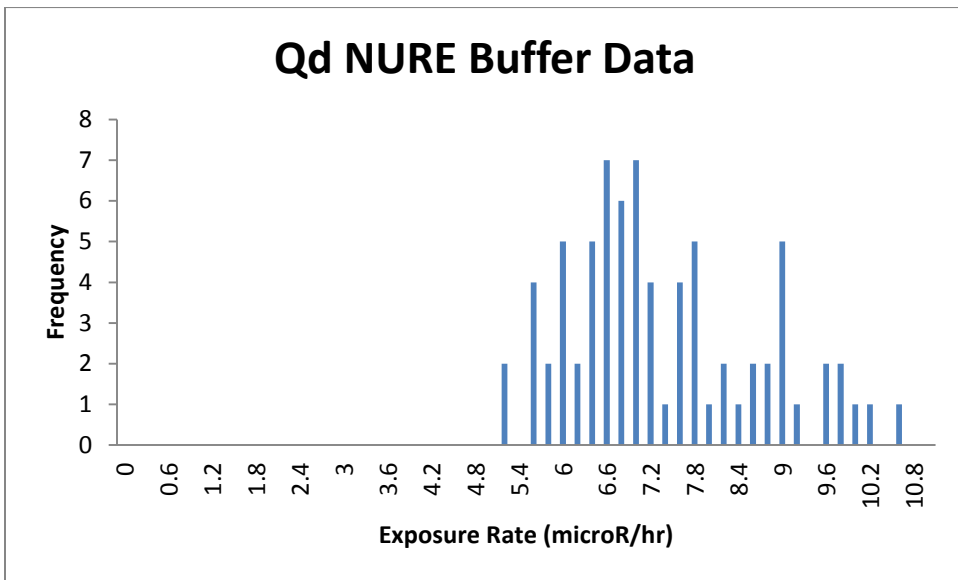
Qd 50 m buffer AMS Histogram:
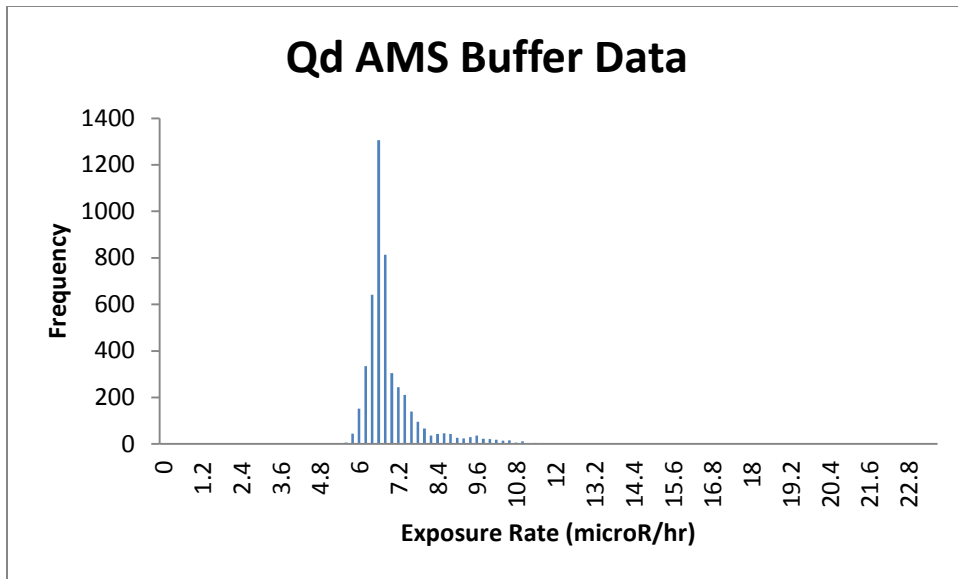
Qd AMS Distribution: This alluvial unit has a wide distribution and some distinct trends. On the east side of the map there are large cool alluvial fans. North of these alluvial fans are smaller very hot areas. On the west side of the map there's more of a random distribution of hotter points, though to the north west in the channels of the Little Colorado River the unit is cooler. Overall this unit has a wide range, from 4.693 to 26.84.

Qd AMS Exposure Rate Data
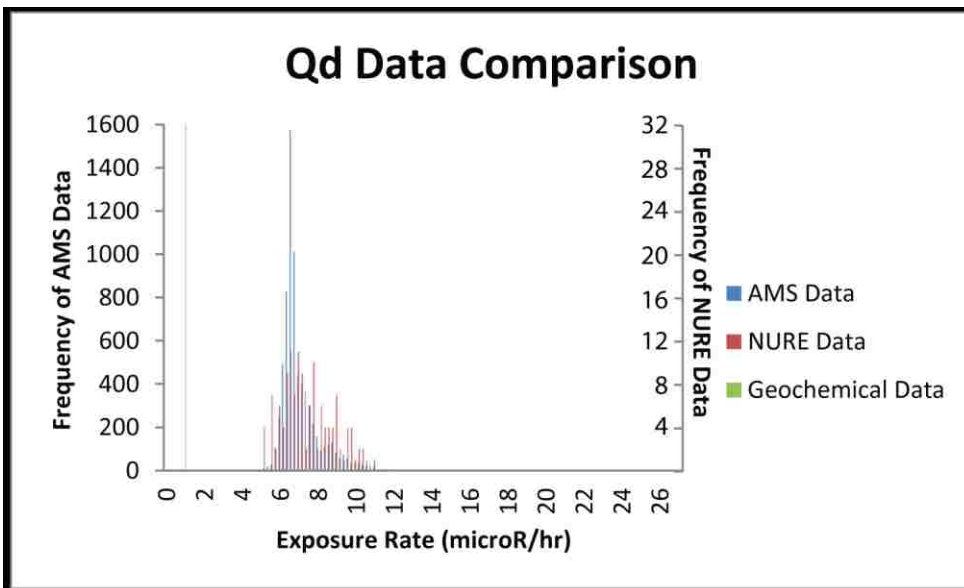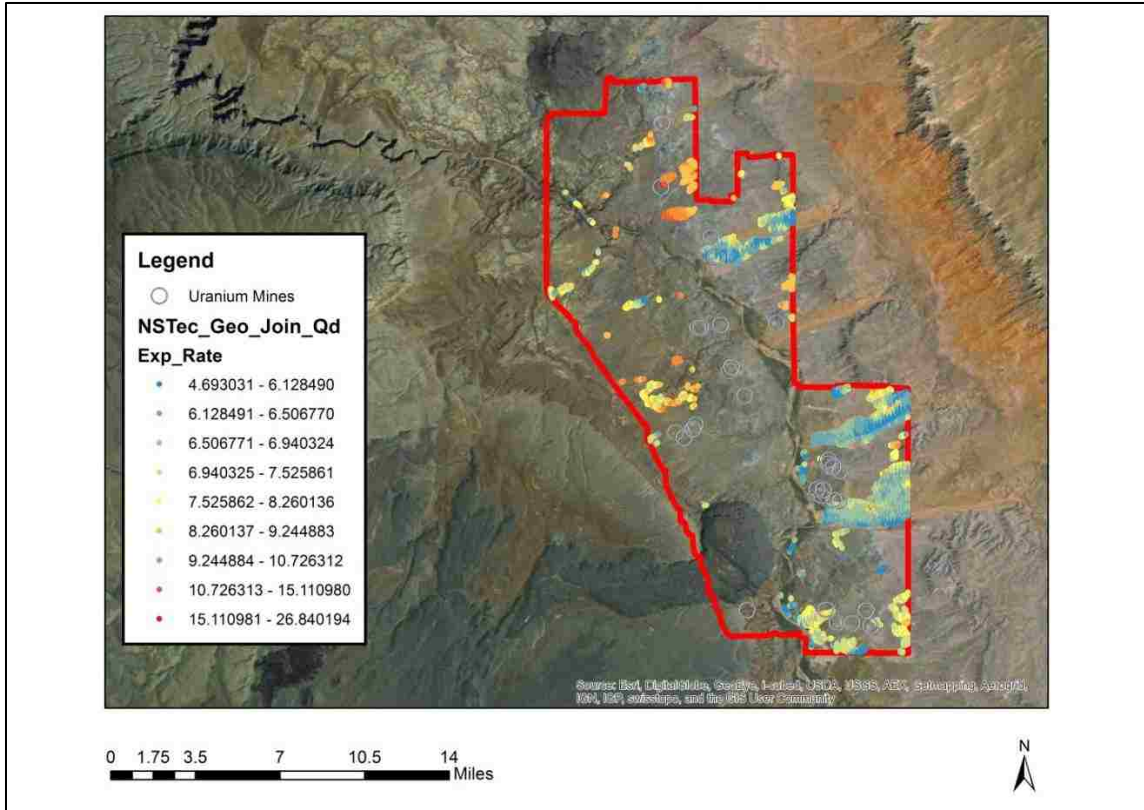
Qes: This unit is extremely similar to Qd, it is classified by the USGS as late Holocene eolian sand sheets consisting of fine to coarse quartz and chert from Pkh (Billingsley et al., 2007). We only have one point from this unit from DIR with 1.5 ppm Uranium.

Qes cool (on basalt) Field Notes: Mostly basaltic sand to aeolian material. Basalt clasts vary from smoothed to angular. Vary in size from fist to sand. Mostly basaltic sand with small basalt clasts. Some eolian material but less than Ts. Moderate to sparse grasses

Qes hot (off basalt) Field Notes: All fine grained material, lacks clasts, no basalt. The amount of vegetation varies from little to medium. Based on sand filling in plants, highly aeolian area. The sand is composed of: basalt, quartz (dominate), feldspar, limestone. Sand varies greatly. Coarse to fine grained. Mud cracks present in some areas.
Fine grained sand and alluvium. No clasts at all. Sand is red to black but dominately red. Moderate grasses and bushes.

Qes hot is more consistent with the USGS description, as it contained all sand, whereas Qes cool contained clasts of basalt, which are not mentioned. Units on the basalt flow are significantly different than off and are not included in the USGS descriptions. Both locations included aeolian sand deposits consistent with the USGS description. Qae cool is mostly likely cooler than Qae hot due to the large presence of basalt.

Qes Soil: This soil is described as occurring in a flat desert scrub environment on a mafic volcanic rock (USGS, 2004). This is not consistent with Qes which is a eolian sand unit. However, basalt occurs widely within the mapping area so it is within reason that some basalt could be within this eolian unit, or the unit could be overlaying basalt, and the basalt could be exposed in some areas. The soil sample had a U concentration of 2.2, and a Th concentration of 9 ppm. The differences between rock and soil could be due to the fact that there is only one data point for each.

Qes NURE Histogram:
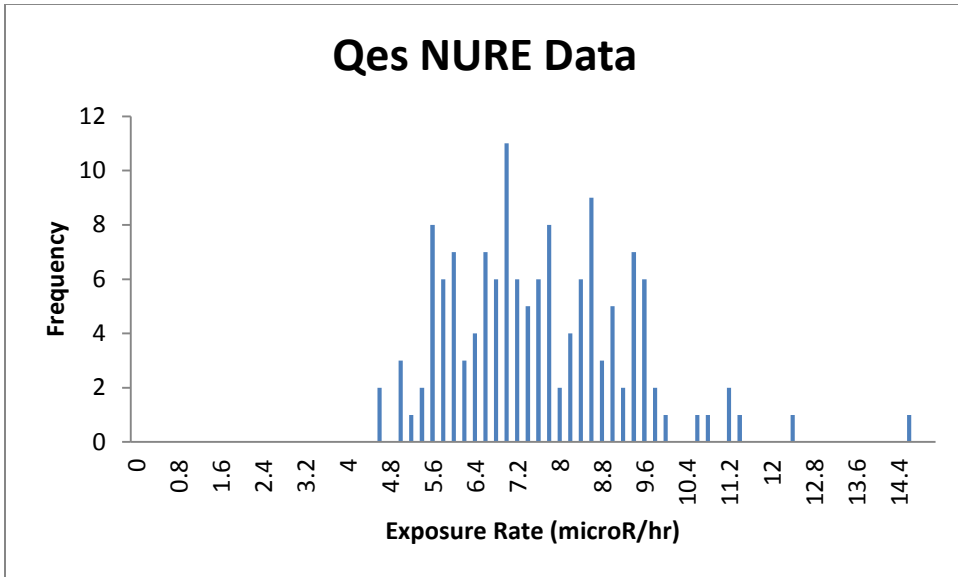
Qes AMS Histogram:
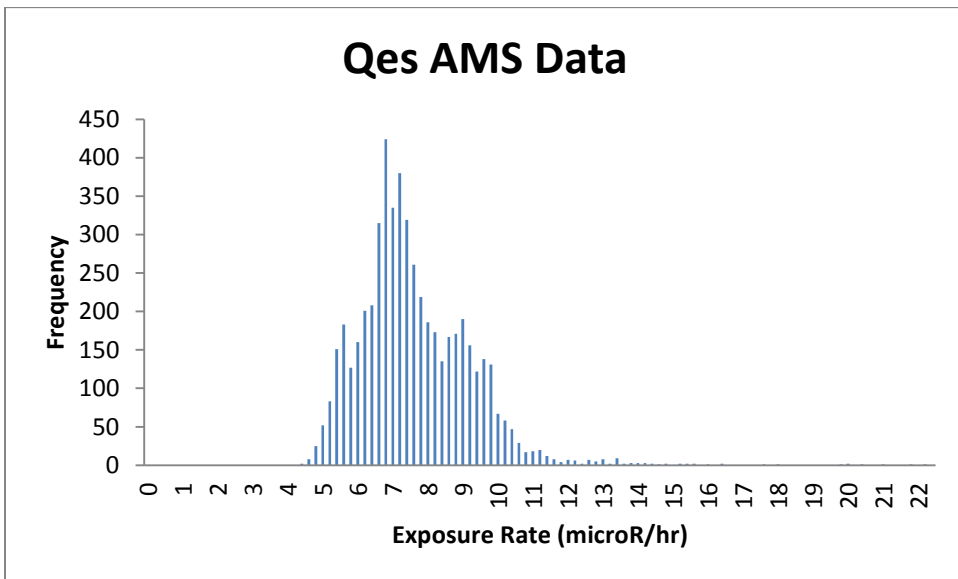
The observed medians between these two histograms look similar. The difference in mean, which is above error, can be explained by the right skewed AMS Histogram.

Qes 50 m buffer NURE Histogram:

Qes NURE Buffer Data

(Histogram: x-axis "Exposure Rate (microR/hr)" from 0 to 14.4 in 0.6 increments; y-axis "Frequency" from 0 to 7.)
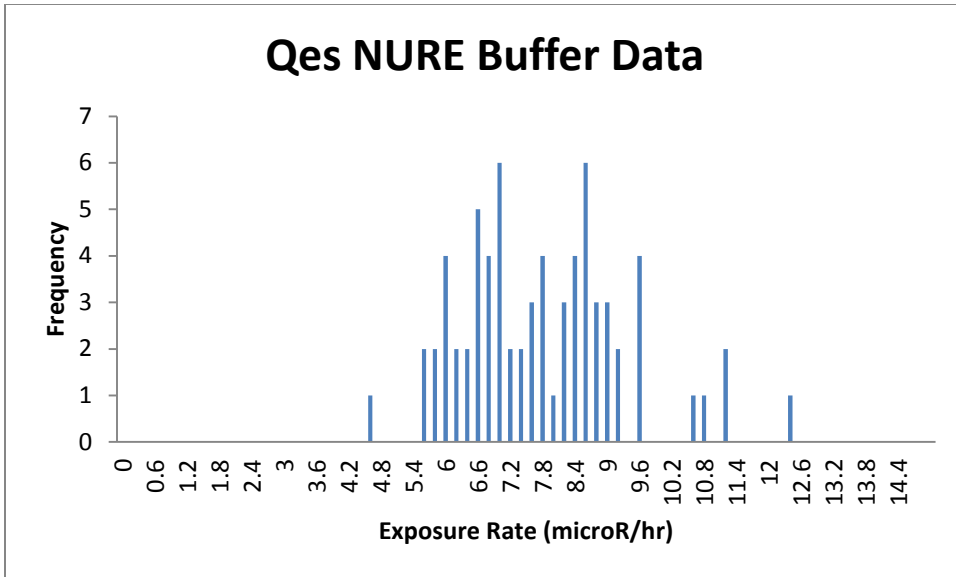
Qes 50 m buffer AMS Histogram:

Qes AMS Buffer Data

(Histogram: x-axis "Exposure Rate (microR/hr)" from 0 to 22; y-axis "Frequency" from 0 to 300.)
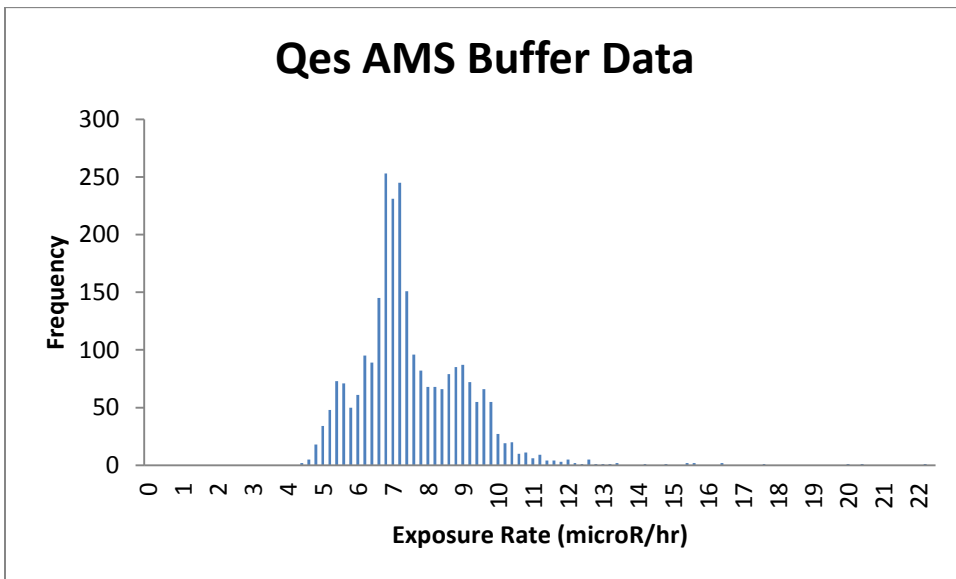
Qes AMS Distribution: This alluvial unit has a wide distribution across the area. There is an observed trend that this unit is cooler in the southeast and gets hotter to the northwest, but this is overly generalized as there are many localized hot and cold areas. The range of this unit is from 4.304 to 22.089.

Qes AMS Exposure Rate Data
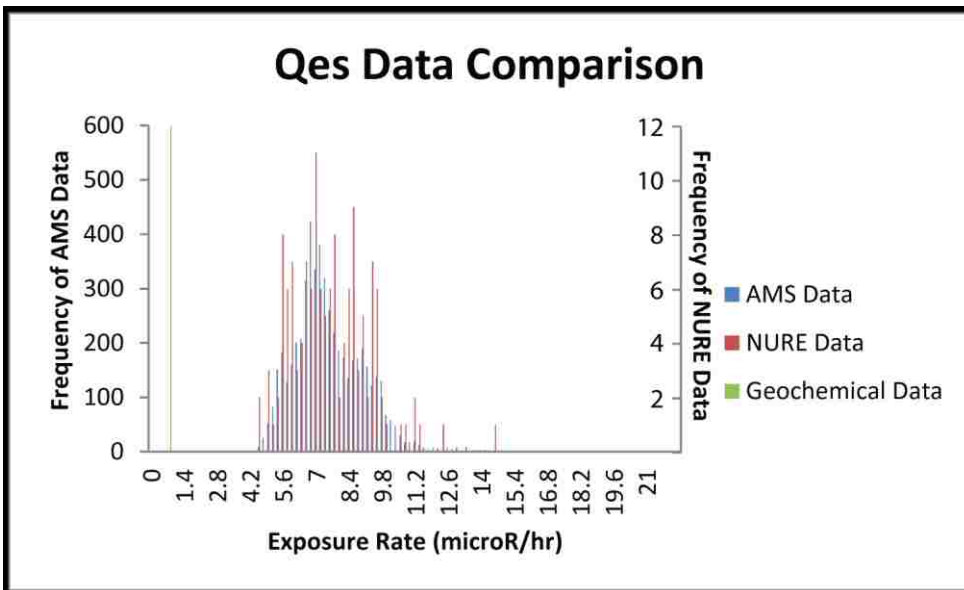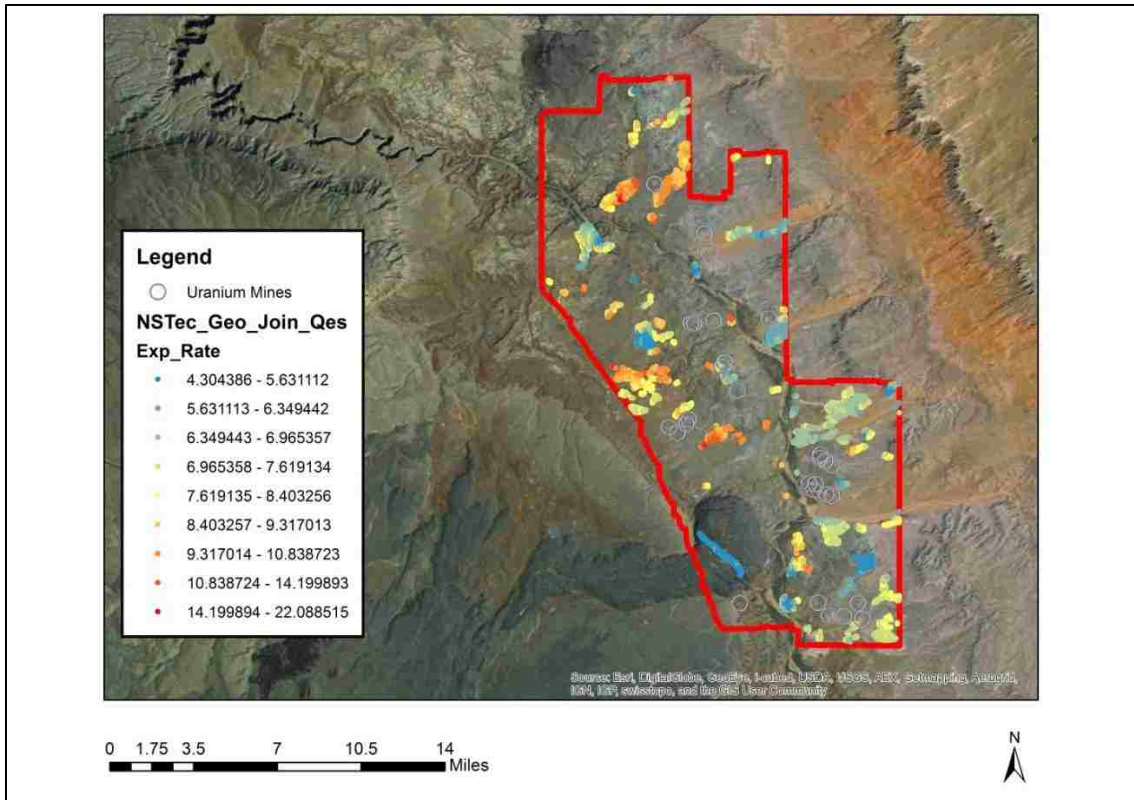
Qg1: These deposits are classified by the USGS as late Holocene terrace-gravel deposits, with silt to boulder sized clasts of sandstone, chert, and limestone of local origin occurring throughout the unit. This unit changes throughout the mapping area with basalt becoming dominant in the south. The unit report also states that clasts of metamorphic rocks such as quartzite appear in the southeast but I've concluded this is outside our survey area (Billingsley et al., 2007). There are 2 data points in this area from NAVDAT and DIR. One point is specified as a basalt, which is consistent with Qg1, and has 1.0875 wt % Potassium. The other point is of an unspecified rock type with 1.9 ppm Uranium.

Qg1 North (cool) Field Notes: Light sand color matrix. Clasts of chert, sandstone, and limestone. Border of this unit is being heavily affected by the sand dunes next to it. Adding more matrix. Medium vegetation, but mostly dead. Clasts are mostly subrounded. Nothing like Qg1 south. Possible petrified wood. Sample taken. Gravel studded surface, weak pavement. Gravels intermixed with eolian sands, gravel composed of sandstone, limestone, and cherts. Small shrubs moderately dispersed.

Qg1 South (hot) Field Notes: No clasts of any kind. Brown-red clay with mudcracks, thick clay. Medium vegetation. Small crystals of gypsum in dirt. Very different from other Qgs.
Mud cracked surface, no clasts, consists of red silt. Moderate thorn bushes with some tall bushes or short trees.

No clasts of basalt were seen in this unit, which is not consistent with the USGS description or database. The hotter Qg1 contained no clasts at all, which is not consistent with a gravel unit. The cool Qg1 is consistent with sandstone, chert, and limestone clasts as in the description. It is strange that the hotter unit contains no clasts at all, the radiation difference may be coming from the clay itself then.

Qg1 NURE Histogram:
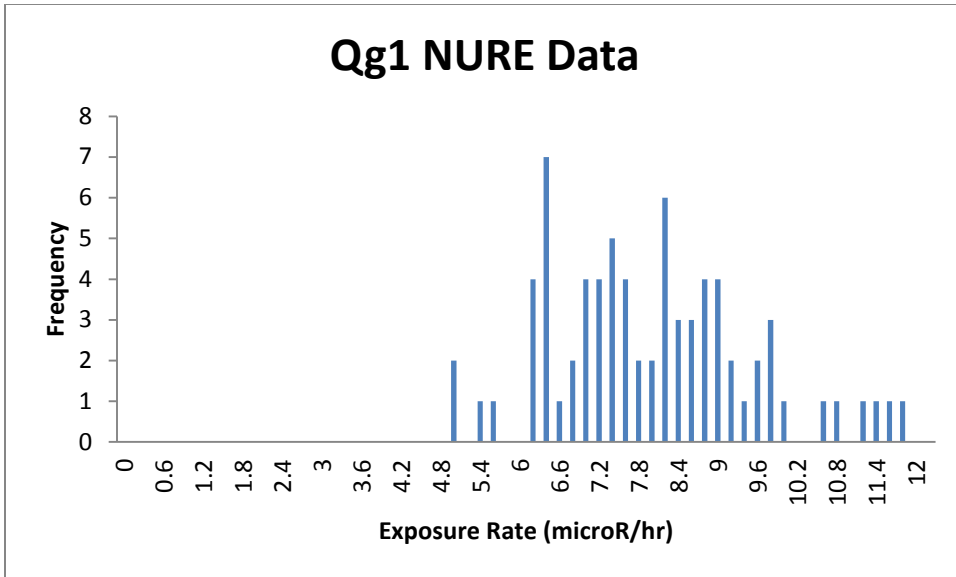
Qg1 AMS Histogram:
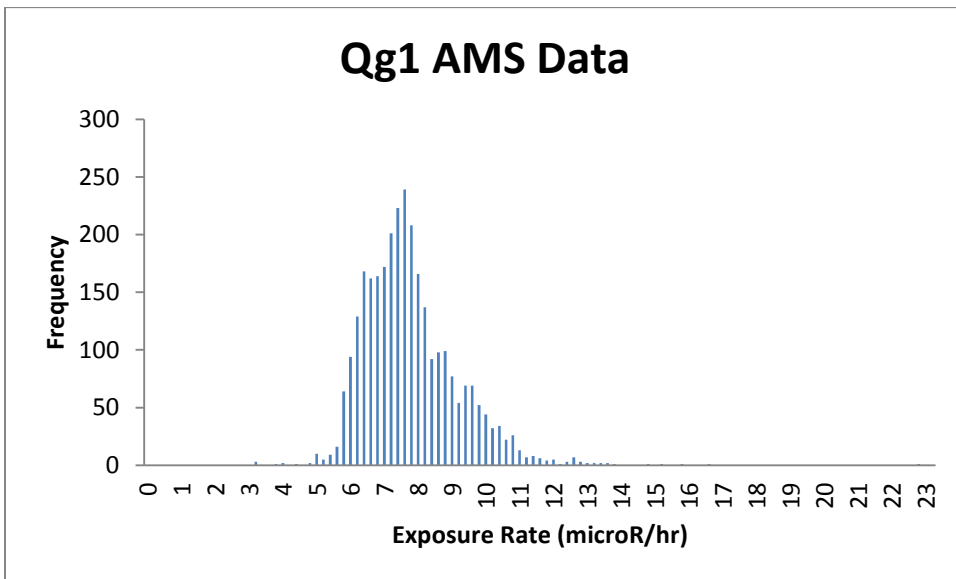
The NURE data does not have a well-developed curve, perhaps there aren't enough data points. The differences between the means are outside of error and most likely due to the right skewedness of the AMS data.

Qg1 50 m buffer NURE Histogram:

Qg1 NURE Buffer Data

Frequency vs Exposure Rate (microR/hr)
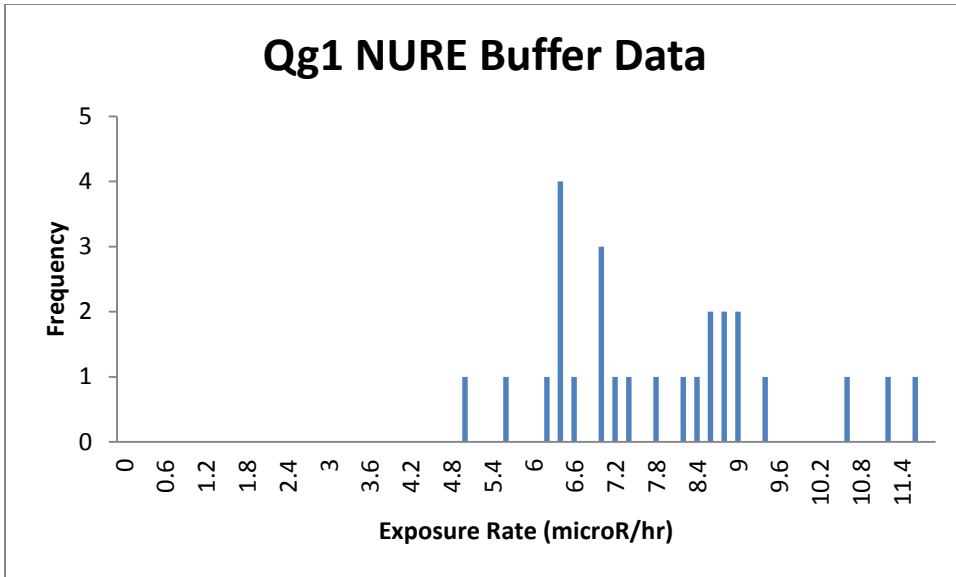
Qg1 50 m buffer AMS Histogram:

Qg1 AMS Buffer Data

Frequency vs Exposure Rate (microR/hr)
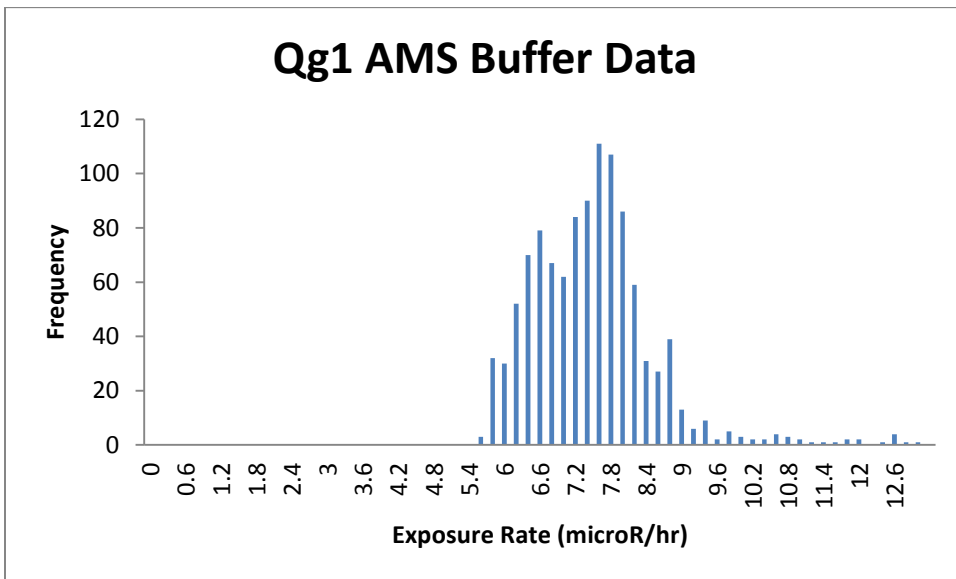
Qg1 AMS Distribution: This unit occurs mostly along the river and its 'tributaries'. The west side of the river is in general hotter than the east side, this is especially obvious in the south. The tributaries west of the river are hotter than those of the east. The range of this unit is from 4.355 to 22.724.

Qg1 AMS Exposure Rate Data

106
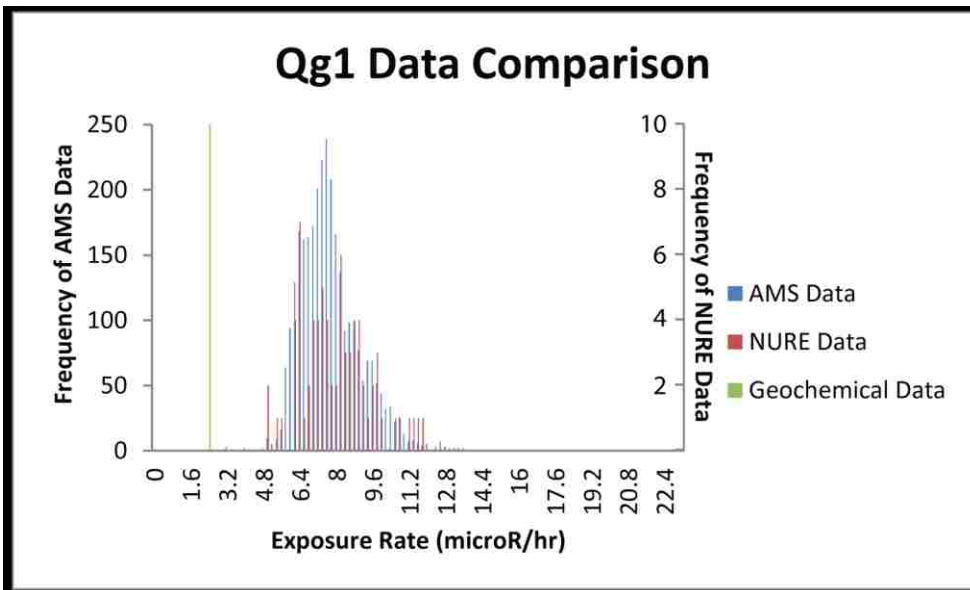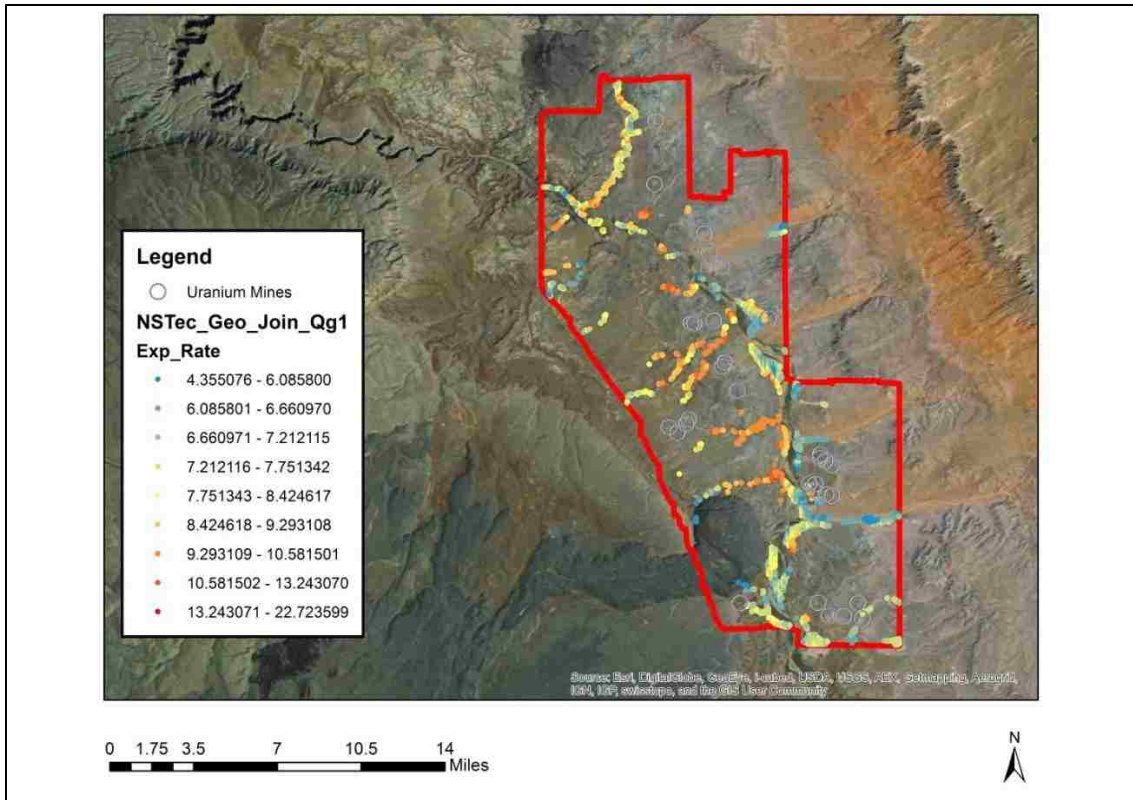
Qa1: Holocene alluvial fan deposits, grain size varies widely (silt to boulder). The composition depends on what area of the survey the deposit is from. To the north it consists of limestone, chert and sandstone clasts from nearby Triassic and Permian units. To the south the USGS states it is dominated by basalt, andesite and pyroclastic fragments (Billingsley et al., 2007). This large variation in composition based on location suggests we should divide this unit into two different radioelement contents, instead of averaging all of the points together. There are 4 rocks identified as basalt, and 4 as sandstone, the other 9 points are unidentified. We could also act on the assumption that all points from DIR are sandstone. The basalt points, which occur farther south than the sandstone points, only have K measurements, with an average of 0.88 K wt %, while the 4 sandstone points have an average of 0.73 K wt %. DIR measurements of K are not being considered. Once multiple measurements from the same rock sample were eliminated, we have 17 data points in this area from the USGS, DIR and NAVDAT. Recorded rock types include basalt, sandstone and arkose, which is consistent with the USGS unit description.

Qa1 Field Notes: Gravel with some sand (mostly sticking to plants, aeolian). Random large basalt float present. Very hard surface under gravel. Gravel is mostly sub angular. Gravel is mostly chert, with some basalt, quartz and sandstone.
Gravels with some sand Coppice dunes around sparse grasses. Gravels less than 5 cm composed of basalt, chert. Hard mud cracked surface under thin gravel layer.

This field observations of chert, sandstone and basalt clasts are consistent with the USGS description and database.

	K (wt %)	U (ppm)	Th (ppm)
mean	0.9341	37.0208	11.9
Standard deviation	0.5063	88.1206	1.2728
range	1.8375	291	1.8
median	0.8800	1.8	11.9
mode	0.8800	1.8	N/A

The median values again are a better representation of the data than the mean for radioelement concentration due to high U concentrations.

Qa1 K wt %

Qa1 U ppm
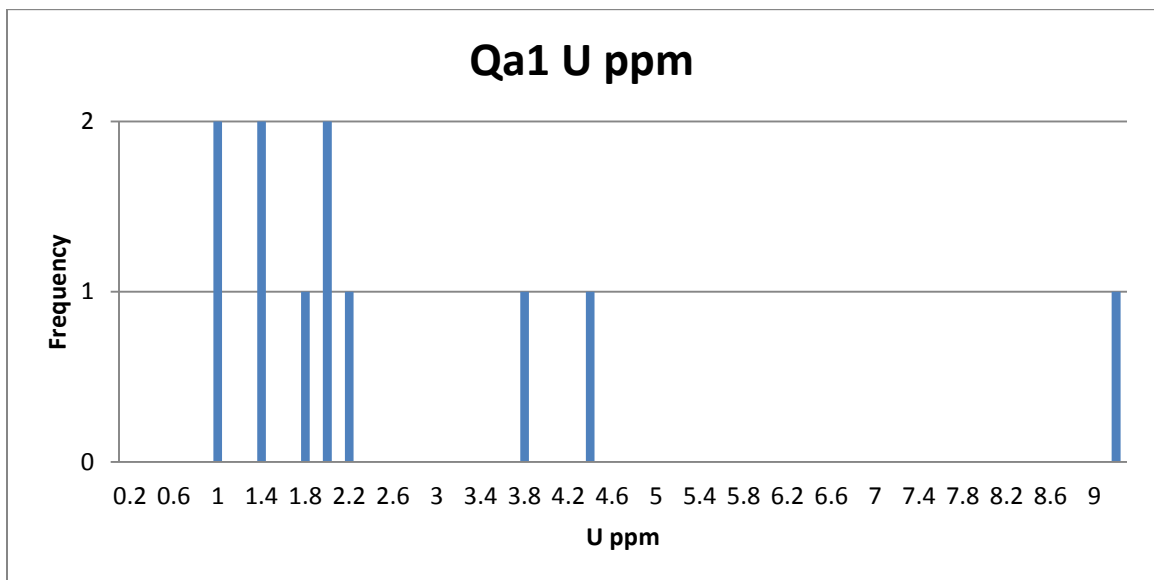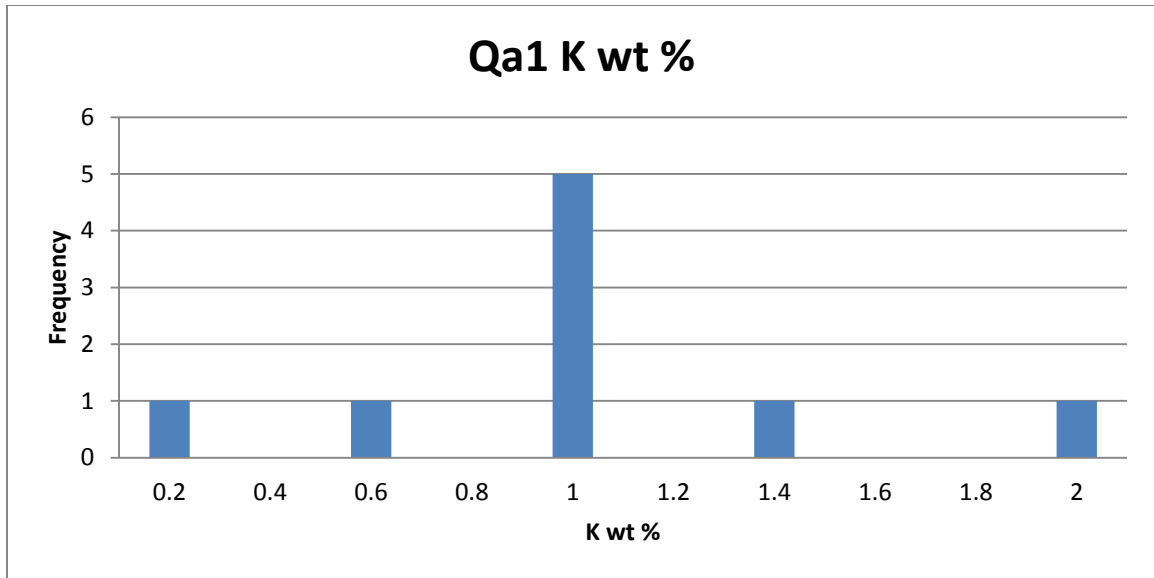
There are 4 outlier values for Uranium of 150, 160, 270, and 292 ppm. These are all values reported by the USGS in the same location in arkose and other unidentified sedimentary rocks.

There are only two Th values of 11 and 12.8 ppm.

Qa1 Soil: This soil is described as low relief, coarse to fine grained gray sand, with sparse vegetation. The soil is reported to be on top of unconsolidated valley fill, felsic and mafic igneous rock, and shale (USGS, 2004). Because this is an alluvial rock unit, all these rock types are possible as they occur in and around the mapping area, though shale is not specifically listed in the USGS description. There are 8 data points from the USGS all collected for NURE.

	K (wt %)	U (ppm)	Th (ppm)
mean	1.5469	2.7575	8.8633
Standard deviation	0.4727	1.2531	2.9402
range	1.159	3.64	7.7
median	1.799	2.915	8.53
mode	1.9	N/A	N/A

Comparing these mean concentrations to the median concentrations of the rock unit, U and K are higher within the soil. For K this is by a less than a factor of 2, though there are values within the rock unit that record K values this high. For U there's a difference of less than 1 ppm. For Th the median value in the rock data is higher than the average value in the soil.
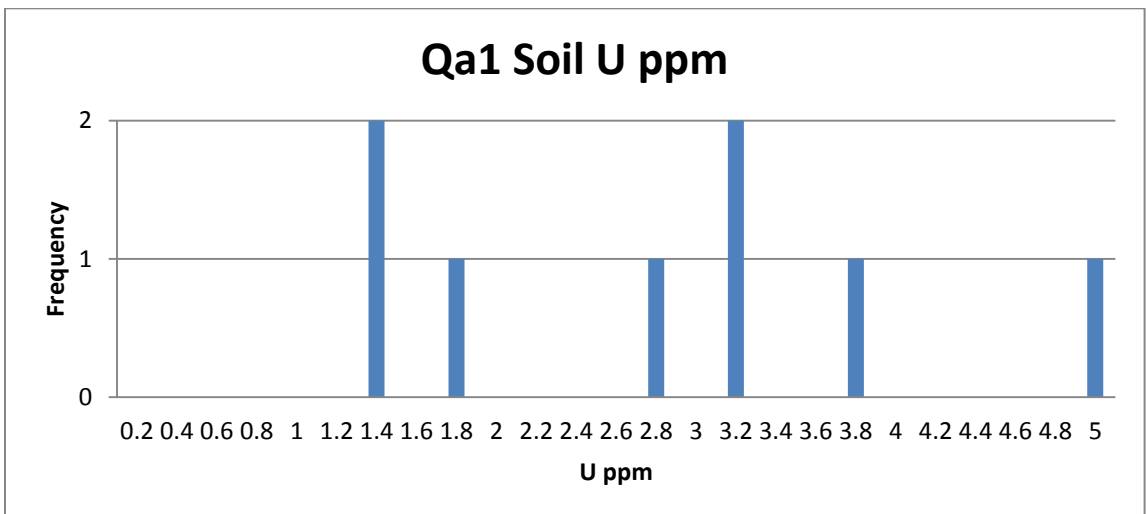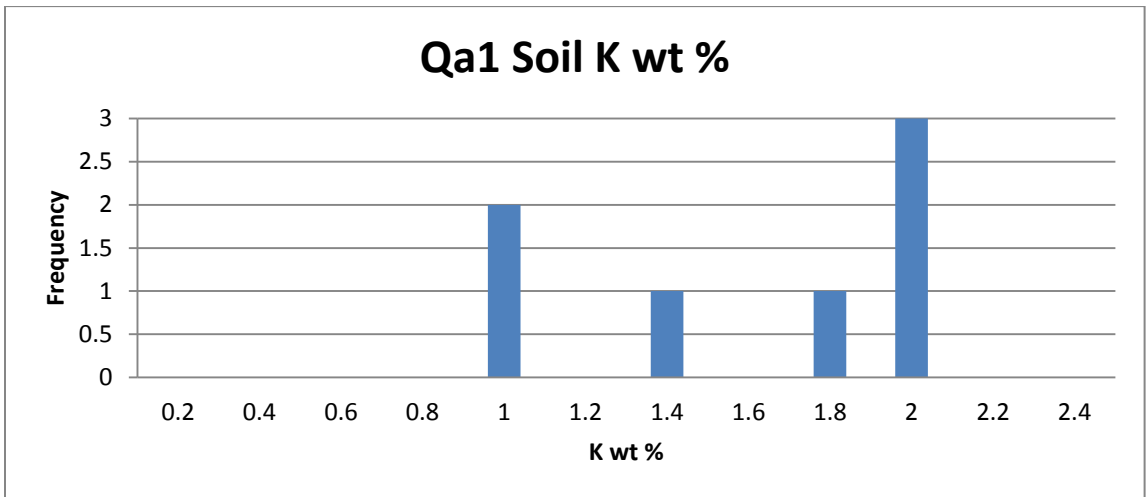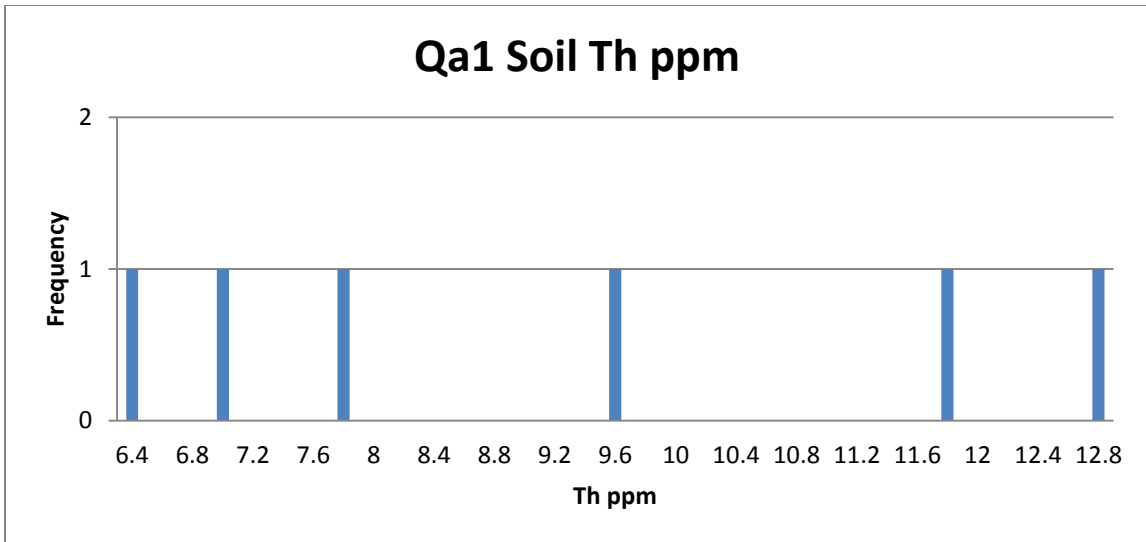
Qa1 NURE Histogram:
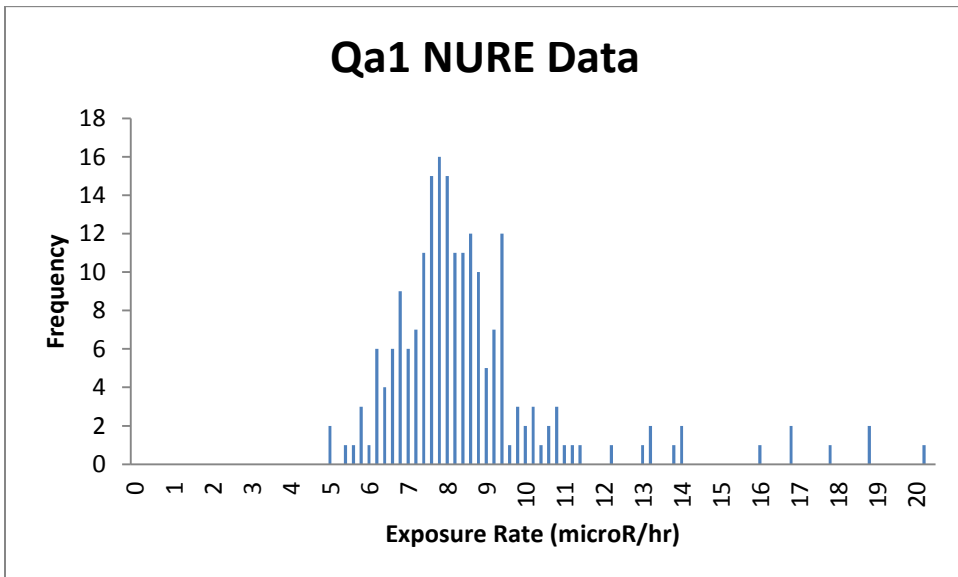
Qa1 AMS Histogram:

Qa1 AMS Data
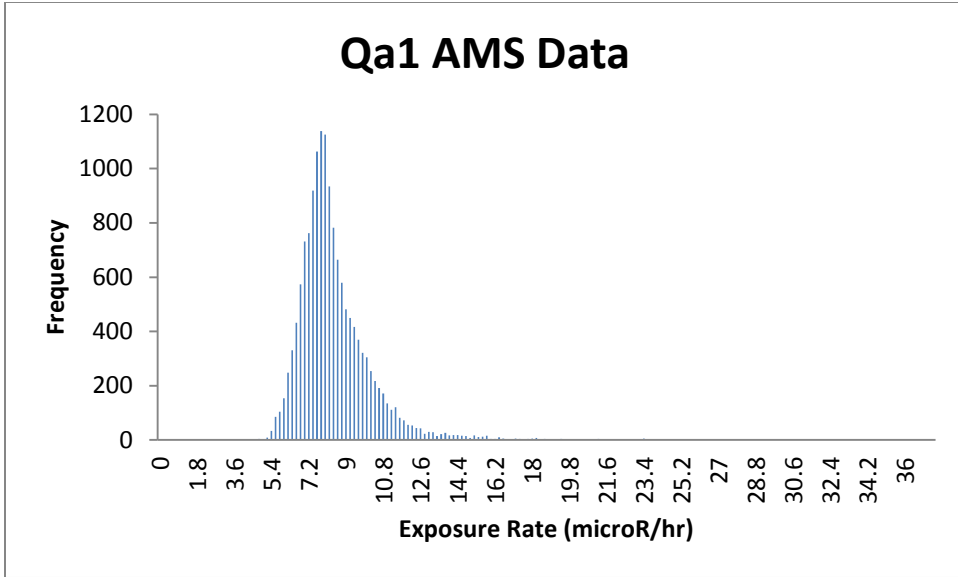
This unit has similar histograms, both are right skewed with averages of about 8. While the differences of the means are not within error, this could be due to the fact that the AMS data is more skewed, with highs more than twice that of the NURE data.

Qa1 50 m buffer NURE Histogram:

Qa1 NURE Buffer Data
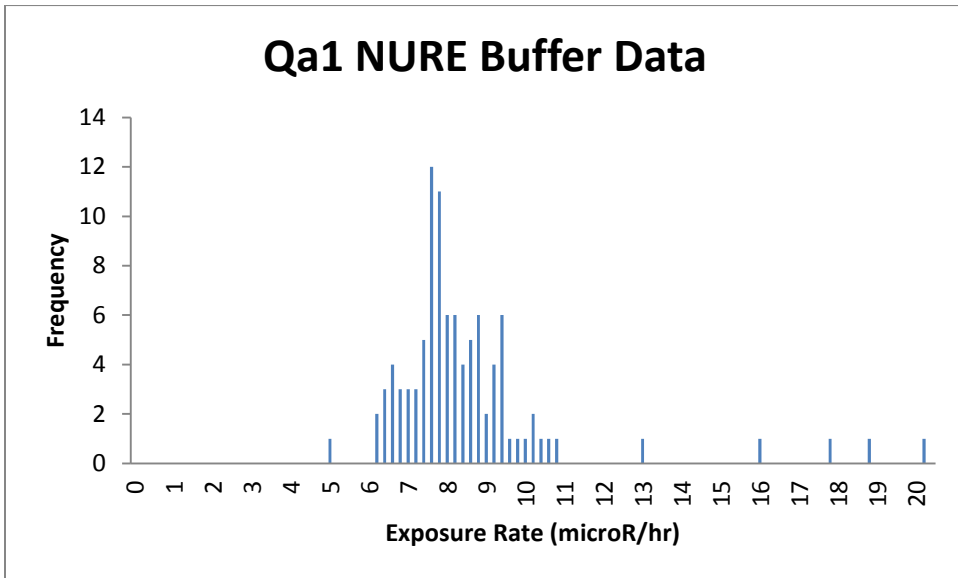
Qa1 50 m buffer AMS Histogram:
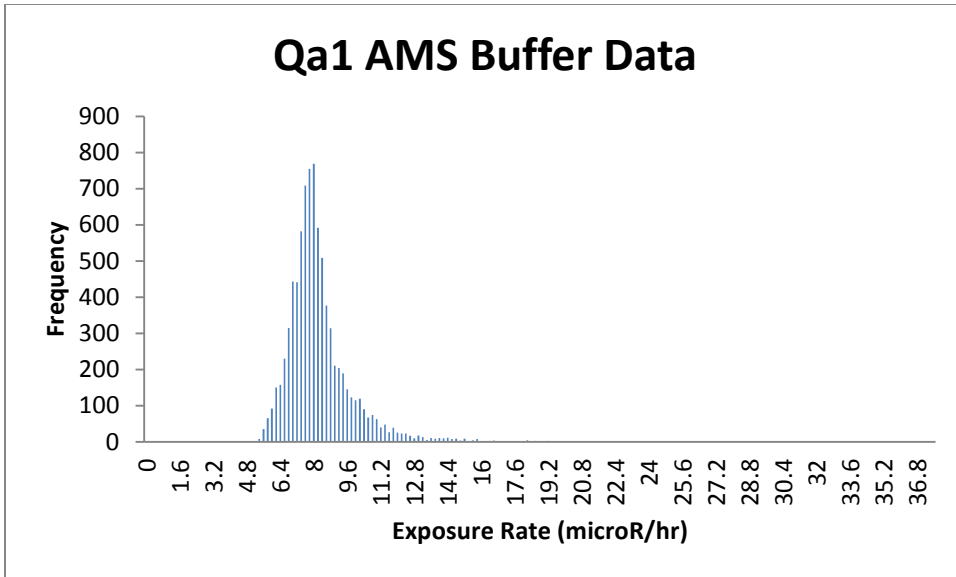
Qa1 AMS Distribution: This is a widespread alluvial unit, so high amounts of variation is expected. We can see that in the east on the alluvial fans this unit is cooler, and even in the north, east of the river is overall cooler than the west. There are localized hot spots, some of them categorized by uranium mines. The exposure rate range of this unit is large, from 3.688 to 37.191

Qa1 AMS Exposure Rate Data
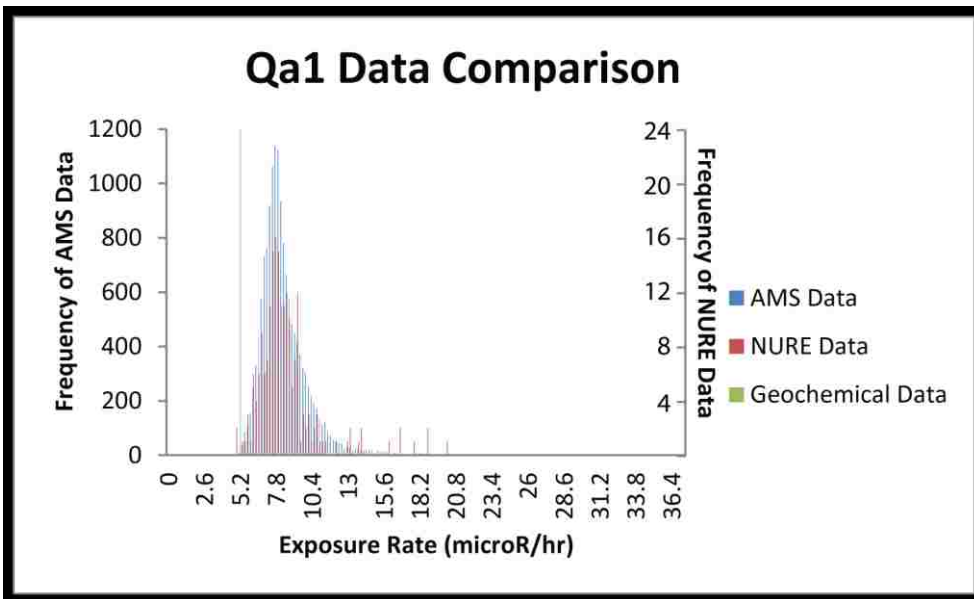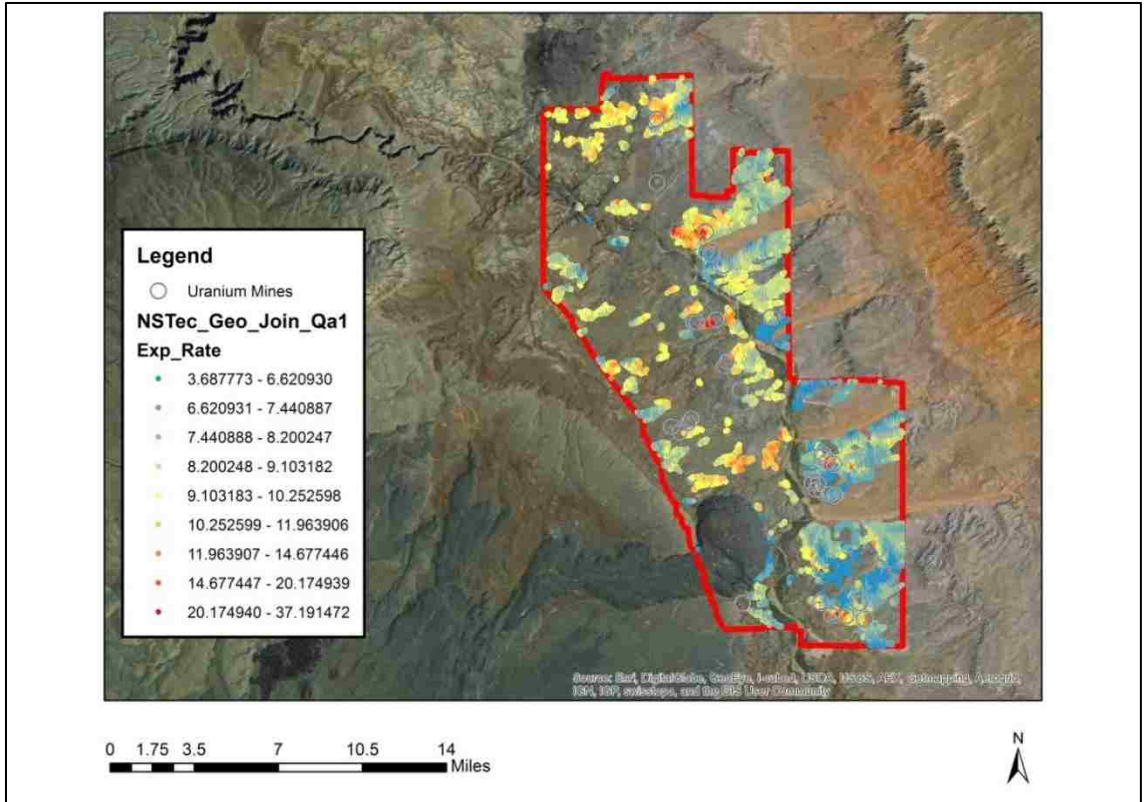
Qa2: The USGS reports that this unit is similar to Qa1, but is 'partly cemented by calcite and gypsum' and is earlier Holocene in age (older). This unit also exhibits the change in composition as one moves across our mapping area. Basalt clasts dominate in the south and chert clasts dominate in the north. Much of this unit is covered by sand (Billingsley et al., 2007), so remote sensing may be best for this unit. All of the data points not listed as basalt will be left in this unit, it is an alluvium, so it is possible that nearby volcanic rocks such as andesite, dacite, latite, rhyolite, gabbro, peridotite, dunite, granulite, and diabase could be present. The USGS does not give a comprehensive composition of this alluvium so the rock type cannot by narrowed further. We have 228 data points for this unit, about one third of all of our data points. There are only 7 points with Uranium concentrations, and 14 points with Thorium concentrations, so for these isotopes this data is not as representative as it may seem. All but one of these data points is from the USGS, the single point is from DIR. The USGS data points are all from igneous rocks, and thus representing only the southern portion of the unit. The rock types recorded are basalt, andesite, dacite, latite, rhyolite, gabbro, peridotite, dunite, granulite, and diabase. Also 225 of these points are listed at the same location (35.5, -111.5). So while there are many points within this unit, they are all very similar (in that many are from the same location and only have K values), and do not give the type of range we would like.

Qa2 hot Field Notes: Fine to coarse sand with clasts of basalt, chert, black sandstone (from Qg2 hot), light grey sandstone from possible TRcs. In order of abundance: mostly chert and smaller pieces of light sandstone, then basalt and grey sandstone.
Float consisting of mostly chert and basalt, some black sandstone like from Qg2 hot, sparse bushes and grasses.

Qa2 cool Field Notes: Mostly sand, raised humps with clasts. Sand is fine grained, about the same composition as aeolian but with clays. Clasts: chert, banded sandstone and limestone, grey brown sandstone, limestone, basalt. Sand lacks ripples.
 Clay infused quartz sand, gravel in places consisting of grey sandstone, chert, sparse limestone. Moderate grasses.

Qa2 hot had more prevalent, larger clasts than Qa2 cool and less vegetation, possibly explaining the difference in radiation. This unit contained basalt, but no other igneous rocks, nothing to explain the extreme amount of igneous rocks reported in the USGS database. However, the clast composition was consistent with the USGS description, though we did not find it to be partially cemented.

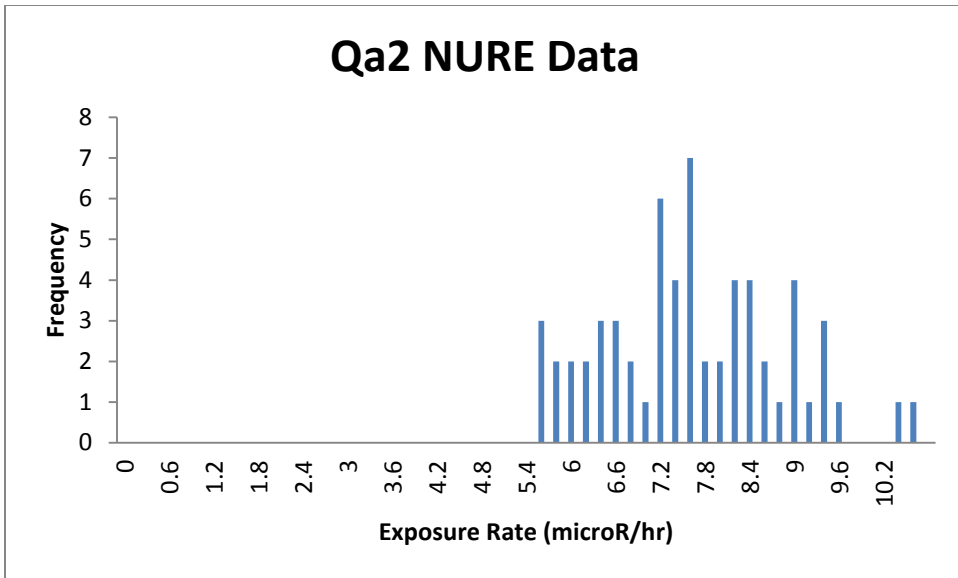|	K (wt %)	U (ppm)	Th (ppm)
mean	1.4847	1.6314	9.781
Standard deviation	0.9806	1.5059	11.3472
range	4.4426	3.89	32.31
median	1.1705	0.979	3.65
mode	0.9962	N/A	1.24

Qa2 U ppm
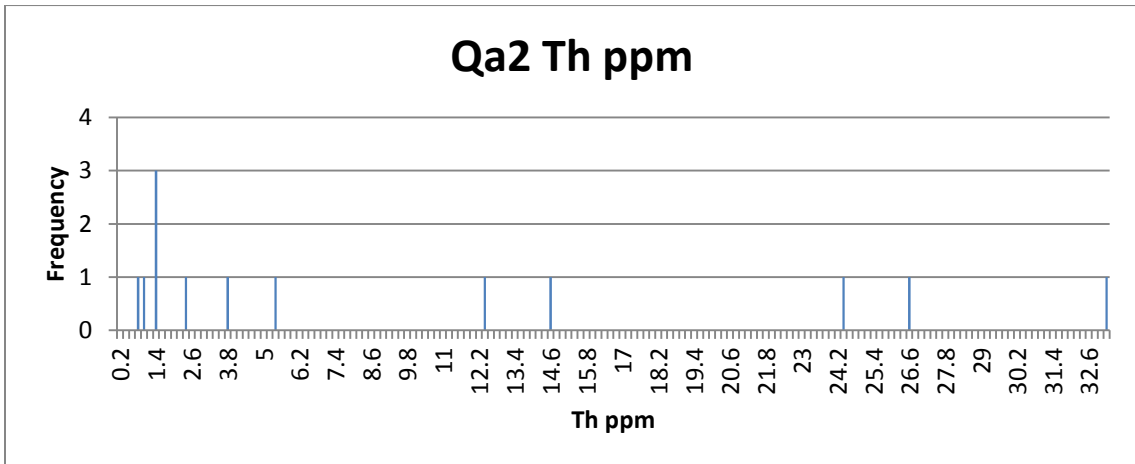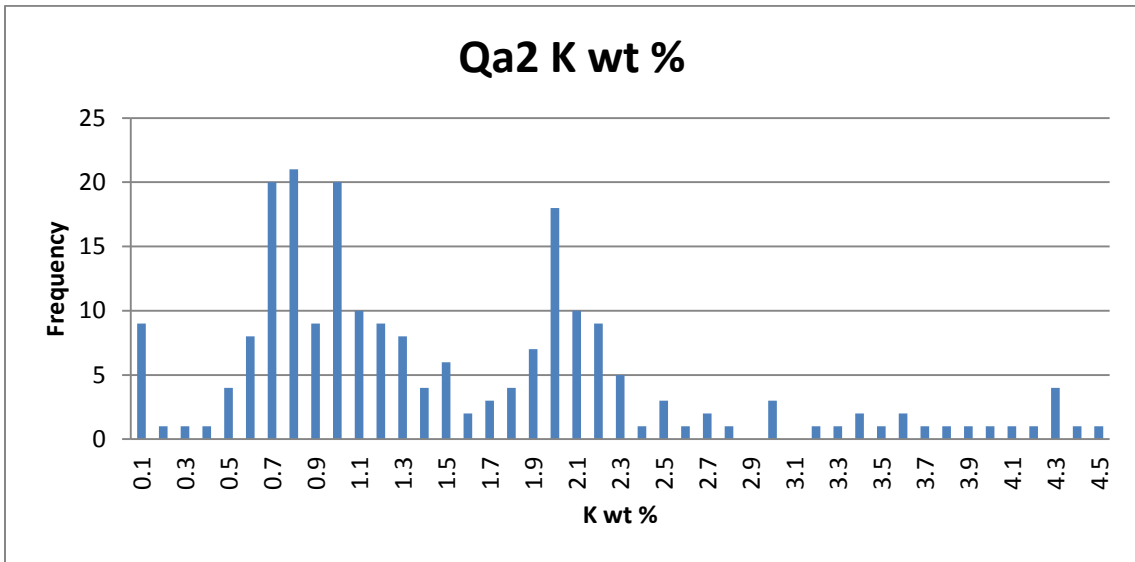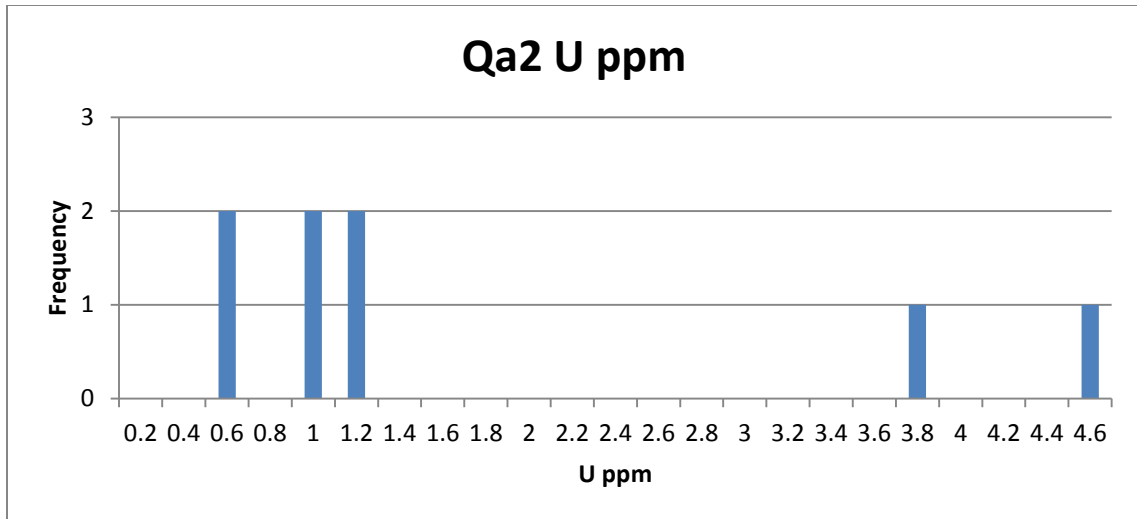
Qa2 Soil: This soil is described as sandy and occurs on top of felsic volcanic and unconsolidated valley fill (USGS, 2004). As this is an alluvium unit this is consistent with the rock unit description. There are 2 soil data points collected by the USGS, with only one K wt % measurement of 1.3.

	K (wt %)	U (ppm)	Th (ppm)
mean	1.3	2.33	8.8485
Standard deviation	N/A	0.5233	2.1425
range	N/A	0.74	3.03
median	1.3	2.33	8.485
mode	N/A	N/A	N/A

Comparing the rock and soil concentrations, the K is similar om rock and soil, while the U and Th are higher in the soil than the rock. However, the soil U and Th values are within the range of the rock U and Th values.

Qa2 NURE Histogram:

Qa2 NURE Data

Frequency vs Exposure Rate (microR/hr)

Qa2 AMS Histogram:

Qa2 AMS Data

Frequency vs Exposure Rate (microR/hr)
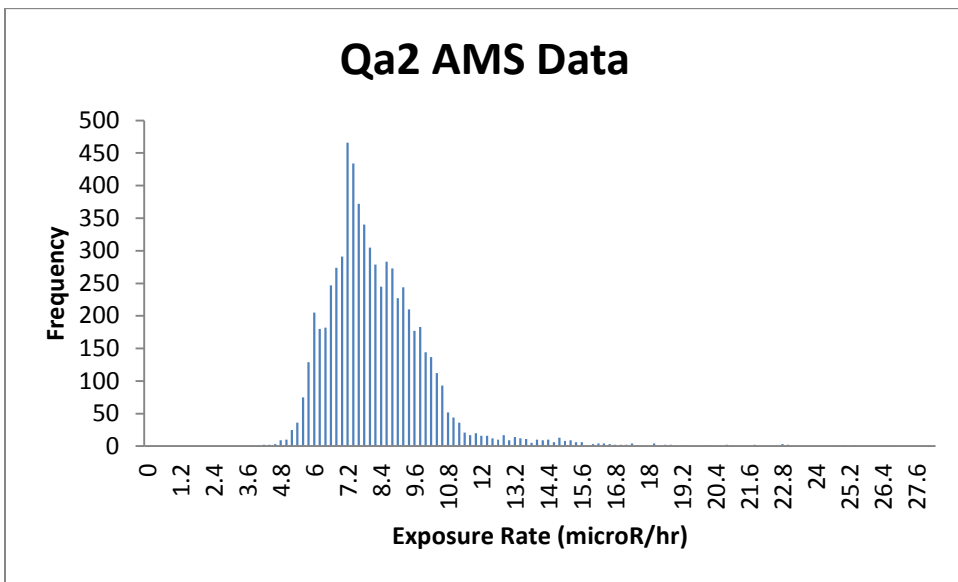
The means vary significantly between these two histograms, this is most likely due to how right skewed the AMS histogram is.

Qa2 50 m buffer NURE Histogram:
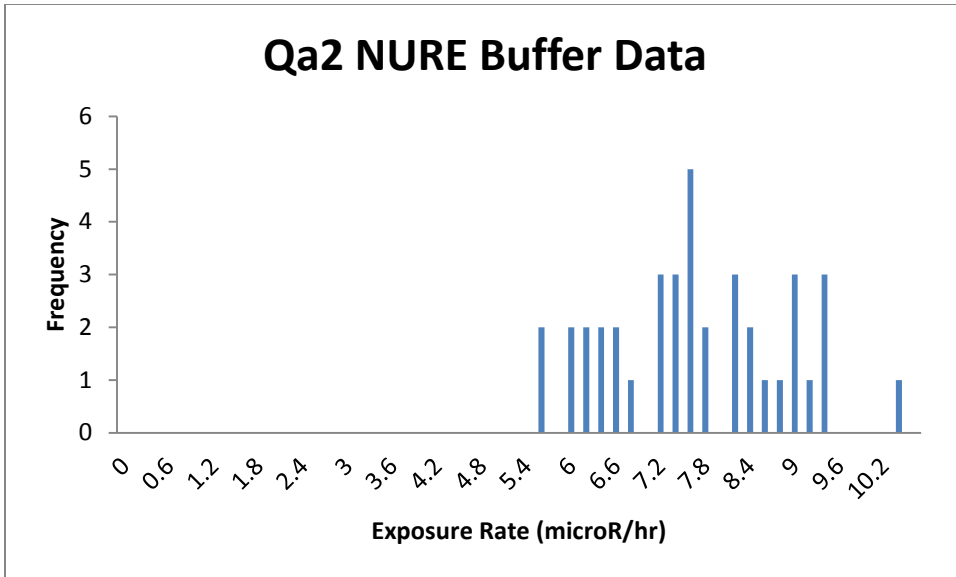
Qa2 50 m buffer AMS Histogram:
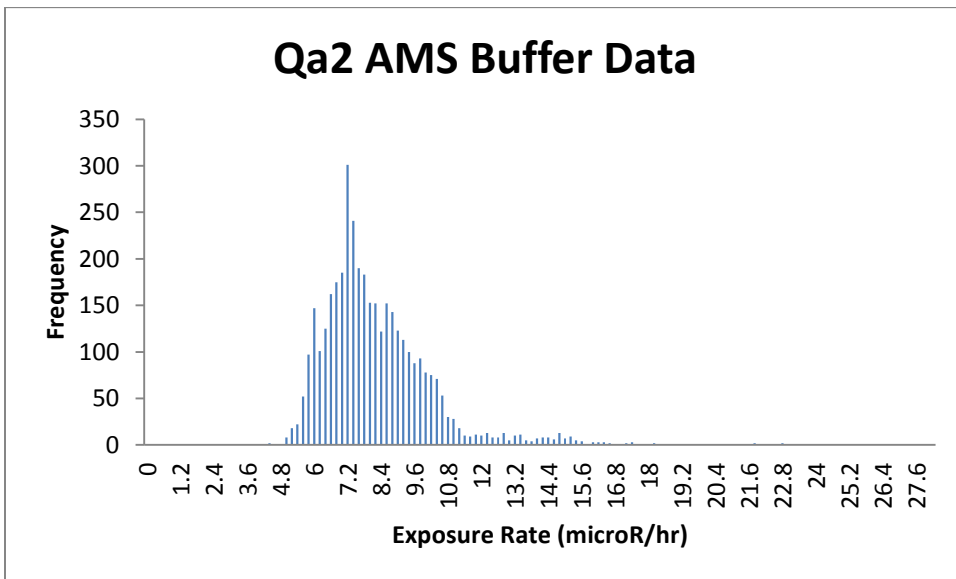
Qa2 AMS Distribution: This unit does not have an overall trend, hotter areas seem to be concentrated just north of Black point, but distribution overall seems random. This alluvial unit has a large range as would be expected: from 3.71 to 27.863.

Qa2 AMS Exposure Rate Data
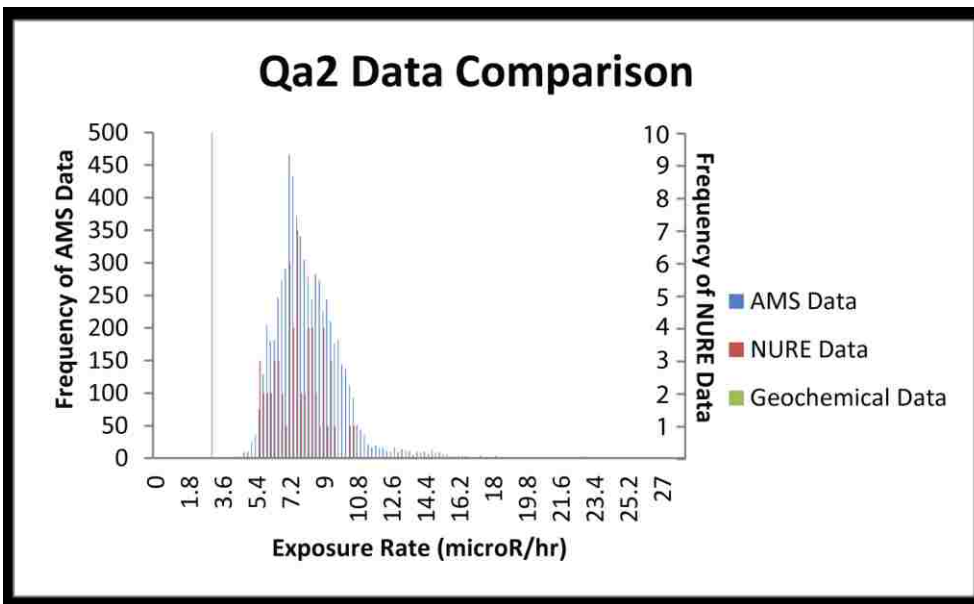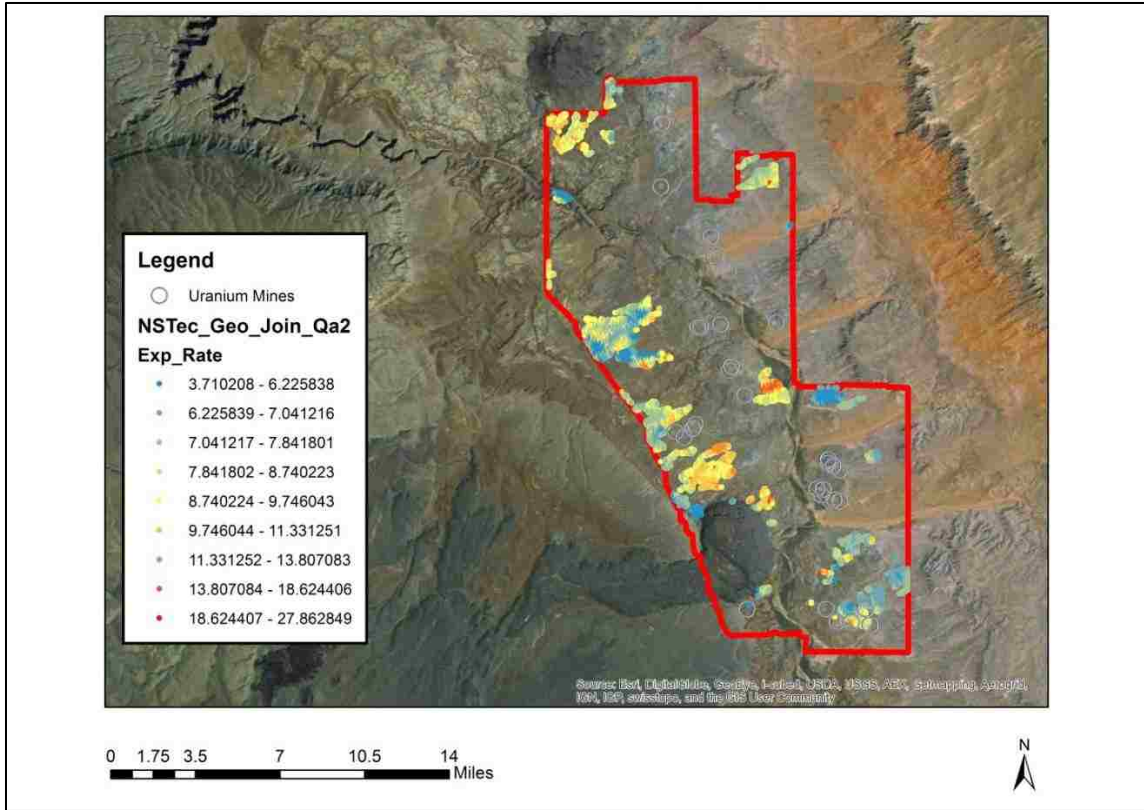
Qg3: This unit is lithologically similar to Qg1, but earlier Holocene in age (older). USGS describes this unit as silt to boulder sized terrace gravel, clasts come mainly from Pkh and Triassic units, and basalt clasts in the southern portion of the mapping area. This unit is partially cemented by gypsum and calcite. The USGS states it differs from Qg1 also by the presence of volcanic and quartzite clasts, though both of these are also reported in Qg1 (Billingsley et al., 2007). There are 4 USGS data points for this unit but they are all the same rock sample, so it has been made into one data point by choosing the point with the sampling method with the highest accuracy. The sample is 0.0249 wt % K, 13.4 ppm U, and 6.79 ppm Th. This rock is listed as a sandstone from the Shinarump Member of the Chinle Formation, consistent with TRcs. I have chosen to leave the data point within Qg3, as Qg3 contains TRcs, and this data point occurs within the mapping area, so it is a good representation of this specific location.

Qg3 Field Notes: This unit was not visited as the road was washed out.

Qg3 NURE Histogram:

Qg3 AMS Histogram:

Qg3 AMS Data
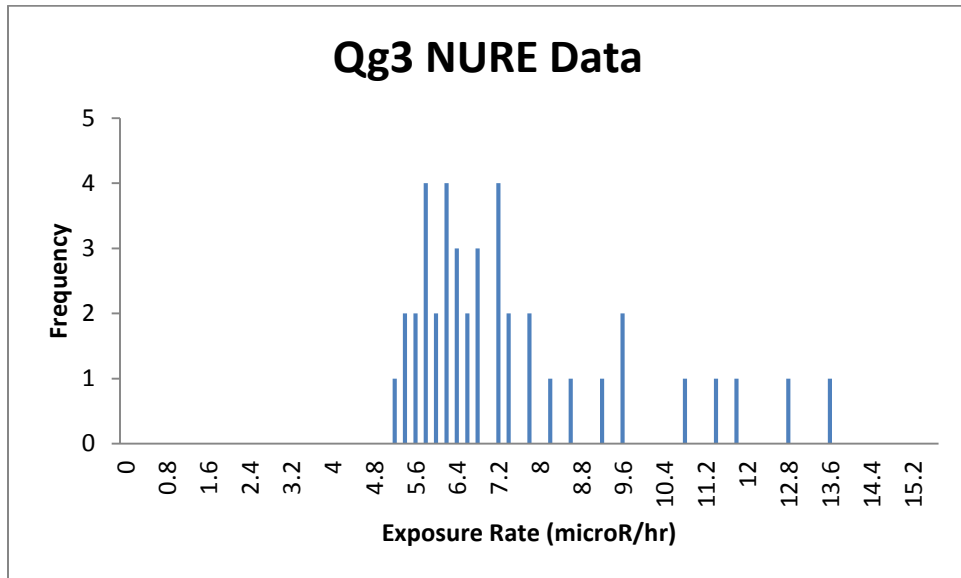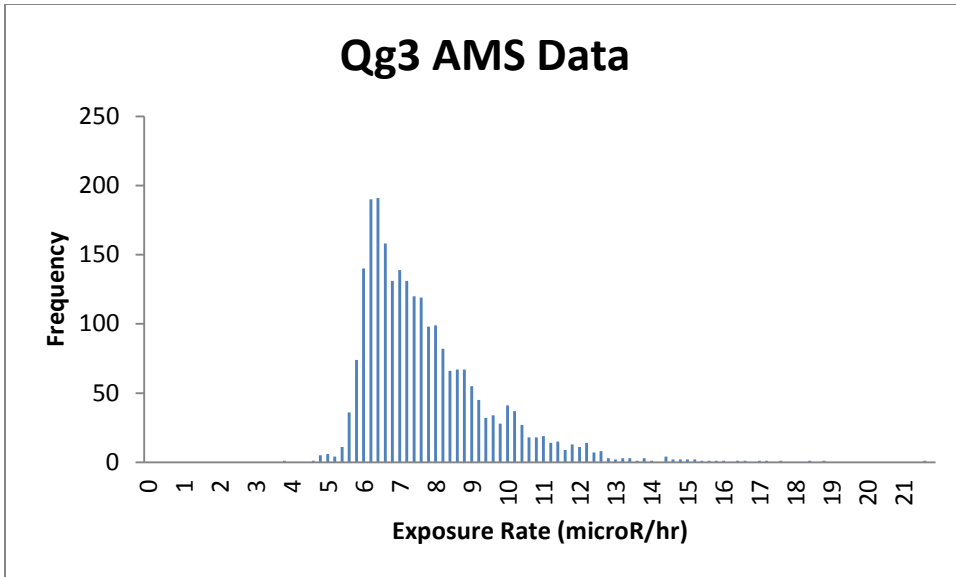
While the means are not within error, the majority of the AMS points appear to be between 4.6 and 10.6 which is about the range of the majority of the NURE model. Thus the difference in means could be due to the right skewedness of the AMS histogram.

Qg3 50 m Buffer AMS Histogram:

Qg3 NURE Buffer Data

Qg3 50 m Buffer AMS Histogram:

Qg3 AMS Buffer Data
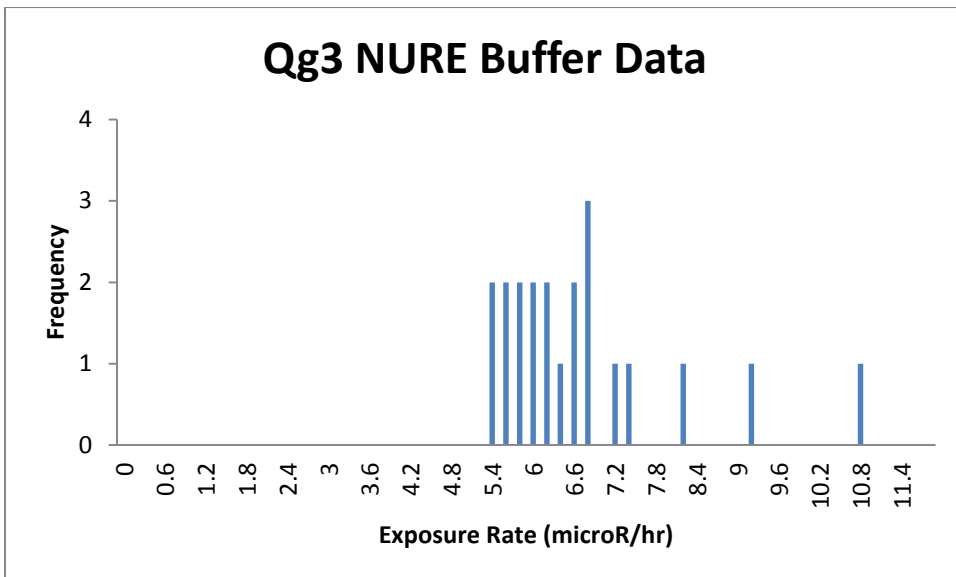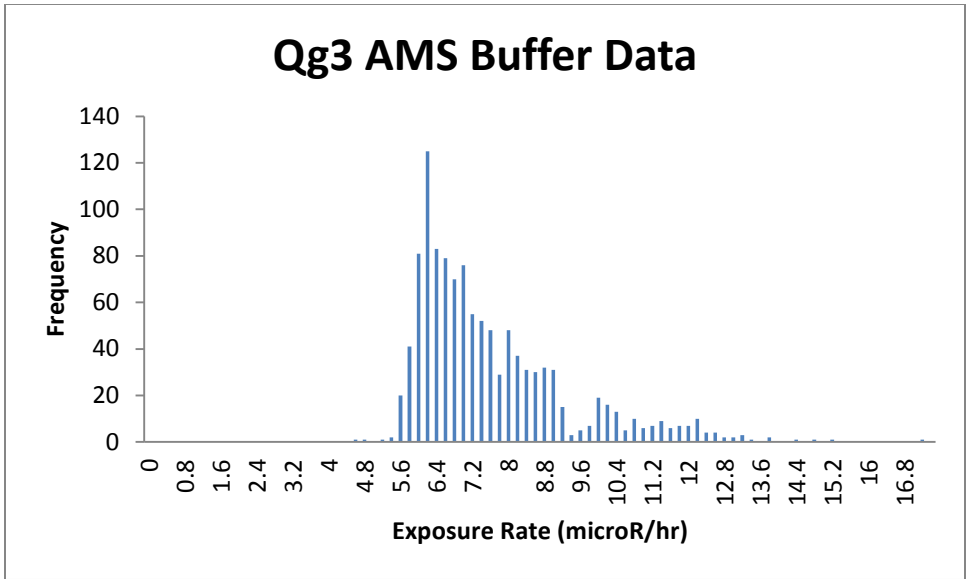
Qg3 AMS Distribution: This alluvial unit lacks overall trends with respect to exposure rate. There seems to be localized highs and lows. The area southeast of the river is a large cool area, but contains a 'hot spot' in relation to the uranium mines. This unit has a large range of exposure rates, from 4.555 to 31.439.

Qg3 AMS Exposure Rate Data
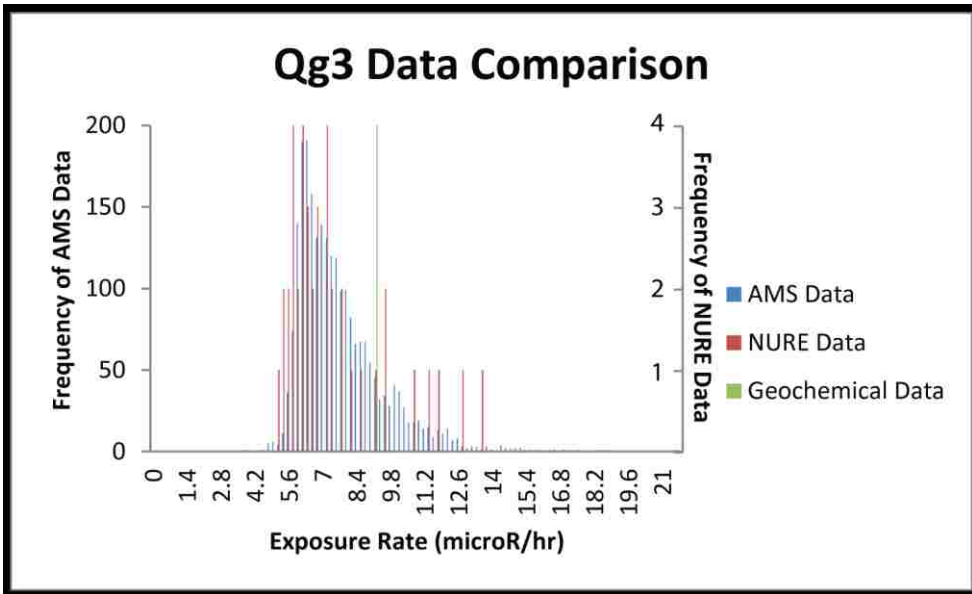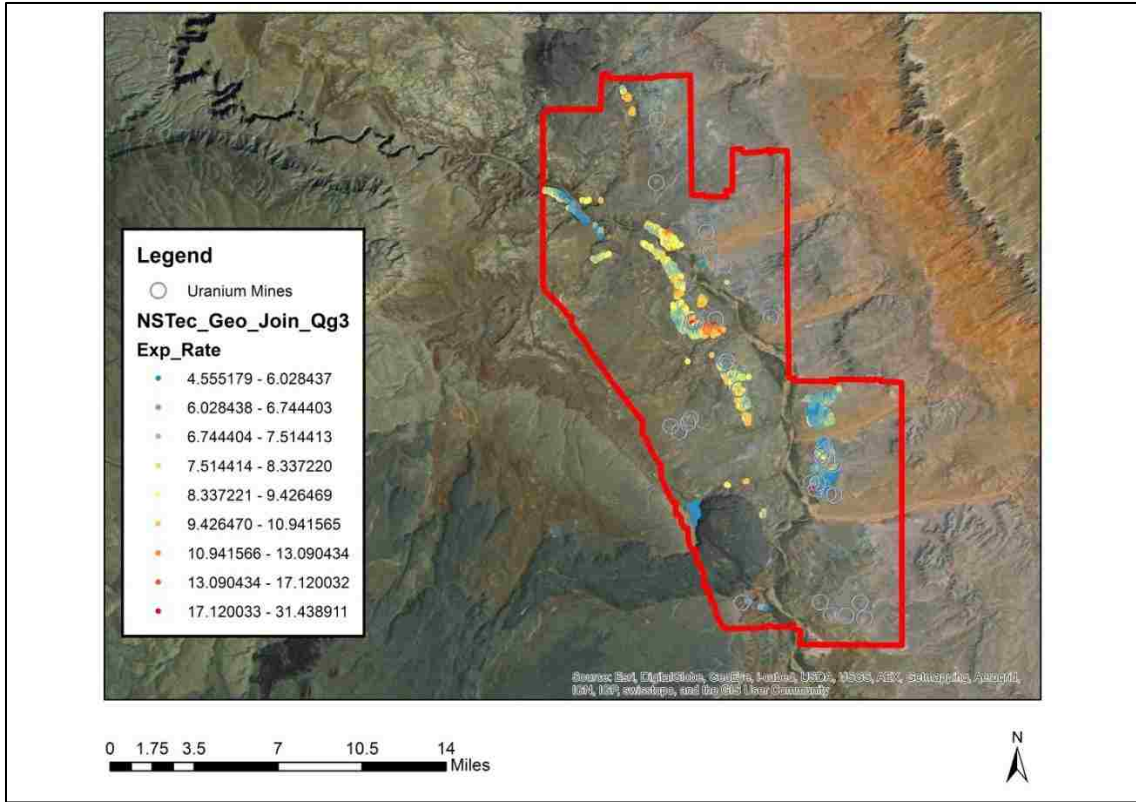
Qae: The USGS describes this unit as Holocene and Pleistocene aged interbedded alluvium and eolian deposits ranging in size from clay to gravel. Consists mainly of chert fragments from Pkh, TRco, and the Navajo Sandstone (Billingsley et al., 2007). The reported rock types are basalt, andesite and a bentonite clay listed as coming from the Chinle Fm by the collector. The Chinle Formation data point is ambiguous because there are three separate members of the Chinle in this mapping area, none of which list a bentonite clay and was removed. The points labeled basalt and andesite should also be removed as they do not represent Qae, but the underlying bedrock. These points are not even within the mapping area, but were correlated in because they fell within the same rock unit. By removing the basalt, andesite, clay, and Chinle Fm data points, and also all data points that were repeats of the same sample we are left with 4 data points, with only 1 K concentration and no Th data.

Qae (on basalt) Field Notes: Basalt clasts, some basalt sand, and aeolian addition in the form of a brown matrix underneath weathered basalt. Basalt clasts range in size from sand to 2 fist size.
Basaltic sand with basalt clasts, brown eolian dust on top of and internatlized with basalt sand. Sparse to moderate vegetation.

Qae hot (off basalt) Field Notes: All fine sand, no clasts, thus incredibly different than on the basalt flow. Overall a lighter brown sand, very thick, sink in. Medium vegetation. Sand is made up of quartz, basalt, limestone, feldspar, chert. No cementation, overall homogenous. Closer to the road is more soil formation, more fine grained.
Red brown fine sand, no clasts or soil formation, moderate to dense grasses and bushes.

Based on our observations in the field the Qae point that was collected as basalt should be added back into the geochemical data, as on the basalt flow, the unit consists entirely of basalt. The basalt dominated Qae is cooler because it is dominated by a rock that is cooler. We are not sure why Qae hot is hot, since it consisted only of sand, mostly likely an aeolian deposit. This sand however is consistent with the USGS description. Strangely enough the presence of basalt clasts is not mentioned by the USGS description.

|	K (wt %)	U (ppm)	Th (ppm)
mean	0.9630	1.3667	N/A
Standard deviation	N/A	0.3215	N/A
range	N/A	0.6	N/A
median	0.9630	1.5	N/A
mode	N/A	N/A	N/A

There is only 1 listed K concentration of 0.9630 wt %.

Qae U ppm
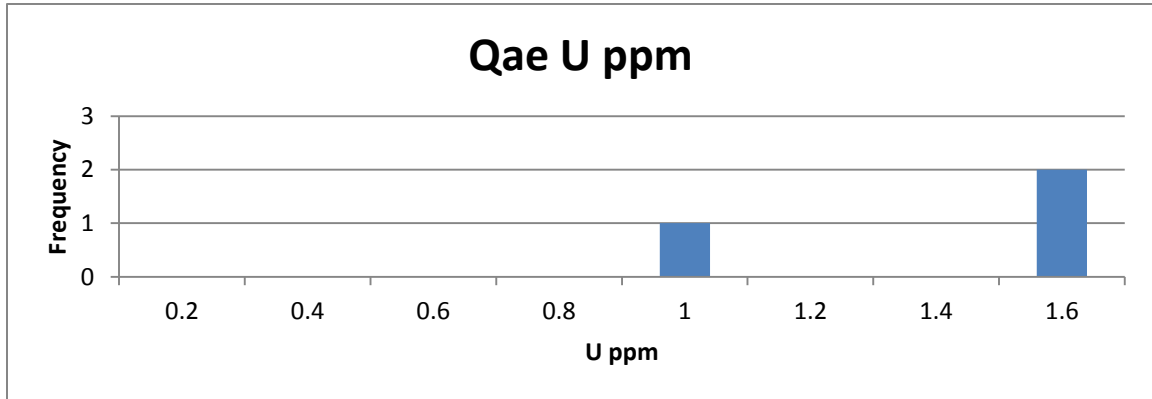
Qae Soil: This soil is described as a coarse, dark grey sand of low relief with moderate vegetation. This soil occurs on unconsolidated valley fill and sandstone (USGS, 2004). The rock description has this unit as an alluvium unit with clasts of sandstone, which is consistent with the Qae soil description. There are 4 data points for this soil.

	K (wt %)	U (ppm)	Th (ppm)
mean	2.100	2.8175	9.7030
Standard deviation	0.3607	0.4538	2.1361
range	0.7	0.82	4.1
median	1.999	2.825	9.01
mode	N/A	N/A	N/A

Comparing these values to that of the rock unit, the K of the soil is more than 2 times that of the rock unit, and the rock unit does not contain any K values that high (though there is only one K value in the rock unit). The U values of the soil are also higher than that of the rock, almost by a factor of 2. There are no Th rock values to compare to the soil.

Qae Soil K wt %

Qae Soil U ppm

Qae Soil Th ppm
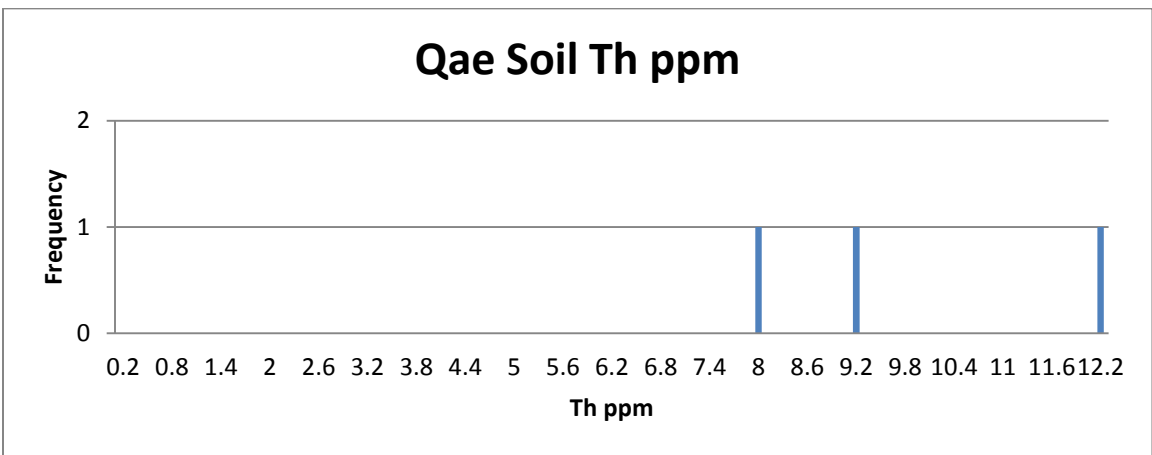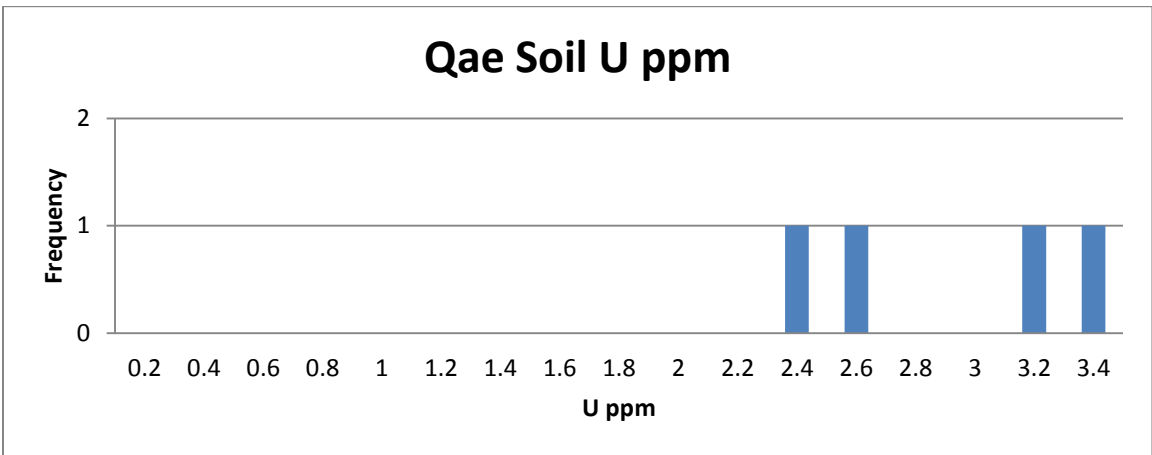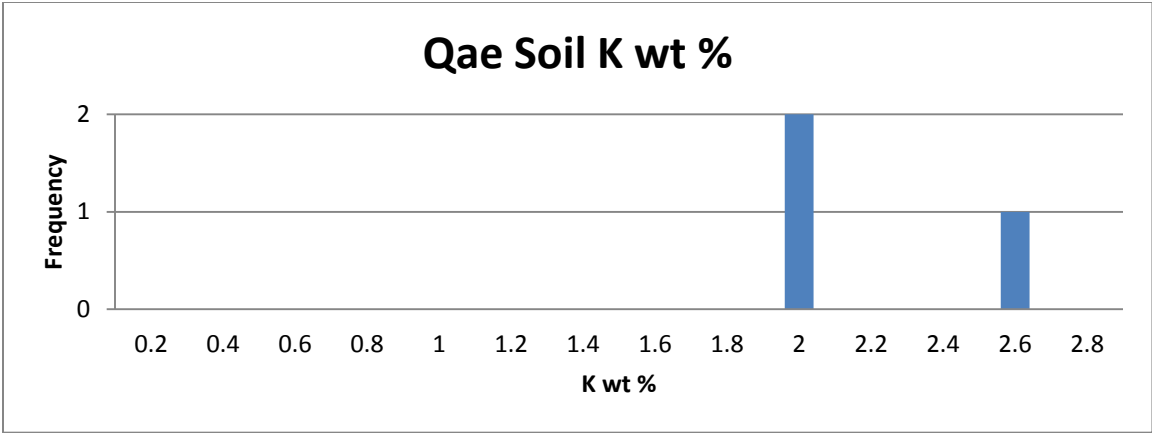
Qae NURE Histogram:
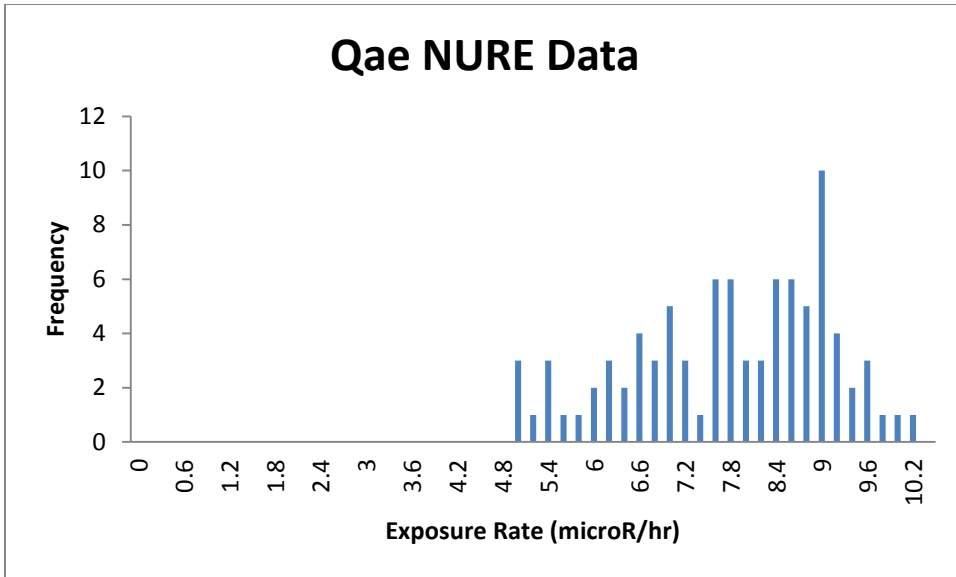
Qae AMS Histogram:
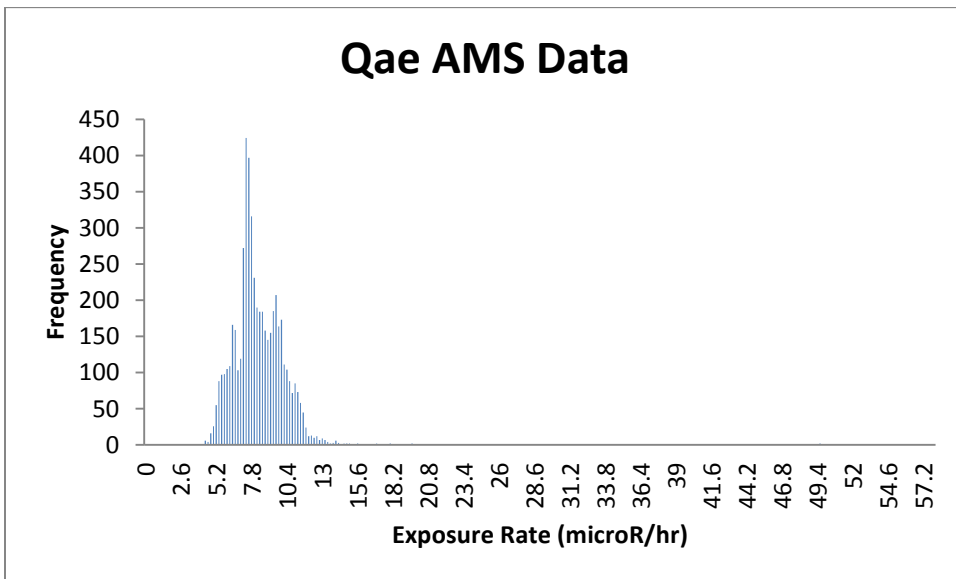
The difference in mean between these two histograms is very large, and this could be due to the right skewedness of the AMS histogram. The majority of the AMS data points occurs between 4.2 and 9.6, this corresponds to about the range of the NURE histogram.

Qae 50 m buffer NURE Histogram:

Qae NURE Buffer Data
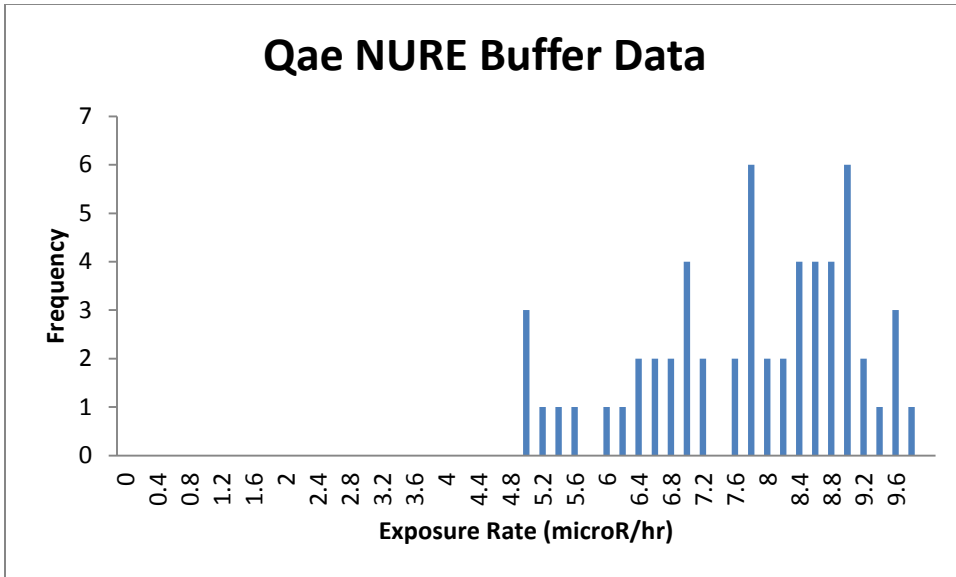
Qae 50 m buffer AMS Histogram:

Qae AMS Buffer Data
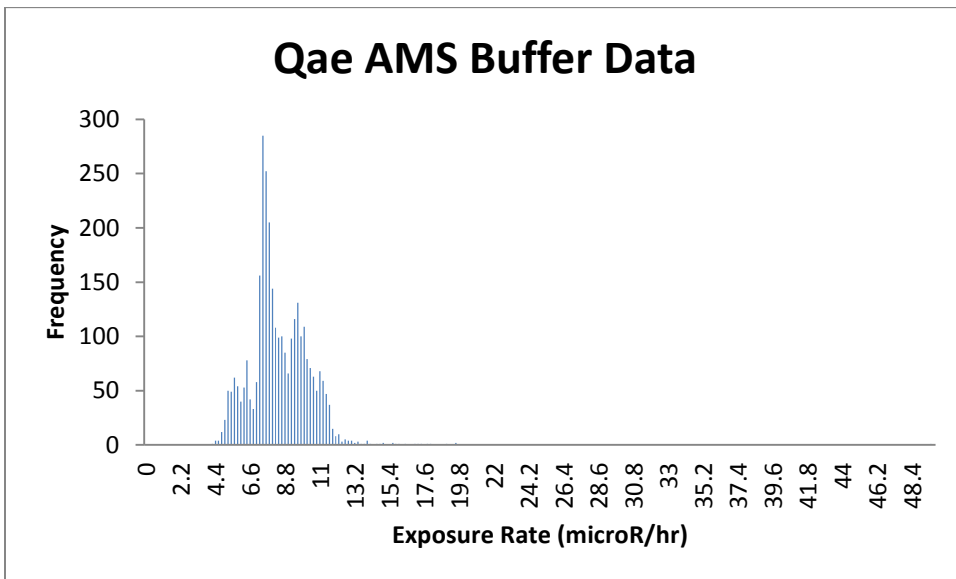
Qae AMS Distribution: This alluvial unit has a wide distribution throughout the mapping area, the general trend seems to be that it is hotter in the north than the south. Black Point seems to be the coolest portion of this unit, and the exposure rate has a large range, from 4.195 to 57.672.

Qae AMS Exposure Rate Data

129
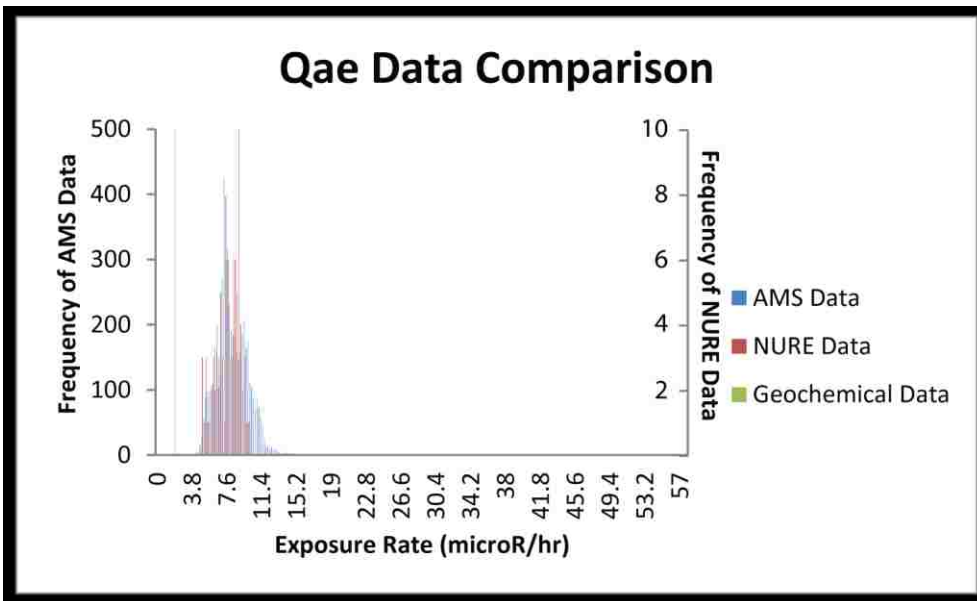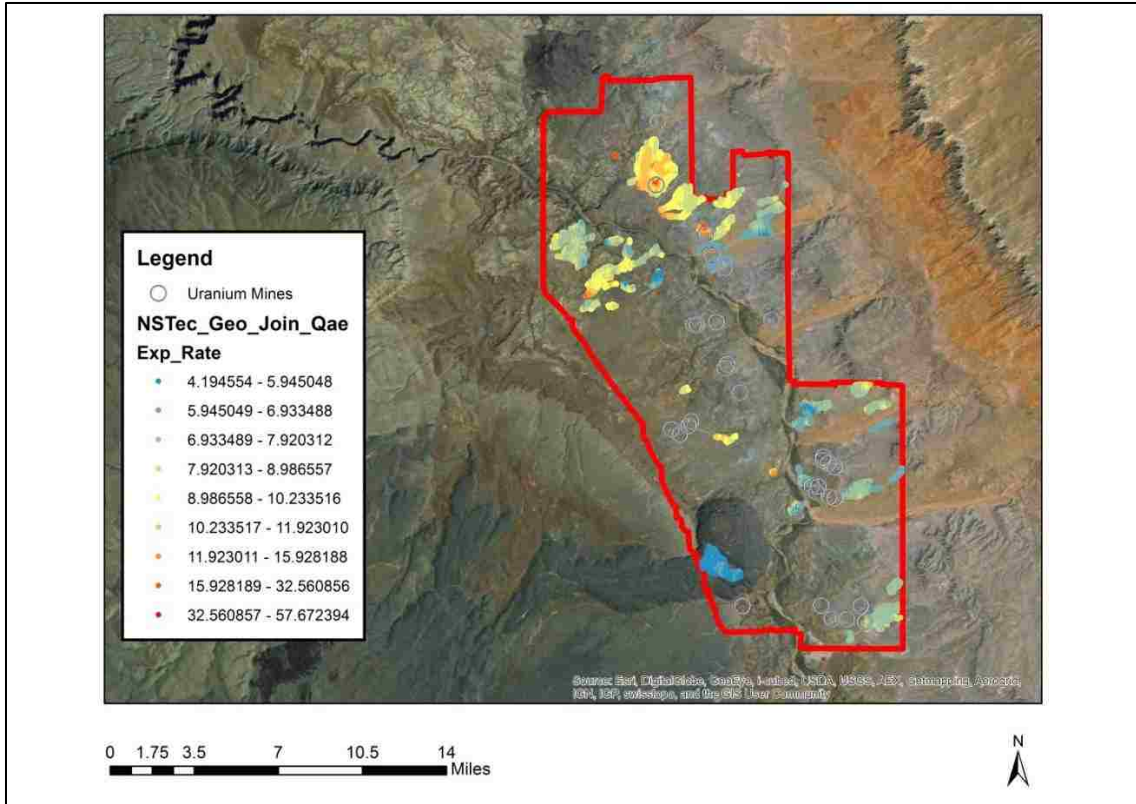
Ql: The USGS classifies this unit as Holocene and Pleistocene landslide deposits (Billingsley et al., 2007). These vary in composition based on location, see map. There are 7 USGS data points within this unit, and all of them are listed as igneous, 5 being basalt and the rest being unknown. Four of these data points are listed at the same location. All data points will be left in Ql, as this unit occurs around Black Point, making it plausible that all the landslide material is basalt.

Ql hot Field Notes: This point was not visited as the road was washed out.

Ql cool Field Notes: While driving around the basalt flow throughout the afternoon we noticed that there are larger boulders at the top of the cliff, and the size fines downward. This unit is coarser basalt, more large clasts, and more variety in the degree of sphericity of clasts. Largest clasts are about 20 cm. Medium vegetative coverage.
Mostly basalt clasts, significant portion greater than 10 cm. Eolian sands, medium grasses, some shrubs.

These field observations are consistent with the USGS descriptions as a landslide deposit off of a basalt flow, and with the basalt rocks in the USGS database.

	K (wt %)	U (ppm)	Th (ppm)
mean	1.6190	4.6367	24.4333
Standard deviation	1.3777	3.1855	18.5149
range	3.62	5.61	34.5
median	0.9132	6.38	32.2
mode	0.9132	N/A	N/A

# Ql U ppm

Ql Th ppm
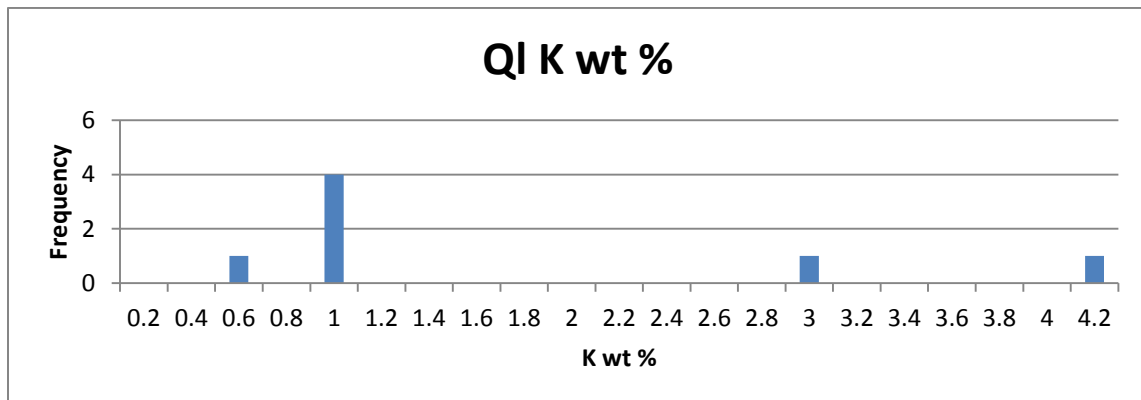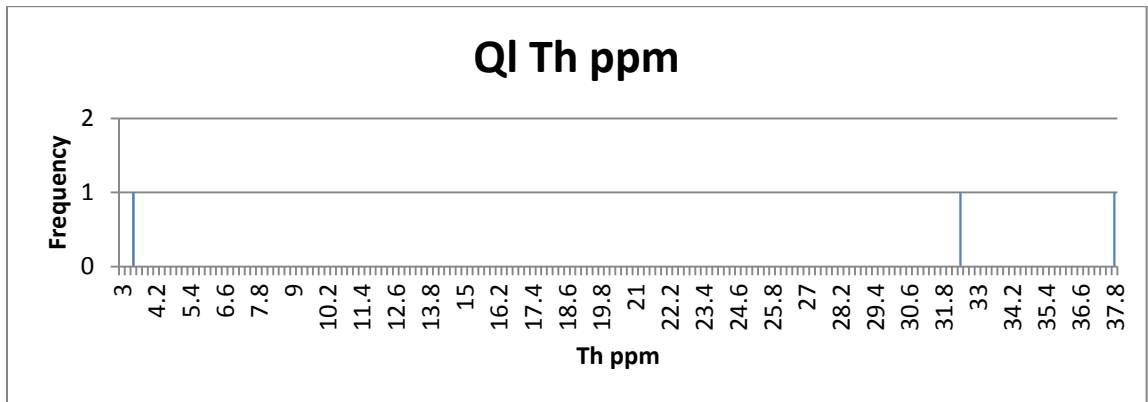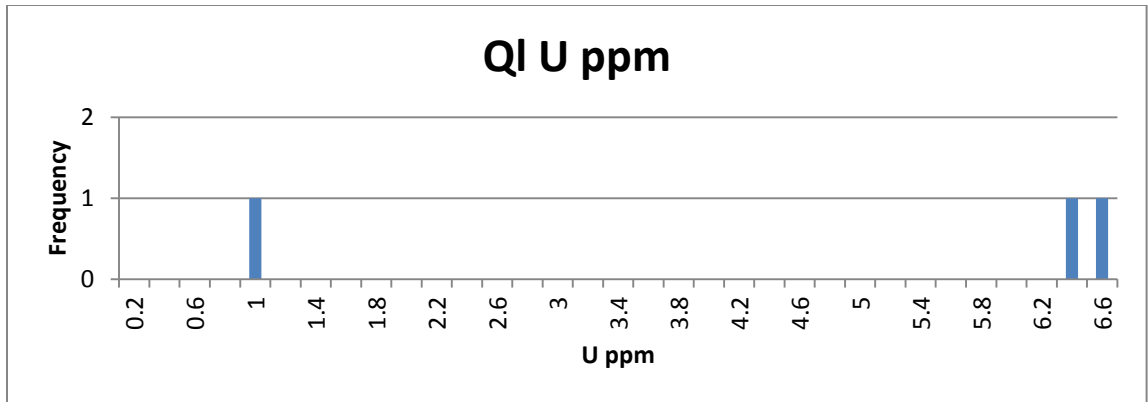
Ql Soil: This soil is described as being collected from a flat area of sparse vegetation occurring on top of felsic volcanic rock (USGS, 2004). This is consistent with the Ql being a landslide deposit and felsic volcanic rock occurring within the mapping area. The soil sample has a K concentration of 1.7 wt %, almost twice as much as the median rock concentration, but within its range; a U concentration of 2.67, less than half that of the median concentration of the rock but within the rock's range, and a Th concentration of 10.1, a third of the median concentration in the rock but also within the rock's range.
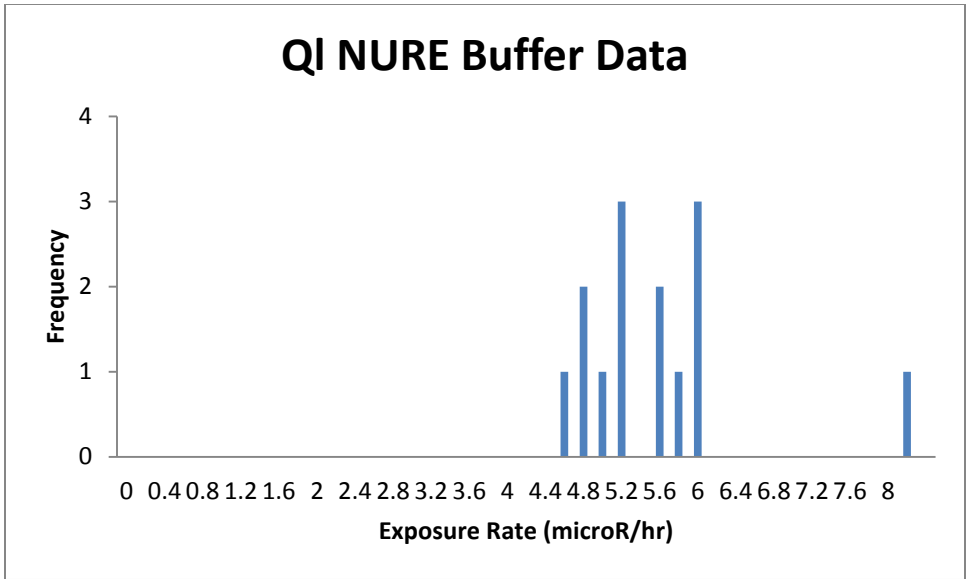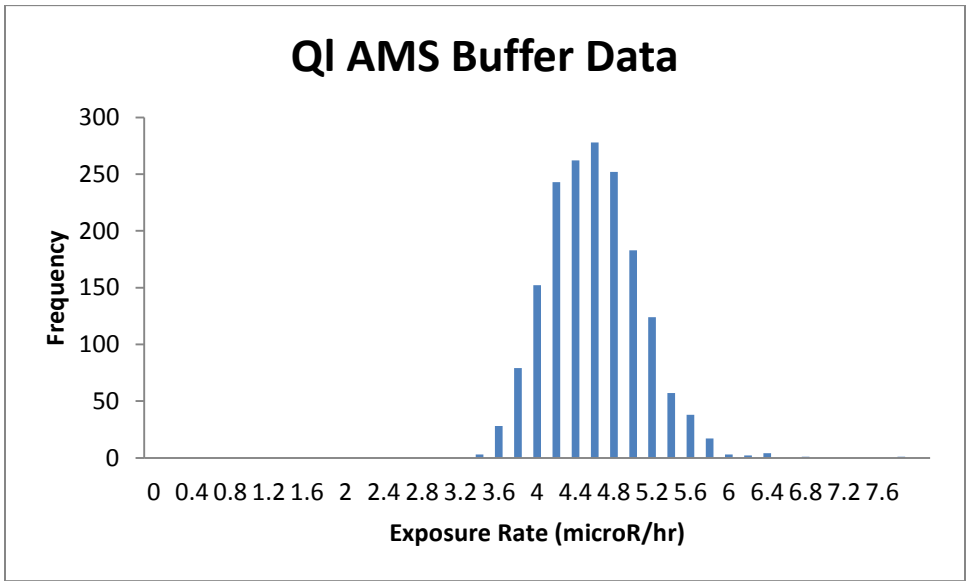
QI NURE Histogram:
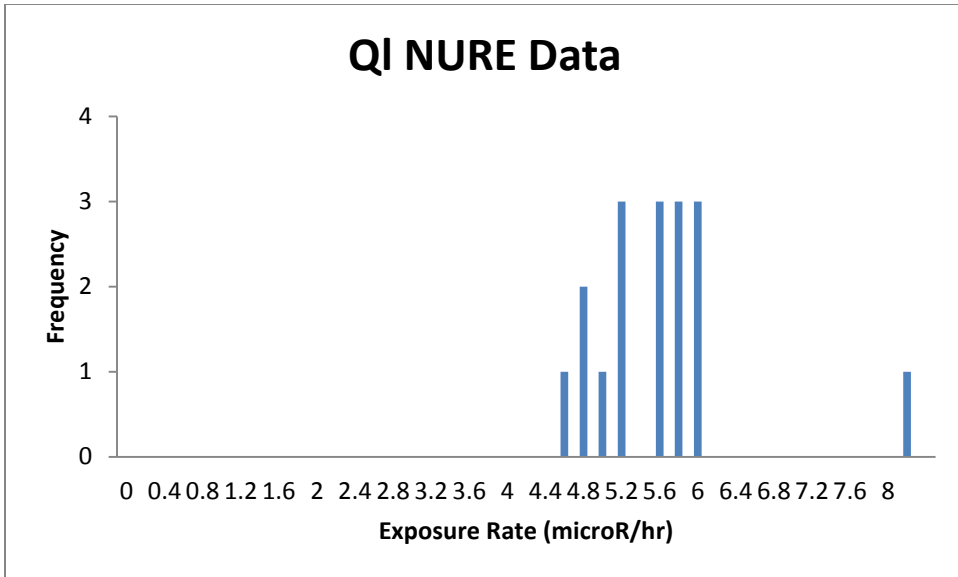
QI AMS Histogram:
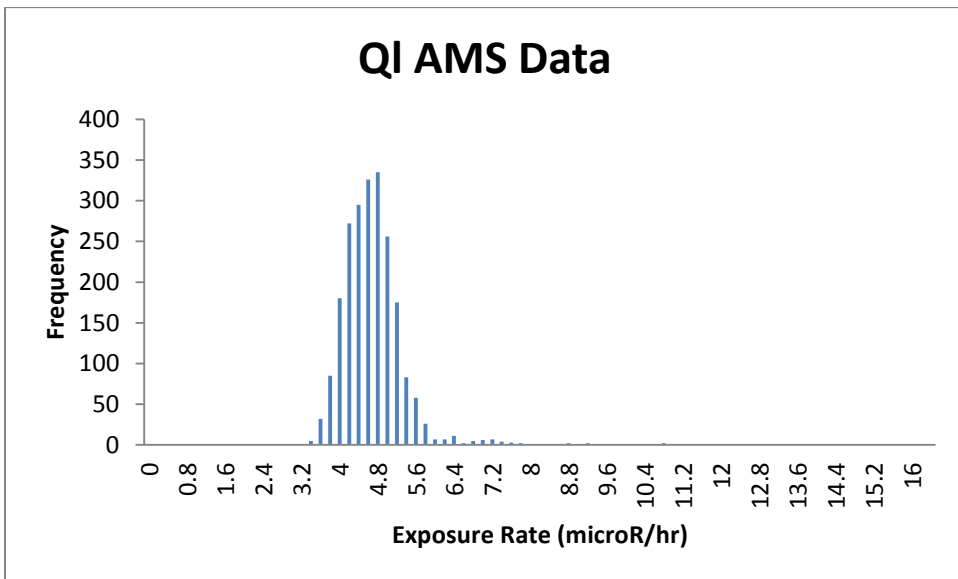
The means of these histograms are within error. That is surprising given the small amount of NURE data points and the right skewedness of the AMS histogram.

Ql 50 m buffer NURE Histogram:

Ql NURE Buffer Data

Frequency vs Exposure Rate (microR/hr)

Ql 50 m buffer AMS Histogram:

Ql AMS Buffer Data

Frequency vs Exposure Rate (microR/hr)

QI AMS Distribution: This unit occurs mostly on the slopes of Black Point and also in a small area in the northwest. This small area is distinctly hot. The area around Black Point displays its own trends, having a hotter outer edge and cooler inside. This unit has a small range of exposure rates, from 3.195 to 11.658.

QI AMS Exposure Rate Data
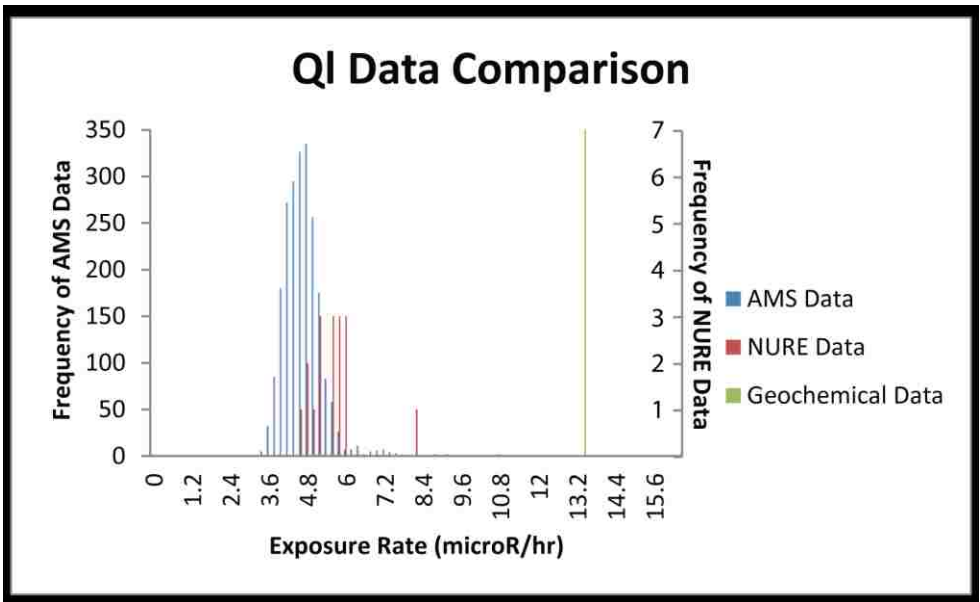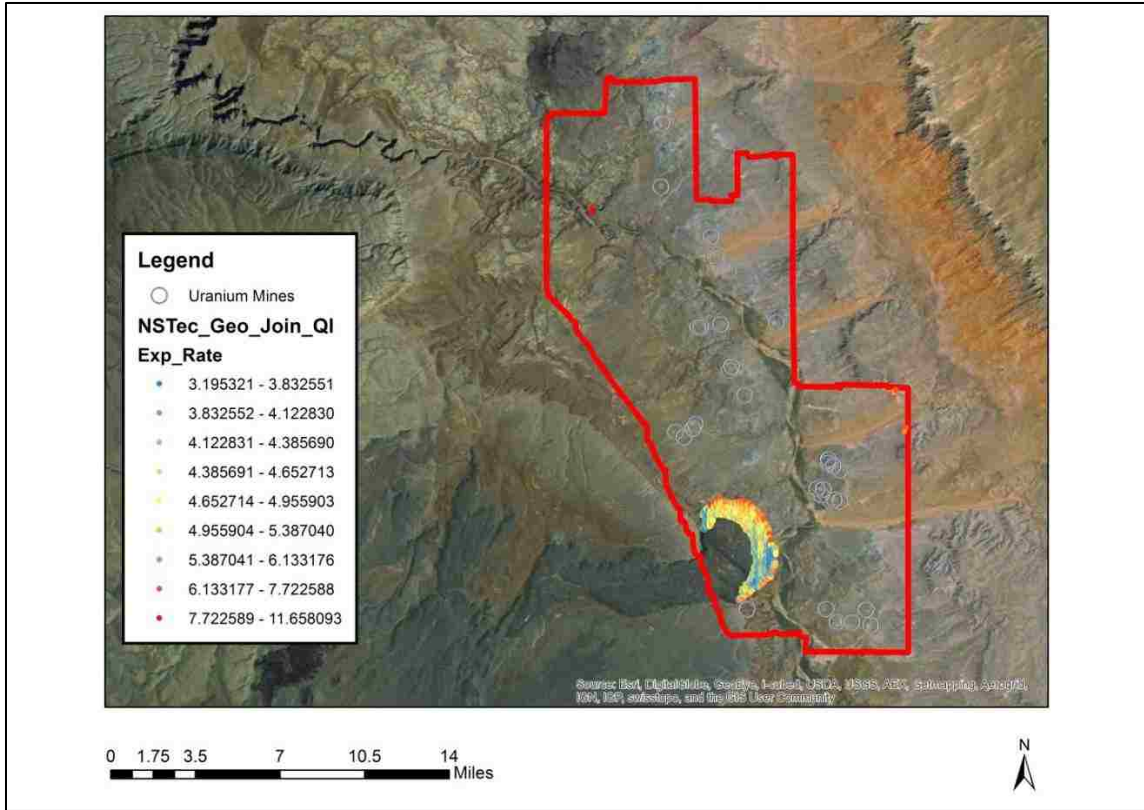
Qv: This unit is Holocene and Pleistocene age valley-fill deposits, with silt to gravel sized clasts of limestone, chert, and basalt, partially cemented by calcite and gypsum, according to the USGS (Billingsley et al., 2007). This is consistent with the recorded rock types of basalt and limestone in the 46 data points in this unit from the USGS, DIR and NAVDAT, so no data points will be removed.

Qv Field Notes: This unit was not visited as it was over a cliff.

|	K (wt %)	U (ppm)	Th (ppm)
mean	0.5612	1.6206	4.78
Standard deviation	0.4913	0.9472	4.2144
range	1.2650	5.311	5.96
median	0.31	1.4	4.78
mode	1.1622	1.1	N/A
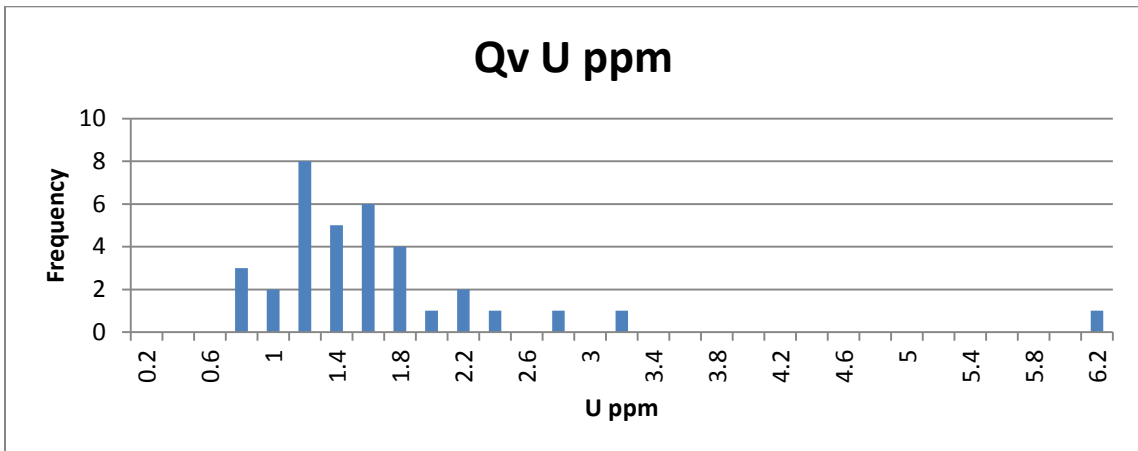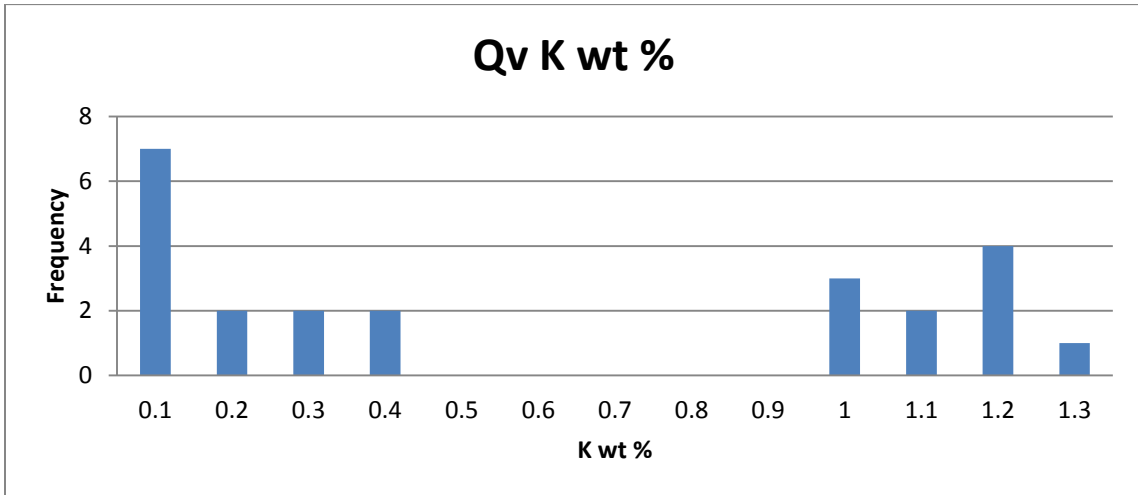
There are 2 reported Th concentrations of 7.76 and 1.8 ppm.

135

Qv Soil: This soil is described as a coarse brown to grey sand with moderate to sparse vegetation occurring on sandstone and unconsolidated valley fill (USGS, 2004). This is consistent with Qv as it is valley fill, and it is possible it could contain sandstone clasts despite the fact that the USGS does not specifically list this in their description. There are 4 data points within this soil unit.

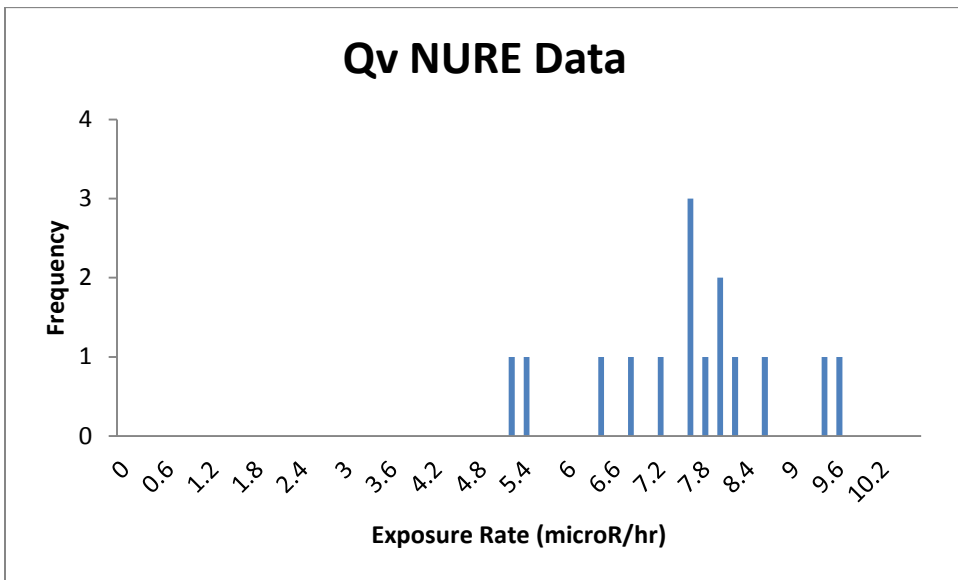|	K (wt %)	U (ppm)	Th (ppm)
mean	2.0648	2.3925	10.85
Standard deviation	0.4401	0.8517	1.0607
range	1.07	1.83	1.5
median	2.0645	2.27	10.85
mode	N/A	N/A	N/A

The mean concentrations of the soil U, K and Th vary from the median rock unit concentrations. K is almost 7 times greater in the soil than the rock, U is much closer with a difference of about 59%, and Th is twice as prevalent in the soil than rock.
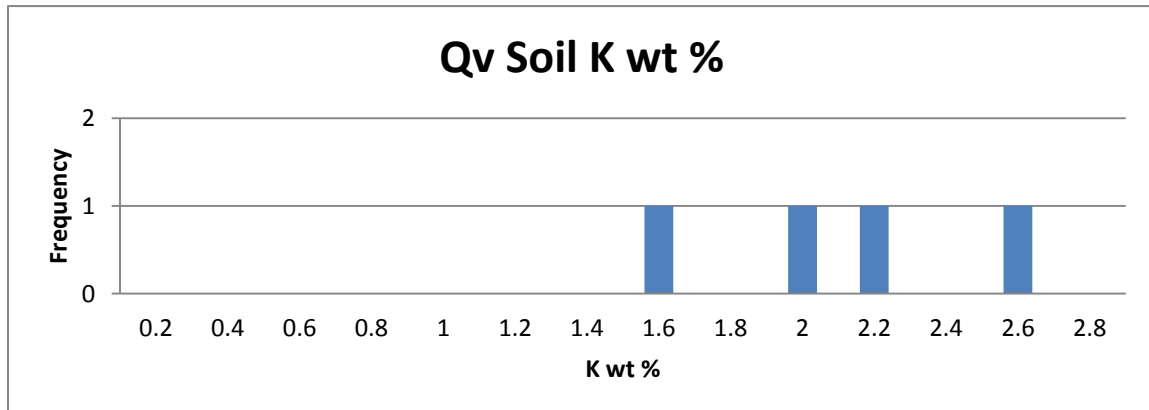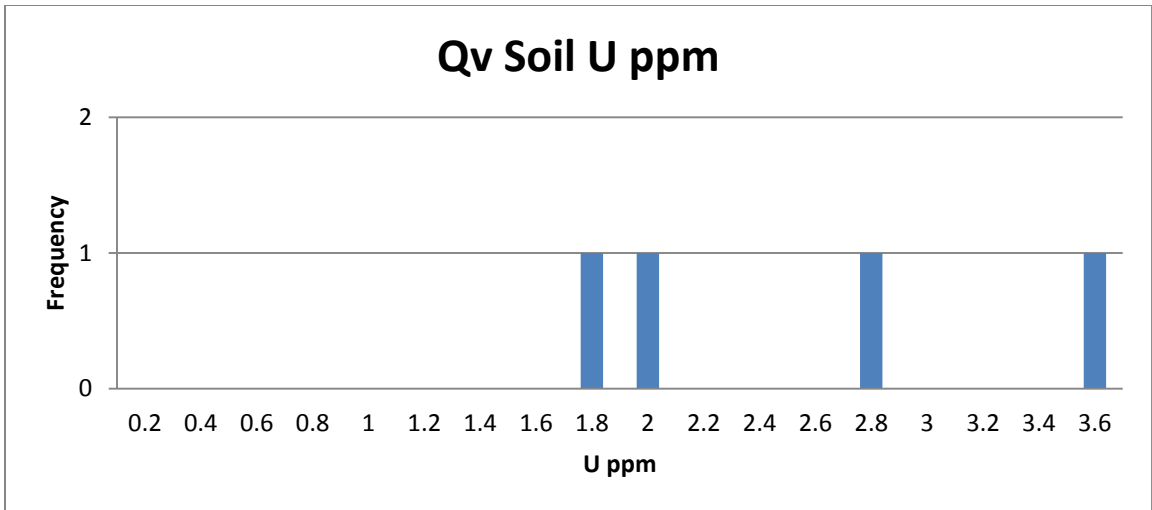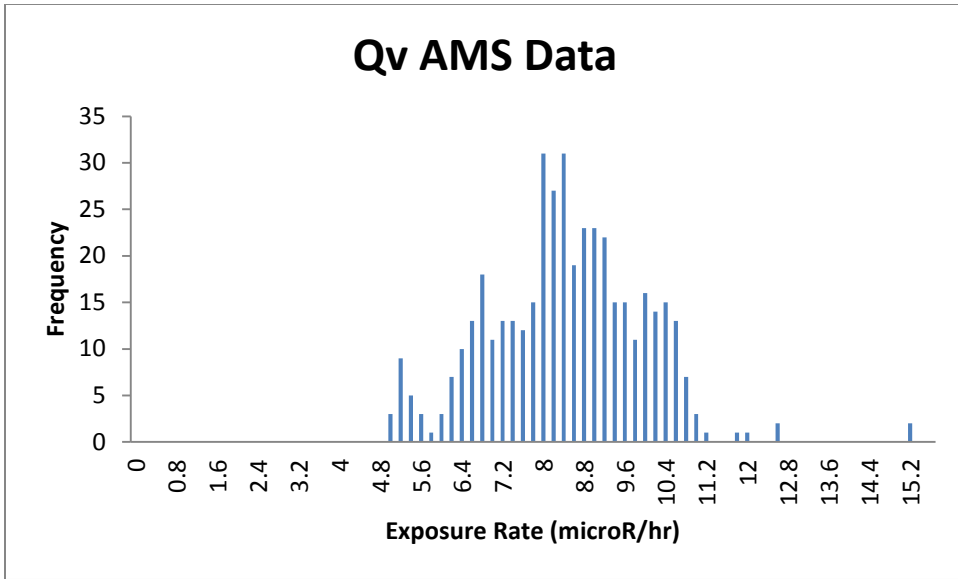
There are two Th concentrations recorded of 10.1 and 11.6 ppm.

Qv NURE Histogram:

Qv AMS Histogram:

Qv AMS Data — histogram with x-axis "Exposure Rate (microR/hr)" and y-axis "Frequency"
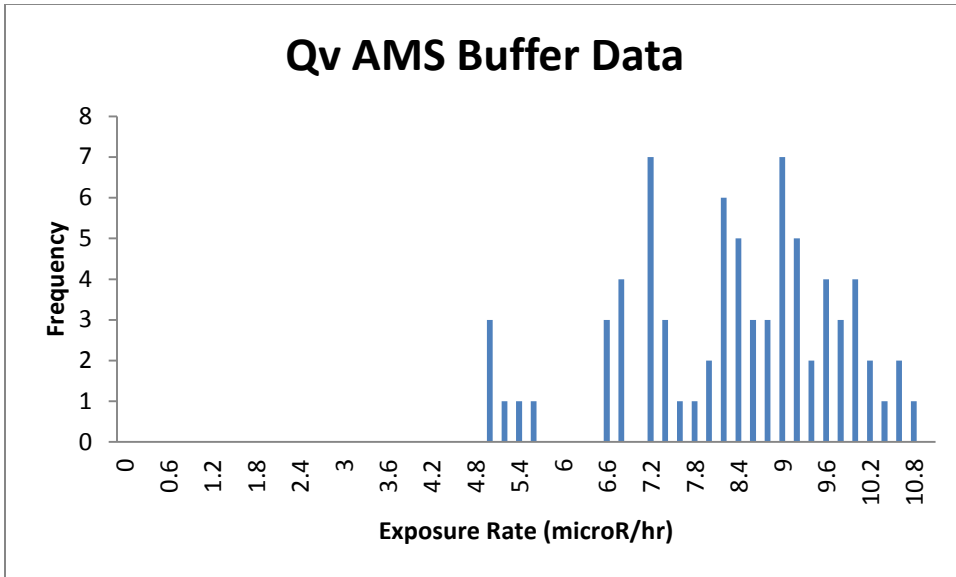
The means of these histograms is not within error, this is probably due to the fact that there are only 17 NURE survey data points and the data is not making a clear curve. However the majority of the AMS data falls between 6.2 and 10.3, a similar range to that of the NURE data.

Qv 50 m buffer NURE Histogram:

Qv NURE Buffer Data — histogram with x-axis "Exposure Rate (microR/hr)" and y-axis "Frequency"
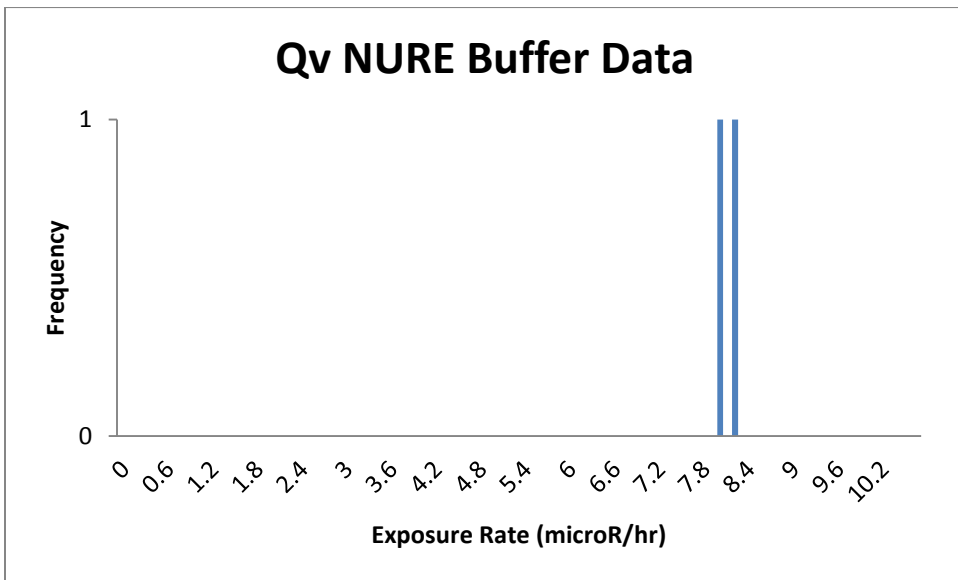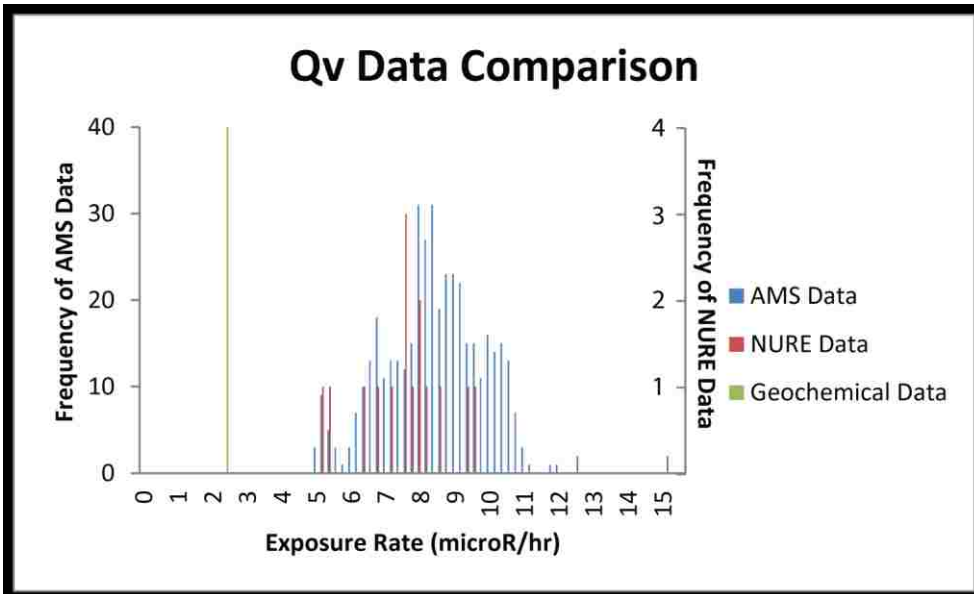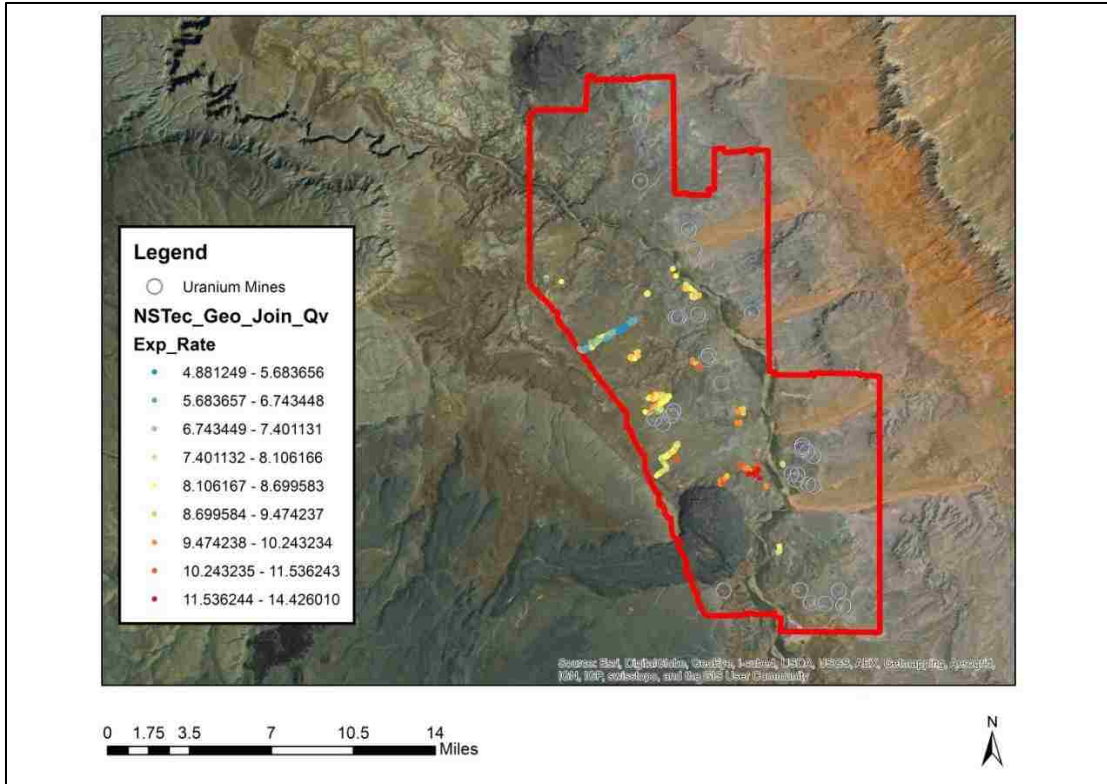
Qv 50 m buffer AMS Histogram:

Qv AMS Distribution: This unit has a trend that is backwards of most other units. Its hottest areas are in the southeast, and it gets cooler to the northwest. However this unit is not very widespread and the range of its exposure rate is not great, 4.881 to 14.426

Qv AMS Exposure Rate Data

Parent Units

TRmhm: Holbrook and Moqui Members of the Moenkopi Formation, Early to Mid Triassic in age. Composed mainly of claystone, siltstone and sandstone, in some locations includes gypsum, limestone and conglomeratic sandstone (Billingsley et al., 2007).

TRmhm Field Notes: Basalt float present, unit is a fine grained red sandstone. When broken unweathered surface is pinkish grey. Lack of ripple marks.
Dull red sandstone, some white, fine grained, rare cross stratification. Vesicular basaltic boulders. Some bushes and grasses, sparse.

These field observations are consistent with the USGS description of a fine grained red sandstone, however, no limestone, claystone, gypsum, or conglomeritic sandstone was observed.

TRmhm NURE Histogram:
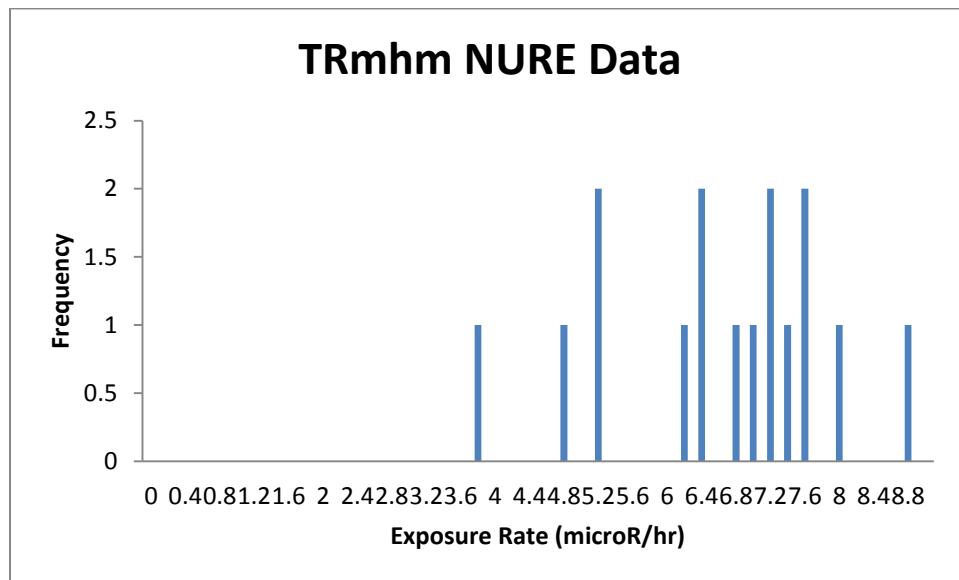
TRmhm AMS Histogram:
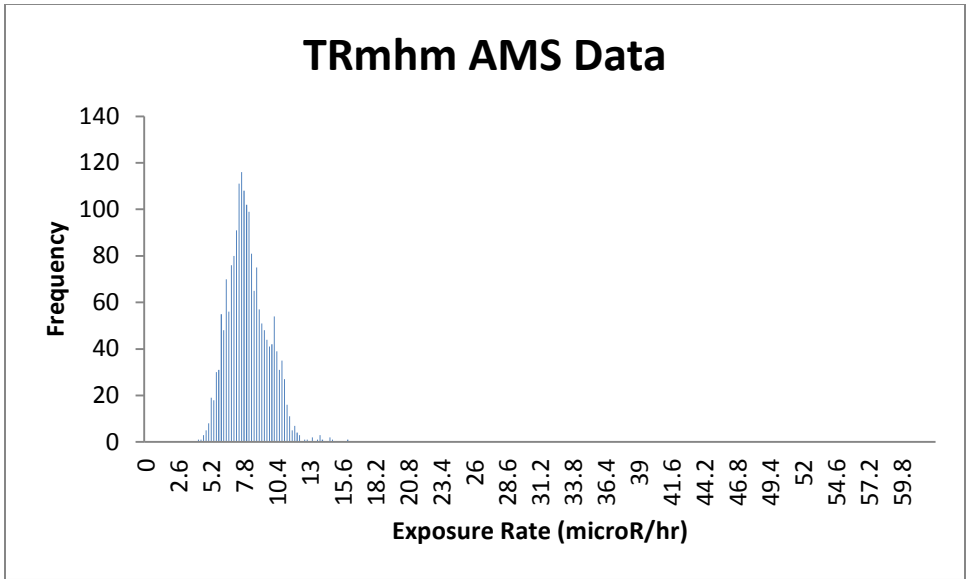
The means of these 2 histograms are significantly different. There are few points in the NURE survey data, and it has a smaller range that is lower in exposure rate than the majority of the AMS data points. The AMS data is also slightly right skewed.
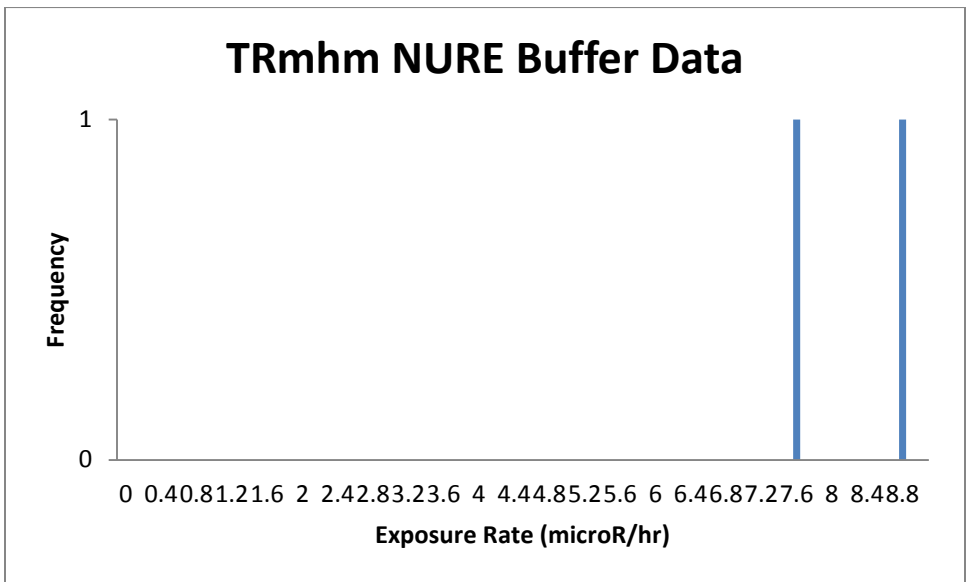
TRmhm 50 m buffer NURE Histogram:

TRmhm 50 m buffer AMS Histogram:
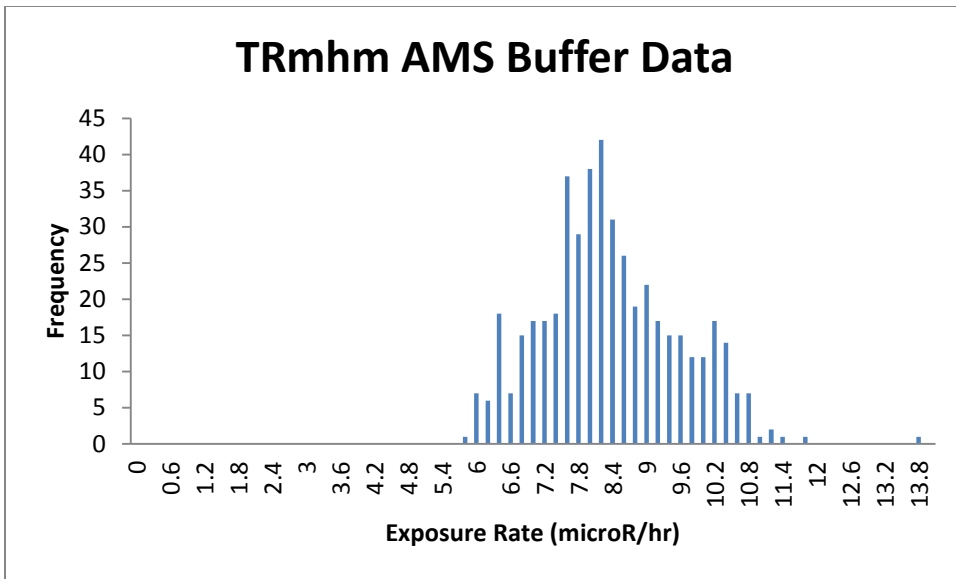
TRmhm AMS Distribution: This unit occurs in two main areas in the south by black point and north surrounding the river. It follows most trends as the south is cooler than the north, but taking a closer look at the points in the north surrounding the river there is a strange trend. The west side of the river is significantly cooler than the east side. It seems strange to see so much variation in a rock unit, and could possibly be due to alluvial contamination. This unit does not have as wide of range as other bedrock units, 4.375 to 14.583.

TRmhm AMS Exposure Rate Data
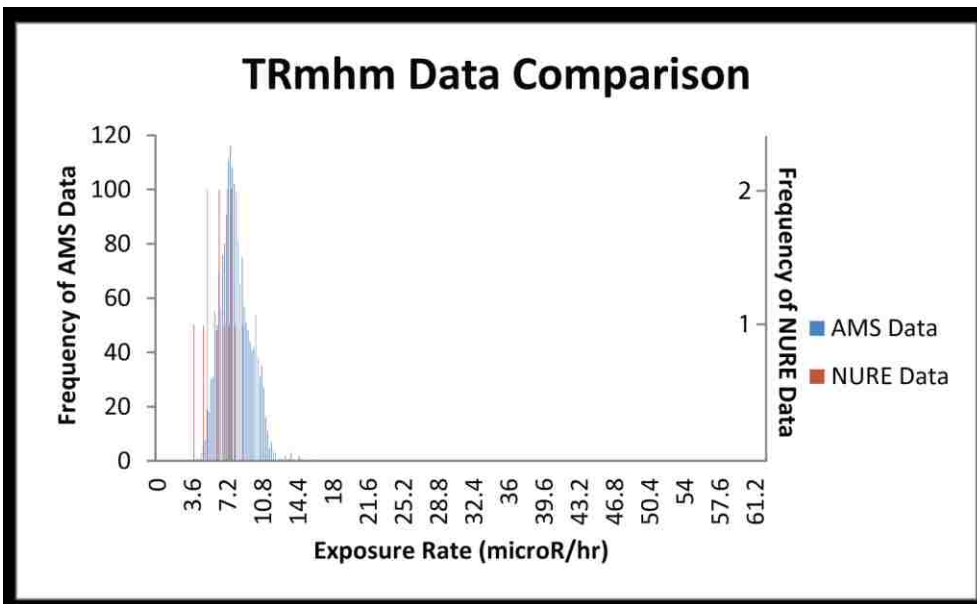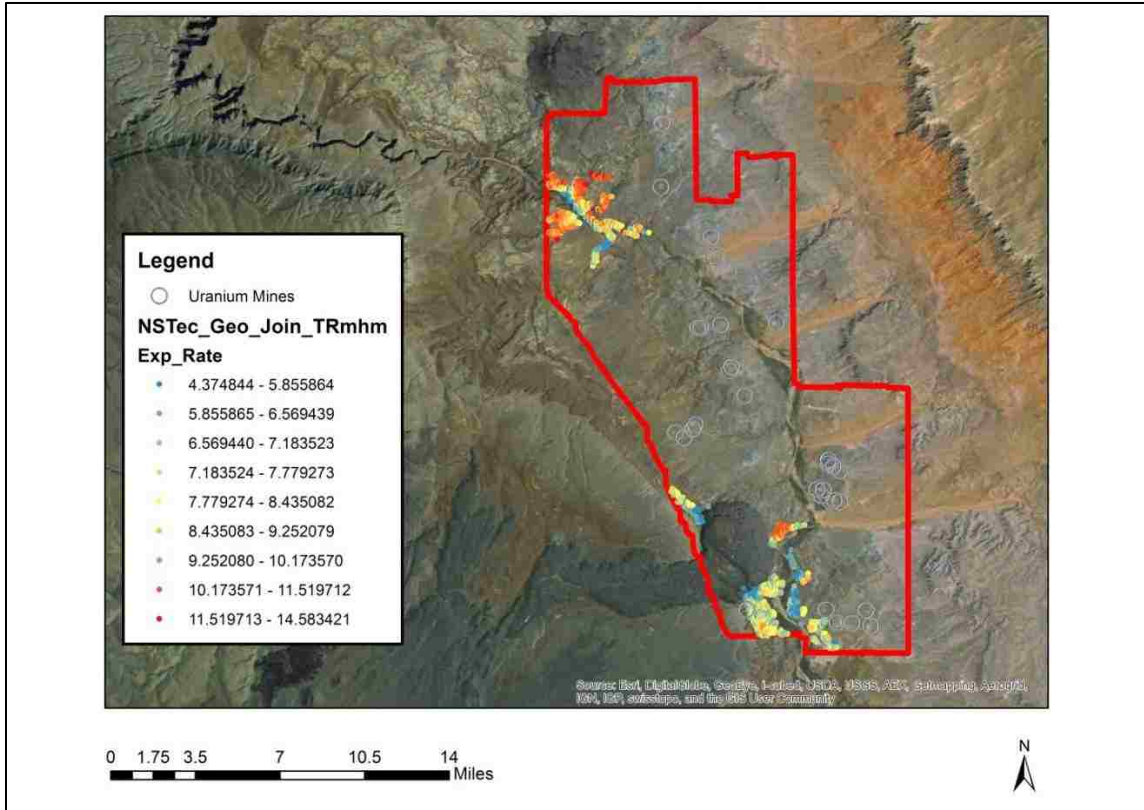
Daughter Units

Qdl: Very few small occurrences. Holocene linear dune deposits, consists of quartz sand (Billingsley et al., 2007).

Qdl Field Notes: This unit was not visited due to road construction.

Qdl NURE Histogram:
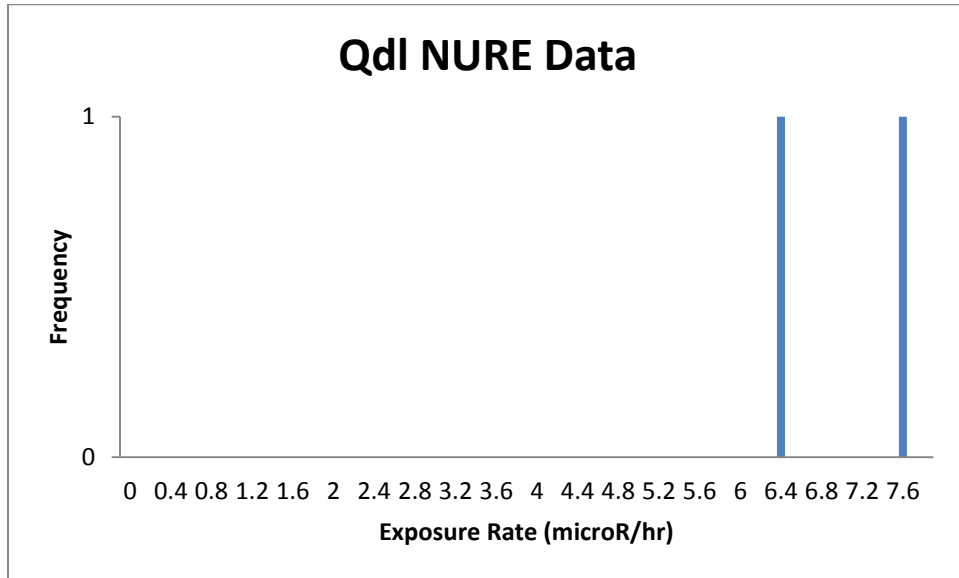
Qdl AMS Histogram:
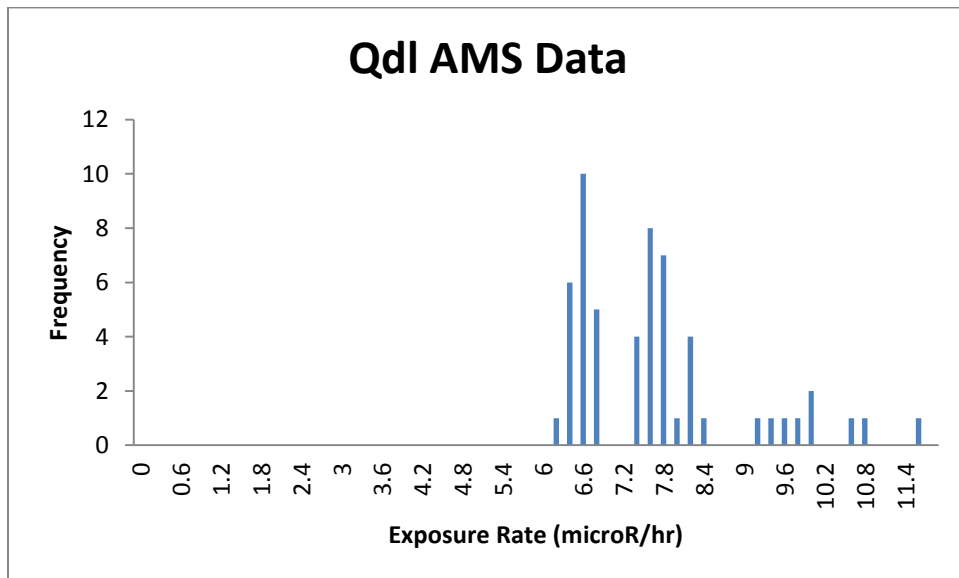
The means of these histograms are not within error. This is most likely due to the fact that there are only two data points for the NURE survey, and one of

them is below the range of the AMS data. The AMS data is right skewed and does not form a good curve.

Qdl 50 m buffer AMS Histogram:
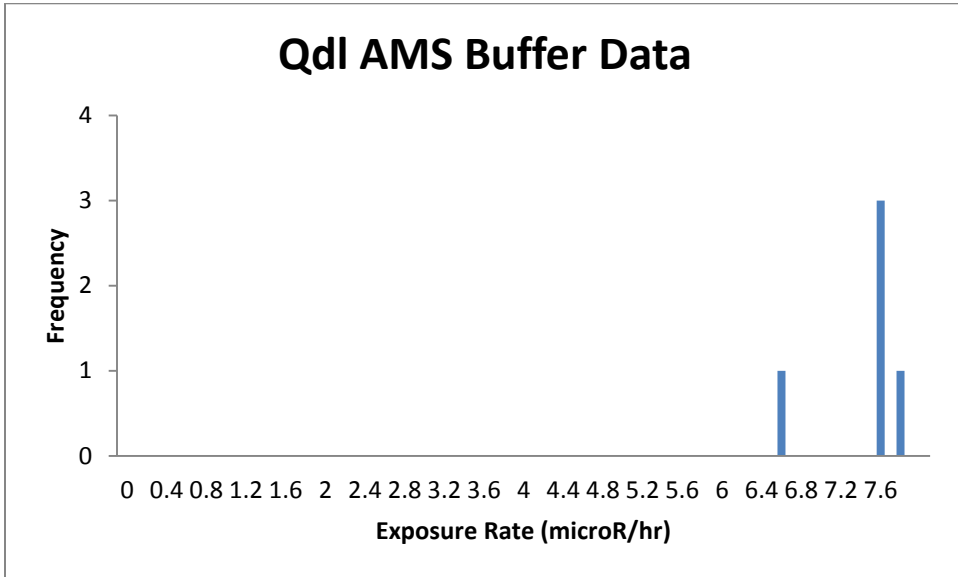
Qdl AMS Distribution: This unit is very small and thus does not display any overall trends. It has a small range of exposure rates, from 6.074 to 13.385. That is a higher minimum than most other units but could be due to small sample size.

Qdl AMS Exposure Rate Data
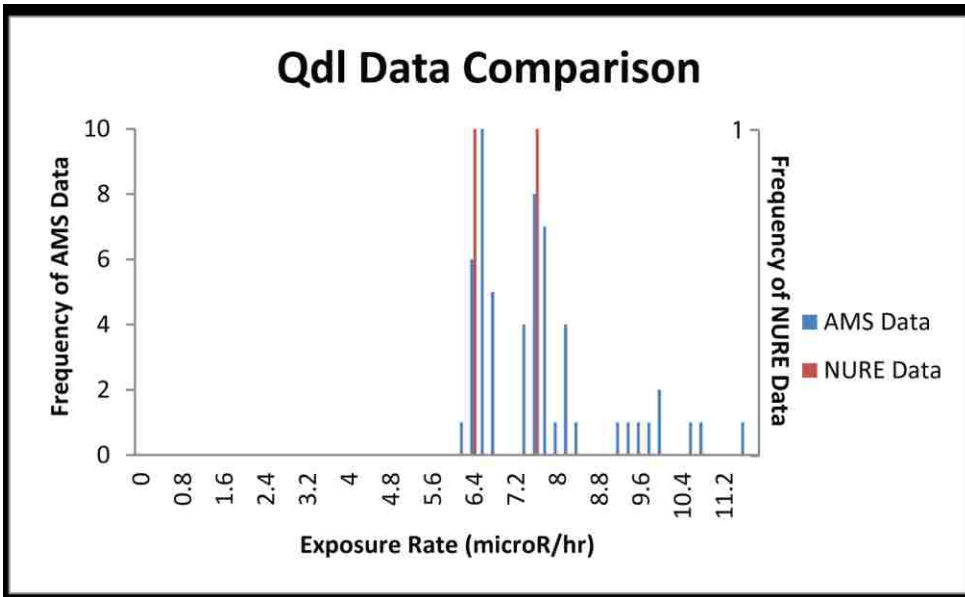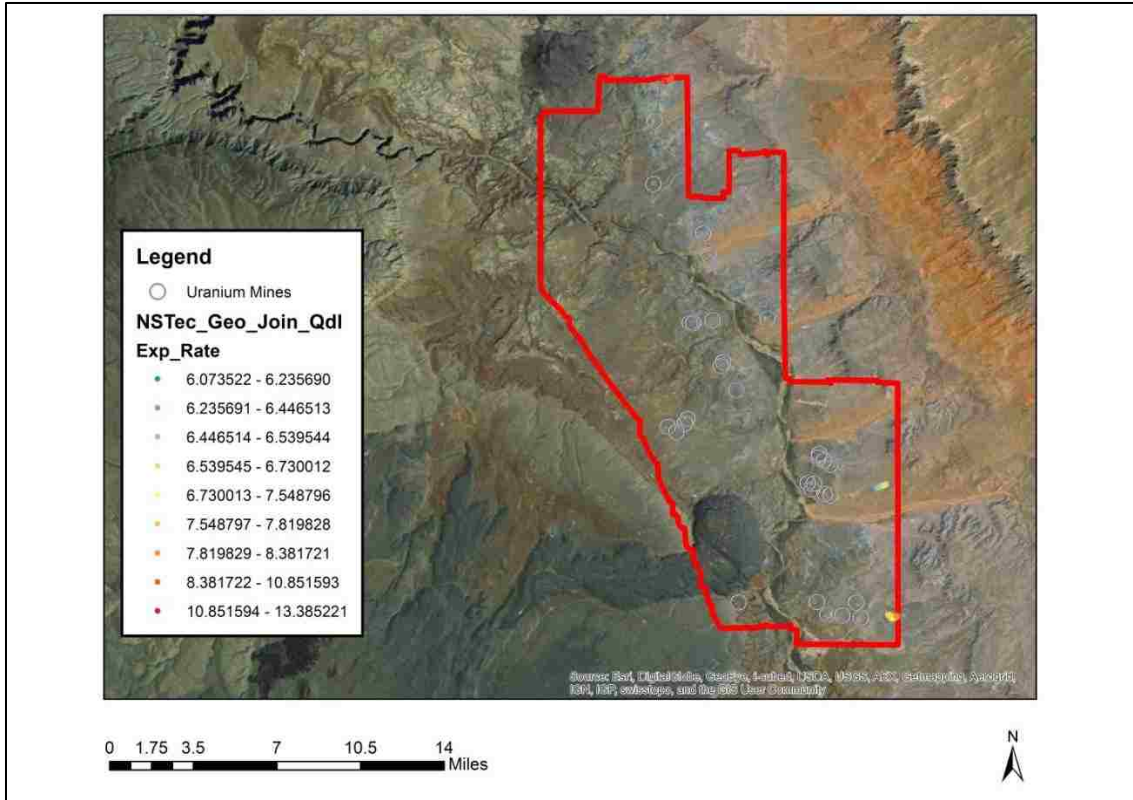
Qdp: Very few small occurrences. Holocene parabolic dune deposits composed of quartz sand. The USGS report states that 'bedrock or older sand accumulations often exposed within interior of isolated parabolic dunes' (Billingsley et al., 2007). This indicates that for modeling an aerial gamma ray survey the unit beneath Qdp may become important.

Qdp Field Notes: Cemented mudcracks, sand surrounding the unit. There is channeling present on the mud cracks. Exposure of bedrock is not apparent. The unit is crescent shaped. Very small unit, not sure it really counts as a dune. Cemented mud cracks with some eolian sands on top. Some channeling with small about 1 cm clasts of limestone, chert, rare basalt, no vegetation.

This unit is not in the correct location on the geologic map, it's about 75 m north. This unit was consistent with the USGS description in shape, but very different in every other way. The USGS describes it as loose unconsolidated quartz sand, whereas we saw mud cracks with very little sand on top. Dunes shift frequently in this windy area, so this type of inconsistency is expected in dune units.

Qdp NURE Histogram:
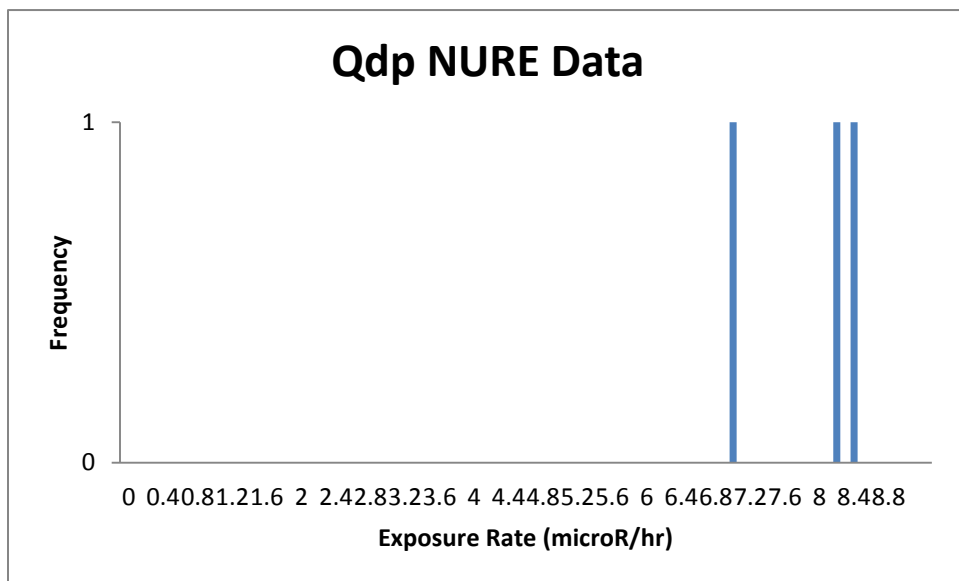
Qdp AMS Histogram:
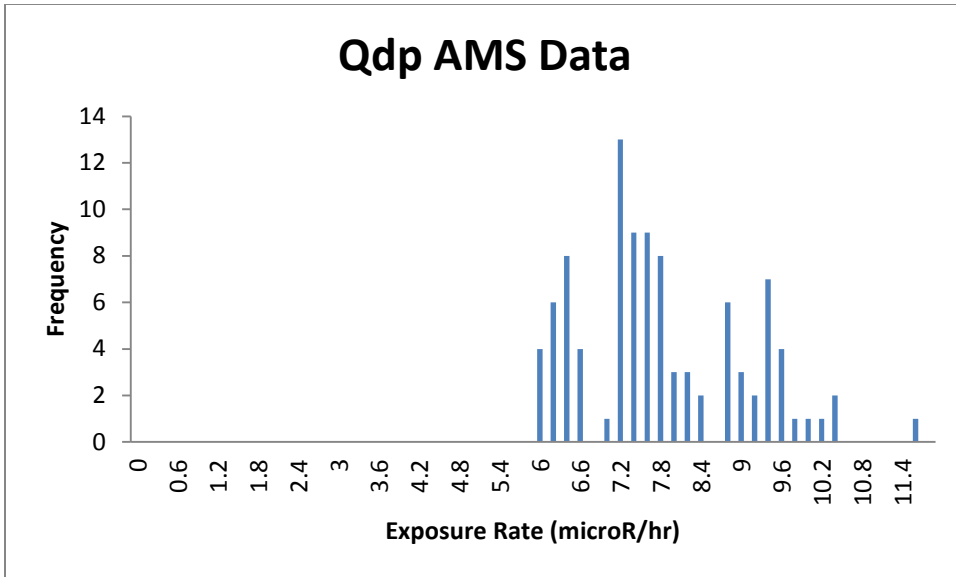
The means of these histograms are not within error. This is due to the fact that there is only one NURE survey data point, and it occurs at the minimum of AMS data.

Qdp 50 m buffer NURE Distribution:
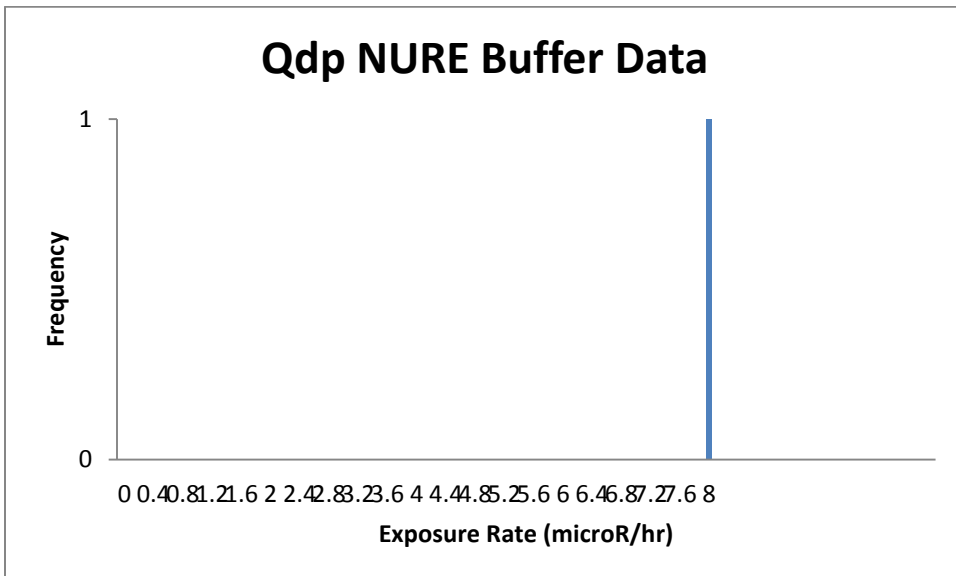
Qdp 50 m buffer AMS Distribution:

Qdp AMS Buffer Data
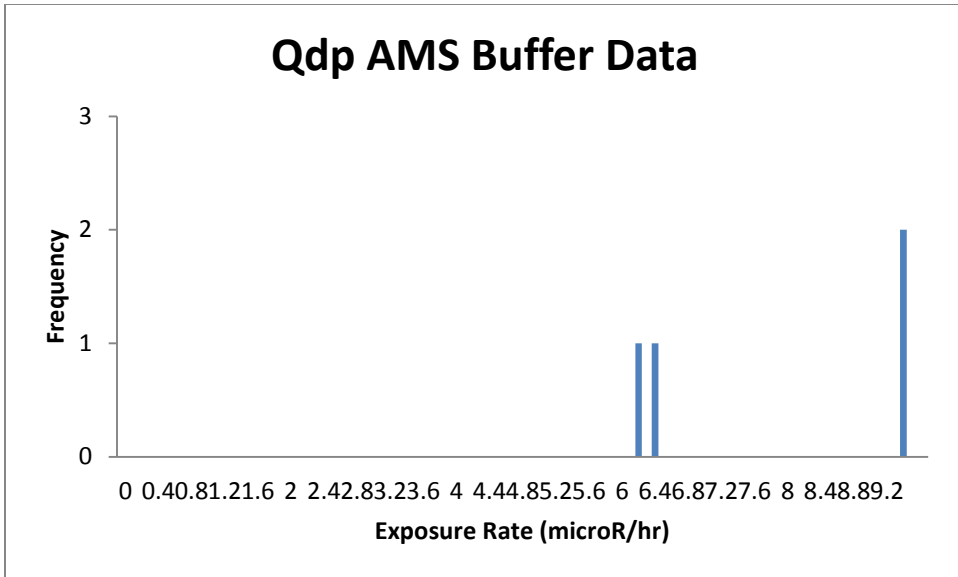
Qdp AMS Distribution: This unit has a small distribution, but appears to become hotter to the southeast, opposite of the trend of most other units. It has a small range of exposure rates, from 5.846 to 10.823.

Qdp AMS Exposure Rate Data

Qdp Data Comparison
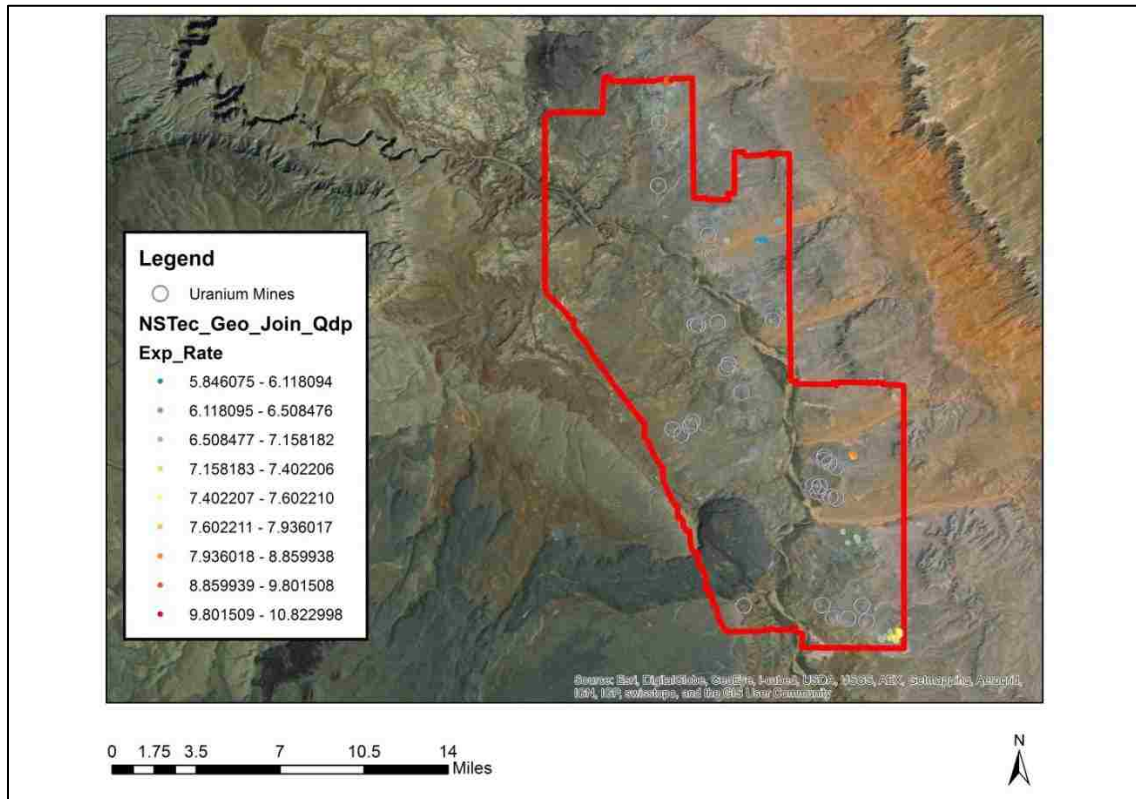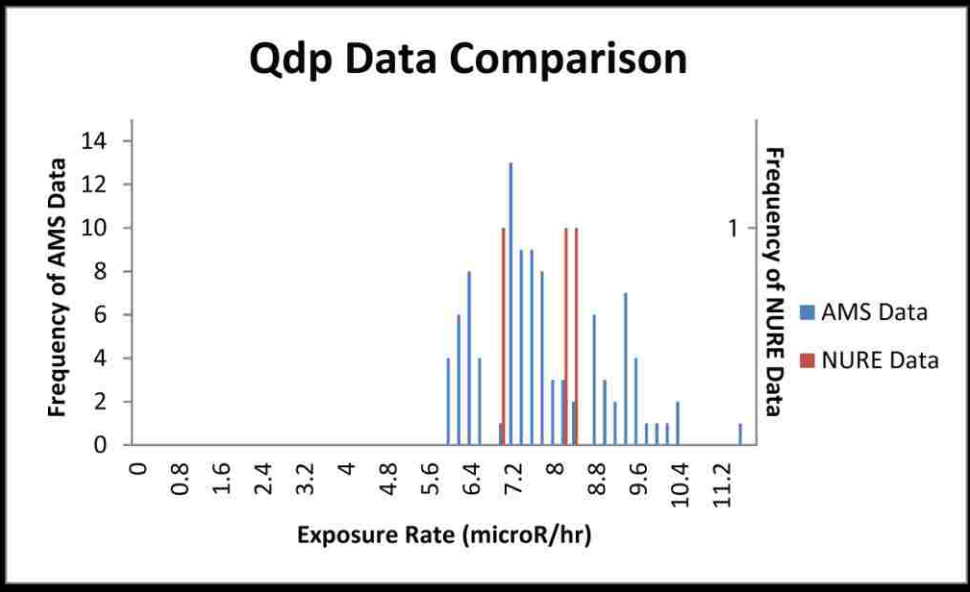
Qdb: This unit only has 2 small occurrences. Holocene barchan dune deposits, consists of quartz sand (Billingsley et al., 2007).

Qdb Field Notes: This unit was not visited.

Qdb AMS Histogram:

Qdb AMS Data

A bar chart titled "Qdb AMS Data" with the y-axis labeled "Frequency" (ranging 0 to 4) and the x-axis labeled "Exposure Rate (microR/hr)" (ranging 0 to 7.6). Two bars are shown: one at 6.4 with a frequency of 2, and one at 7.6 with a frequency of 3.
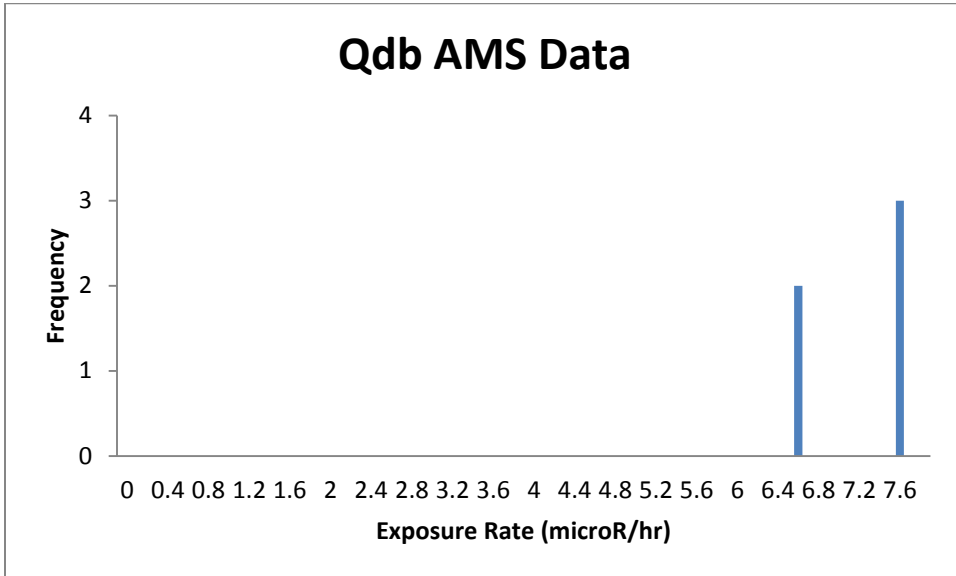
Qdb 50 m buffer AMS Distribution: The 50 m buffer causes an elimination of this unit.

Qdb AMS Distribution: This unit is very small and does not display overall trends. There are so few points it could not be separated into nine classes. Its range of exposure rates is very small, from 6.425 to 7.354.

Qdb AMS Exposure Rate Data

Legend

○ Uranium Mines

NSTec_Geo_Join_Qdb
Exp_Rate
- 6.425355
- 6.425356 - 6.508802
- 6.508803 - 6.510175
- 6.510176 - 7.250716
- 7.250717 - 7.353959

0   1.75 3.5   7   10.5   14
Miles

N
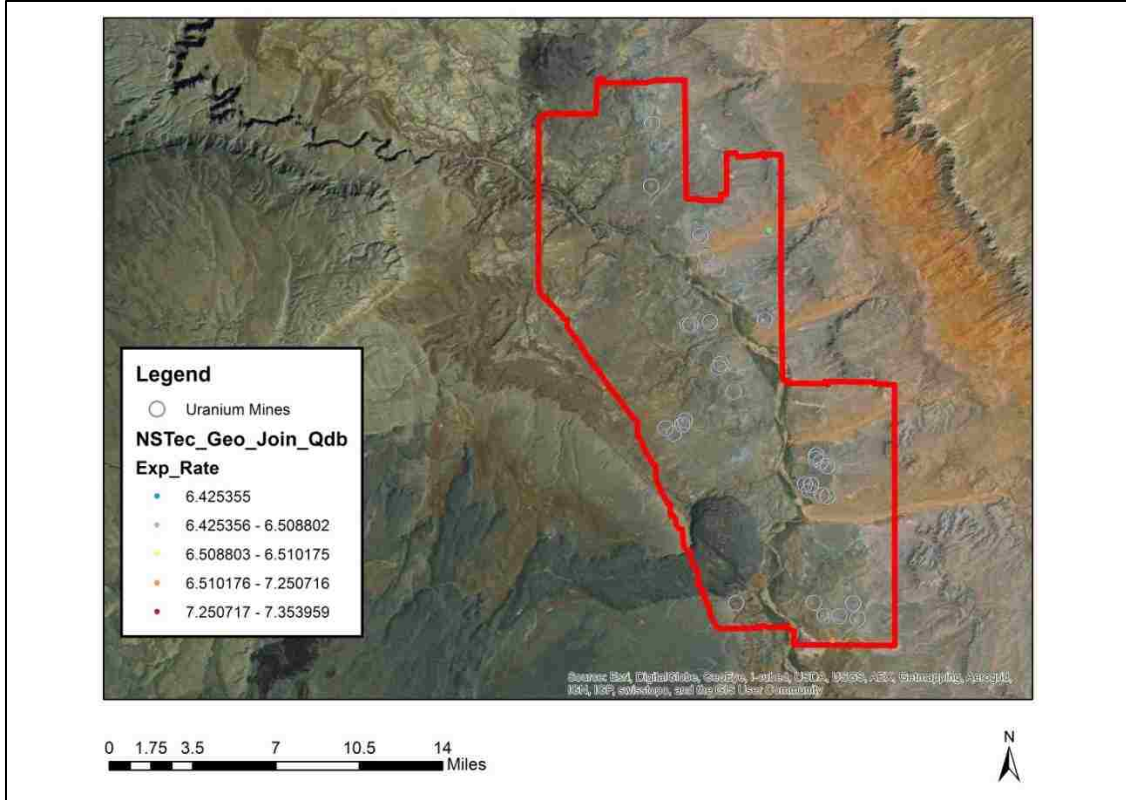
Qg2: Holocene gravel deposit, silt to gravel sized clasts. Matrix of silt and sand with clasts of Pkh and basalt in the southern portion of the map. USGS classifies this unit as lithologically similar to Qg1 (Billingsley et al., 2007).

Qg2 hot Field Notes: This gravel unit consists of mostly clasts of dark sandstone we haven't yet seen. It could be TRcp, but it's a very dark grey. Little basalt and chert. The sandstone is mostly quartz and feldspar with black matrix, sample in bag. Sand underneath is brown, poorly sorted, coarse to fine, composed mainly of rock fragments including basalt and limestone.
Dark sandstone covered in eolian dust, some mud cracks. Sandstone possibly derived from basalt at black point. Little vegetation.

Qg2 cool Field Notes: Channeling with respect to clast size. More rounded clasts. Dominated by chert. Moderate vegetation. Fine aeolian sand beneath clasts. Extremely different from other Qg2. No bedrock outcrops. Fairly continuous in composition, seems continuous underneath top layer. This unit has clasts in the sand, not just sand.
Weak desert pavement, bars of clasts about 1-2 cm in width. Channels of finer clasts less than 1 cm. Clasts consist of chert. Moderate vegetation.

These field observations are consistent with the USGS description of a gravel unit with sandstone and basalt clasts, chert is not mentioned specifically, but it was most likely derived from the limestone the USGS lists as a source rock. Qg2 hot could be hotter due to the larger clast size and also the dark grey sandstone that wasn't present in Qg2 cool.

Qg2 NURE Histogram:

Qg2 AMS Histogram:

Qg2 AMS Data
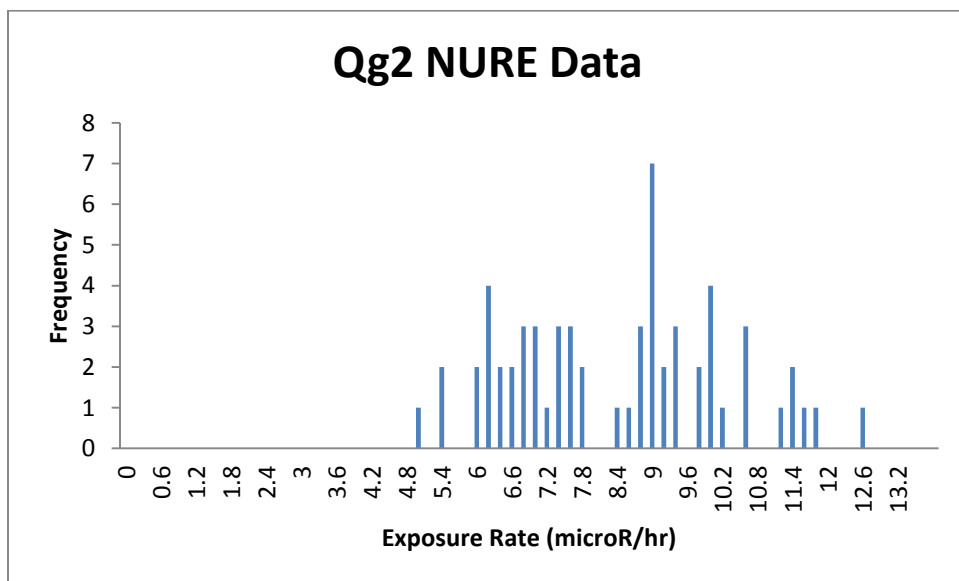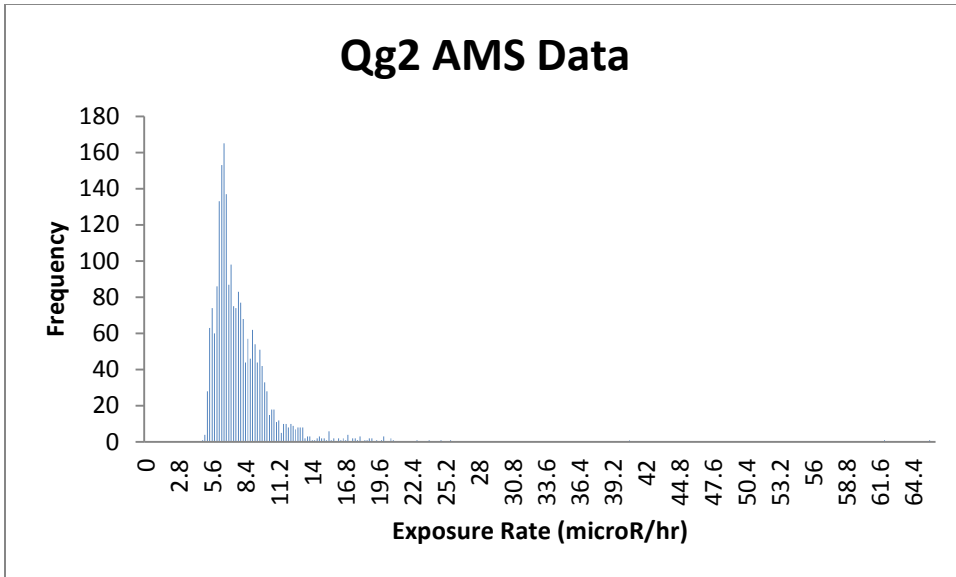
These histograms have means that are within error. They are both right skewed, though the AMS histogram is significantly more so.

Qg2 50 m buffer NURE Histogram:

Qg2 NURE Buffer Data
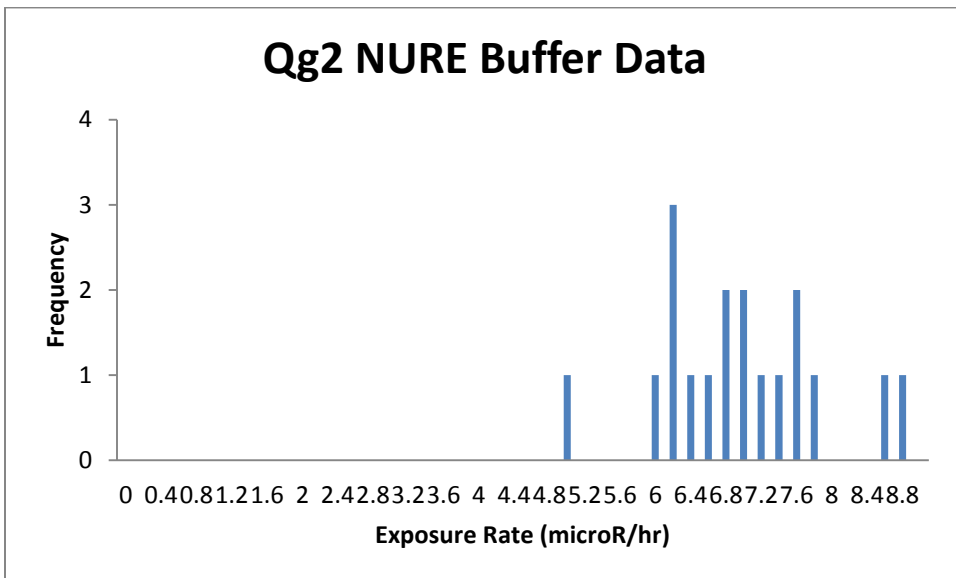
Qg2 50 m buffer AMS Histogram:

Qg2 AMS Buffer Data
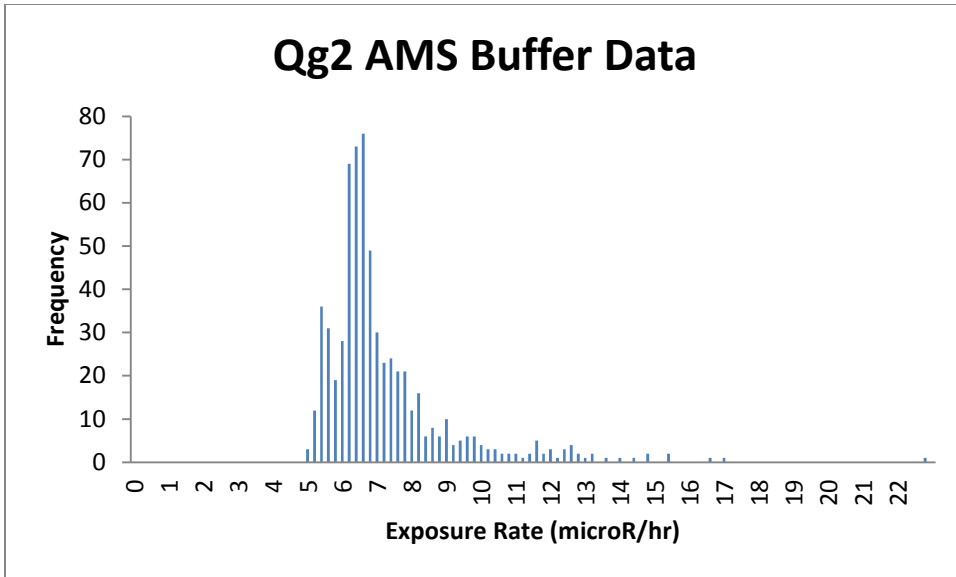
Qg2 AMS Distribution: This unit has a large distribution and a large range of exposure rates, from 4.766 to 61.883. A trend occurs in the southern portion of the map where west of the river is hotter than the east.

Qg2 AMS Exposure Rate Data

Qg2 Data Comparison
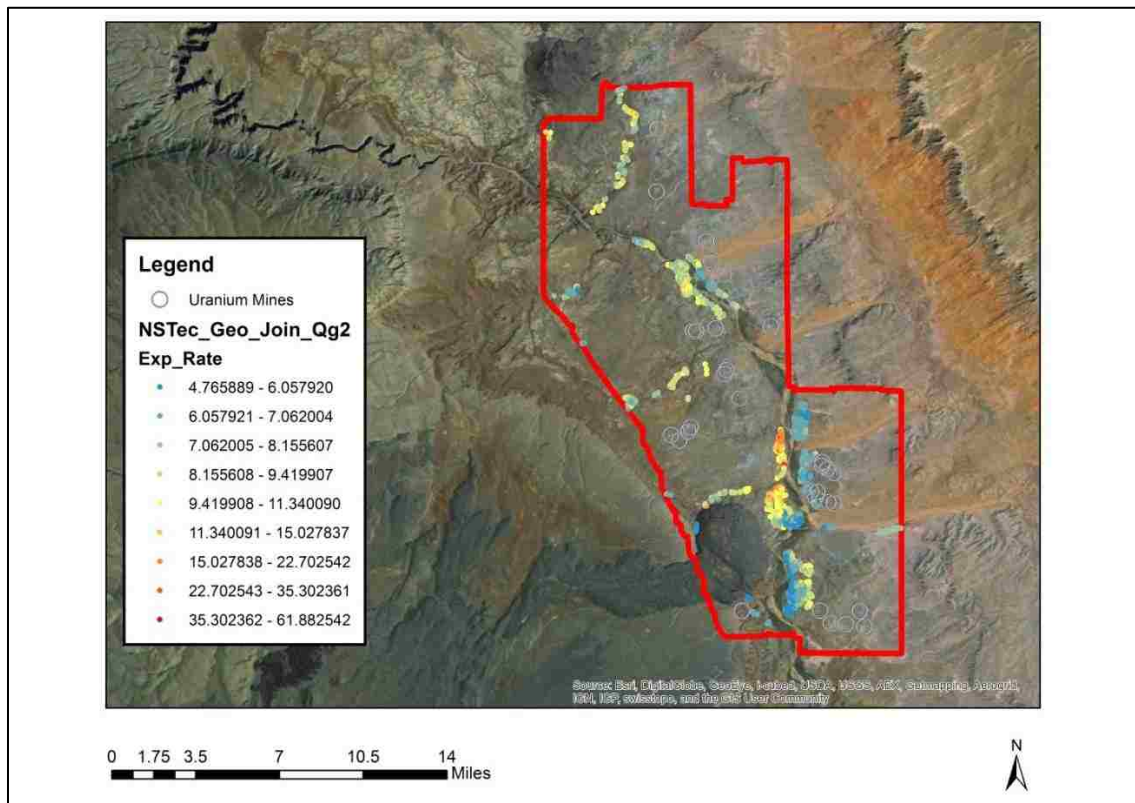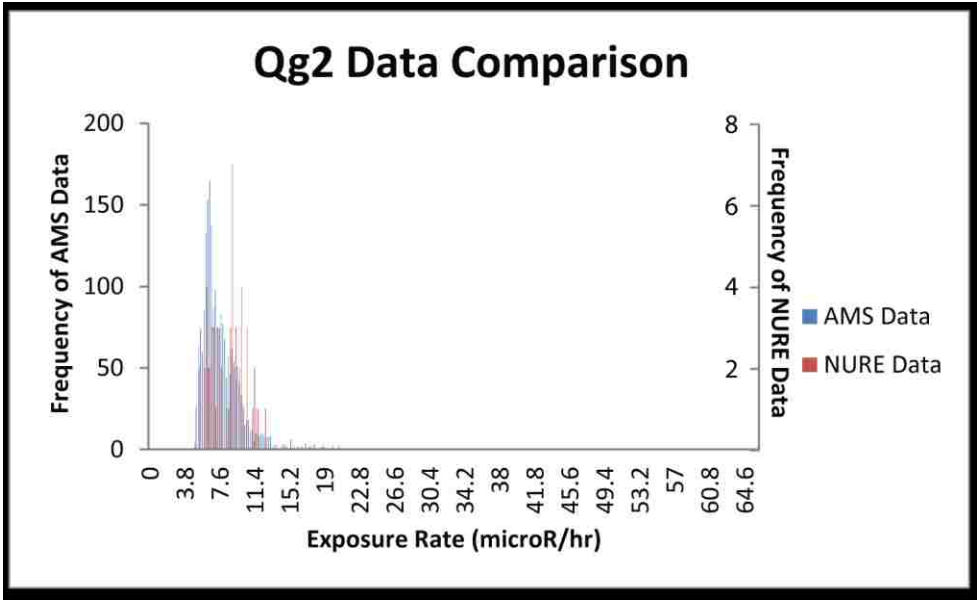
Qa3: Holocene and Pleistocene alluvial fan deposit, silt to gravel in size, partially cemented by gypsum and calcite. Lithologically similar to younger alluvial deposits, Qa1 and Qa2 (Billingsley et al., 2007).

Qa3 Field Notes: More developed surface. Surface is all clasts (large) underneath is a grey brown soil. Clasts are conglomerate, chert, basalt, and brown sandstone like TRmhm or the like. There is also light sandstone like TRcs (large) and black limestone, found a piece with 2 large calcite crystals in it. Black limestone is fine grained and lacks other clasts (mudstone). More basalt as move towards black point.
Large clasts less than 5-10 cm of basalt, red sandstone, conglomerate, chert, white sandstone, black limestone. Below the surface is fine eolian sand, mud cracked when exposed.

These field observations are inconsistent with the USGS descriptions as we saw much larger clasts than are reported. Though we did find the surface to be more cemented as in the USGS description. The USGS description also only mentions basalt and chert as clasts, we found these to be clasts, but also had more varied rock types that would be expected to be seen in alluvial units in the area.

Qa3 NURE Histogram:

Qa3 AMS Histogram:

Qa3 AMS Data
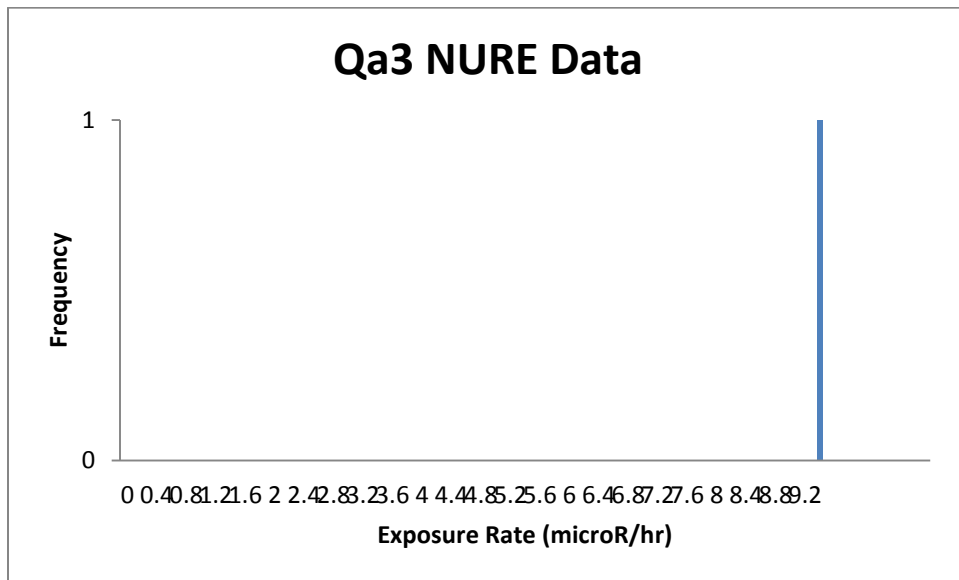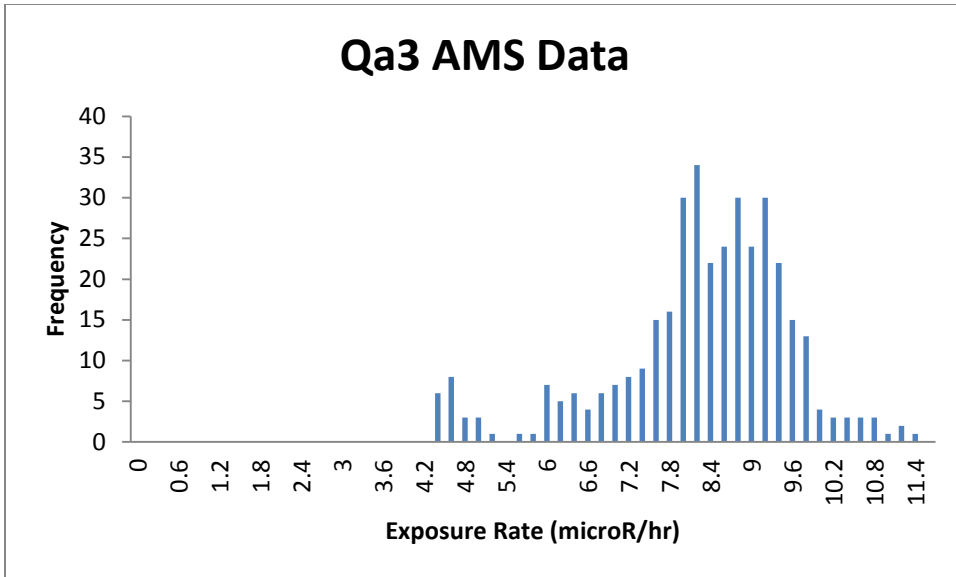
The means of these two histograms are significantly different. This is expected as there are only 6 NURE survey data points. The AMS histogram is left skewed, but this skewed portion represents the range of the NURE data.

Qa3 50 m buffer AMS Distribution:

Qa3 AMS Buffer Data
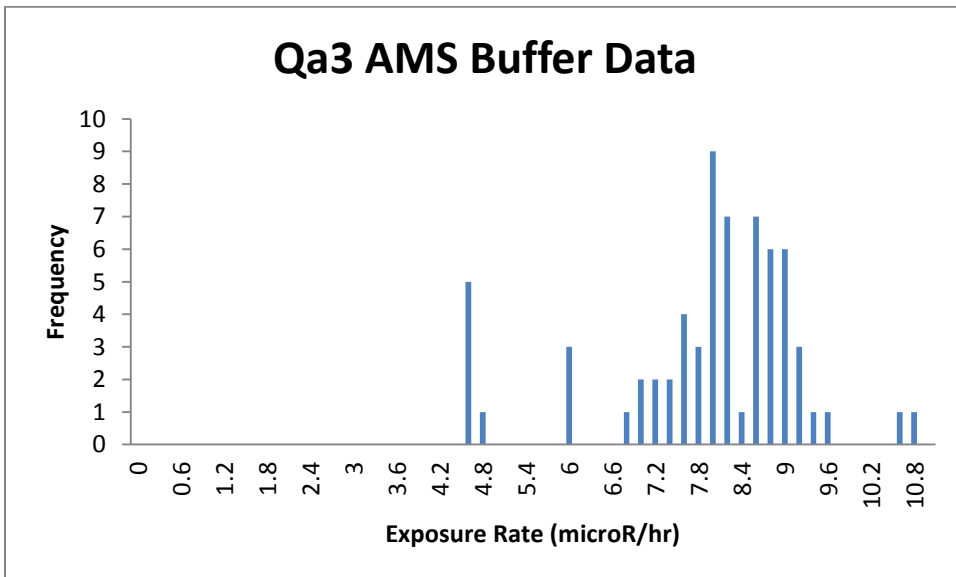
Qa3 AMS Distribution: This unit does not have a large distribution and lacks overall trends. It has a small range of exposure rates, from 4.36 to 11.51.

Qa3 AMS Exposure Rate Data
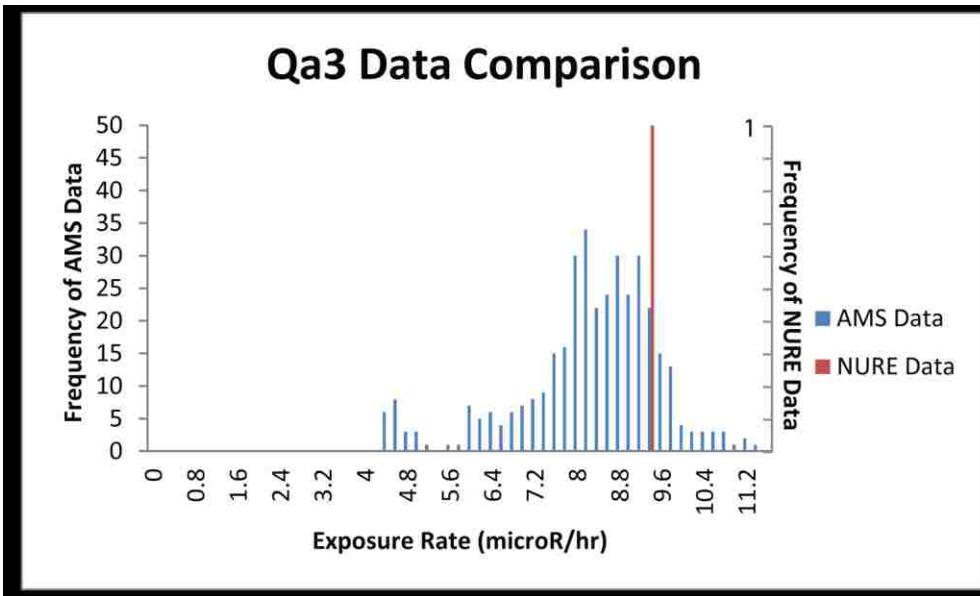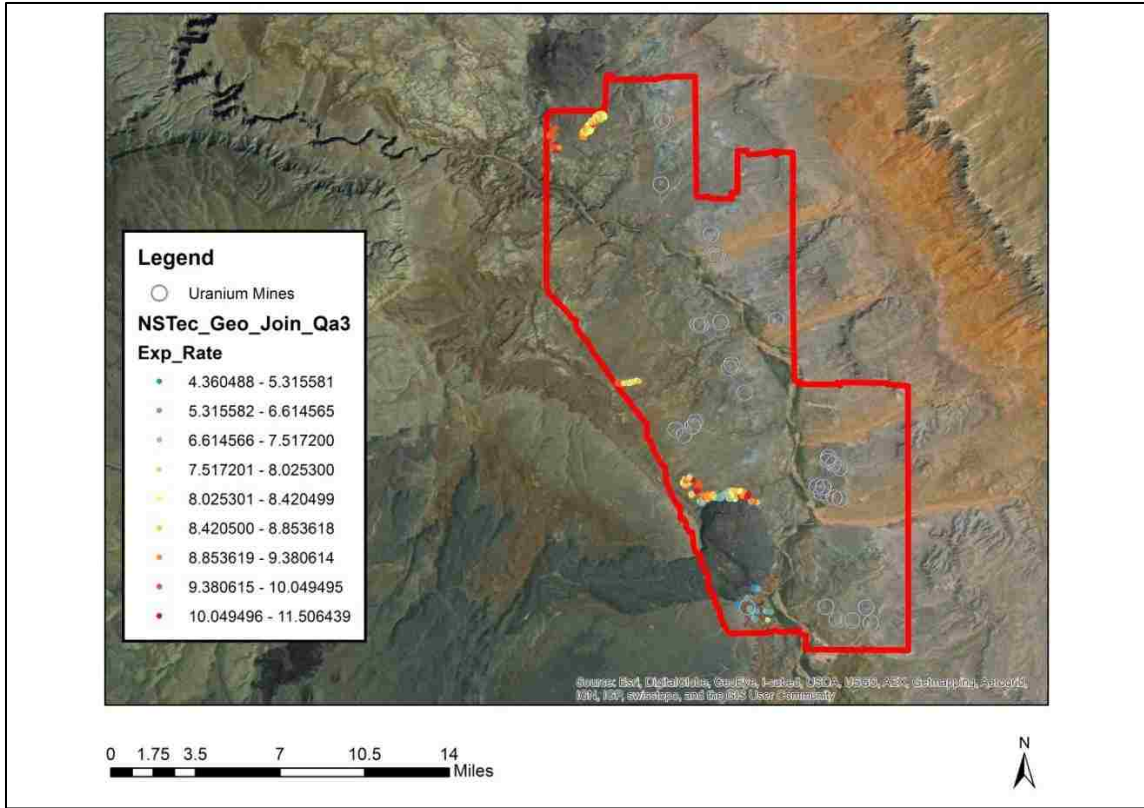
Qps: Holocene and Pleistocene age ponded sediments, composed mainly of clay to sand with some chert and limestone gravel, partially cemented by calcite and gypsum. The USGS classifies this unit as similar to Qf (Billingsley et al., 2007).

Qps (on basalt) Field Notes: Fine brown aeolian material/dust. Mudcracks present in this material. There are vesicular basalt clasts on top.Basalt clasts appear more weathered and rounded here than in Ts and Qae (on basalt). Clasts range from sand sized to 2 fists. This unit has no apparent variation. Little vegetation is present in this unit.
Brown mudcracked sediment with basalt clasts on top. Clasts less than 1 mm to 10 cm.

Qps hot (off basalt) Field Notes: Large chert nodules and small basaltic gravel present on top of red brown dirt. There is a lot of variation in the amount of chert nodules. The basaltic gravel appears to be lineated by the wind (present in stripes). There are mud cracks in the red brown dirt.
Brown mud cracked surface. Cherty clasts sparse to moderate about 5 cm in size. Some basaltic pebbles, non continuous. Sparse/no vegetation.

These field observations were consistent with the USGS description as partially cemented sediments with chert gravel, though no mention was made of basalt gravel that we saw at both sites. The only real difference between Qps hot and cool was the presence of chert and the basalt clasts were smaller in Qps hot, the pictures even look very similar. This unit did not resemble Qf, there was no basalt present in Qf (which dominated Qps) and the surface was not as well developed.

Qps Soil: This soil is described as sandy with moderate vegetation occurring on mafic volcanic rock (USGS, 2004). This is consistent with Qps as Qps is a sediment unit that occurs on top of basalt. There is one data point for this unit with a K wt % of 1.7% and a U concentration of 1.8 ppm.

Qps NURE Histogram:

Qps NURE Data — histogram of Frequency vs Exposure Rate (microR/hr)

Qps AMS Histogram:

Qps AMS Data — histogram of Frequency vs Exposure Rate (microR/hr)
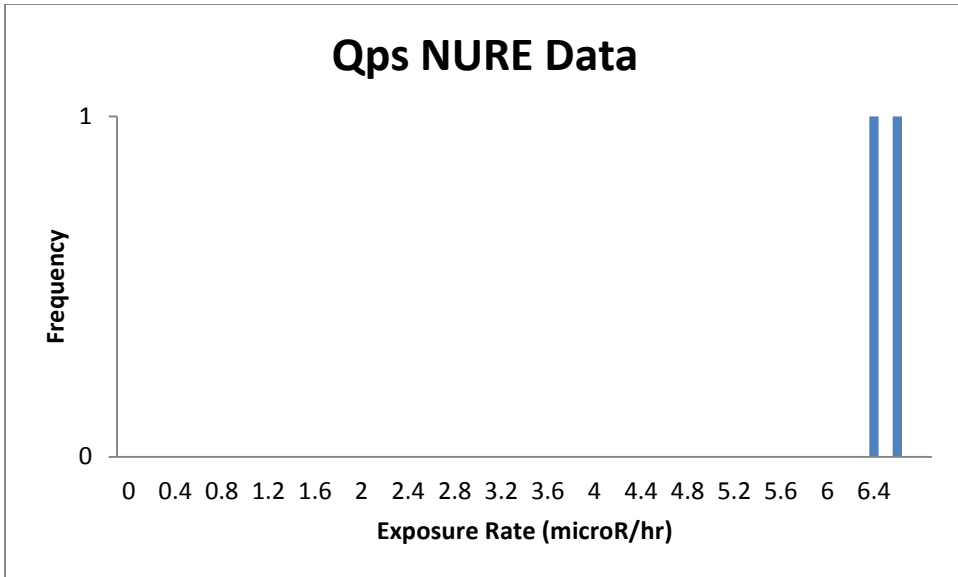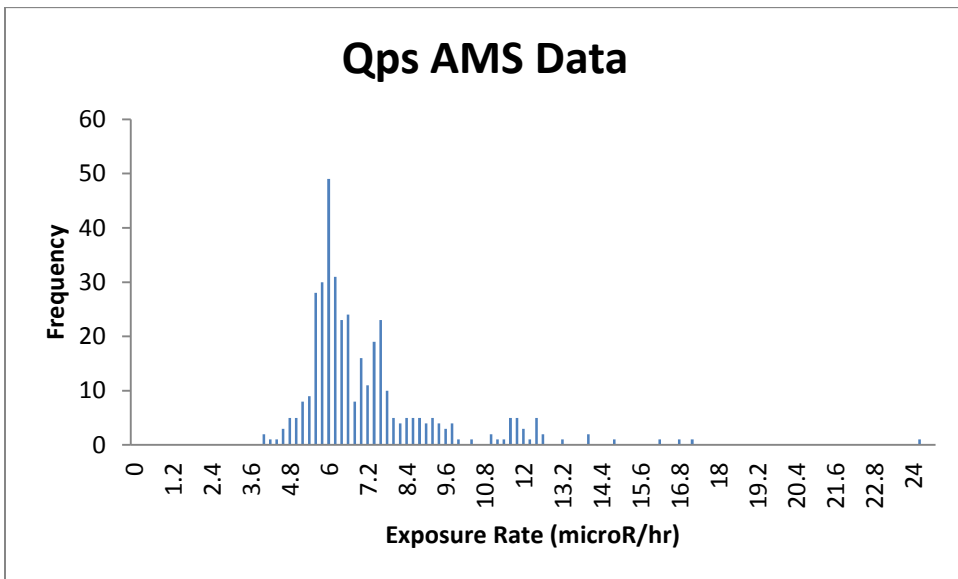
The means for these histograms are almost within error, this is surprising since there are only 3 data points from the NURE survey and the AMS data is right skewed.

Qps 50 m buffer AMS Histogram:

Qps AMS Buffer
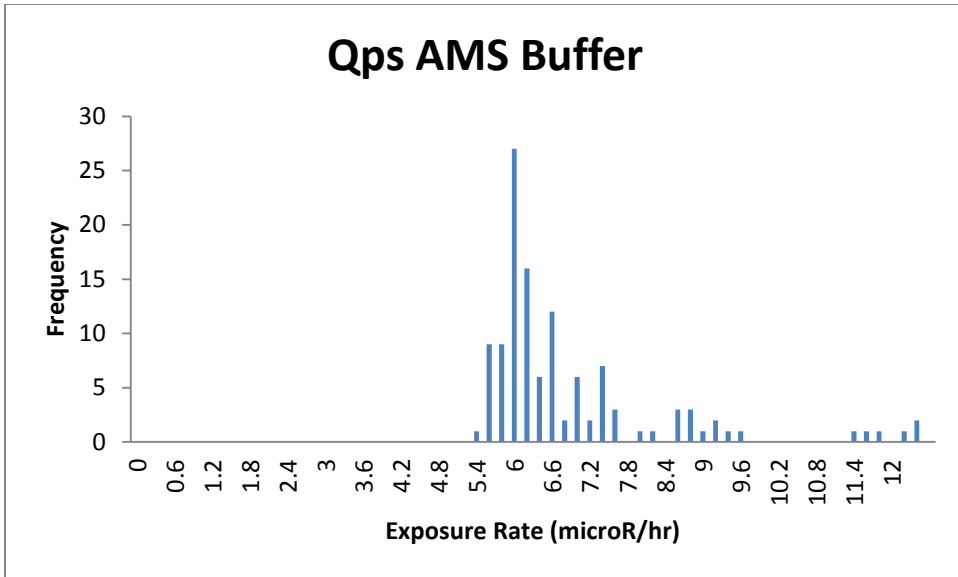
Qps AMS Distribution: This unit occurs throughout the mapping area in very small pockets. It does not display any overall trends, though the portion on Black Point is cooler than the rest of the unit.

Qps AMS Exposure Rate Data
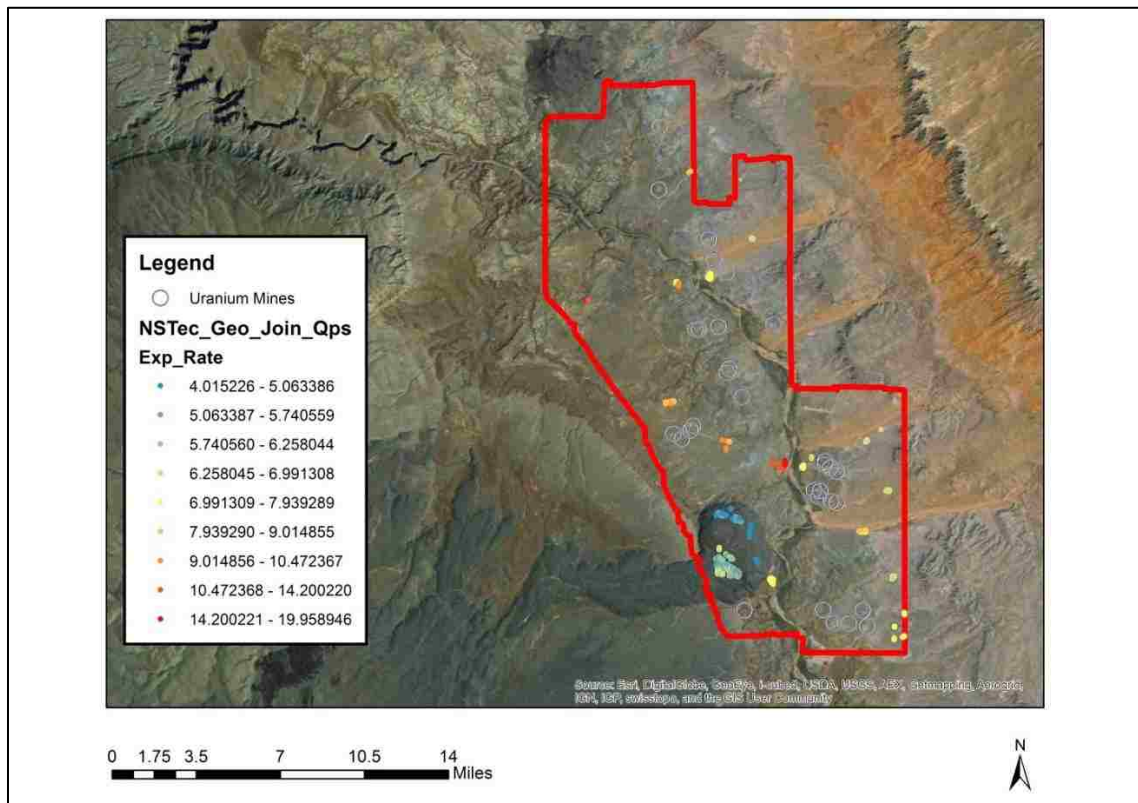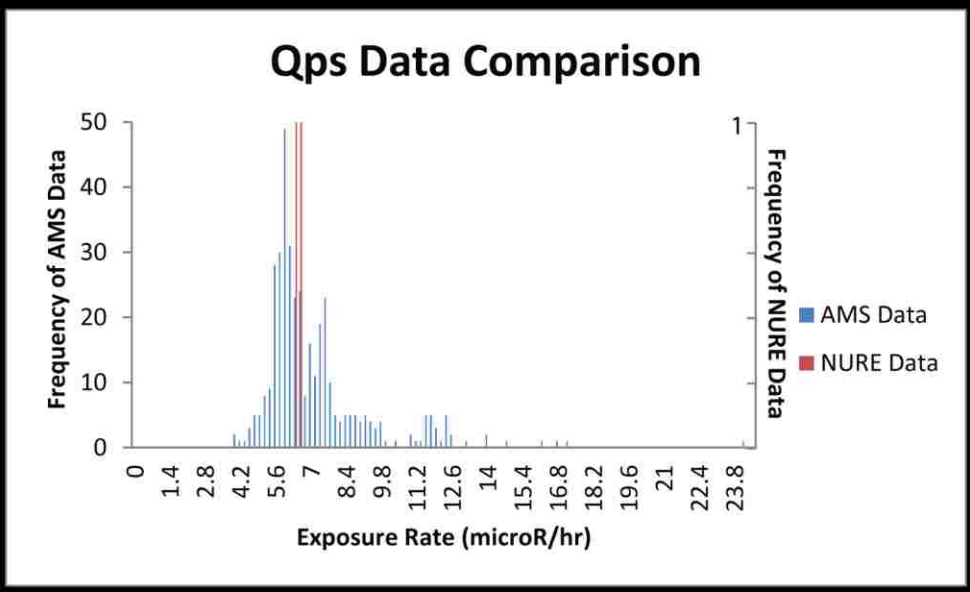
Qtr: Holocene and Pleistocene age talus and rock fall deposits. Silt to gravel matrix with boulders of limestone, chert and sandstone from Pkh and others, partially cemented by calcite and gypsum (Billingsley et al., 2007).

Qtr Field Notes: This unit was inaccessible in the field area.

Qtr AMS Histogram:
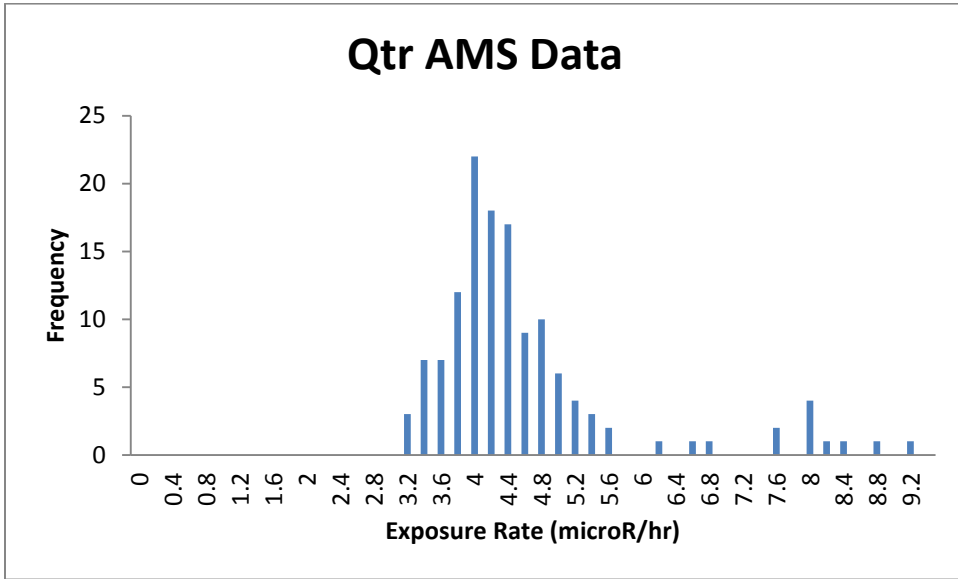
Qtr 50 m buffer AMS Histogram:
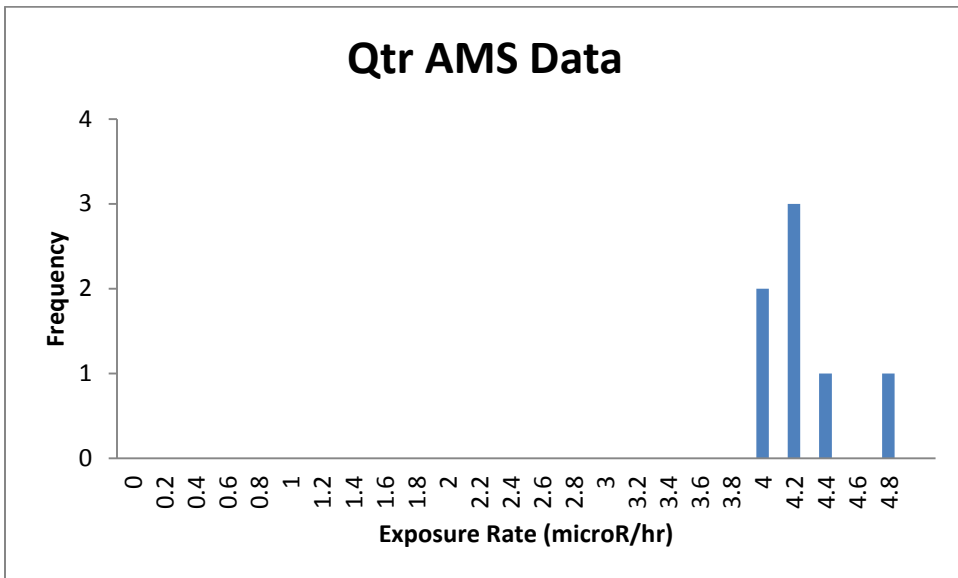
Qtr AMS Distribution: This unit has a small range, lacks any overall trends or patterns, and has a small range of exposure rates, 3.368 to 9.597.

Qtr AMS Exposure Rate Data
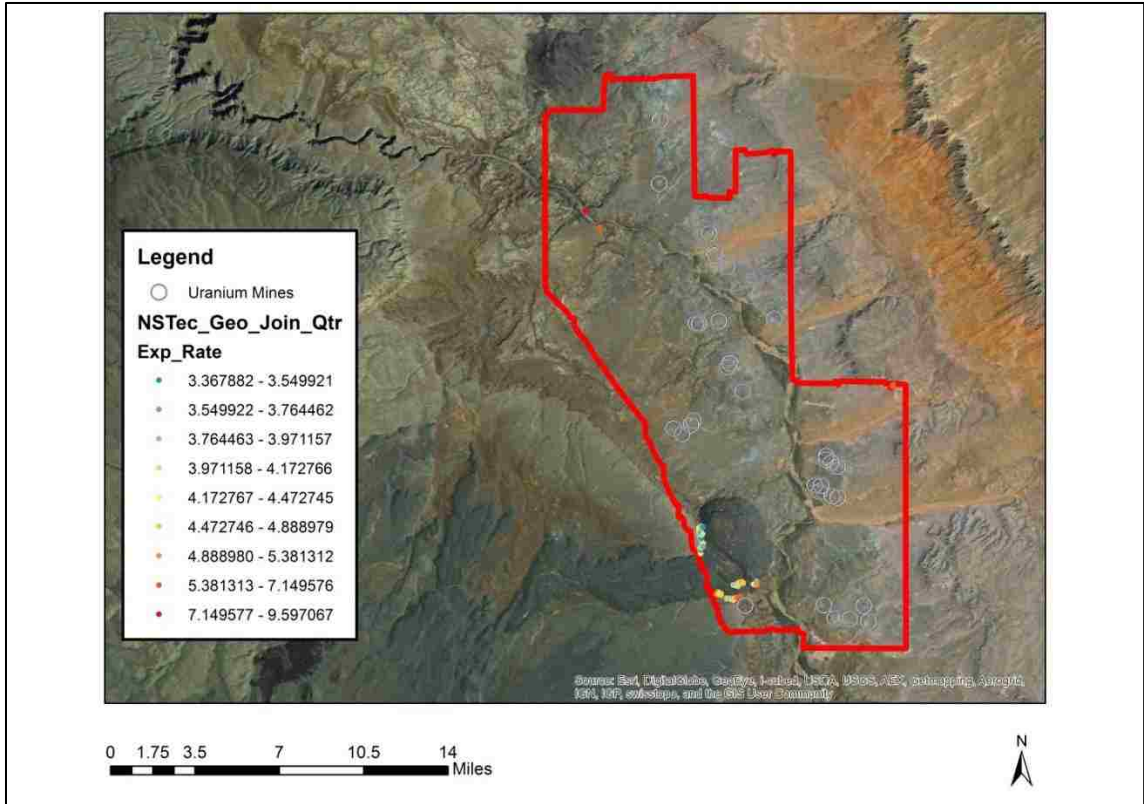
QTg4: Pleistocene terrace-gravel deposits, clasts ranging in size from silt to boulder, though largely sand and gravel clasts from Pkh, TRmw, TRmhm and TRmss. Some locations include basalt clasts from the southern portion of the mapping area (Billingsley et al., 2007).

QTg4 hot Field Notes: Construction prevented us from viewing this point.

QTg4 cool Field Notes: sand and clay matrix, moderate vegetation, light grey limestone clasts dominate, TRcs? Chert also present, clasts are overall angular. Limestone is very fine grained, has red chert clasts, only red, dull light grey overall. Some basalt. Some green alteration.
Lime mudstone. Sandy with moderate gravels. Gravel composed of altered limestone, chert and unaltered fine grey limestone. Sand is mostly quartz, red in color. Sparse vegetation mostly bushes.

These field observations are consistent with the USGS description of a gravel deposit with basalt, limestone, and chert clasts.

QTg4 NURE Histogram:
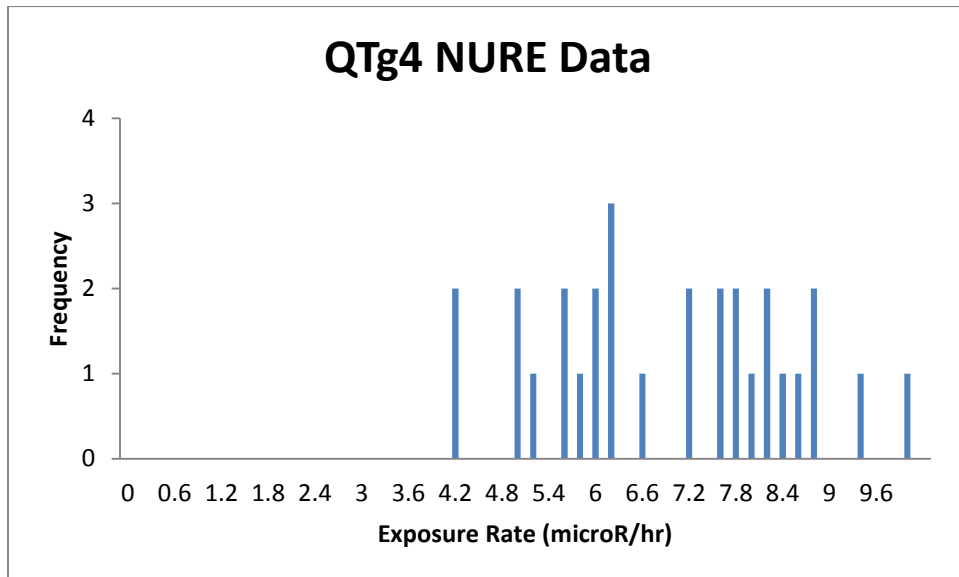
QTg4 AMS Histogram:

QTg4 AMS Data
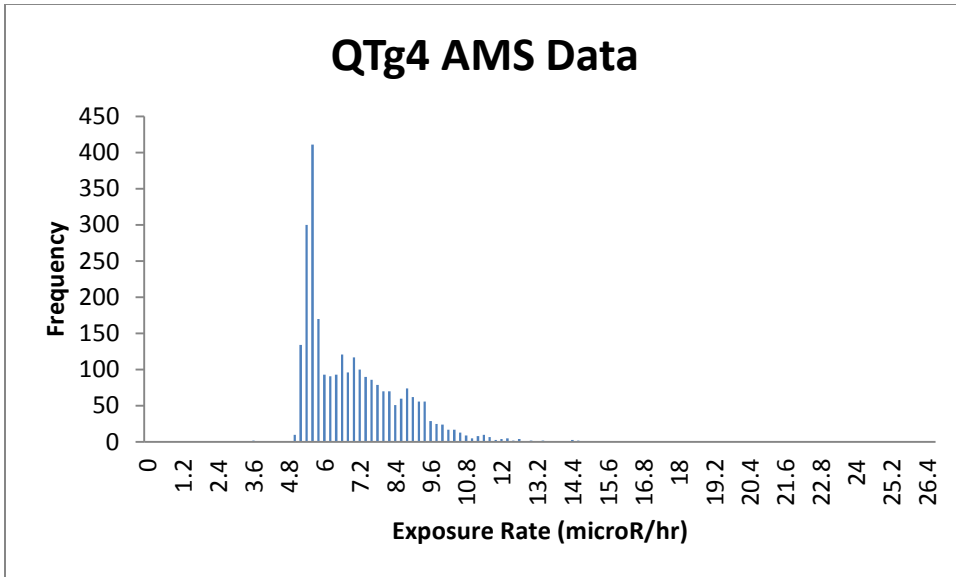
The difference between these two histograms' means is greater than error. There are few points in the NURE histogram, and the AMS histogram has a large right skewed 'tail' probably both causes of error.

QTg4 50 m NURE Distribution:

QTg4 NURE Buffer Data
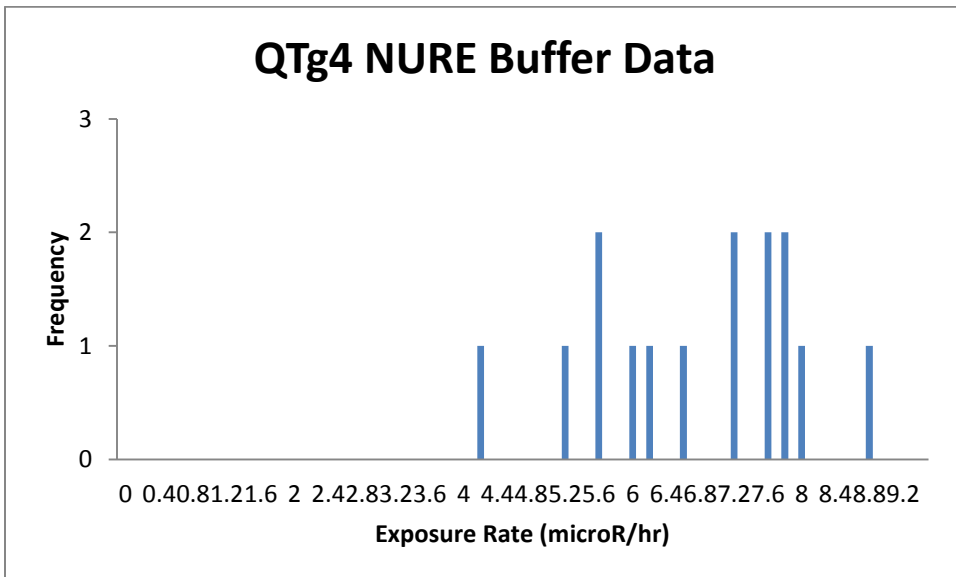
QTg4 50 m AMS Distribution:

QTg4 AMS Buffer Data
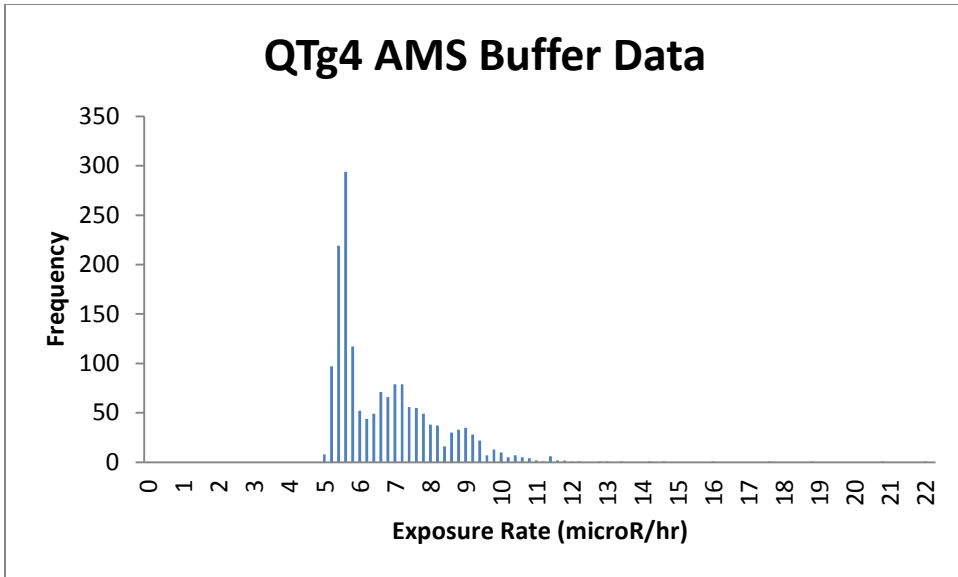
QTg4 AMS Distribution: This unit occurs as 2 main blobs, a cooler blob to the south east and a hotter blob to the northwest, following the trend that occurs through most of the units. This unit has a range of exposure rate from 4.125 to 24.41.

QTg4 AMS Exposure Rate Data
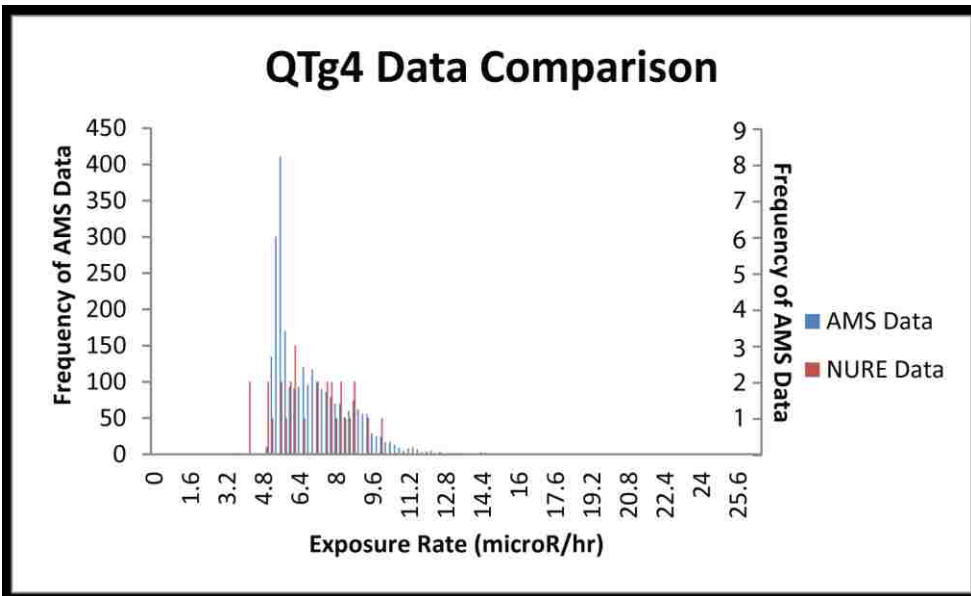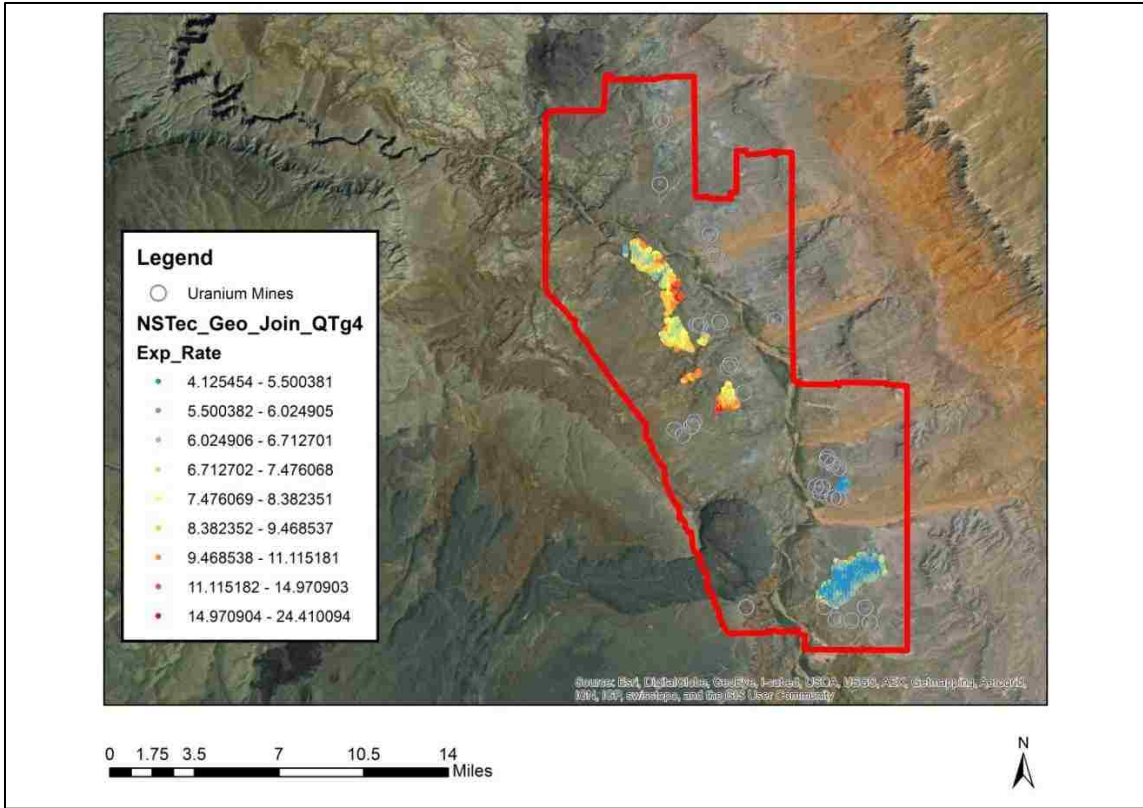
QTg5: Pleistocene and Miocene terrace gravel deposits, silt to cobble in size. Consist of limestone and chert clasts from Pkh, and sandstone clasts from TRmw, TRmhm and TRmss. Hypothesized to be equivalent to Ts (Billingsley et al., 2007).

QTg5 Field Notes: Mostly dark brown very fine grained sandstone clasts with clay underneath. Also clasts of chert and basalt present. Not homogenous, large variation across unit with respect to clast size. Gravel, mostly dark brown sandstone (less than 1 cm), some cherts (2-5 cm)

These field observations are consistent with the USGS description of this gravel unit. However, we did not agree that the unit was similar to Ts, which was dominated by basaltic sand and basalt clasts, though it did contain limestone and chert clasts like QTg5.

QTg5 NURE Histogram:
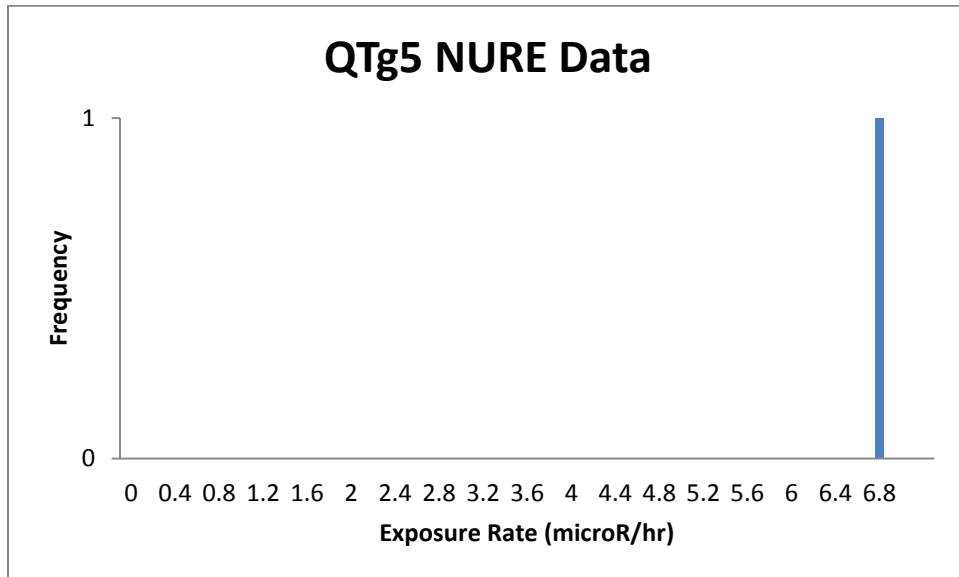
QTg5 AMS Histogram:

QTg5 AMS Data
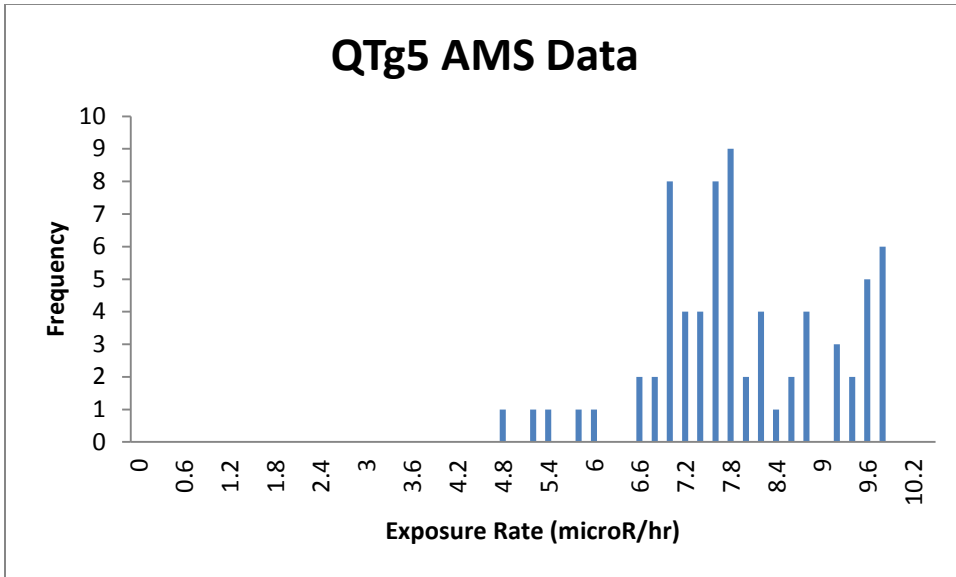
It is not surprising that these histograms do not have means that are within error. The NURE data contains only 3 data points, not enough to create a curve or show trends. The AMS data has 2 separate peaks and is left skewed, which should only help in making the means closer together.

QTg5 50 m buffer AMS Distribution:

QTg5 AMS Buffer Data
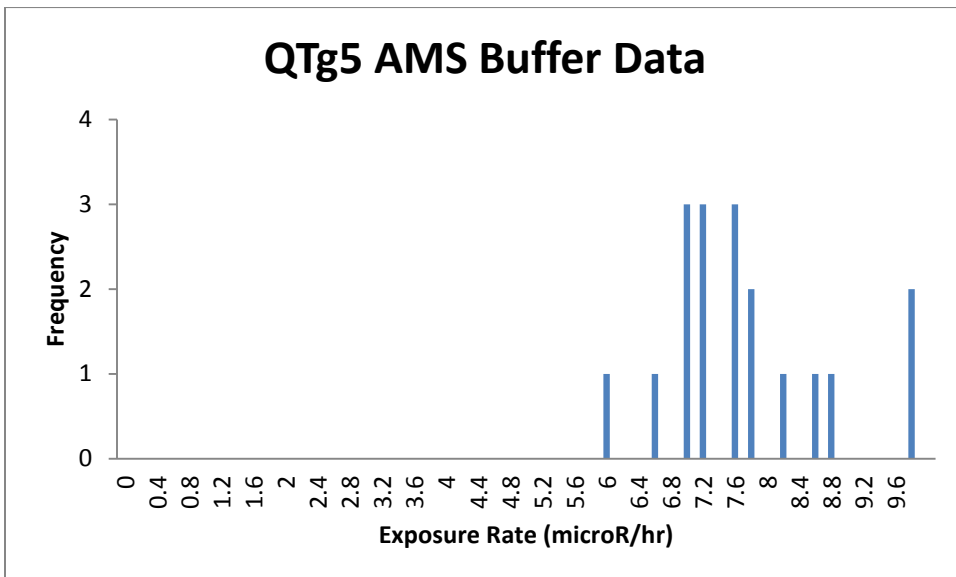
QTg5 AMS Distribution: This unit has a small distribution, and is hotter to the northwest, following the trend of most other units. It has a small range of exposure rates of 4.26 to 9.66.

172

QTg5 AMS Exposure Rate Data
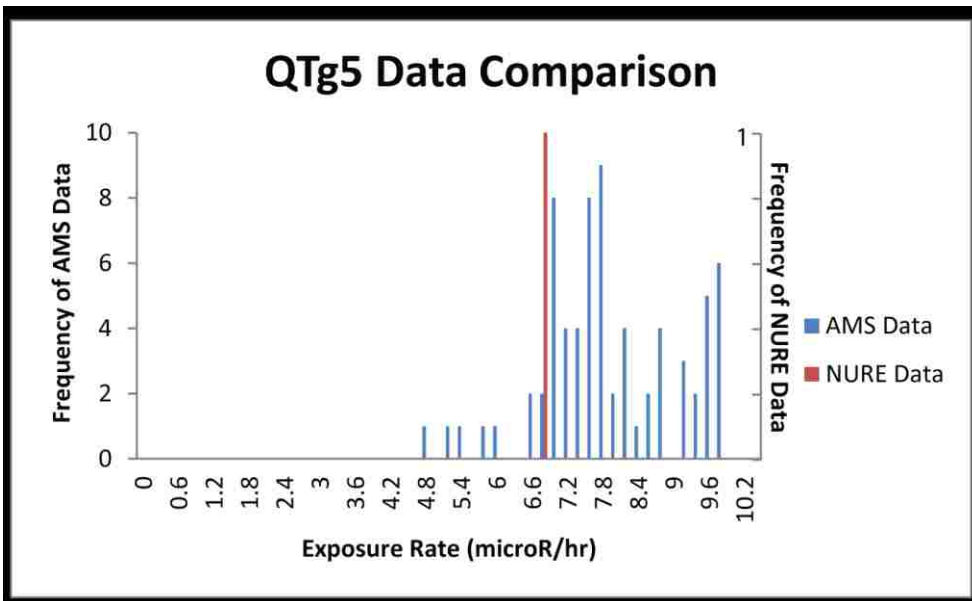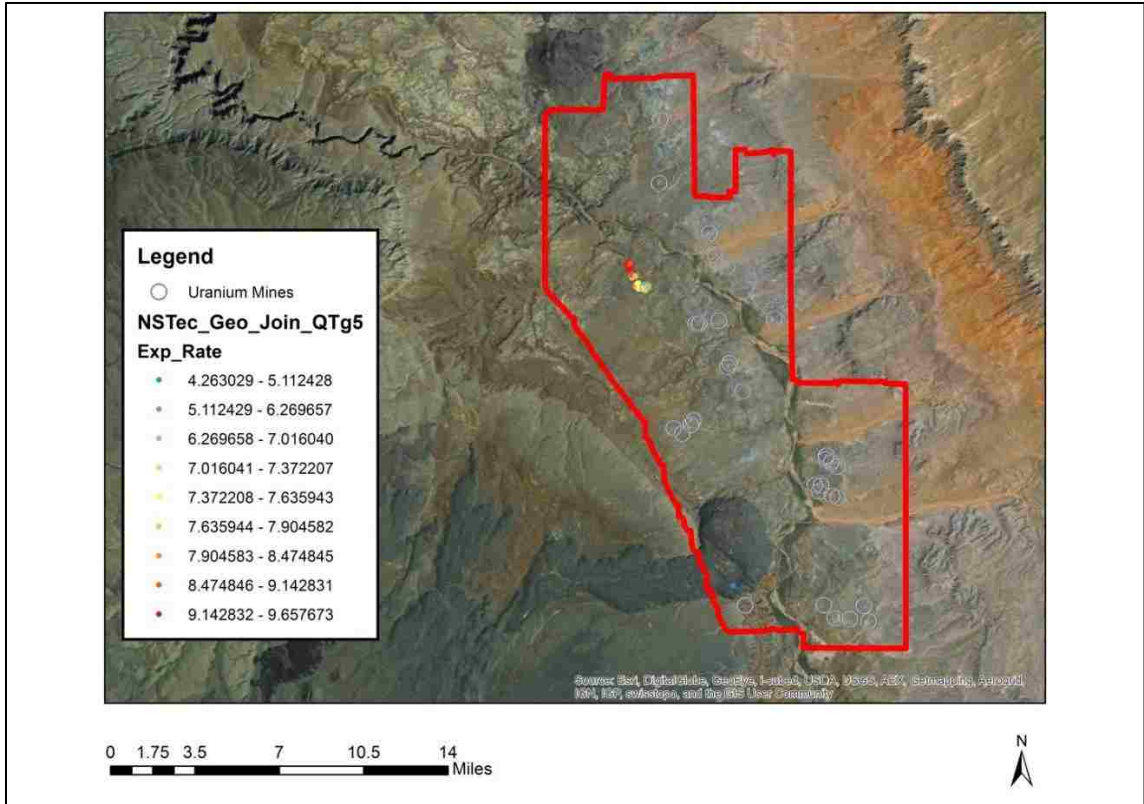
Ts: Occurs in the Black Point area in the south of the map, near Tbpb. Pleistocene and Miocene stream-channel deposits. Contains siltstone, sandstone, 'arkosic gravel and lenticular conglomerate' according to the USGS (Billingsley et al., 2007).

Ts Field Notes: Does not appear recently active, no cementation observed. Contains: fist sized vesicular basalt clasts and smaller (sub angular, larger=smoother), chert clasts of 1-3 cm, rough limestone, smooth chert. Medium amount of vegetation.
Mostly basaltic sand and basalt float about a decimeter in size. Some cherty float. Little aeolian addition. Moderate grasses and bushes.

These field observations are not consistent with the USGS description in that no sandstone, siltstone, arkosic gravel or lenticular conglomerate were observed. We saw only basalt and chert (which is not mentioned in the USGS description. However we only observed this stream channel at the top at Black Point, not at the base where these rock types may accumulate.

Ts AMS Histogram:
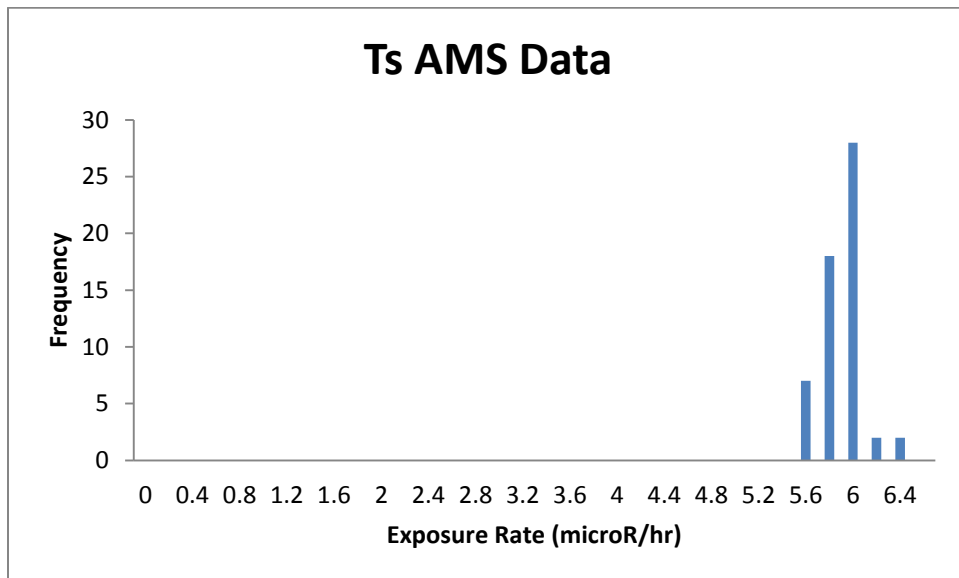
Ts 50 m buffer AMS Histogram:

Ts AMS Buffer Data
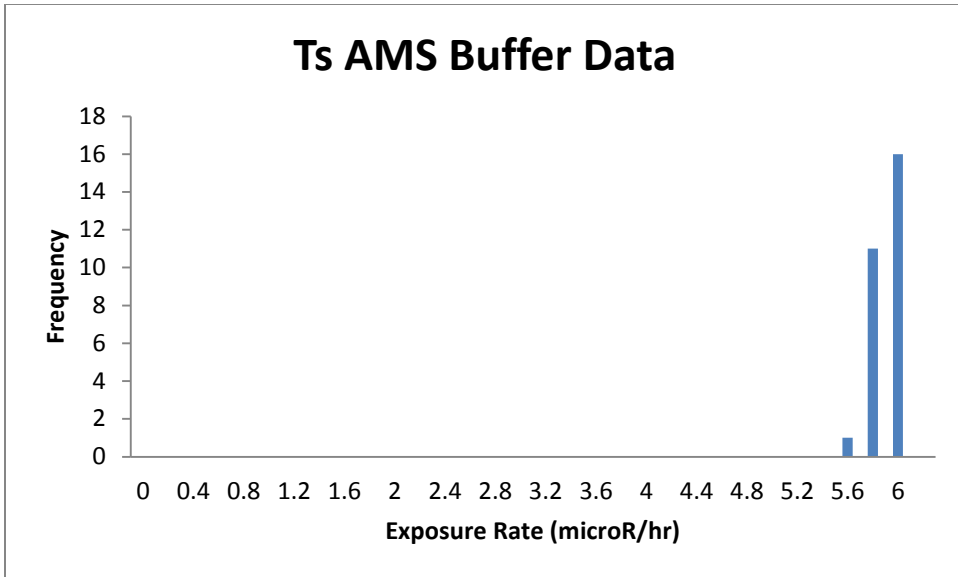
Ts AMS Distribution: This unit has a very small range on Black Point, and a very small range of exposure rates from 5.372 to 6.19. There are no observable patterns or trends.

Ts AMS Exposure Rate Data
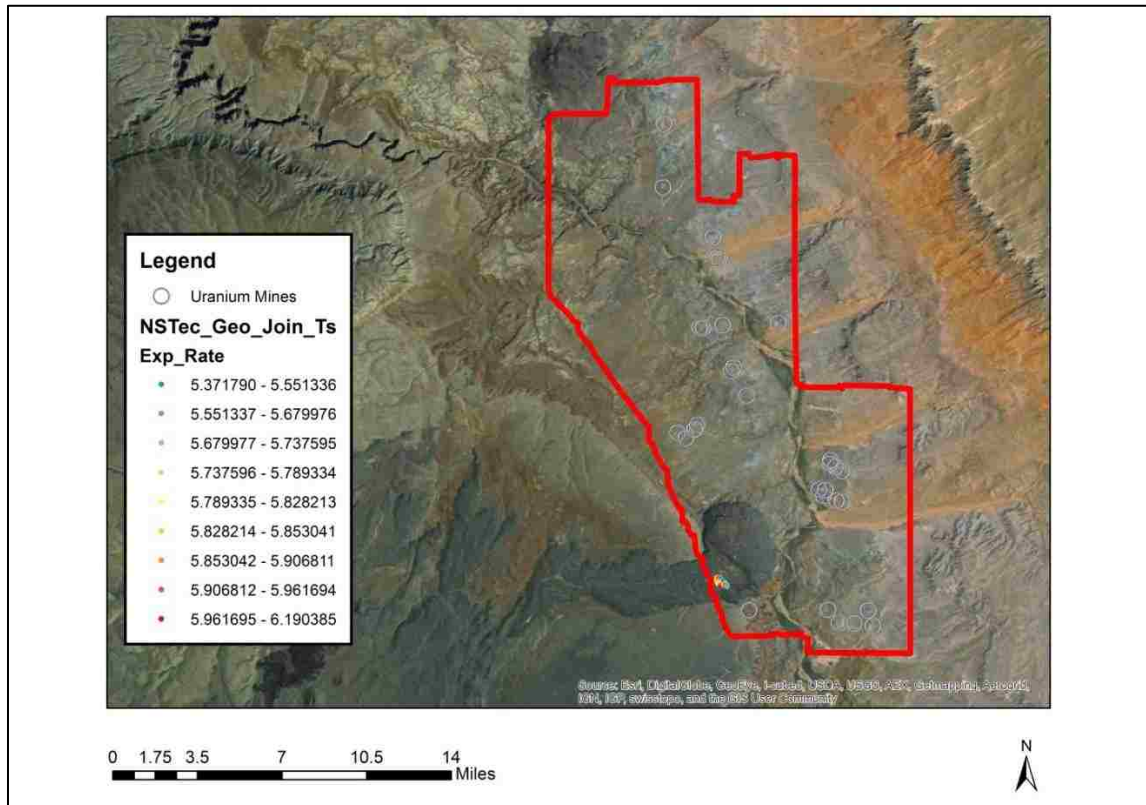
Units in the Literature

Chinle Fm (TRc prefix): The Petrified Forest Member of the Chinle Formation contains silicified wood, formed in the bottom of a swamp or stagnant pond. The sandstone occurring coeval with the wood contains clay formed from volcanic ash, the source of the silica. Petrified wood can also occur in other members of the Chinle. The shales and sandstones of the Chinle were deposited by 'streams meandering northward across a broad depositional basin containing numerous shallow lakes and swamps' (Sigleo, 1979). This is confirmed by Howell and Blakey (2013), who states it 'is a mud-dominated fluvial system deposited within a backarc basin.' These streams were flowing to the south to the late Triassic Sea of Nevada. Of most interest to this research is the Uranium concentrations which are found in the Chinle Fm and more specifically the Shinarump conglomerate. We also concluded that conglomerates tend to have very high U values from our database findings. Clays in the Chinle also have high U, and it is proposed by Hinckley (1955), that these clays are the source of the U, with a solution containing U being forced into the underlying sand and gravel layers, by compaction from the volcanic ash and debris. This corresponds with his findings that U favors coarser material. U deposits are usually found as bedded deposits, lens deposits, and in silicified trees. Perhaps the most relevant portion of his research is that he also did aerial radiation mapping, and when radiation anomalies were found, ground checks were done. Usually during these ground checks a silicified tree was found. Around these logs are oxidized halos of bedrock. Since these logs tend to occur in clusters, they could be the cause of the small areas of high radioelement content in the west of the aerial gamma ray survey (Hinckley, 1955).

San Francisco Volcanic Field (Tbpb): The basalt flow known as Black Point (Tbpb) is on the edge of the San Francisco Volcanic Field (SFVF). There are approximately 600 vents in the SFVF, all of which formed in the last 5 Ma. Silicic and mafic rocks were being produced at the same time in this area. The source is thought to be upper mantle, with interaction between upper mantle basalts and the silicic crust (Chen and Arculus, 1995). The composition of the SFVF varies so much over its area, that data points outside the mapping area are not likely to be relevant to the composition of flows within the mapping area.

Harrisburg Member, Kaibab Formation (Pkh): This unit was deposited in a dolomitic mudflat or Sabkha environment, with a gypsum precipitating lagoonal environment to the west. It was an arid environment with shallow water (Clark, 1981).

DIR Report

Pkh with DIR:

	K (wt %)	U (ppm)	Th (ppm)
mean	0.1987	185.26	0.7250
Standard deviation	0.5464	1670.2507	1.7651
range	4.2238	16599.7	14.2
median	0.03	1.45	0.3
mode	0.02	1.9	0.2

Pkh without DIR:

	K (wt %)	U (ppm)	Th (ppm)
mean	0.6352	898.5842	6.5386
Standard deviation	0.9207	3645.4628	5.2315
range	4.1938	16599.596	13.1
median	0.37	1.875	6.52
mode	0.04	1.39	0.2

Pkh DIR only:

	K (wt %)	U (ppm)	Th (ppm)
mean	0.03672	1.5267	0.4176
Standard deviation	0.04301	0.8935	0.3574
range	0.31	5.6	1.7
median	0.02	1.4	0.3
mode	0.02	1.9	0.2

Pkh Soil:

	K (wt %)	U (ppm)	Th (ppm)
mean	1.8225	2.14	7.56
Standard deviation	0.1776	0.0490	N/A
range	0.4	0.1	N/A
median	1.815	2.13	7.56
mode	N/A	2.1	N/A

While removing DIR for Pkh limited our data to only 52 points (down from 184), the averages without DIR are significantly closer to the soil values, especially with regards to Th. When looking at the table with only DIR data it becomes obvious that K and Th are significantly lower than expected for this area.

Qa1 with DIR:

	K (wt %)	U (ppm)	Th (ppm)
mean	0.5104	37.0208	2.77
Standard deviation	0.5856	88.1206	4.848
range	1.9475	291	12.6
median	0.13	1.8	0.35
mode	0.02	1.8	0.3

Qa1 without DIR:

	K (wt %)	U (ppm)	Th (ppm)
mean	0.9341	93.454	11.9
Standard deviation	0.5063	129.7129	1.2728
range	1.8375	290.2	1.8
median	0.8800	9.19	11.9
mode	0.8800	N/A	N/A

Qa1 DIR only:

	K (wt %)	U (ppm)	Th (ppm)
mean	0.03375	1.75	0.4873
Standard deviation	0.01685	0.8767	0.4673
range	0.04	2.7	1.4
median	0.03	1.55	0.3
mode	0.02	1	0.3

Qa1 Soil:

	K (wt %)	U (ppm)	Th (ppm)
mean	1.5469	2.7575	8.8633
Standard deviation	0.4727	1.2531	2.9402
range	1.159	3.64	7.7
median	1.799	2.915	8.53
mode	1.9	N/A	N/A

For Qa1 elimination the DIR data points brought K closer to that of the soil, but drove U and Th over the recorded concentrations of the soil, though Th

was overall closer in value. Without the DIR data we went from 17 data points to 10, with only two Th measurements and 4 U measurements, 2 of which are outliers. This is probably the cause of the extreme increase of U median value. If we average the 2 non-outlier U concentrations we get 3.04 ppm, very close to the soil average of 2.7575 ppm. When looking at the DIR only statistics it becomes obvious that K and Th values are much lower than expected.

Qa2 is interesting in that it has a large amount of data points (228) only 1 of which is DIR, and this is the unit that has averages that are similar, in this unit it may be applicable to look only at the averages as the rock values lack outliers. Perhaps we should define an outlier and use that to decide what units should be defined by mean or median. Qa2's DIR data point is 0.05 wt % K, 1.1 ppm U, and 0.7 ppm Th. We expect the Th values for DIR's data to be low, but K is also a problem.

Qa2 with DIR:

	K (wt %)	U (ppm)	Th (ppm)
mean	1.4782	1.6314	9.1324
Standard deviation	0.9832	1.5059	11.1689
range	4.4426	3.89	32.31
median	1.1705	0.979	3.025
mode	0.9962	N/A	1.24

Qa2 without DIR:

	K (wt %)	U (ppm)	Th (ppm)
mean	1.4847	1.7073	9.781
Standard deviation	0.9806	1.6100	11.3472
range	4.4426	3.89	32.31
median	1.1705	0.898	3.65
mode	0.9962	N/A	1.24

Qa2 Soil:

	K (wt %)	U (ppm)	Th (ppm)
mean	1.3	2.33	8.8485
Standard deviation	N/A	0.5233	2.1425
range	N/A	0.74	3.03
median	1.3	2.33	8.485
mode	N/A	N/A	N/A

For Qa2 removing the DIR data point made the rock averages for K and Th go farther away from the soil averages, while the U concentration was closer to that of the soil. An important thing to remember is despite the large amount of data points there were only 7 data points with U, and 14 with Th. The fact that

removing the DIR data point had the most positive effect on the category with the least data points may speak to this being a good idea.

Qg1: This unit has one data point from NAVDAT and one from DIR, NAVDAT only lists K so this is all we can compare. DIR reports a K of 0.05 wt %, while NAVDAT reports a K of 1.0875 wt %. This is a significant difference in values.

Qae: By removing the DIR data points from Qae we are only left with one data point with only a K value of 0.963 wt % K, compared to an average K of 0.2532% and a median of 0.02%. Eliminating the DIR data points brings us closer to the soil values as the average for soil was 2.1%. It's also important to note that for this unit the rock had ridiculously little U and Th compared to the soil.

Qae with DIR:

	K (wt %)	U (ppm)	Th (ppm)
mean	0.2532	1.3667	0.1667
Standard deviation	0.4732	0.3215	0.0577
range	0.953	0.6	0.1
median	0.02	1.5	0.2
mode	0.02	N/A	0.2

Qae Soil:

	K (wt %)	U (ppm)	Th (ppm)
mean	2.100	2.8175	9.7030
Standard deviation	0.3607	0.4538	2.1361
range	0.7	0.82	4.1
median	1.999	2.825	9.01
mode	N/A	N/A	N/A

Qae DIR Only:

	K (wt %)	U (ppm)	Th (ppm)
mean	0.017	1.3667	0.1667
Standard deviation	0.006	0.3215	0.0577
range	0.01	0.6	0.1
median	0.02	1.5	0.2
mode	0.02	N/A	0.2

QI: This unit has no DIR data points, but it is also interesting to note that this is the first unit that has a K concentration in the soil that is extremely close to that in the rock, and a U and Th that are significantly higher in the rock than the soil (see unit report for graphs).

Qs with DIR:

	K (wt %)	U (ppm)	Th (ppm)
mean	0.2638	1.7065	1.4
Standard deviation	0.3724	0.5913	1.8385
range	1.09	2.018	2.6
median	0.1	1.6	1.4
mode	N/A	1.6	N/A

Qs without DIR:

	K (wt %)	U (ppm)	Th (ppm)
mean	0.3	1.7217	2.7
Standard deviation	0.3867	0.6370	N/A
range	1.05	2.018	0
median	0.12	1.6	2.7
mode	N/A	N/A	N/A

Qs Soil:

	K (wt %)	U (ppm)	Th (ppm)
mean	1.6495	3.12	10.38
Standard deviation	0.4943	0.5515	0.8768
range	0.699	0.78	1.24
median	1.6495	3.12	10.38
mode	N/A	N/A	N/A

Qs went from 8 data points to 7 with the elimination of DIR, and this caused little change in any of the values, but all of that change was closer to soil averages. It should be noted that now there is only one recorded Th concentration. Qs has one DIR data point of 0.01 K, 1.6 ppm U and 0.1 Th. The Th and K values of this data point are unreasonable compared to the rest of the data.

Qv with DIR:

	K (wt %)	U (ppm)	Th (ppm)
mean	0.2963	1.6206	0.7344
Standard deviation	0.4360	0.9472	1.5137
range	1.2850	5.311	7.66
median	0.04	1.4	0.4
mode	0.03	1.1	0.4

Qv without DIR:

	K (wt %)	U (ppm)	Th (ppm)
mean	0.5612	1.7433	4.78
Standard deviation	0.4913	1.4222	4.2144
range	1.2650	5.311	5.96
median	0.31	1.27	4.78
mode	1.6221	N/A	N/A

Qv just DIR:

	K (wt %)	U (ppm)	Th (ppm)
mean	0.0313	1.5565	0.3826
Standard deviation	0.02361	0.6021	0.2741
range	0.11	2.4	0.9
median	0.03	1.5	0.4
mode	0.04	1.1	0.4

Qv Soil:

	K (wt %)	U (ppm)	Th (ppm)
mean	2.0648	2.3925	10.85
Standard deviation	0.4401	0.8517	1.0607
range	1.07	1.83	1.5
median	2.0645	2.27	10.85
mode	N/A	N/A	N/A

Eliminating DIR data points was a positive change for K, U and Th. When comparing the means of the soil and rock they are closer without DIR, supporting my theory that DIR is skewing our averages lowers, especially in a unit like Qv where it makes up a large portion of the data points. Before Qv had 46 data points, now there are 23.

By eliminating DIR data points we lost all data for the following units: Qes, Qf

References

Beck, H., DeCampo, J., and Gogolak, C., 1972, In-situ Ge(Li) and NaI(Tl) Gamma-ray Spectrometry: Health and Safety Laboratory: No. HASL—258, 75 p.

Billingsley, G. H., Priest, S. S., & Felger, T. J., 2007, Geologic Map of the Cameron 30' x 60' Quadrangle, Coconino County, Northern Arizona: USGS Geological Survey.

Books, K. G., 1962, Aeroradioactivity survey and related surface geology of parts of the Los Angeles region, California (ARMS-I): Biological and Medical Research Division semiannual report: Argonne National Laboratory: Division of Biological and Medical Research, v. 59, p. 1-25.

Chen, W., and Arculus, R., 1995, Geochemical and isotopic characteristics of lower crustal xenoliths, San Francisco Volcanic Field, Arizona, U.S.A: Lithos, v. 36, p. 203-225, doi: 10.1016/0024-4937(95)00018-6.

Clark, R. A., 1981, Stratigraphy, depositional environments, and carbonate petrology of the Toroweap and Kaibab Formations (Lower Permian), Grand Canyon region, Arizona [PhD Thesis]: State Univ. of New York, Binghamton.

Dickson, B.L., and Scott, K.M., 1997, Interpretation of aerial gamma-ray surveys-adding the geochemical factors: AGSO Journal of Australian Geology and Geophysics, v. 17, p. 187-200.

Dickson, B., Fraser, S., and Kinsey-Henderson, A., 1996, Interpreting aerial gamma-ray surveys utilising geomorphological and weathering models: Journal of Geochemical Exploration, v. 57, p. 75-88, doi: 10.1016/s0375-6742(96)00017-9.

Dickson, B., 1995, Uranium-series disequilibrium in Australian soils and its effect on aerial gamma-ray surveys: Journal of Geochemical Exploration, v. 54, p. 177-186, doi: 10.1016/0375-6742(95)00032-1.

Grasty, R., Carson, J., Charbonneau, B., and Holman, P., 1984, Natural background radiation in Canada: Geological Survey of Canada Bulletin 360, 39 p.

Griscom, A., and Peterson, D. L., 1961, Aeromagnetic, aeroradioactivity, and gravity investigations of Piedmont rocks in the Rockville quadrangle, Maryland: US Geol. Survey Prof. Paper, p. D267-D271.

Hendricks, T. J., 2001, An Aerial Radiological Survey of Abandoned Uranium Mines in the Navajo Nation: Report for Bechtel Nevada Remote Sensing Laboratory: U.S. Department of Energy, 24 p.

Hinckley, D. N., 1955, Reconnaissance in the Cameron area, Coconino County, Arizona: US Atomic Energy Comm: RME-81, 21p.

Howell, E., and Blakey, R., 2013, Sedimentological constraints on the evolution of the Cordilleran arc: New insights from the Sonsela Member, Upper Triassic Chinle Formation, Petrified Forest National Park (Arizona, USA): Geological Society of America Bulletin, v. 125, p. 1349-1368, doi: 10.1130/b30714.1.

Løvborg, L., and Kirkegaard, P., 1974, Response of 3″ × 3″ NaI(Tl) detectors to terrestrial gamma radiation: Nuclear Instruments and Methods, v. 121, p. 239-251, doi: 10.1016/0029-554x(74)90072-x.

Mernagh, T. P., & Miezitis, Y., 2008. A review of the geochemical processes controlling the distribution of Th in the Earth's crust and Australia's Th resources: Geoscience Australia Record 2008/05, 48 p.

Minty, B., 1997, Fundamentals of airborne gamma-ray spectrometry: AGSO Journal of Australian Geology and Geophysics, v. 17, p. 39--50.

Moxham, R., 1963, Natural Radioactivity in Washington County, Maryland: Geophysics, v. 28, p. 262-272, doi: 10.1190/1.1439174.

Pitkin, J., Bates, R., and Neuschel, S., 1964, Aeroradioactivity surveys and geologic mapping (Nuclear facility background gamma radiation measured by aerial radiological measurement): The natural radiation environment, p. 723-736.

Sigleo, A., 1979, Geochemistry of silicified wood and associated sediments, Petrified Forest National Park, Arizona: Chemical Geology, v. 26, p. 151-163, doi: 10.1016/0009-2541(79)90036-6.

Ulbrich, H. H. G. J., Ulbrich, M. N. C., Ferreira, F. J. F., Alves, L. S., Guimarães, G. B., & Fruchting, A. (2009). Levantamentos gamaespectrométricos em granitos iferenciados. I: revisão da metodologia e do comportamento geoquímico dos elementos K, Th e U. Geologia USP. Série Científica, 9(1), 33-53.

U.S. Geological Survey, 2004, National Uranium Resource Evaluation (NURE) Hydrogeochemical and Stream Sediment Reconnaissance data: U.S. Geological Survey, Denver, CO.

van der Meer, F., van der Werff, H., van Ruitenbeek, F., Hecker, C., Bakker, W., Noomen, M., van der Meijde, M., Carranza, E., Smeth, J., and Woldai, T., 2012, Multi- and hyperspectral geologic remote sensing: A review: International Journal of Applied Earth Observation and Geoinformation, v. 14, p. 112-128, doi: 10.1016/j.jag.2011.08.002.

Curriculum Vitae

Kara Marsac
UNLV Geoscience, 4505 Maryland Parkway, Las Vegas, NV 89154
248-701-6812
Marsac@unlv.nevada.edu

Education:

M.S. Geology, University of Nevada: Las Vegas   Expected: May 2015

Near Surface Geophysics Short Course: GSA Annual Meeting   2014

Research Experience in Carbon Sequestration (RECS) Program   2014

Exxon Mobile Geophysics Short Course   2014

Field Camp in Ireland, James Madison University, Harrisonburg, VA   2013

B.S., Eastern Michigan University, Ypsilanti, MI   2013
    Major: Highest Honors in Professional Concentration Geology
    GPA: 4.0

Biology Field Course, Ecuador and the Galapagos, Eastern Michigan University   2012

High School Diploma, Clarkston High School, Clarkston, MI   2010
    Graduated Valedictorian out of 670 students

Research Experience

2013-Present, Research Assistant, University of Nevada: Las Vegas, Pamela Burnley
    Using ArcGIS and geochemistry to model radiation of soil and bedrock
    Collection and mapping of geochemical data
    Field work including soil sampling
    Research and development of improving radiation detection technique

2012-2013, Eastern Michigan University, with Steven LoDuca
    Senior Thesis: Compendium of Paleozoic Noncalcified Algae.
    Project largely involved library research, data analysis and mapping, also went to the
    Smithsonian Institution as a visiting researcher to examine Burgess Shale specimens

Fall 2011-Winter 2012, Eastern Michigan University, with Steven LoDuca
    Using Scanning Electron Microscopes to tell the difference between algae and
    hemichordates in problematic early Paleozoic macrofossils.

Fall 2010-Winter 2011, Eastern Michigan University, with Christine Clark
   Using Optical Microscopes to identify minerals in thin section from rocks collected near
   Poughkeepsie, NY.

Honors and Awards:

First Prize for an oral presentation at the Association of Environmental and Engineering Geologists
Southern Nevada Section Student Night   2014

Highest Honors from Eastern Michigan University   2013
   Departmental Honors in Geology and University Honors for general education

Outstanding Geology Major from the Department of Geography and Geology   2011

Mineralogical Society of America Undergraduate Prize   2012

Dean's List at Eastern Michigan University   2010-2013

Presidential Scholarship from Eastern Michigan University   2010-2013

Raytheon MathMovesU Bonus Award Scholarship, $20,000   2010

Fellowships and Grants:

GSA Research Grant, Summer 2014, $607
   Funding to visit the field area for my Master's Thesis and collect samples

Michigan Space Grant, from the Michigan Space Grant Consortium of NASA, Summer 2012-Winter
2013, $2,500
   A Preliminary Study of the Burgess Shale Taxon *Yuknessia simplex* Walcott, 1919 Using
   Backscattered Electron Imaging

Symposium Undergraduate Research Fellowship, from the Symposium Undergraduate Research
Fellow Program at Eastern Michigan University, Fall 2010-Winter 2013, $3,000 per academic year
   Fall 2010-Winter 2011: Thin Section Investigation of the Metamorphic Sequence near
      Poughkeepsie, New York
   Fall 2011-Winter 2012: Investigation of Problematic Early Paleozoic Macrofossils using
      Scanning Electron Microscopy
   Fall 2012-Winter 2013: Compendium of Paleozoic Noncalcified Algae

Undergraduate Research Stimulus Fellowship, from the Provost at Eastern Michigan University,
Summer 2012, $2,000
   Compendium of Noncalcified Macroalgae
   Investigation of Problematic Early Paleozoic Macrofossils using Scanning Electron
      Microscopy

Honors Undergraduate Research Fellowship, from the Honors College at Eastern Michigan University, Winter 2013, $2,000

Conference and Symposium Presentations

GSA Annual Meeting, October 2014, Poster titled 'Modeling Background Radiation in our Environment using Geochemical Data'

AEG Annual Meeting, September 2014, Poster titled 'Modeling Background Radiation in our Environment using Geochemical Data'

Geosymposium at UNLV, April 2014, Poster titled 'Connecting Aerial Gamma Ray Surveys and Geochemical Data'

GSA Annual Meeting, November 2012, Poster titled 'A Preliminary Study of the Burgess Shale Taxon *Yuknessia simplex* Walcott, 1919 Using Backscattered Electron Imaging'

Michigan Space Grant Consortium Conference, October 2012, Poster titled 'A Preliminary Study of the Burgess Shale Taxon *Yuknessia simplex* Walcott, 1919 Using Backscattered Electron Imaging'

Symposium for Undergraduate Research, Expected March 2013, Senior Thesis entitled 'Compendium of Noncalcified Paleozoic Macroalgae'

Symposium for Undergraduate Research, March 2012, Presentation titled 'Investigation of Problematic Early Paleozoic Macrofossils using Scanning Electron Microscopy'

Symposium for Undergraduate Research, March 2011, Poster titled 'Thin Section Investigation of the Metamorphic Sequence near Poughkeepsie, New York'

Volunteer Experience

Geology Club President, Eastern Michigan University, Ypsilanti, MI   2011-2013
          Organized events and field trips, managed finances and communications

Zookeeper Assistant, Potter Park Zoo, East Lansing, MI   2009
          Assisted zookeepers in tasks and interacted with visitors

Intern, Michigan House of Representatives, Lansing, MI   2010

Classroom Aide, Springfield Plains Elementary, Clarkston, MI   2007-2010
          Aide to Kristine Simek, graded papers and tutored students

Math & Physics Tutor, Clarkston Community Schools, Clarkston, MI   2004-2010

Accomplishments at Eastern Michigan University

President of Geology Club from 2011-2013
    Started an Earth Science Lecture Series: The William Sherzer Memorial Lecture Series

Featured on the Eastern Michigan University Homepage for my research   2013